Optimizing CRISPR–Cas technologies in *Caenorhabditis elegans*: Nested CRISPR and expanded targeting with Cas variants

Jeremy Vicencio

TESI DOCTORAL UPF / 2021

Thesis Supervisor

Dr. Julián Cerón Madrigal

Modeling Human Diseases in *C. elegans* group

Genes, Disease, and Therapy Program. IDIBELL.

Department of Experimental and Health Sciences

Universitat Pompeu Fabra Barcelona

To my parents, Vergel and Imelda,

for your infinite love and support

ACKNOWLEDGMENTS

While it is only my name that appears on the front cover, there were a ton of people involved in making this dream turn into reality. I would like to dedicate a few words to the people who have made this journey worthwhile and unforgettable.

First and foremost, my sincerest gratitude to my supervisor, Julián Cerón, for being an exceptional mentor during these past three and a half years. Thank you for trusting me despite having zero experience with *C. elegans* when I started in the lab, and above all, thank you for putting my well-being before anything else. I have learned a lot from you, both academically and about life in general, and I can only hope that more students get the chance to learn from you as much as I did. Your positivity and creativity have gotten us through some tough times and I learned that looking at things from a different perspective can make a great deal of difference. I wish you and the future generations of Ceron Lab all the happiness and success not only in the lab, but in life as well.

Some people say you cannot have it all but I suppose I am the exception to the rule. How often does one get to work on a topic that they like, have a supportive mentor, and at the same time work with an amazing team of people? My heartfelt thanks go to my lab mates who have become not just friends, but also family during my time here in Barcelona. Dmitri, thank you for teaching me all the basics when I first arrived in the lab and for all your silly moments and catchphrases that always lightened up everyone. David, my half-brother from another mother, thanks for being my go-to person for all things bleaching-related and for helping me take some wonderful photos of the bright and shiny worms that we have created over the years. Also, thanks to the both of you for helping me carry the load during these last few months.

Carmen, I will always remember you every time I see the color purple. I admire your passion, resilience, and cheerfulness, and you will always be my favorite malagueña. Xènia, thanks for putting up with my incessant nematode-related questions and article requests when I cannot find them. I might be older than you chronologically but I've always looked up to you as a senior member of the lab. Thank you for all the support, starting with the first paper that you, Carmen, and I co-wrote together, up until the final stretch of my PhD journey even though you're now in Toronto. Thanks to the four of you for all the fond memories that I will forever carry in my heart. *Amigos para siempre, ¿vale?*

To all the Master's students I have had the pleasure of working with over the years: Isabel, Hildegard, Miguel, Nuria, and Mariona, thank you for letting me impart a small piece of my *C. elegans* know-how to you. I appreciate your curiosity and willingness to learn and I enjoyed all of our moments together, both on and off the lab. Thanks as well to my former co-predocs Laura and Ana Pilar for making an impact in the lab despite your short time with us. I wish all of you the utmost success in whatever goals you pursue in the future.

To the rest of the Molecular Genetics Lab, especially to Laura, Leire, Juanjo, and Ana: thank you for all the late afternoon banter in the pre-docs office. I hope you had fun listening to my rants as much as I had fun listening to yours. I am glad that somehow, we were able to support each other despite working in different groups. Thanks as well to Javi and Antonia for making sure that things run smoothly in the department.

I would also like to take this opportunity to thank everyone who have helped behind the scenes. First and foremost, to La Caixa foundation for ensuring that we have the best PhD experience possible. My special thanks go out to Gisela for dealing with all the paperwork that made it possible for me to work on my PhD here in Spain, and for the relentless support over the years.

I would also like to thank IDIBELL, especially Human Resources for always responding to my queries and concerns, Research Grant Management for coordinating between La Caixa and IDIBELL, and Accounting and Viatges i Dietes for always making sure that my expenses get reimbursed ;) I would also like to thank Alberto Villanueva from ICO and Nick Stroustrup from the CRG for sharing precious reagents and equipment.

I have had the wonderful opportunity to embark on a short research stay at the Centro Andaluz de Biología del Desarrollo in Seville. I would like to thank More and his team, especially Carlos, Ismael, Luis, and Miguel for teaching me the ropes about working with zebrafish. I would also like to thank Marta for hosting me in her lab and Machupi, David, and Patricia who made sure that I had everything I needed during my stay. I had so much fun working with you guys and those six weeks flew by really fast!

I would like to thank my new CRG family for welcoming me to their team. My deepest gratitude goes out to Nick, for his patience and understanding during this time of transition. I would also like to thank the rest of the team, especially Natasha and Daisuke, for all your support.

To all my friends and colleagues in the Philippines, especially to my Department of Biology family at the University of the Philippines Manila: I am so lucky to have crossed paths with all of you. I miss everyone dearly and I sincerely hope to get the chance to work with all of you once more. My special thanks to Ma'am Lhen for your everlasting mentorship and support, and to Ma'am Anna for entertaining my questions about statistical analysis. Thanks to the DB FAM and boo teh teh 3.0 groups.

To my second family here in Barcelona: Tita Mercy and Tito Carlito, thank you for treating me as your own during these past few years. Thank you for all the wonderful homecooked Filipino meals that I would otherwise have bought from a restaurant due to my lack of cooking skills. To all my friends

here in Barcelona: Mig, Angelo, Miriam, Xavi, Mitch, Ate Ann, and Ate Juliet. I miss all the get-togethers we used to have every once in a while to distract us from the harsh realities of life. I'm sure we'll get to see each other more often once this thesis (and pandemic) is over.

To my Erasmus travel buddies: Cova, Sara, and Ifeanyi. Thank you for never losing touch after all these years. I always have so much fun whenever I'm around you guys and I can't wait to go on more adventures with you and see where life takes us!

To Miguel, thank you for your overflowing love and support over the past few years. Your encouragement and understanding mean the world to me. Thanks for everything.

And finally, and most important of all, to my family in the Philippines. It's tough being away from you all these years but I always feel your love and support wherever I am. Thanks to my siblings: Mark, Dan, and Ruth for sending me silly stuff online that make me smile every now and then. To all my aunts, uncles, and cousins who are far too many to name: thank you for always being my biggest supporters and for never refusing to help when I ask for it. To my grandparents, especially to Lola Norma who has been my biggest fan for as long as I can remember: I couldn't have made it without you. To my dad, Vergel: You are one of the reasons why I decided to pursue a career in science and I hope that I have made you proud. You may not be here with us anymore but I will always carry you in my heart. You are dearly missed and I love you very much. Finally, to my mom, Imelda: *you find ways* cannot describe it any better. You are the strongest woman I know and I am very blessed to have you as my mom. Thanks for always sticking with me through thick and thin and I know that there is nothing that we cannot conquer together.

For all His love, wisdom, and guidance, to God be the glory.

ABSTRACT

ABSTRACT

CRISPR–Cas technology is evolving at a monumental pace, and therefore, genome editing protocols in *Caenorhabditis elegans* must be updated correspondingly. While the creation of indels and missense mutations is quite straightforward, the insertion of long DNA fragments can occasionally pose challenges. Here, I describe Nested CRISPR, an alternative, cloning-free method for the creation of translational and transcriptional reporters. We demonstrate that Nested CRISPR is an efficient method that can be customized for the insertion of a suite of fluorescent tags and epitopes at endogenous loci using a combination of single-stranded and double-stranded DNA repair templates.

One of the main features of CRISPR–Cas systems is the requirement for a protospacer adjacent motif (PAM) that aids in the recognition of target sequences. In the case of SpCas9, the most widely used Cas9 ortholog, the 5'-NGG-3' PAM requirement limits the number of targetable sites in the genome. Here, I demonstrate that the natural Cas12 ortholog AsCas12a can be used to efficiently target 5'-TTTV-3' sites in the genome. By contrast, several orthologs of the Cas12f1 family presented limited activity in *C. elegans.*

Finally, we demonstrate that the structurally engineered near-PAMless Cas9 variants SpG and SpRY can efficiently mediate genome editing in *C. elegans* at 5'-NGN-3' and 5'-NYN-3' sites, respectively, via error-prone and precise repair mechanisms under optimized conditions. Overall, the methods presented here expand genome editing possibilities in *C. elegans*, therefore contributing to the advancement of functional genomics and human disease modeling in this model organism.

RESUMEN

La tecnología CRISPR-Cas está evolucionando a un ritmo frenético y, por lo tanto, los protocolos de edición del genoma en *Caenorhabditis elegans* deben actualizarse con frecuencia. Si bien la creación de inserciones y deleciones, y de mutaciones de cambio de sentido, son relativamente sencillas, la inserción de fragmentos largos de ADN, ocasionalmente, puede presentar complicaciones. En esta tesis describo *Nested CRISPR*, un método alternativo para la creación de reporteros de traducción y transcripción, sin necesidad de realizar clonajes moleculares. Demostramos que *Nested CRISPR*, utilizando ADN de cadena sencilla y doble como secuencias de reparación, es un método eficaz para la inserción de etiquetas fluorescentes y otros epítopos en *loci* endógenos.

Una de las principales características de los sistemas CRISPR-Cas es el requerimiento de un Motivo Adyacente al *Protospacer* (PAM) para reconocer las secuencias diana. En el caso de SpCas9, el ortólogo Cas9 más utilizado, la PAM requerida es 5'-NGG-3', lo cual limita el número de sitios editables en el genoma. Aquí demuestro que la nucleasa AsCas12a se puede usar para editar de manera eficiente regiones del genoma con la PAM 5'-TTTV-3'. Por el contrario, varios ortólogos de la familia Cas12f1 mostraron actividad limitada en *C. elegans*.

Finalmente, demostramos que las variantes de Cas9 SpG y SpRY, creadas con ingeniería molecular, en condiciones optimizadas, pueden mediar de manera eficiente la edición del genoma de *C. elegans* en sitios PAM 5'-NGN-3' y 5'-NYN-3' respectivamente, a través de mecanismos de reparación precisos o propensos a errores. En general, los métodos aquí presentados amplían las posibilidades de edición del genoma en *C. elegans*, contribuyendo al avance de la genómica funcional y al modelado de enfermedades humanas en este organismo modelo.

PREFACE

Genome editing refers to the alteration of DNA sequences in cells or living organisms by deletions, insertions, substitutions, or replacements. Genome editing technologies have given researchers the ability to manipulate virtually any genomic sequence, allowing the facile generation of isogenic cell lines and animal models for studying genetics, development, and human disease. Specifically, the ease with which CRISPR–Cas9 can be adapted to recognize new genomic sequences has led to a genome editing revolution that has propelled scientific breakthroughs and applications in areas such as synthetic biology, disease modeling, gene therapy, drug discovery, molecular diagnosis, and agricultural and environmental sciences.

The genetic tractability of the model organism *Caenorhabditis elegans*, when coupled to the adaptability of CRISPR–Cas9, transforms this popular model organism to an even more powerful system for interrogating gene function and uncovering novel molecular mechanisms. Thanks to its rapid life cycle and hermaphroditic nature, the rate at which heritable genomic changes can be made and propagated in this nematode is unparalleled by any other model organism.

Since the introduction of CRISPR–Cas9 several years back, the development of improved genome editing methods and novel applications has not decelerated. Therefore, the *C. elegans* community is constantly working to adapt these new discoveries for use in the nematode. While several protocols exist for inserting large DNA fragments into endogenous loci, we encountered issues in reproducing the results reported in these studies. Therefore, we aimed to develop a method that would allow us to create endogenous fluorescent reporters with relative ease, and thus, Nested CRISPR was born. Most of the reagents required for Nested CRISPR are commercially available, thus facilitating its reproducibility in other labs. In fact, our methodology has been applied by many labs worldwide.

The main thrust of our lab is to model human diseases in *C. elegans*. In several instances, we have found that Cas9 alone was not sufficient for mimicking human mutations as accurately as possible in the nematode. Therefore, we began exploring the use of another commercially available protein, AsCas12a, and we found that the same conditions we use for CRISPR–Cas9 are also applicable to this nuclease.

Throughout the course of this study, we have collaborated with other groups for studying previously uncharacterized Cas proteins in *C. elegans*. These include collaborations with Dr. Virginijus Šikšnys from the Institute of Biotechnology at Vilnius University for the characterization of Cas12f1 proteins and Dr. Benjamin Kleinsteiver from the Center for Genomic Medicine at the Massachusetts General Hospital and Harvard Medical School for the characterization of near-PAMless engineered Cas9 variants. I also did a short research stay at the Andalusian Center for Developmental Biology in Seville, Spain under the guidance of Dra. Marta Artal Sanz and Dr. Miguel Angel Moreno-Mateos, who also characterized the near-PAMless Cas9 variants in parallel in zebrafish.

This work was carried out under the guidance of Dr. Julián Cerón at the *Modeling human diseases in C. elegans* group at the Bellvitge Biomedical Research Center (IDIBELL) in L'Hospitalet de Llobregat, Spain. In addition, this work has been made possible by an INPhINIT fellowship from the La Caixa Foundation (LCF/BQ/IN17/11620065) and has received funding from the European Union's Horizon 2020 research and innovation program under the Marie Skłodowska-Curie grant agreement no. 713673, as well as institutional support from the CERCA (Research Centers of Catalonia) Institute and Generalitat de Catalunya.

KEYWORDS

KEYWORDS

CRISPR

Genome editing

Caenorhabditis elegans

Genetic engineering

Cas9 variants

CRISPR

Edición genómica

Caenorhabditis elegans

Ingeniería genética

Variantes de Cas9

TABLE OF CONTENTS

LIST OF FIGURES AND TABLES

List of figures

INTRODUCTION

RESULTS I - Nested CRISPR

RESULTS IIA - Cas12 orthologs

RESULTS IIB - SpG and SpRY

DISCUSSION

List of tables

INTRODUCTION

RESULTS I - Nested CRISPR

RESULTS IIA - Cas12 orthologs

DISCUSSION

MATERIALS AND METHODS

SUPPLEMENTARY TABLES

INTRODUCTION

1. *Caenorhabditis elegans* as a model organism.

Caenorhabditis elegans is a free-living nematode with worldwide distribution and is commonly present and readily isolated from rotting fruits and flowers, which are considered its natural habitat (Kiontke et al., 2011). The reference strain Bristol or N2 was originally isolated by Sydney Brenner to study the effects of mutations on behavior and development (Brenner, 1974). Since then, *C. elegans* has been used in hundreds of laboratories as an animal model, leading to crucial discoveries in molecular and cellular biology such as RNA interference (RNAi) (Fire et al., 1998), the genetic pathway of apoptosis (Sulston et al., 1983; Sulston & Horvitz, 1977), and the use of green fluorescent protein as a biological marker (Chalfie et al., 1994).

C. elegans is small, with adult worms growing to a length of approximately 1 mm, and easily maintained on agar plates or in liquid media, with the uracil auxotrophic *Escherichia coli* OP50 as food source, at growth temperatures between 15°C and 25°C. Unlike other multicellular organisms, strains can be frozen indefinitely at -80°C or in liquid nitrogen at -196°C, making it possible to store hundreds of strains in a single laboratory (Stiernagle, 2006). In addition, thousands of mutant strains are readily available to the research community (*Caenorhabditis* Genetics Center, University of Minnesota, Minneapolis, MN)[1]. To this day, *C. elegans* is firmly established as a model organism of reference and a powerful tool for studying a wide range of biological processes (Corsi et al., 2015). This is due in great part to its genetic tractability, allowing the manipulation of gene expression with ease using a variety of transgenic methods (Nance & Frøkjær-Jensen, 2019).

[1] https://cgc.umn.edu/

The value of *C. elegans* as a model organism stems from the genetic conservation between humans and nematodes. *C. elegans* homologs have been identified for 60–80% of human genes (Kuwabara & O'Neil, 2001; Lai et al., 2000; O'Reilly et al., 2014; Sonnhammer & Durbin, 1997), and approximately 53% of genes identified in human disease have an ortholog in *C. elegans* (W. Kim et al., 2018). Thus, *C. elegans* is an attractive model for modeling human diseases, and its rapid life cycle and numerous progeny facilitates the discovery of new drug targets through massive drug screens.

A myriad of tools is available to the *C. elegans* research community including WormBase[2], the central online repository for information regarding *C. elegans* which aims to deliver an integrative view of nematode biology through extensive curation of research on *C. elegans* and other related nematodes. It combines genomic sequences and annotations with curated data from decades of experimental data regarding *C. elegans* genetics, development, physiology, behavior, and evolution (Harris et al., 2020; Howe et al., 2012). In addition, WormAtlas[3] is an online resource featuring the behavioral and structural anatomy of *C. elegans*; and finally, WormBook[4] is an in-depth, open-access collection of original, peer-reviewed material that deal with *C. elegans* biology and that of related nematodes.

[2] https://wormbase.org/

[3] https://www.wormatlas.org/

[4] http://www.wormbook.org/

1.1. *C. elegans* biology

1.1.1. Life cycle

One of the most remarkable features of *C. elegans* as a model organism is its rapid life cycle. After the eggs are laid, embryos progress through a series of rapid cell divisions during the first three hours (early-stage embryos), followed by an eight-hour period that is practically devoid of cell division (late-stage embryos) (Clejan et al., 2006a). After the embryo hatches, cell division resumes for a few hours and it develops into an L1 larva. The worm goes through a series of four larval stages (named L1 to L4) and completes development as egg-laying adults (**Figure 1**). The rate of development is directly related to temperature and takes about three days at 25°C (Corsi et al., 2015). A period of transition between each larval stage is characterized by molting during which the old cuticle is shed and exchanged for a new, stage-specific cuticle. This period is accompanied by a temporary cessation of pharyngeal pumping and inactivity or lethargy (Altun & Hall, 2009).

Worms can temporarily arrest development at the L1 stage (L1 diapause) if food is unavailable and is the basis for a protocol to synchronize worm populations. A sodium hypochlorite solution can be used to destroy the cuticle of gravid hermaphrodites to release the developing embryos, which are then grown in the absence of food. Thus, the eggs enter L1 arrest upon hatching and synchronously resume development upon feeding (Porta-de-la-Riva et al., 2012). Alternatively, under crowded conditions and starvation, the L1 can enter the stress-resistant Dauer state, in which the worms can survive for months under harsh conditions, resuming development when favorable conditions are reestablished (Jorgensen & Mango, 2002).

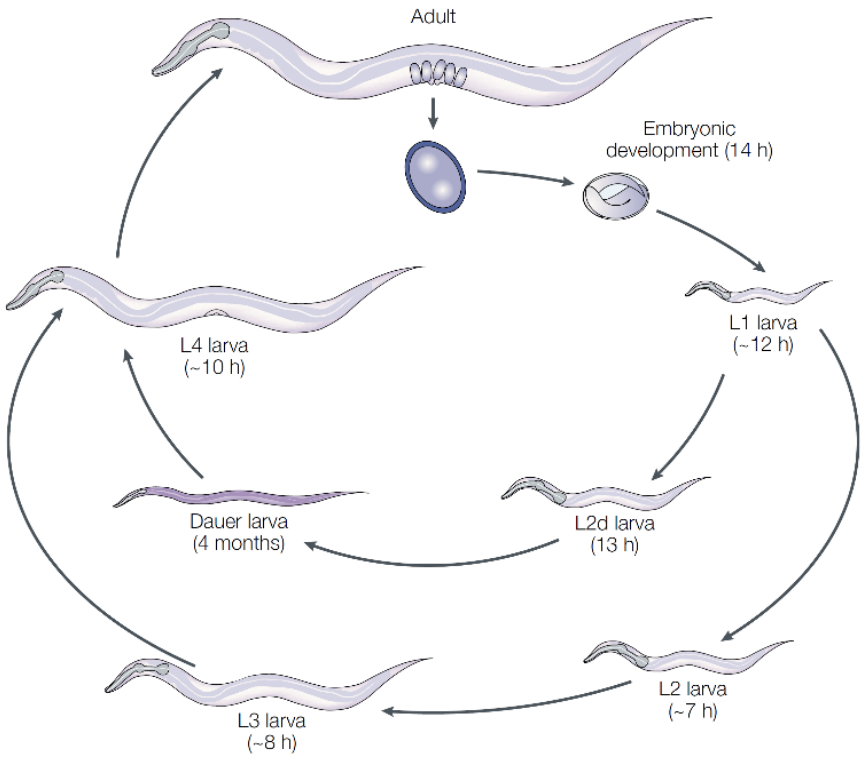

Figure 1. The life cycle of *C. elegans*. This diagram represents the various stages of *C. elegans* development from egg to adult and the approximate duration of each stage at 25°C is specified. Figure reproduced from Jorgensen & Mango, 2002.

1.1.2. Reproduction

C. elegans is a metazoan that exists in two sexual forms: self-fertilizing hermaphrodites and males (**Figure 2**). Both sexes are diploid for five autosomal chromosomes, with hermaphrodites having two X chromosomes and males having one (Hodgkin, 2005; Zarkower, 2006). Hermaphrodites possess a gonad that produces sperm during the L4 stage, then switches to oocyte production near adulthood. Hermaphrodites can give rise to approximately 300 self-progeny by using its stored sperm for fertilization. Most self-fertilized offspring are hermaphrodites, with males comprising

only 0.1 – 0.2% of offspring since nondisjunction of the X chromosome during meiosis is rare. However, hermaphrodites mated with males can produce approximately 1000 offspring, of which approximately half are males (Corsi et al., 2015). Working with self-fertilizing hermaphrodites is advantageous since homozygotes can be easily derived from heterozygotes through Mendelian segregation, whereas genetic crosses between worms of different genotypes can be facilitated by crossing males with hermaphrodites.

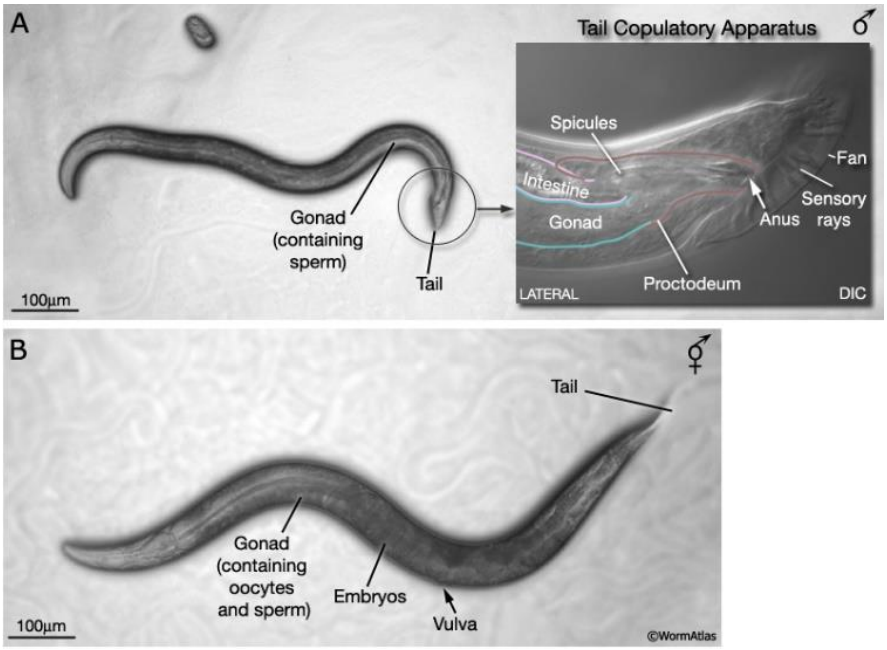

Figure 2. Sexual dimorphism in *C. elegans*. (A) Representative differential interference contrast (DIC) image of an adult male. Males can be distinguished from age-matched hermaphrodites by their slimmer bodies, clear ventral gonad, and distinctive tail. The encircled area and inset at the right demonstrate the details of the male copulatory apparatus located at the tail (lateral view). (B) Representative DIC image of an adult hermaphrodite showing its distinguishing features: the vulva, embryos, and a voluminous gonad which forms an ovotestis. Reproduced from Lints & Hall, 2009 in *WormAtlas*.

1.1.3. Development

Embryonic development occurs for about 14 hours in the egg case and is comprised of a series of stages that can be visually distinguished through Nomarski or DIC microscopy (**Figure 3**). After fertilization, the single cell embryo undergoes a series of highly stereotyped cell divisions during the first 150 minutes at 22°C. These events occur *in utero*, and the embryo is laid outside at approximately the 30-cell stage. Further cellular proliferation occurs (with certain daughter cells undergoing apoptosis) and the process of gastrulation begins. In this stage, individual cells become internalized and migrate to the center of the embryonic mass, resulting in the establishment of the three germ layers that will give rise to the different cell lineages (Hall et al., 2017). The ectoderm gives rise to the hypodermis and most of the nervous system; the mesoderm gives rise to the pharynx, coelomocytes, and muscles; and the endoderm gives rise to the intestine and germline (Sulston et al., 1983; Sulston & Horvitz, 1977).

The next phase of development is morphogenesis which overlaps with the end of gastrulation. During morphogenesis, cells join tissue subgroups and undergo terminal differentiation in line with their eventual cell fates within specialized tissue compartments. The latter part of morphogenesis then coincides with elongation, wherein the different tissues are folded inside the eggshell, and the embryo decreases in circumference and increases in length, until it is ready for hatching (Hall et al., 2017; Sulston et al., 1983).

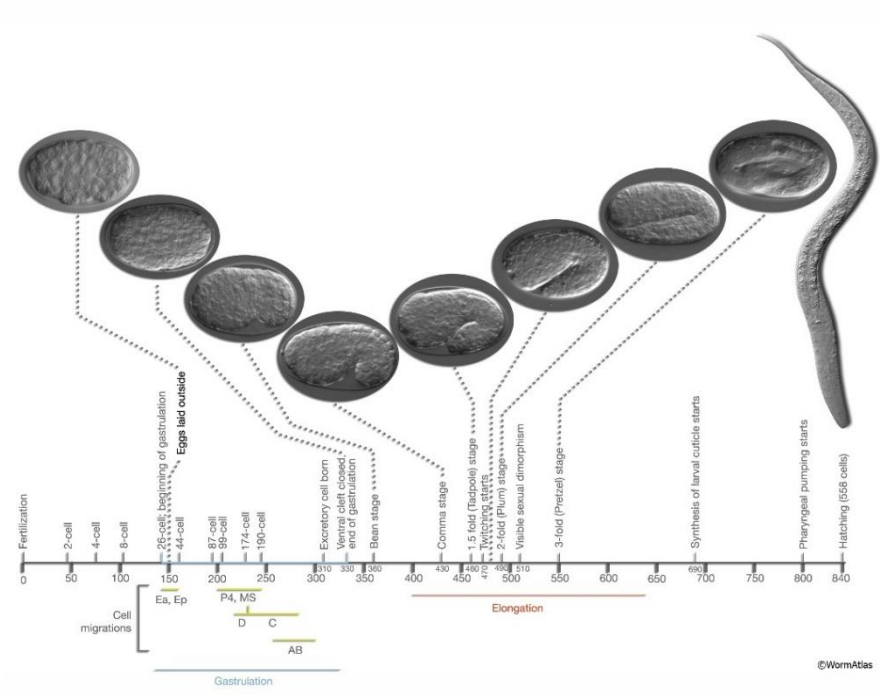

Figure 3. The stages of embryonic development in *C. elegans*. The different embryonic stages from fertilization (0 minutes) to hatching (840) minutes and marker events are arranged along a temporal horizontal axis. Marker events and representative DIC images of selected stages are shown above the axis. The duration of gastrulation, elongation, and cell migrations to their specific lineages is indicated by the blue, red, and yellow lines, respectively. Gut precursors (E), Mesoderm (MS), Germline precursors (P4), Hypodermis and neurons (AB). Reproduced from Altun & Hall, 2009 in *WormAtlas*.

C. elegans is formed by a fixed number of somatic cells and its transparency has facilitated the tracing of its invariant somatic cell lineage throughout its embryonic (Sulston et al., 1983) and post-embryonic (Sulston & Horvitz, 1977) development. After embryonic development, there are 558 somatic cells in a newly hatched L1 larva, and 55 of these cells undergo postembryonic division to reach generate 1090 somatic cells in an adult hermaphrodite (Sulston & Horvitz, 1977). These post-embryonic somatic dividing cells include epidermal seam cells, intestinal cells, migratory and

non-migratory neuroblasts, and mesoblasts (Lambie, 2002; Sulston & Horvitz, 1977). However, 131 cells undergo programmed cell death at characteristic times, and therefore, an adult hermaphrodite has 959 somatic nuclei which includes 302 neurons (Sulston et al., 1983). In contrast, males have 1031 somatic nuclei, 385 of which are neurons, with the extra neurons mostly dedicated to male mating behavior (Cook et al., 2019).

1.1.4. Germline

The adult hermaphrodite germline is composed of two tubular gonad arms exhibiting distal–proximal polarity wherein the germ cells advance from the mitotically active distal end toward the proximal end as they differentiate and progress through meiosis (Hirsh et al., 1976; Kimble & White, 1981) (**Figure 4**). The meiotic germ cells are spatiotemporally organized, with sequential phases of meiosis I prophase extending from the distal arm, around the loop into the proximal arm of the gonad, paralleled by dynamic changes in chromosome organization. Each arm contains hundreds of germ cells sharing a central core of cytoplasm known as the rachis, thus forming a syncytium with intercellular bridges connecting the germ cells to the rachis (Hubbard & Greenstein, 2005).

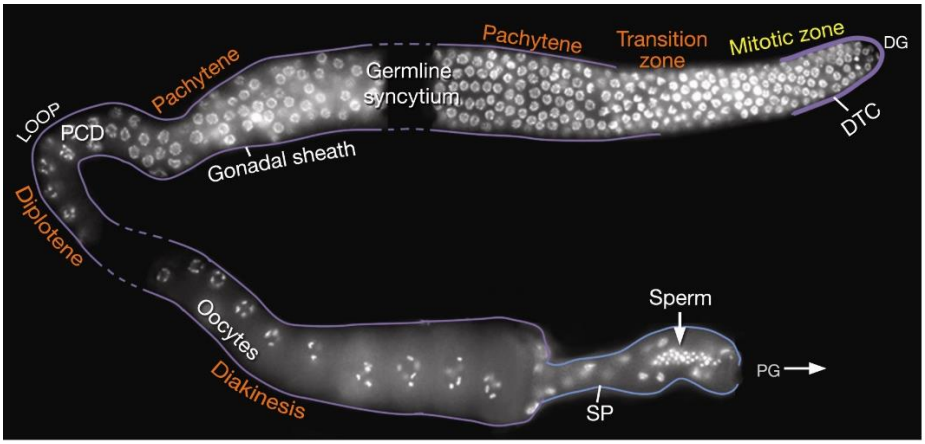

Figure 4. Distal–proximal polarity of the *C. elegans* germline. This photograph is an epifluorescent image of a dissected, DAPI-stained adult hermaphrodite gonad comprised of a montage of three individual gonad arms (dashed lines correspond to regions not covered by the individual gonad images). The different stages of meiotic prophase I are indicated by the orange text and the colored lines represent the relative positions of the somatic tissues. DG: distal gonad, DTC: distal tip cell, PCD: programmed cell death, SP: spermatheca, PG: proximal gonad. Reproduced from Lints & Hall, 2009 in *WormAtlas*.

During L4, the first ~40 germ cells to enter meiotic prophase at the most proximal end of the germline commit to sperm development, generating about 160 sperm per gonad arm. Afterwards, the germline switches from spermatogenesis to oogenesis during the remainder of development and throughout adulthood. Oocytes then proceed to ovulation and enter the spermatheca for fertilization (Hubbard & Greenstein, 2000).

1.2. The *C. elegans* genome

The *C. elegans* genome was the first metazoan genome to be completely sequenced (The *C. elegans* Sequencing Consortium, 1998) and using new sequencing technologies, subsequent efforts have been made to recomplete the genome from telomere to telomere (Hillier et al., 2005) and to include new genome regions (Yoshimura et al., 2019). The nuclear genome is comprised of five autosomes and a sex (X) chromosome (Brenner, 1974;

Nigon, 1949) that encode for approximately 20,000 protein-coding genes (The *C. elegans* Sequencing Consortium, 1998; WormBase web site, http://www.wormbase. org, release WS280, May 2021).

The median size of protein-coding genes is 1,956 bp, ranging from ~80 bp to more than 100 kbp, due to the presence of long introns (Spieth et al., 2014). Like most eukaryotic protein-coding genes, *C. elegans* genes contain exons separated by introns. The median exon size is 123 bp (Spieth et al., 2014), and is therefore, similar in size to human gene exons (131 bp) (Piovesan et al., 2019). Meanwhile, the most common size of introns is 47 bp, with a median of 65 bp (Spieth et al., 2014), which is much shorter than the median intron size in humans of 1747 bp (Piovesan et al., 2019). Just like in all other eukaryotic nuclear pre-mRNAs, the *C. elegans* splice site follows the GU-AG rule, with infrequent usage of GC in the 5' splice site (Blumenthal & Steward, 1997). There appears to be a positive correlation between intron size and local recombination rates (Prachumwat et al., 2004), and highly expressed genes preferentially contain short introns (Castillo-Davis et al., 2002).

C. elegans genes demonstrate spatial clustering, that is, the expression patterns of genes are more similar when they are in closer proximity as compared to when they are physically far apart. In addition, many genes that are expressed in the same tissue type tend to physically cluster along chromosomes (Cutter et al., 2009). Finally, chromosome centers possess greater gene density, lower recombination rates (Barnes et al., 1995), and higher operon density (Blumenthal et al., 2002). They also tend to encode more highly conserved proteins (The *C. elegans* Sequencing Consortium, 1998), and genes have stronger codon usage bias (Marais et al., 2001) and stronger effects on viability, reproduction, and other phenotypes when knocked down by RNA interference (Kamath et al., 2003; Rual et al., 2004) or mutagenic screens (Brenner, 1974; Johnsen et al., 2000).

2. Functional genetics in *C. elegans*

2.1. Mutations

One of the primary reasons Sydney Brenner adopted the nematode *Caenorhabditis elegans* as a model organism is due to its ease of genetic manipulation (Brenner, 1974). Its hermaphroditic nature allows homozygous mutations to be maintained through self-propagation without the need for mating. Coupled with its rapid life cycle, this means that mutant homozygotes can be isolated in just two generations (~1 week) after mutagenesis.

Traditionally, gene functions were characterized in *C. elegans* using forward genetics approaches, which begins with mutagenesis using chemicals or irradiation to induce random DNA lesions followed by screening of mutants with a specific phenotype. The wild-type role of the gene is then inferred from the nature of the mutant phenotype. In *C. elegans*, one of the simplest screening methods involves mutagenesis with ethyl methanesulfonate (EMS), an ethylating agent (Brenner, 1974). In addition, a variety of screening and selection methods can be used in *C. elegans* to identify mutations that lead to novel phenotypes (Jorgensen & Mango, 2002).

Over the years, genome sequencing has facilitated the identification of mutations and polymorphisms, resulting in a readily available collection of mutant strains (Doitsidou et al., 2010; Minevich et al., 2012; The *C. elegans* Deletion Mutant Consortium, 2012; Thompson et al., 2013; Zuryn et al., 2010). Moreover, the availability of the complete *C. elegans* genomic sequence has promoted the development of reverse genetics approaches, wherein gene function is elucidated by observing phenotypic effects caused by changes in the genotype. In *C. elegans*, these approaches include RNA

interference (Ravi S Kamath & Ahringer, 2003; J. Rual et al., 2004) as well as a constantly expanding toolbox for transgenesis (Nance & Frøkjær-Jensen, 2019). These approaches are further discussed below.

2.2. RNA interference

RNA interference (RNAi) is a conserved biological response to double-stranded RNA (dsRNA) that can be used to regulate the expression of protein-coding genes based on sequence-specific silencing (Hannon, 2002). This phenomenon was initially discovered in *C. elegans* when Fire and colleagues discovered that injecting dsRNA into the germline led to the depletion of endogenous messenger RNA (mRNA) transcripts upon hybridization (Fire et al., 1998). RNAi is conserved across almost all eukaryotes and has been demonstrated in *Drosophila* (Kennerdell & Carthew, 1998) and mammalian cell cultures (Caplen et al., 2001; Elbashir et al., 2001); and is known as co-suppression or post-transcriptional gene silencing (PTGS) in plants (Waterhouse et al., 1998), or quelling in fungi (Romano & Macino, 1992).

RNAi is particularly convenient in *C. elegans* because it can be performed by microinjection (Fire et al., 1998), by feeding animals with bacterial clones expressing the double-stranded RNA (dsRNA) of interest (Timmons & Fire, 1998), or by soaking (Tabara et al., 1998), and there are libraries with RNAi feeding clones targeting most *C. elegans* genes (Kamath & Ahringer, 2003; Rual et al., 2004). Furthermore, the parental animal requires exposure to only a few molecules of dsRNA per cell to trigger gene silencing in the entire animal (systemic silencing) as well as in its first-generation progeny (F_1) (Timmons & Fire, 1998). However, RNAi is not without disadvantages. First, it is subject to off-target cross reaction, that is, it can affect other genes with high sequence similarity to the target gene

(Rual et al., 2007). Second, weak RNAi effects are also frequent due to the different sensitivities of each gene to RNAi (Simmer et al., 2002). Third, different phenotypes may be observed depending on the method used (Kamath et al., 2001). And finally, some neuronal cells are refractory to RNAi treatment due to low expression levels of a dsRNA transporter required for systemic RNAi (Winston et al., 2002).

3. Transgenesis in *C. elegans*

3.1. Extrachromosomal arrays

One of the earliest methods for *C. elegans* transgenesis is by injecting a mix of genetically marked molecules that assemble into extrachromosomal arrays composed of tandem or inverted repeats, depending on the nature of the DNA molecule (plasmid vs. linear) (Mello et al., 1991; Stinchcomb et al., 1985) (**Figure 5**).

Extrachromosomal arrays form after fertilization through a combination of HR and NHEJ (Yuen et al., 2011; Zhu et al., 2018). The arrays are heritable and exhibit non-Mendelian segregation patterns (Mello et al., 1991), and often there is a random loss of extrachromosomal DNA during mitotic division, giving rise to various patterns of mosaicism (Stinchcomb et al., 1985). While the creation, maintenance, and detection of extrachromosomal arrays are facile, they are usually overexpressed, leading to toxicity; and may suffer from heterogeneous expression which do not reflect endogenous expression patterns (Mello & Fire, 1995; Nance & Frøkjær-Jensen, 2019). In addition, their repetitive nature leads to their silencing over the course of a few generations (Kelly et al., 1997). However, following a few design rules can help alleviate transgene silencing in the germline (Aljohani et al., 2020). Extrachromosomal arrays also occasional-

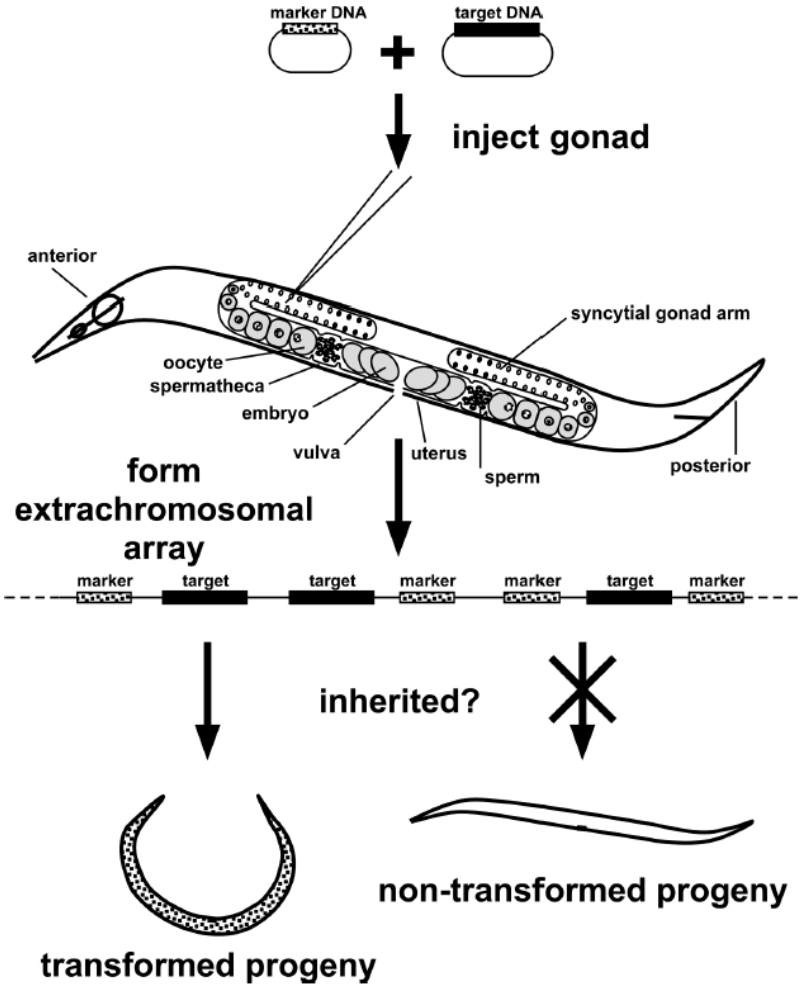

Figure 5. Transformation of *C. elegans* with extrachromosomal arrays. Plasmids containing marker and target DNA are injected into the syncytial hermaphrodite gonad. The injected DNA then forms large concatemers or extrachromosomal arrays with numerous copies of the injected DNA. Progeny that inherit the array display the marker phenotype.
Reproduced from Kadandale et al., 2009.

ly insert into the genome via homologous and nonhomologous integration (Mello & Fire, 1995) but they may also be intentionally integrated via micro-particle bombardment (Praitis et al., 2001) or through the induction of chromosomal breaks through irradiation or mutagenesis (Mariol et al., 2013; Mello & Fire, 1995). The integration of multicopy arrays prevents their loss during mitosis and meiosis and improves the homogeneity of expression (Evans, 2006).

3.2. MosSCI

The many disadvantages of multicopy arrays that limit their utility in some experiments can be overcome through the insertion of single-copy transgenes. One such method for accomplishing this is though Mos-1 mediated single copy insertion (MosSCI, **Figure 6**) (Frøkjær-Jensen et al., 2008).

MosSCI is a form of transposon-mediated transgenesis that relies on the insertion of the non-native Mos1 transposon from *Drosophila mauritana* into the *C. elegans* genome followed by its re-excision, generating a DSB (Bessereau et al., 2001). The break is then concurrently repaired with the insertion of a single-copy transgene into a “safe harbor” genomic landing site that does not cause overt mutant phenotypes nor influenced by neighboring regulatory regions. Single-copy transgenes present several advantages. They enable protein expression at near-native levels, facilitate stable transgene expression in the germline, and allow comparisons between single-copy transgenes inserted in identical genomic environments to determine structure-function relationships (Frøkjær-Jensen et al., 2008; Nance & Frøkjær-Jensen, 2019).

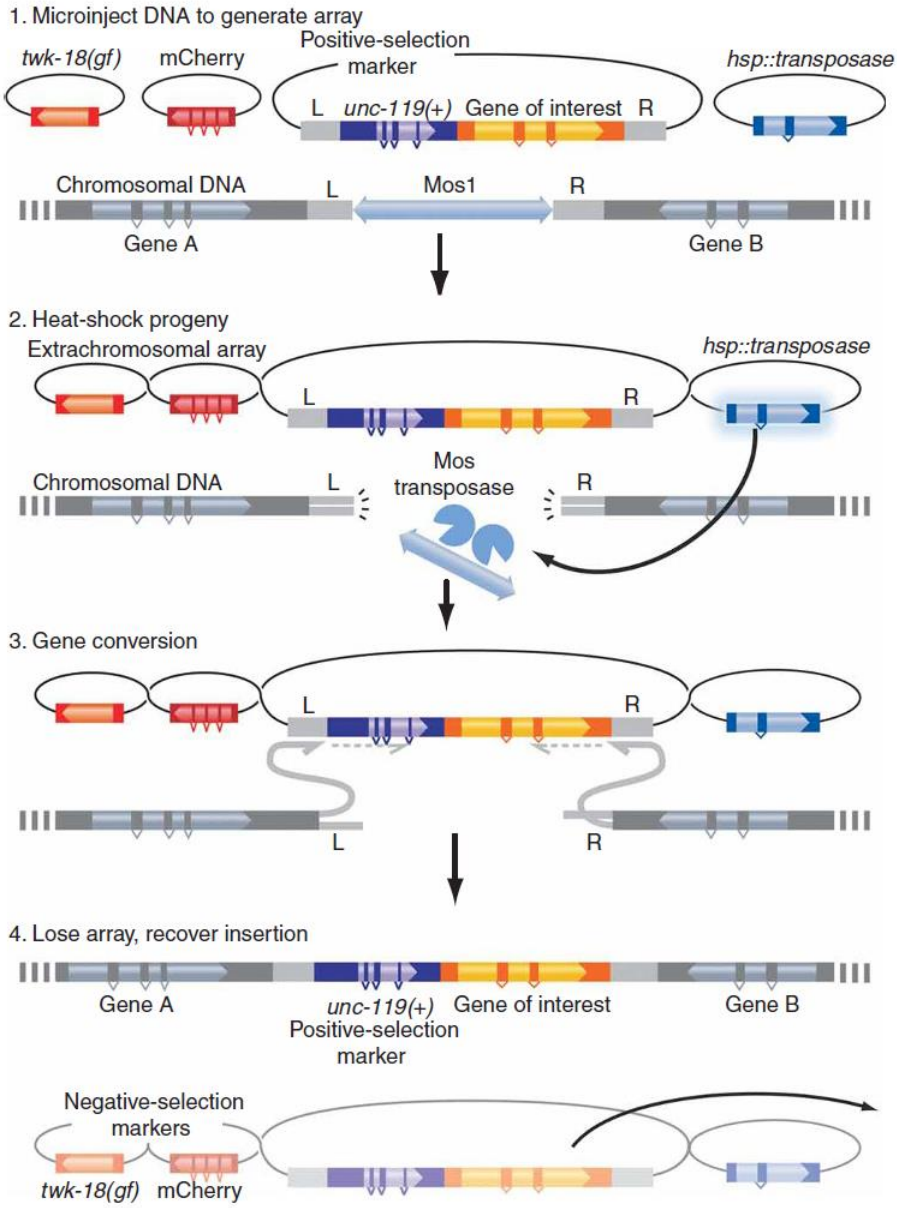

Figure 6. Single-copy transgene insertion via MosSCI. (1) *unc-119(ed3)* mutant worms with the ttTi5605 Mos1 insertion are injected with a mix consisting of several components which form an array: these include negative selection markers such as the temperature-sensitive dominant mutation *twk-18(gf)* or fluorescent mCherry, a plasmid containing an *unc-119(+)* positive selection marker and the (*continued on page 19*)

3.3. ZFNs and TALENs – The predecessors of CRISPR

Genome-editing techniques can be classified based on the mechanisms with which DNA modifications are carried out. Some of the earlier techniques include conventional genome editing systems involving homologous recombination in yeast (Orr-Weaver et al., 1981) as well as chemical modalities that utilize artificial restriction DNA cutters (ARCUT) (Komiyama, 2014). However, these techniques have fallen out of favor since the emergence of newer methods that rely on nucleases. These include homing endonuclease (HE) systems, protein-based nuclease systems such as zinc fingers (ZFNs) and transcription activator-like effector nucleases (TALENs), and the RNA-protein based system, CRISPR–Cas.

ZFNs and TALENs employ the tethering of the *Fok*I restriction endonuclease to modular DNA-binding proteins for inducing targeted double-strand breaks (DSBs) in the DNA at specific genomic loci. Both these methods have been demonstrated to be effective for genomic manipulation but suffer from the significant drawback of the need to engineer a specific protein for each dsDNA target site (Miller et al., 2011; Urnov et al., 2010; Wood et al., 2011). Meanwhile, the CRISPR–Cas9 system also induces DSBs at a target genomic locus but instead relies on

---

(*continued from Figure 6, page 18*)
gene of interest flanked by ~1.5 kbp-long left (L) and right (R) homology arms, and a heat-shock inducible transposase source (*hsp::transposase*). (2) Phenotypically rescued young adult worms with stable array transmission are heat-shocked for 1 h at 34°C, inducing transposase expression that leads to Mos1 excision and DSB generation. (3) The exposed 3' ssDNA flanks in the chromosomal DNA anneal to the homology arms in the array and the gene of interest is inserted via SDSA, repairing the break. (4) Insertion events are screened with the aid of negative-selection markers by selecting nonparalyzed, nonfluorescent worms, and the insertion is subsequently homozygosed. Reproduced from Frøkjær-Jensen et al., 2008.

the Cas9 nuclease guided by short RNA molecules through complementary base pairing with the target DNA (Garneau et al., 2010; Gasiunas et al., 2012; Jinek et al., 2012). Thus, in contrast to other genome-editing technologies based on ZFNs and TALENs, the specificity of RNA-guided endonucleases (RGENs) can be customized by constructing a specific guide RNA molecule without changing the protein component. Therefore, it is significantly easier to design with high specificity and efficiency and is well-suited for high-throughput and multiplexed gene editing for a diverse set of cell types and organisms. A comparison between ZFNs', TALENs', and CRISPR's biotechnological differences, side effect profiles, and clinical and research applications is reviewed in Khan (2019).

4. Overview of selected CRISPR–Cas systems

4.1. Discovery of CRISPR and its function

The clustered, regularly interspaced, short palindromic repeats (CRISPR)–CRISPR-associated protein (Cas) system is a defense mechanism present in many Bacteria and most Archaea that allow them to withstand viral predation and exposure to invading nucleic acids. The first clue of their existence came in 1987 when Ishino and colleagues described an unusual sequence element comprised of a series of 29-nucleotide repeats separated by unique 32-nucleotide "spacer" sequences in the *Escherichia coli* genome. Later, repetitive sequences with a similar repeat–spacer–repeat pattern were also found in the genome of the archaeon *Halofax mediterranei* (Mojica et al., 1993). However, the function of these repeats was not elucidated until many spacer sequences were linked to viral and plasmid sequences, correctly leading to the hypothesis that CRISPR is an adaptive immune system (Mojica et al., 2005; Pourcel et al., 2005).

A comprehensive description of the discovery of CRISPR in archaea and bacteria can be found in Mojica & Rodriguez-Valera, 2016.

4.2. Discovery of Cas9 and PAM

An *in silico* analysis of several prokaryotic genomes by Jansen and colleagues in 2002 confirmed the presence of four CRISPR-associated (*cas*) genes that were invariably located adjacent to a CRISPR locus, suggesting a functional relationship between the two. Based on sequence similarity with proteins of known function, they predicted that Cas3 was a helicase and that Cas4 was a RecB-like exonuclease. Conserved functional domains were not found for the Cas1 and Cas2 proteins, although it was later demonstrated that these two proteins form a stable complex required for spacer acquisition (Nuñez et al., 2014).

In 2005, two additional core *cas* genes named *cas5* and *cas6* were discovered by Bolotin et al. after performing *in silico* analysis of the *Streptococcus thermophilus* genome. The *cas5* gene belonged to a family of large proteins (>1100 aa) that contain an HNH motif, suggesting endonuclease activity. In addition, they identified a short, conserved sequence (5'-NNpu-py-A-A-a-3' — where N is A, T, C, or G; pu is any purine; and py is any pyrimidine) at a constant position relative to the protospacer, which was believed to be responsible for directing Cas5 to its target. In 2009, Mojica et al. demonstrated the apparent universality of these short sequence motifs adjacent to protospacers in other prokaryotic genomes, leading to the first usage of the term protospacer adjacent motif (PAM). An update of the CRISPR–Cas classification eventually led to the classification of the "HNH"-type or *Streptococcus*-like system as a type II system wherein the single, large effector for DNA cleavage was designated as Cas9 (Makarova et al., 2011).

4.3. The three stages of CRISPR–Cas immunity

CRISPR–Cas systems are comprised of *cas* genes organized in operons and a CRISPR array containing unique genome-targeting sequences (called spacers) interspersed with identical repeats. The acquisition of adaptive immunity through CRISPR–Cas occurs in three stages (**Figure 7**).

First, upon viral or plasmid challenges, bacteria and archaea which harbor CRISPR loci integrate short fragments of foreign sequence (protospacers) into the host chromosome at the proximal end of the CRISPR array (**adaptive phase**). These repetitive loci establish adaptive immunity by maintaining a genetic record of prior encounters with foreign invaders.

In the **crRNA biogenesis phase** (also called the expression or maturation phase), the CRISPR locus containing the spacers is expressed, generating a long primary CRISPR transcript (the pre-crRNA) that is processed via enzymatic cleavage into a library of short CRISPR RNAs (crRNAs) that each carries a sequence complementary to a previously encountered foreign nucleic acid. Each crRNA associates with tracrRNA and a Cas protein to form a surveillance ribonucleoprotein (RNP) that monitors the intracellular environment and facilitates the detection and destruction of foreign nucleic acids and targets.

Finally, the **interference phase** is initiated upon reinfection, resulting in the cleavage of the invading nucleic acid (Jinek et al., 2012; Makarova et al., 2011; Wiedenheft et al., 2012).

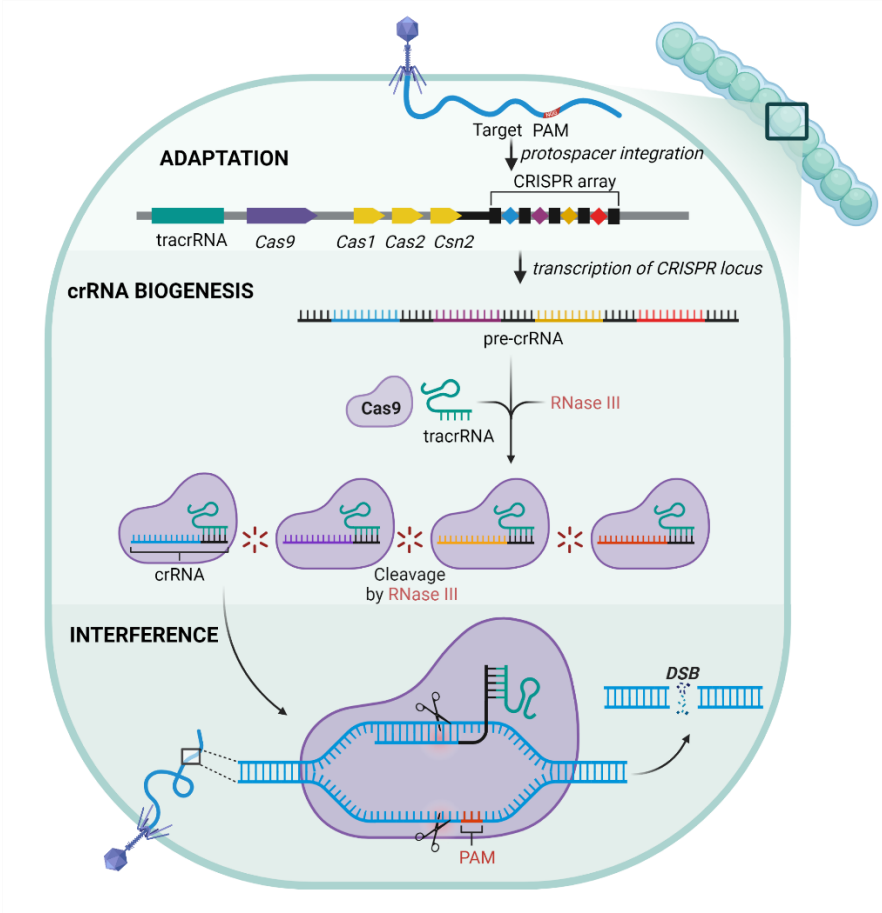

Figure 7. The three stages of CRISPR–Cas immunity in a type II system (*Streptococcus pyogenes*). The type II CRISPR–Cas loci such as that of *S. pyogenes* are comprised by an operon of four genes encoding the proteins Cas9 (purple), Cas1, Cas2, and Csn2 (yellow); a CRISPR array composed of a leader sequence followed by identical repeats (black rectangles) interspersed with unique genome-targeting spacers (colored diamonds); and a sequence encoding the trans-activating CRISPR RNA (tracrRNA). CRISPR–Cas systems act in three stages: adaptation, crRNA biogenesis, and interference. **Adaptation:** After the initial recognition step, the Cas1–Cas2 complex selects a part of the foreign DNA (protospacer) which is preferentially integrated at the leader end of the CRISPR array to form spacers (Barrangou et al., 2007; Garneau et al., 2010). In type II CRISPR–Cas systems, the selection of protospacers in invading nucleic acid depends on a protospacer-adjacent motif (PAM) (Bolotin et al., 2005). **crRNA biogenesis:** In the next stage, the CRISPR array is transcribed into a long precursor CRISPR RNA (pre-crRNA). Then, the tracrRNA pairs with the repeat (*continued on page 24*)

4.4. CRISPR–Cas Classes and Types

CRISPR–Cas systems fall under two classes. Class 1 systems are composed of multi-subunit effectors while class 2 systems are those in which the effector consists of a single, large protein (**Figure 8**).

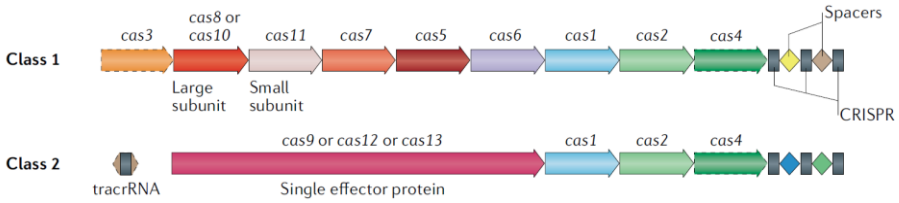

Figure 8. The generic organization of the two CRISPR–Cas systems. Class 1 systems have multiple Cas genes that form multiple effector modules that function together in binding and processing of the target. On the other hand, class 2 systems possess a single, multidomain crRNA-binding protein that carries out all the functions of the entire class 1 effector complex. Reproduced from Makarova et al., 2020.

The latest classification of CRISPR–Cas systems includes six types and 33 subtypes, divided on the basis of gene conservation and locus organization (Makarova et al., 2020). Class 1 includes types I, III, and IV whereas class 2 includes types II, V, and VI. A brief overview of the CRISPR–Cas subtypes related to this thesis (II-A, V-A, V-F, and V-U3) follows below (**Figure 9**).

(*continued from Figure 7, page 23*)
fragment of the pre-crRNA, forming a duplex, followed by cleavage within the repeats by the housekeeping endoribonuclease RNAse III in the presence of the Cas9 protein (Deltcheva et al., 2011). In this ternary complex, the tracrRNA:crRNA duplex serves as guide RNA that directs Cas9 to the cognate target DNA. **Interference:** Target recognition commences by scanning the invading DNA molecule for homology between the protospacer sequence in the target DNA and the spacer-derived sequence in the crRNA. After the RNA duplex pairs with the protospacer sequence, an R-loop is formed and Cas9 subsequently produces a double-strand break (DSB) in the DNA (Marraffini & Sontheimer, 2008; Semenova et al., 2011). Created with BioRender.com.

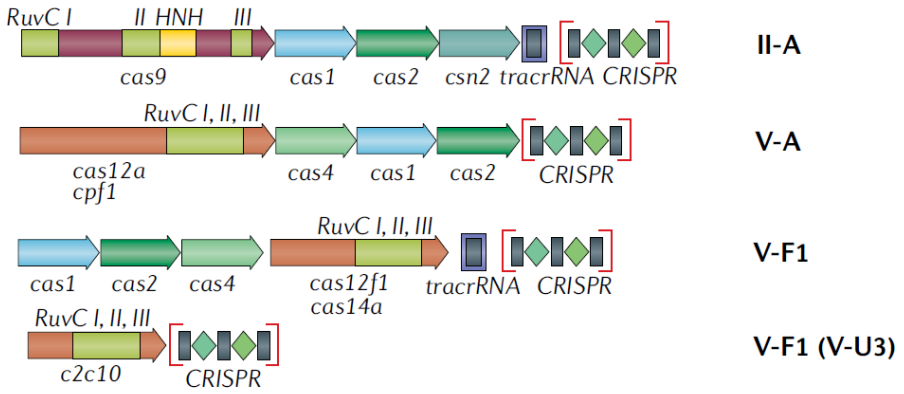

Figure 9. Representative architectural organization of selected class 2 subtypes. The representative type II-A, V-A, V-F1, and V-U3 CRISPR–*cas* loci are based on the organisms *Streptococcus thermophilus*, *Francisella cf. novicida Fx1*, *Uncultured archaeon*, and *Bacillus thuringiensis*, respectively. Homologous genes are color coded and are designated by a family name according to the classification in Makarova et al., 2015. If a gene is commonly known by both a systematic name and a legacy name, the legacy name is given under the systematic name. CRISPR–Cas systems with Cas12a and C2c10 do not require tracrRNA. The RuvC-like nuclease domain is shown in yellow, and the HNH nuclease domain, in green. The elements of the CRISPR array (rectangles – CRISPR repeats, and diamonds – spacers) are enclosed in red brackets.
Adapted from Makarova et al., 2020.

4.4.1. Type II-A

Type II CRISPR–Cas systems are the simplest in terms of gene number, with *cas9* as the signature gene. In addition, all type II systems contain *cas1* and *cas2*, and most loci also encode a tracrRNA (Makarova et al., 2015). Subtype II-A systems are characterized by an additional gene, *csn2*, which is the hallmark of this subtype. The Csn2 protein plays a role in spacer integration but is not necessary for interference (Barrangou et al., 2007; Garneau et al., 2010). The effector for type II systems, Cas9, has two nuclease domains — an HNH domain inserted within the tri-split RuvC-

like domain, that cleave the complementary and non-complementary strands of the target DNA, respectively (Jinek et al., 2012). In addition to target cleavage, Cas9 also contributes to adaptation as it contains a PAM recognition motif which facilitates the selection of functional spacers (Heler et al., 2015; Wei et al., 2015).

Cas9 produces blunt double-stranded breaks (DSBs) at sites defined by a 20-nucleotide guide sequence contained within an associated crRNA transcript. The DSB occurs at three base pairs upstream of the PAM (Garneau et al., 2010). The work of Jinek et al. (2012) in *S. pyogenes* and Gasiunas et al. (2012) in *S. thermophilus* have demonstrated that the Cas9 protein cleaves double-stranded DNA (dsDNA) that bears a protospacer sequence complementary to a mature crRNA in a PAM-dependent manner. Moreover, crRNA alone is insufficient for Cas9-catalyzed DNA cleavage and requires the presence of tracrRNA, which performs complementary base pairing with the repeat sequence of crRNA. On the other hand, the cleavage of single-stranded DNA (ssDNA) by Cas9 is PAM-independent. Therefore, the Cas9–crRNA:tracrRNA RNP complex functions as a guided endonuclease that relies on RNA for target site recognition and Cas9 for DNA cleavage. In addition, it has been demonstrated that the crRNA:tracrRNA complex can be redesigned as a single transcript called the single-guide RNA (sgRNA) that maintains the essential features for both Cas9 binding and DNA target site recognition (Jinek et al., 2012, 2013).

4.4.1.1. Near-PAMless variants

While Cas9 is versatile and has many biotechnological applications, its main limitation is the requirement for a PAM sequence. In the case of the most widely used variant, *S. pyogenes* Cas9 (SpCas9), an NGG motif must immediately follow the sequence specified by the crRNA or sgRNA (F. Jiang et al., 2015; Jinek et al., 2012; Sternberg et al., 2014). Targeting can be expanded by using other naturally occurring Cas orthologs with divergent noncanonical PAMs (Gasiunas et al., 2020) such as SaCas9 (*Staphylococcus aureus*) with an NGGRRT PAM (Ran et al., 2015), or NmCas9 (*Neisseria meningitidis*) with an NNNNGATT PAM (Yan Zhang et al., 2013). However, their longer PAMs make them even more limiting than SpCas9. In addition, despite the relatively wide targeting range of SpCas9, the NGG PAM requirement is still an obstacle for applications requiring high-resolution target site positioning such as base editing and homology-directed repair. To overcome this limitation, nuclease variants have been purposely engineered to relax the PAM requirement. Some examples of structurally engineered Cas9 variants are listed in **Table 1**.

In this study, we investigate the use of the near-PAMless variants SpG and SpRY via RNP delivery. These variants were created by Walton et al., (2020) through structure-guided mutagenesis of SpCas9. The recognition of the optimal NGG PAM by SpCas9 relies on the interaction between the guanine DNA bases and the amino acid side chains of R1333 and R1335.

Table 1. Structurally engineered Cas9 variants with altered PAM requirements.

Variant	PAM (5'-3')	Reference
SpCas9 VQR (*S. pyogenes*)	NGAN	Kleinstiver et al., 2015
SpCas9 VRER (*S. pyogenes*)	NGCG	Kleinstiver et al., 2015
SpCas9 VRQR (*S. pyogenes*)	NGA>NGNG[4]	Kleinstiver et al., 2016
RHA FnCas9[1] (*Francisella novicida*)	YG	Hirano et al., 2016
xCas9 *(S. pyogenes)*	NG, GAA, GAT	Hu et al., 2018
SpCas9-NG (*S. pyogenes*)	NG	Nishimasu et al., 2018
iSpyMac (*S. pyogenes/ S. macacae* hybrid)[2]	NAAN	Chatterjee, Lee, et al., 2020
Cas9–Sc^{++} (*S. canis*)[3]	NNG	Chatterjee, Jakimo, et al., 2020
SpG (*S. pyogenes*)	NGN	Walton et al., 2020
SpRY (*S. pyogenes*)	NRN>NYN[4]	Walton et al., 2020

[1] The natural PAM of FnCas9 is 5'-NGG-3'.

[2] iSpyMac is produced by grafting the SmacCas9 PAM-interacting domain with a natural 5'-NAAN-3' PAM into a truncated SpCas9.

[3] Cas9–Sc^{++} is the structurally engineered variant of ScCas9 which also has an NNG PAM.

[4] > indicates preferential targeting. R = A or G and Y = C or T.

However, the modification of either arginine residue substantially diminishes nuclease activity against NGG PAMs while the modification of both abolishes activity (Anders et al., 2014; Kleinstiver et al., 2015). Therefore, together with changes to R1333 or R1335, other residues in the PAM-interacting (PI) domain must also be altered to retain SpCas9 function while also altering PAM preference. Using SpCas9 VRQR which demonstrates a more relaxed PAM preference of NGA > NGNG as a scaffold, Walton and colleagues (2020) introduced additional substitutions to further relax PAM preferences (**Figure 10**). In the case of the SpG variant which recognizes NGN PAMs, six structure-motivated substitutions are introduced: D1135L/S1136W/G1218K/E1219Q/R1335Q/ T1337R. This variant exhibits even tolerance across NGAT, NGCC, NGGG, and NGTA PAMs based on a high-throughput PAM determination assay (HT-PAMDA) and displays high average activity across the four sites in human cells.

Finally, the additional substitution of R1333 in the SpG variant further relaxes the PAM preference by altering the recognition of the second position of the PAM, specifically through the formation of a base-specific contact with adenine. However, as this substitution alone abolished activity in human cells harboring NRN PAMs (where R is A or G), additional substitutions were necessary to rescue activity through the formation of novel nonspecific DNA contacts. This additional set of 5 substitutions over the SpG derivative: A61R/L1111R/N1317R/A1322R/R1333P — led to the SpRY variant which is capable of targeting NRN > NYN PAMs (where Y is C or T) (Walton et al., 2020).

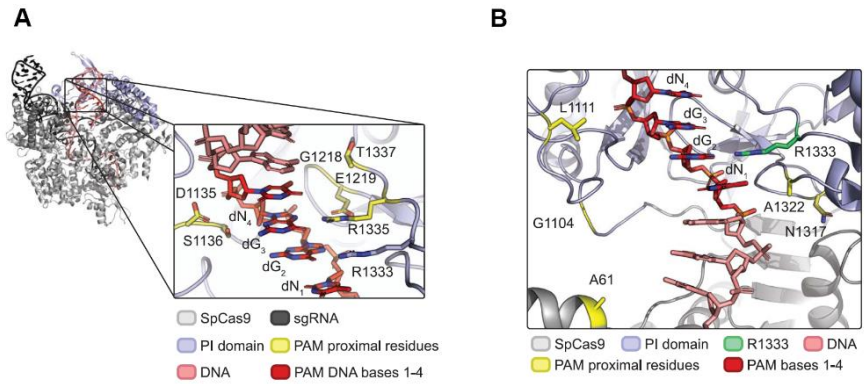

Figure 10. Rendering of crystal structure of SpCas9 showing the substituted residues in the SpG (A) and SpRY (B) variants. PAM recognition by SpCas9 occurs through bidentate hydrogen bonds between R1333 and R1335 in the PI domain and dG_2 and dG_3 of the NGG PAM, respectively. Modification of either arginine to alter PAM recognition in the 2nd or 3rd position abolishes nuclease activity, thus requiring additional substitutions to rescue activity. (A) In the case of SpG, R1335Q alters the 3rd PAM position preference, D1135L and S1136W compensate for the shortened sidechain length of R1335Q through displacement of the PAM DNA bases, G1218R forms non-specific DNA contacts that interact with the PAM DNA phosphate backbone, E1219Q supports alternative conformations of R1335Q, and T1337R stabilizes PAM DNA binding and contributes to DNA displacement towards R1335Q. (B) In the case of SpRY, R1333P enables access to sites bearing NAN PAMs via base-specific contact with adenine, L1111R and A1322R form nonspecific DNA contacts that compensate for the loss of activity due to R1333 substitution, and A61R and N1317R increase activity by forming novel nonspecific DNA contacts. Adapted from Walton et al., 2020.

4.4.2. Type V-A

The main difference of type V systems from type II systems lies in the domain architecture of their effector proteins. As previously mentioned, type II effectors contain two nuclease domains (HNH and Ruv-C) which are each responsible for the cleavage of one strand of target DNA. On the other hand, type V effectors only possess a RuvC-like domain that cleaves both strands (**Figure 9**). In addition, DNA cleavage in type V systems results in a 5-nt 5' overhang instead of blunt ends generated by Cas9 (**Figure 11**). The PAM of type V effectors is generally T-rich instead of G-rich as in Cas9, and is located at the 5' end of the protospacer instead of the 3' end (Zetsche et al., 2015). Some examples of commonly used type V effectors, their respective PAMs, and descriptions of their DSBs are listed in **Table 2**.

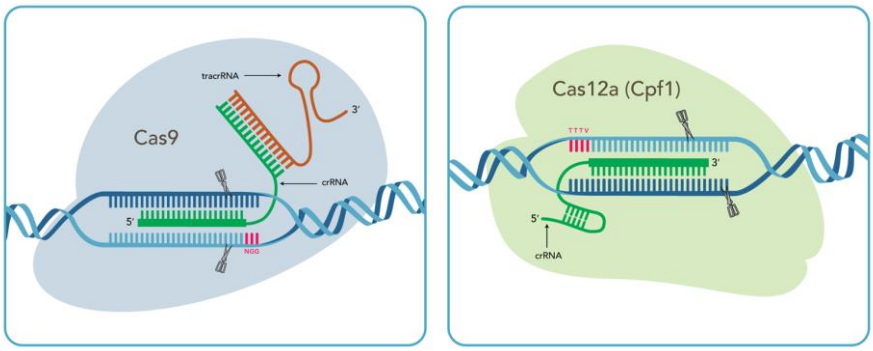

Figure 11. Key Differences between Cas9 and Cas12a (Cpf1). Diagrams of RNP assemblies consisting of Cas9 and Cas12a are shown on the left and right, respectively. Cas9, the effector for type II systems, requires tracrRNA for DNA interference. This crRNA:tracrRNA duplex may be substituted with a single guide RNA (sgRNA) instead. Cas9 recognizes an NGG PAM immediately following the 3' end of the protospacer on the NTS, and produces a blunt DSB 3 bp upstream of the PAM. Meanwhile, Cas12a, the effector for subtype V-A systems, only requires crRNA, and not tracrRNA, for DNA cleavage. It recognizes a TTTV PAM immediately preceding the 5' end of the protospacer on the NTS and generates a staggered DSB with 5' overhangs. Reproduced from IDT (n.d.)

Table 2. Examples of commonly used type V effectors

Nuclease (source organism)	**PAM (5'-3')[1]**	**DSB[2]**	**Reference**
FnCas12a (*Francisella novicida U112*)	TTV	18th base on the + strand and 23rd base on the – strand	Zetsche et al., 2015
AsCas12a (*Acidaminococcus sp. BV3L6*)	TTTV	19th base on the + strand and 23rd base on the – strand	Kim et al., 2017; Zetsche et al., 2015
LbCas12a (*Lachnospiraceae bacterium ND2006*)	TTTV	19th base on the + strand and 23rd base on the – strand	Kim et al., 2017; Zetsche et al., 2015

[1] Where V is A, G, or C

[2] + strand: non-target strand (NTS), – strand: target strand (TS)

In addition to the general characteristics of type V systems described above, subtype V-A systems do not require tracrRNA for DNA interference (Zetsche et al., 2015), and the effector (Cas12a) is also responsible for pre-crRNA processing RNAse activity (East-Seletsky et al., 2016; Fonfara et al., 2016; L. Liu et al., 2017), in contrast to type II and other type V subtypes where this role is fulfilled by a non-Cas enzyme, RNAse III.

4.4.3. Types V-F and V-U3 (miniature nucleases)

As with type V-A systems, type V-F also encodes an adaptation module comprised of the Cas1, Cas2, and Cas4 proteins. On the other hand, type V-U3 lack the proteins involved in adaptation (Koonin et al., 2017; Shmakov et al., 2017). However, the principal feature of the Cas12f1 effectors of the type V-F and V-U3 systems is that they can be two or three times smaller than Cas9 or Cas12 proteins (Harrington et al., 2018; Koonin

et al., 2017; Makarova et al., 2020; Shmakov et al., 2017). Whereas Cas9 proteins can range from 950 to 1700 AARs (amino acid residues) and Cas12a from 750 to 1500 AARs, Cas12f1 proteins are only 400 to 700 AARs long. This size difference is mostly due to the significant length reduction in the N-terminal half of Cas12f1 proteins when compared to other Cas12 orthologs (Karvelis et al., 2020). Due to their small size, Cas12f1 effectors are being developed for their potential use in therapeutics since the size of Cas9 and Cas12 orthologs pose a challenge to cellular delivery (Lino et al., 2018). The Cas12f1 effectors examined in this study are listed in **Table 3**.

Table 3. List of Cas12f1 effectors tested in this thesis

Nuclease	**Type**	**PAM (5'-3')**	**Size (AARs)**	**Reference**
Un1Cas12f1 (*Uncultured archaeon*)	V-F	TTTR	529	Karvelis et al., 2020
AsCas12f1 (*Acidibacillus sulfuroxidans*)	V-U3	YTTN	422	Karvelis et al., 2020
SpCas12f1 (*Syntrophomonas palmitatica*)	V-U3	TTC	497	Karvelis et al., 2020

4.5. Cas derivatives

In addition to the typical cut-and-paste application of CRISPR–Cas systems, a number of Cas proteins have been engineered with unique features that permit distinct gene editing approaches. Since Cas9 has two endonuclease domains, a mutation in either domain ($RuvC^{D10A}$ or HNH^{H840A}) will abolish activity only in that domain while retaining activity

in the other, thereby producing a DNA nick instead of a DSB (Ran et al., 2013). Since both nickases are required to produce a DSB by targeting opposing strands of the DNA, this double nicking strategy can enhance the specificity of genome editing (Ran et al., 2013; B. Shen et al., 2014). Furthermore, mutations in both endonuclease domains of Cas9 or in the single RuvC domain of Cas12a completely abolishes activity, thus transforming them into dead nuclease variants designated as dCas9 (Qi et al., 2013) and dCas12a (X. Zhang et al., 2017).

Specific applications for dCas proteins can be achieved by fusing them to effector domains which perform additional functions. For instance, dCas proteins can be used to modulate gene expression by coupling them to transcriptional activators (CRISPRa) (Cheng et al., 2013; Konermann et al., 2015) or transcriptional repressors (CRISPRi) (Gilbert et al., 2013; Qi et al., 2013). In addition, the conjugation of dCas9 to deaminase enzymes has led to the development of cytosine base editors (CBE) (Komor et al., 2016) and adenine base editors (ABE) (Gaudelli et al., 2017). These base editing systems enable the direct and irreversible conversion of a target base in the DNA into a different one without inducing DSBs, and thus are viewed as a safer alternative to CRISPR–Cas9. However, base editors can only produce a limited range of base changes, an issue that can be addressed by prime editing. Prime editors utilize an RNA template with the desired genomic change that is integrated into genomic DNA by a Cas9 nickase-guided reverse transcriptase enzyme (Anzalone et al., 2019). Finally, the fusion of dCas9 to transposase enzymes is being studied for the active insertion of large payloads in the genome, with potential therapeutic applications and genetic modification of clinically relevant cell types (Goshayeshi et al., 2021).

5. CRISPR–Cas methodologies in *C. elegans*

The advent of CRISPR–Cas technology and demonstration of its applicability in worms has led to it being favored over single-copy transgenic approaches such as MosSCI. In addition, CRISPR–Cas9 has the added advantage of editing genes at their endogenous loci, therefore preserving important regulatory information present in enhancers, gene structure, or genomic location (Nance & Frøkjær-Jensen, 2019). The use of CRISPR–Cas9 in worms is comprehensively reviewed in the WormBook chapters by Dickinson & Goldstein (2016) and by Nance & Frøkjær-Jensen (2019).

Several methods exist for performing CRISPR–Cas transgenesis in *C. elegans* and they differ based on how the components (crRNA, tracrRNA, and Cas nuclease) are expressed in the gonad. These components can be expressed from mRNA (Chiu et al., 2013; Katic & Großhans, 2013; Lo et al., 2013), plasmids that express Cas9 and sgRNA (Dickinson et al., 2013; Friedland et al., 2013; Frokjaer-Jensen, 2013; Waaijers et al., 2013), or added as commercially available independent molecules that form ribonucleoprotein complexes (RNPs) (Cho et al., 2013; Paix et al., 2015). However, regardless of the expression system chosen, all components must be delivered to the *C. elegans* germline via microinjection (**Figure 12**). Due to the hermaphroditic nature of these nematodes coupled with their fast life cycle, homozygous lines can be isolated in as quick as 10 days from the time of injection, without the need for genetic crosses.

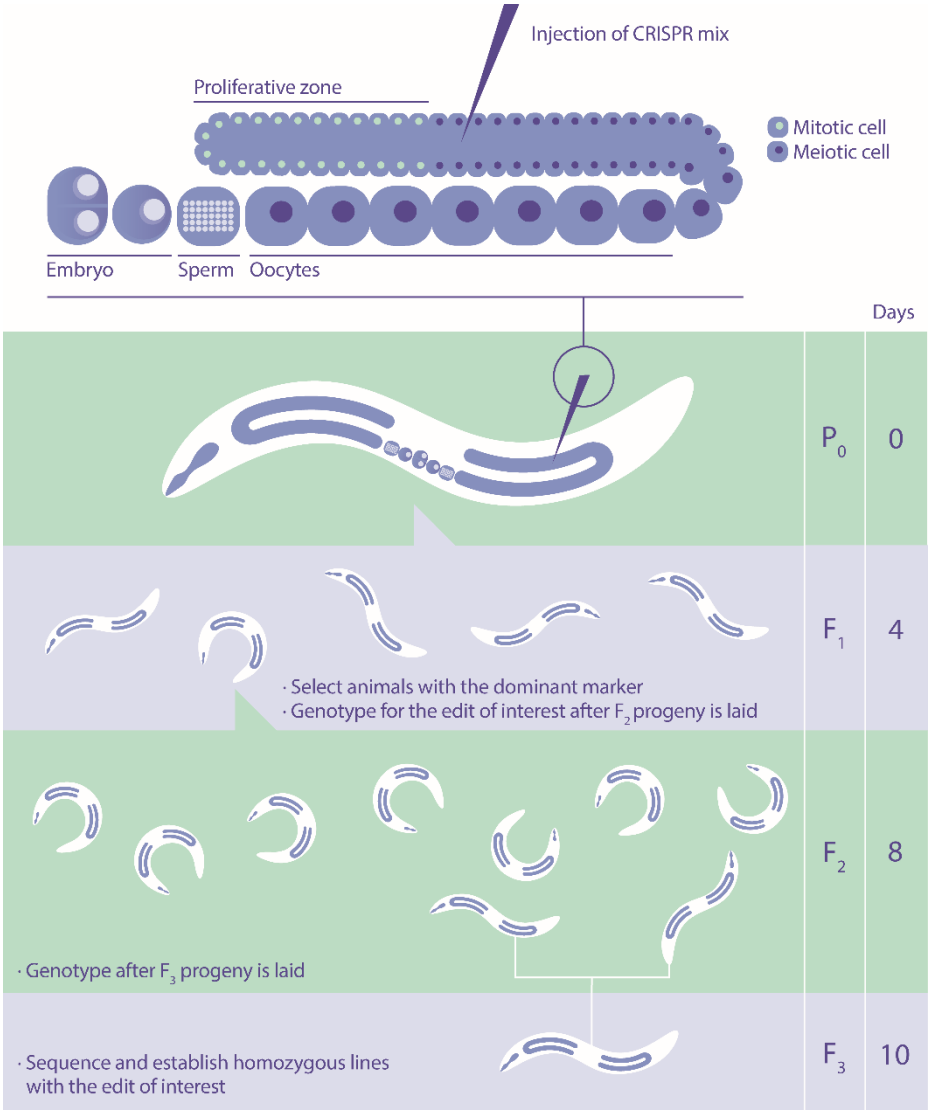

Figure 12. Schematic of CRISPR–Cas genome editing in *C. elegans*. CRISPR reagents are injected in the germline of an adult hermaphrodite which contains hundreds of mitotic and meiotic cells sharing a common cytoplasm (syncytium). F_1 animals displaying the dominant mutation (marker) are separated, allowed to lay eggs, and then genotyped to find the edit of interest. F_2 animals with the edit of interest are allowed to lay F_3 progeny and then genotyped and sequenced to establish a strain harboring the edit in homozygosis. Reproduced from Vicencio & Cerón, 2021.

5.1. Selection of edited genomes

Choosing an important selection strategy is important not only to control injection quality, but also to obtain a population enriched in edited animals, thus reducing the screening load. Such a population could be obtained by using a plasmid carrying a fluorescent marker, an antibiotic resistant gene, or a dominant allele, which is transiently expressed in the F_1 generation (H. Kim et al., 2014; Norris et al., 2015; Prior et al., 2017; Waaijers et al., 2013; P. Zhao et al., 2014). A popular marker is the pRF4 plasmid that expresses the dominant allele *rol-6(su1006)*, causing animals to corkscrew around in circles that are easily spotted under a dissecting microscope (Kramer et al., 1990; Mello et al., 1991). In this strategy, the markers serve as indicators of efficient microinjections and competent loading of the injection mix in the nuclei and are therefore referred to as co-injection markers.

For HDR-mediated editing, an effective strategy is co-CRISPR, where a marker locus is simultaneously edited. The edited marker locus results in a visible dominant phenotype that is used to enrich for edits at the target locus (**Table 4**).

Thus, in addition to indicating successful uptake of the RNP payload, these co-CRISPR strategies also serve as indicators of nuclease activity. Alternatively, edited animals can be selected by knock-in of genes providing antibiotic resistance, which are later removed by the Cre–Lox recombination system, leaving just the insertion of interest in the genome (Dickinson et al., 2015; Norris et al., 2015).

Table 4. List of selected co-CRISPR strategies.

Locus (allele)	**Description of strategy**	**Reference**
dpy-10 (*cn64*)	Produces the Rol (roller) phenotype causing animals to move in a circular instead of a sinusoidal pattern	Arribere et al., 2014; H. Kim et al., 2014
pha-1 (*e2123*) *zen-4* (*cle10ts*)	Rescue of temperature-sensitive mutants that are viable at 15°C but not at 25°C	Farboud et al., 2019; Ward, 2015
unc-119 (*ed3*)	Rescue of the Unc (uncoordinated) phenotype characterized by short morphology and curled appearance	Schwartz & Jorgensen, 2016; D. Zhang & Glotzer, 2014
ben-1	Confers benzimidazole resistance allowing drug selection-based rescue of benzimidazole-induced Unc and Dpy (dumpy) phenotypes	Farboud et al., 2019
NF-GFP (non-fluorescent GFP)	Correction of the NF-GFP sequence to produce functional GFP	D. Zhang & Glotzer, 2014

5.2. Guide RNA considerations

A number of important factors can influence crRNA (or sgRNA) choice: the distance of the desired edit from the cut site, its predicted efficiency, and potential off targets. Since crRNA choice is limited by the PAM requirement (NGG in the case of Cas9), the DSB produced will frequently lie a few base pairs away from the desired edit site. It has been demonstrated that there is an inverse relationship between a mutation's incorporation rate and its distance to the cleavage site (Farboud et al., 2019; Paix et al., 2017; Paquet et al., 2016). While minimizing the cut-to-edit distance improves precise repair via HDR, the closest gRNA does not always ensure maximal results if it has poor inherent genomic cleavage efficiency (X. Liang et al., 2017).

Several tools are available online for selecting the most efficient gRNAs based on various algorithms (Labun et al., 2019; Moreno-Mateos et al., 2015; Stemmer et al., 2015). These algorithms provide scores based on the experimental quantitation of the target efficiencies of hundreds of gRNAs. For instance, the CRISPRater score used in the CCTop[10] online target predictor takes into consideration the PAM-distal GC-content as well as an additional set of nine predictive features as criteria for predicting gRNA activity (Labuhn et al., 2018). However, as these algorithms are based on the verification of gRNA activity in mammalian cells (Doench et al., 2016; Labuhn et al., 2018) or *in vivo* using zebrafish (Moreno-Mateos et al., 2015), caution must be exercised when using these algorithms for predicting gRNA activity in *C. elegans*.

5.3. Repair template considerations

Choosing the appropriate type of repair template depends on the type of mutagenesis desired and the distance of the DSB to the edit site (Dickinson & Goldstein, 2016). Generally, point mutations and short insertions of less than 140 bp long benefit from the use of a single-stranded repair template such as ssODNs. Farboud et al., (2019) demonstrated that HDR was less efficient when using dsDNA repair templates compared to ssDNA when there is only a single DSB. In addition, the orientation of the ssDNA repair template appears to influence editing efficiencies (Farboud et al., 2019; Katic et al., 2015; Paix et al., 2017; Ward, 2015).

The use of ssODNs as repair templates is very convenient since they can be rapidly synthesized by commercial providers. However, the price of synthesis significantly increases past the length of 200 nucleotides, in which case, long ssDNA fragments called megamers need to be used. Therefore, for longer insertions, dsDNA repair templates either in the form of a PCR product or a plasmid can be used. PCR products with short homology arms of ~35 bp can direct the efficient insertion of long sequences (e.g., GFP; ~850 bp) (Paix et al., 2014, 2015). However, the editing efficiencies using this technique has been challenged by other groups (Dokshin et al., 2018; Vicencio et al., 2019).

In addition, the use of linear repair templates facilitates *recombineering* (the use of overlapping PCR and/or ssODN fragments) to generate long insertions by taking advantage of the SDSA pathway for templated repair (Paix et al., 2016). However, editing efficiencies using linear repair templates with short homology arms is restricted by the cut-to-edit distance. In general, editing efficiencies drop when this distance is greater than 10 bp (Arribere et al., 2014; Farboud et al., 2019; Paix et al., 2014, 2015, 2016; 2017). In addition, recoding of homologous sequences between the DSB

and the edit site is recommended to prevent recutting by Cas9 as well as premature template switching that hinders the copying of inserts at a distance from the DSB (Paix et al., 2016).

6. DSB repair mechanisms

Eukaryotic cells employ overlapping repair pathways to repair DSBs and genome editing technologies exploit these pathways to introduce permanent genetic changes. These different pathways result in distinct outcomes, and thus, the ability to favor a specific pathway is paramount to achieving the desired genomic alteration. The different DSB repair mechanisms in the context of CRISPR-Cas genome editing are extensively reviewed in Yeh et al., 2019 and Xue & Greene, 2021. However, a brief overview of each repair pathway in the context of *C. elegans* genome editing follows below.

Generally speaking, DSBs are reversed through two major pathways: re-ligation of the broken ends through end-joining pathways such as non-homologous end joining (NHEJ) or alternative end joining (alt-EJ) that lead to insertions and deletions (indels), or precise repair in the presence of a separate donor DNA molecule (template) through homology-directed repair (HDR) (**Figure 13**) (Ranjha et al., 2018; H. Yang et al., 2020).

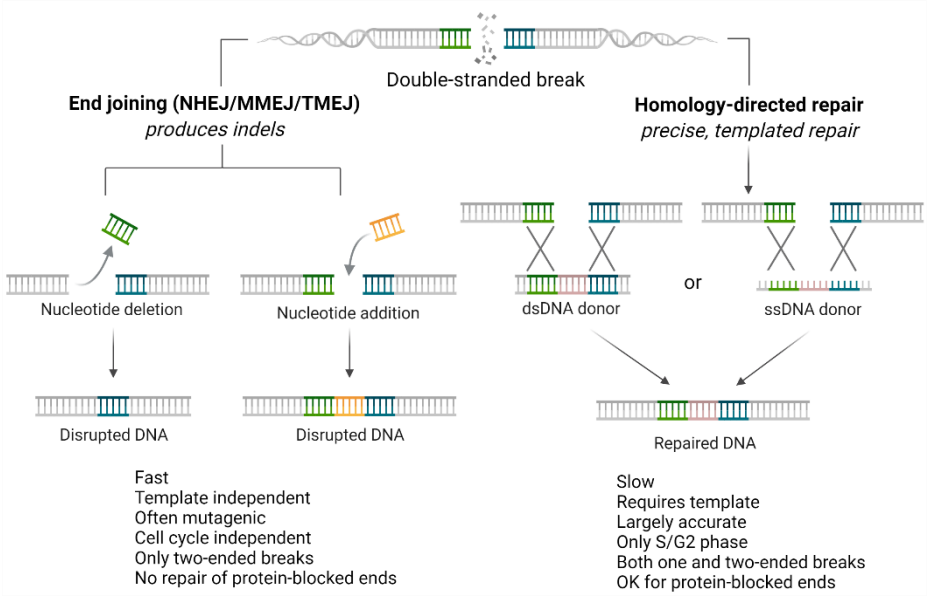

Figure 13. The two major DSB repair pathways, their repair outcomes, and key features. In the absence of a repair template, the end joining pathways (NHEJ, MMEJ, or TMEJ) seal DSBs with little or no homology, leading to random gene editing outcomes (insertions or deletions [indels] at the cleavage site). In contrast, when exogenous DNA molecules are provided in the form of dsDNA or ssDNA, these are utilized by the HDR pathway as a template for repair and produces a precise gene editing outcome. Key features adapted from Ranjha et al., 2018. Figure made with BioRender.com.

6.1. Nonhomologous end joining (NHEJ)

NHEJ is the primary DSB repair pathway in mammalian cells throughout all stages of the cell cycle (excluding mitosis). It is a fast but inaccurate form of repair involving the direct ligation of two DSB ends with little or no sequence homology required, often leading to mutagenesis (Chang et al., 2017; Lieber, 2010). After DSB formation, NHEJ begins with the binding of Ku70-Ku80 heterodimer (Ku) (CKU-70 and CKU-80 in *C. elegans*) to blunt or near-blunt DNA ends, forming a ring that encircles the duplex DNA (Gottlieb & Jackson, 1993; Ramsden & Geliert, 1998). This process

protects the blunt DNA ends, inhibiting end resection and preventing MMEJ and HDR (Mimitou & Symington, 2010; Shim et al., 2010; S. H. Yang et al., 2013). While Ku recruits and activates more than a dozen factors in vertebrates, the entire known NHEJ mechanism in *C. elegans* consists of only three core components: CKU-70, CKU-80, and LIG-4 (Clejan et al., 2006a); and one accessory factor: NHJ-1 (Vujin et al., 2020). This mode of end joining is more specifically referred to as classical-NHEJ (c-NHEJ) to contrast it from other forms of end-joining (alt-EJ) that lack one or more c-NHEJ components (Chang et al., 2017; Ochi et al., 2014).

In *C. elegans*, NHEJ is restricted to, and is the major pathway in non-dividing somatic cells, playing little to no role in the repair of DSBs in the germline. (Clejan et al., 2006a). In addition, it has been demonstrated in *C. elegans* that NHEJ is actively suppressed in the germline to prevent error-prone repair by channeling meiotic DSBs into homologous recombination (HR) instead of NHEJ (Adamo et al., 2010; Lemmens et al., 2013; Martin et al., 2005; Smolikov et al., 2007), ensuring stable genome transmission from one generation to the next.

6.2. Polymerase theta-mediated end joining (TMEJ)

Polymerase theta-mediated end joining refers to an error-prone pathway for DSB repair that requires DNA polymerase theta (Pol θ) that operates independently of both Rad51-mediated HR and c-NHEJ (Chan et al., 2010; Roerink et al., 2014; Yousefzadeh et al., 2014). The term TMEJ was coined to distinguish it from other forms of alt-EJ which include polymerase theta-independent microhomology-mediated end joining. Repair of DSBs via TMEJ is characterized by deletions with single-nucleotide homology at the

junctions, and to a lesser extent, by insertions of short stretches of DNA that come from the regions flanking the DSB (Chan et al., 2010; Koole et al., 2014; Lemmens et al., 2015; Roerink et al., 2014; van Schendel et al., 2015; 2016).

TMEJ is the dominant error-prone DSB repair pathway in the *C. elegans* germline (van Schendel et al., 2015). It has been demonstrated that TMEJ is used to repair DSBs that are induced by replication fork barriers that are caused by DNA lesions from endogenous sources (Koole et al., 2014; Lemmens et al., 2015; Roerink et al., 2014), as well as transposon-induced breaks (van Schendel et al., 2015). Meanwhile, in the context of genome editing, it has been shown that TMEJ, and not c-NHEJ, is responsible for the repair of CRISPR-Cas9 induced DSBs, with most alleles consisting of small deletions with a median size of ~ 13 bp. This is supported by the typical signature of TMEJ action that leads to a majority of deletions and a small fraction of templated insertions, similar to the signature obtained in the processing of transposon-induced breaks. In addition, the inactivation of c-NHEJ via the disruption of *lig-4* or *cku-80* did not alter the frequency or type of mutations, ruling out a canonical role of NHEJ for CRISPR–Cas9 mediated repair in the germline.

6.3. Microhomology-mediated end joining (MMEJ)

Like c-NHEJ, MMEJ is an error-prone pathway that does not require a repair template. The process commences with short-range (~ 20 bp) end resection of the 5' ends, resulting in short 3' ssDNA overhangs (Lee & Paull, 2004; Sartori et al., 2007; Truong et al., 2013) (**Figure 14A**). After short-range end resection, the DSB ends are realigned using short (5–25 bp) stretches of microhomology present near the broken ends. Any remaining 3' ssDNA flaps are cleaved off, resulting in the loss of sequence information (Seol et al., 2018; Sfeir & Symington, 2015). The remaining gaps are closed via gap-filling DNA synthesis, and the process concludes with the sealing of nicks through ligation by DNA ligases I and III (L. Liang et al., 2008) (**Figure 14B**).

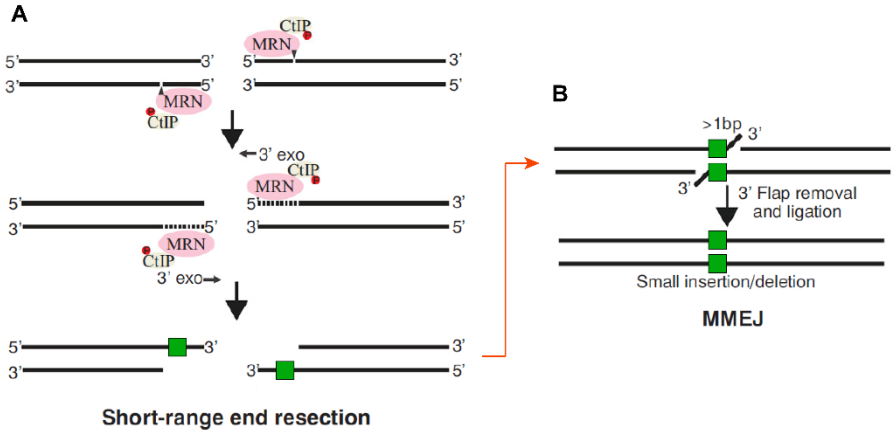

Figure 14. Short-range end resection and MMEJ. (A) DSBs are processed by the MRN complex [MRE11 and RAD50 in *C. elegans* (Chin & Villeneuve, 2001; Hayashi et al., 2007)] and CtIP [COM-1 in *C. elegans* (Lemmens et al., 2013)] to generate short 3' ssDNA overhangs, exposing regions of microhomology (green boxes). (B) The short 3' ssDNA overhangs can be channeled into the MMEJ pathway in which the microhomologous sequences are annealed, followed by removal of excess 3' heterologous flaps and ligation. Modified from Xue & Greene, 2021.

6.4. Homology-directed repair (HDR)

The term HDR encompasses a number of DSB repair pathways and is related to the nature of the DNA donor template used to direct the DSB repair reaction, and falls under either double-stranded DNA donor templated repair (DSTR) and single-stranded DNA donor templated repair (SSTR) (Xue & Greene, 2021; Yeh et al., 2019). In contrast to NHEJ which is based on DNA end protection, HDR, like MMEJ, is based on DNA-end resection. After DSB induction, the repair process begins with the nucleolytic degradation of the 5' strands to expose 3' single-stranded DNA (ssDNA) tails (Pâques & Haber, 1999). However, in contrast to MMEJ, HDR involves long-range end resection (Grabowski et al., 2005; Jung et al., 2014; Nimonkar et al., 2011; Sturzenegger et al., 2014). The exposed ssDNA then forms a nucleoprotein filament with the RAD51 recombinase that effectuates homologous pairing, strand invasion, and subsequent DNA synthesis reactions (Krogh & Symington, 2004) (**Figure 15A**). Most branches of HDR rely on a repair template, and the search for an appropriate repair template, including exogenous donors, is conducted by RAD51 (Renkawitz et al., 2013; Sugiyama et al., 1997).

In the context of DSBs produced by CRISPR-Cas9, template-dependent DSB repair pathways utilize an exogenous donor template to attain precise gene editing (Doudna & Charpentier, 2014). DSTR mainly occurs via homologous recombination (HR, also known as double-strand break repair; DSBR) or synthesis-dependent strand annealing (SDSA) whereas SSTR mainly occurs via SDSA or single-strand annealing (SSA) (Xue & Greene, 2021; Yeh et al., 2019).

6.4.1. Double-stranded DNA donor templated repair (DSTR)

In the context of genome editing, DSTR is initiated when the donor template is a PCR product or a plasmid. The 3' filament bound by RAD51 initiates homology searches, followed by strand invasion of the homologous DNA template by the ssDNA, forming a displacement loop (D-loop). After D-loop formation, DNA polymerase δ (Pol δ) engages the 3' end of the invading strand, facilitating the extension of the broken DNA end using the homologous donor dsDNA as template (Ceccaldi et al., 2016; Kowalczykowski, 2015; McVey et al., 2016; San Filippo et al., 2008; Sung & Klein, 2006).

As previously mentioned, DSTR mainly occurs via HR or SDSA. In HR, the second DSB end undergoes strand capture, forming an intertwined double Holliday junction (dHJ) structure, resulting in either crossover or non-crossover repair products depending on the pattern of resolution (Ranjha et al., 2018) (**Figure 15B**). However, DSTR may also occur via SDSA wherein the newly synthesized DNA dissociates from the invaded exogenous template and anneals to the other DSB end (Verma & Greenberg, 2016) (**Figure 15C**).

Theoretically, Cas9-induced breaks can be repaired using linear donors via direct integration at the DSB. For instance, MMEJ can facilitate the ligation of donor ends to each side of the DSB if there is sufficient microhomology (Nakade et al., 2014; Yao et al., 2017). On the other hand, the homology arms on the donor can stimulate HR via the formation of Holliday junctions with sequences on each side of the DSB. The donor sequence can then be integrated at the DSB due to crossover resolution of both Holliday junctions via HR. This mode of HDR has been shown to be the predominant type of repair when plasmid or viral donors are supplied (Kan et al., 2014, 2017).

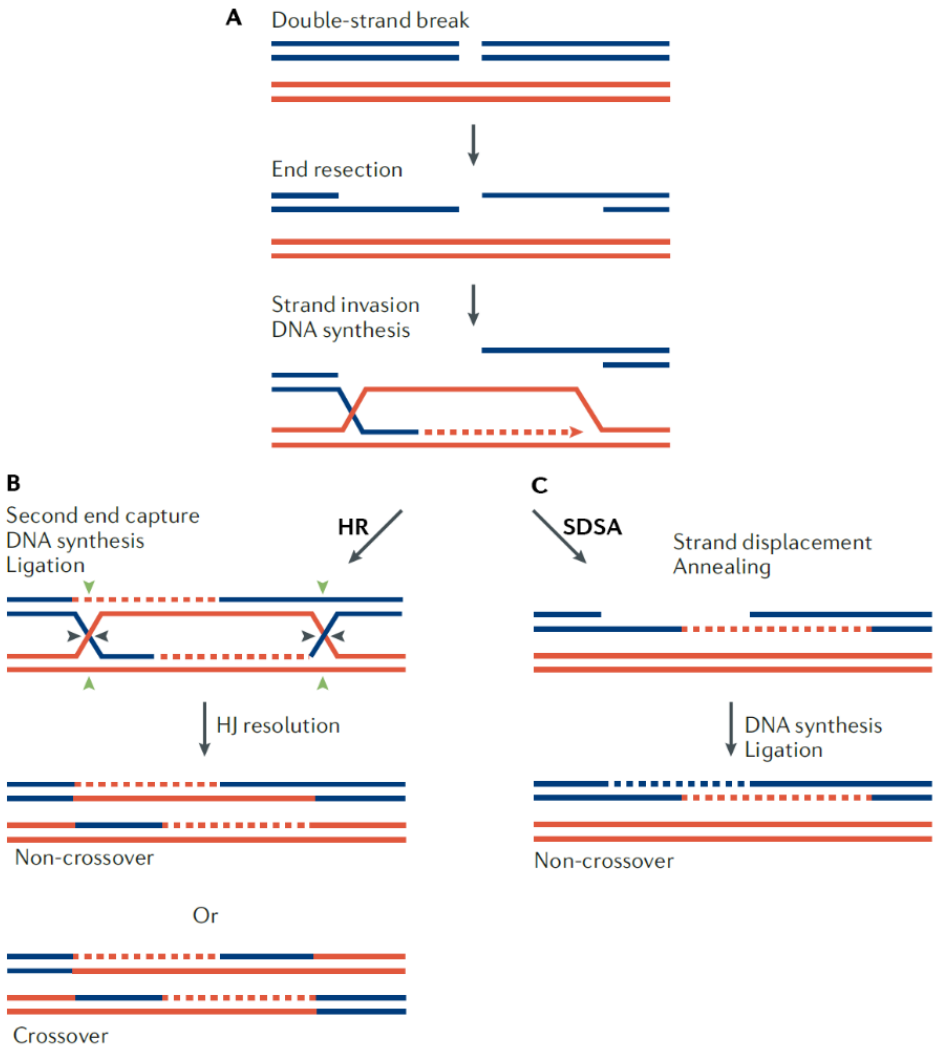

Figure 15. DSB repair via HR and SDSA. (A) In both pathways, repair commences with end resection of the DSB (genomic DNA in blue), resulting in 3' ssDNA overhangs. These overhangs then invade a homologous donor (donor dsDNA in red) and is followed by DNA synthesis at the invading end. (B) In the HR pathway, the second DSB end undergoes strand capture, forming an intermediate with two Holliday junctions (HJ). This is followed by gap-repair DNA synthesis and ligation, and resolution of the HJs in a non-crossover (black arrow heads at both HJs) or crossover (green arrow heads at one HJ and black arrow heads at the other HJ) pattern. (C) In the SDSA pathway, the newly synthesized DNA strand is displaced and anneals to the ssDNA on the other break end. The process is completed with gap-filling DNA synthesis and ligation, and the repair product is always non-crossover. Modified from Sung & Klein, 2006.

However, studies by Paix and colleagues in *C. elegans* and mammalian cells demonstrate that repair with linear donors is sensitive to polarity and that it occurs via an asymmetric, likely replicative, process that is more consistent with SDSA (Paix et al., 2016, 2017).

6.4.2. Single-stranded DNA donor templated repair (SSTR)

SSTR is an attractive option for channeling HDR since short ssDNA templates can be easily synthesized as single-stranded oligodeoxy-nucleotides (ssODNs) with multiple modifications to improve editing efficiency and *in vivo* stability (F. Chen et al., 2014; Harmsen et al., 2018; Paquet et al., 2016). Precise HDR occurs via SDSA (**Figure 15C**) or SSA (**Figure 16**) at the broken end that is complementary to the 3' end of the ssDNA template, whereas the mechanism for repairing the other broken end is currently not fully understood (Xue & Greene, 2021).

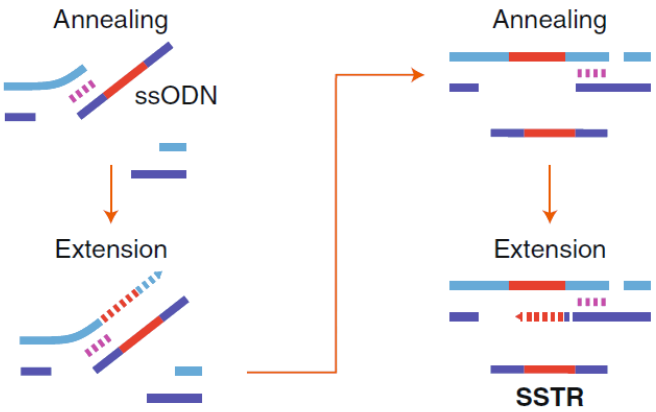

Figure 16. SSTR via an SDSA-like process. The exact mechanism by which SSTR occurs is still being defined but is thought to mirror an SDSA-like process wherein the donor ssODN anneals to the resected DSB end which is then extended using the donor as a template. After extension, the donor is displaced and homology between the newly synthesized strand and the other DSB end enables annealing and ligation, repairing the DSB. Modified from Yeh et al., 2019.

6.4.2.1 Single-strand annealing (SSA)

Like MMEJ, SSA involves end resection to expose annealable homologies followed by gap filling (Bhargava et al., 2016). In contrast, SSA requires longer end resection and homology than MMEJ (Yeh et al., 2019). The annealing in SSA creates heterologous flaps that are removed by the ERCC1-XPF nuclease complex (Ahmad et al., 2008; Al-Minawi et al., 2008). This process is followed by gap-filling DNA synthesis and concludes with ligation by currently unknown enzymes (Bhargava et al., 2016; McVey et al., 2016; Scully et al., 2019; Verma & Greenberg, 2016). SSA leads to large deletions in normal conditions but results in accurate repair in the presence of an ssDNA repair template (Xue & Greene, 2021) (**Figure 17**).

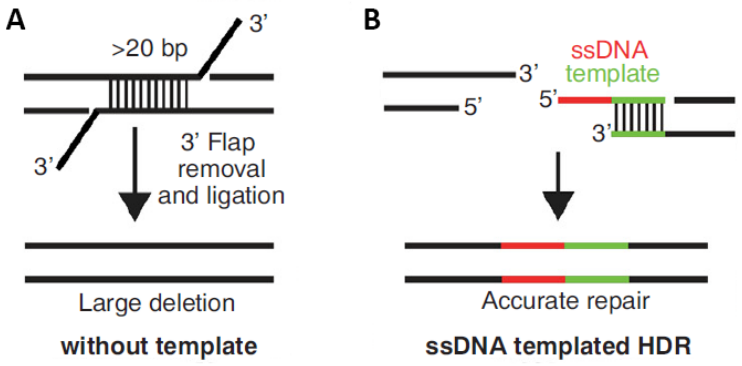

Figure 17. SSTR via SSA. SSA is a RAD51-independent pathway that involves long-range resection followed by annealing of homologous sequences between the two DSB ends. (A) In the absence of a repair template, SSA resembles MMEJ in that it involves removal of the 3' heterologous flaps followed by gap filling, leading to a large deletion. (B) However, in the presence of a repair template, the 3' end of the ssDNA donor anneals to the exposed, complementary 3' overhang of one of the broken ends. The other broken end is repaired via an unknown mechanism. Nevertheless, the process results in accurate repair. Modified from Xue & Greene, 2021.

7. Reporter gene fusions in *C. elegans*

Since the first use of GFP for labeling cells in *C. elegans* by Martin Chalfie in 1994 (Chalfie et al., 1994), the use of reporter technology has been a staple tool for investigating spatiotemporal patterns of gene expression in *C. elegans*. Its transparency and relative thinness permit its microscopic analysis *in vivo* with little to no sample preparation. Other than providing information about the promoter activity of a gene, reporters can also be used for a variety of purposes such as protein localization, visualization of cellular anatomy, cell identification, and visualization of cellular and physiological processes (Boulin et al., 2006).

The creation of transgenic reporter gene fusions was initially carried out by generating fluorescent reporter constructs through cloning (Dupuy et al., 2004; Fire et al., 1990) or PCR fusion (Hobert, 2002) followed by injection of the DNA into the gonad to form extrachromosomal arrays. While the multicopy nature of arrays can potentially offer a higher level of sensitivity, it also has disadvantages such as potential overexpression artifacts, gene silencing, or promoter-titration artifacts (Hobert & Loria, 2005). Advances in array technology have mitigated some of these issues such as the use of complex arrays to license germline expression (Aljohani et al., 2020; Kelly et al., 1997) or delivery via microparticle bombardment to generate low-copy number arrays that more closely reflect endogenous gene expression levels (Praitis et al., 2001). However, these methods have fallen out of favor to CRISPR–Cas technologies which permits tagging of genes at their endogenous loci, reducing artifacts while providing a more faithful reflection of gene expression levels.

In the following sections, the applications of translational and transcriptional reporters are discussed, and some practical considerations for creating reporter gene fusions are explained.

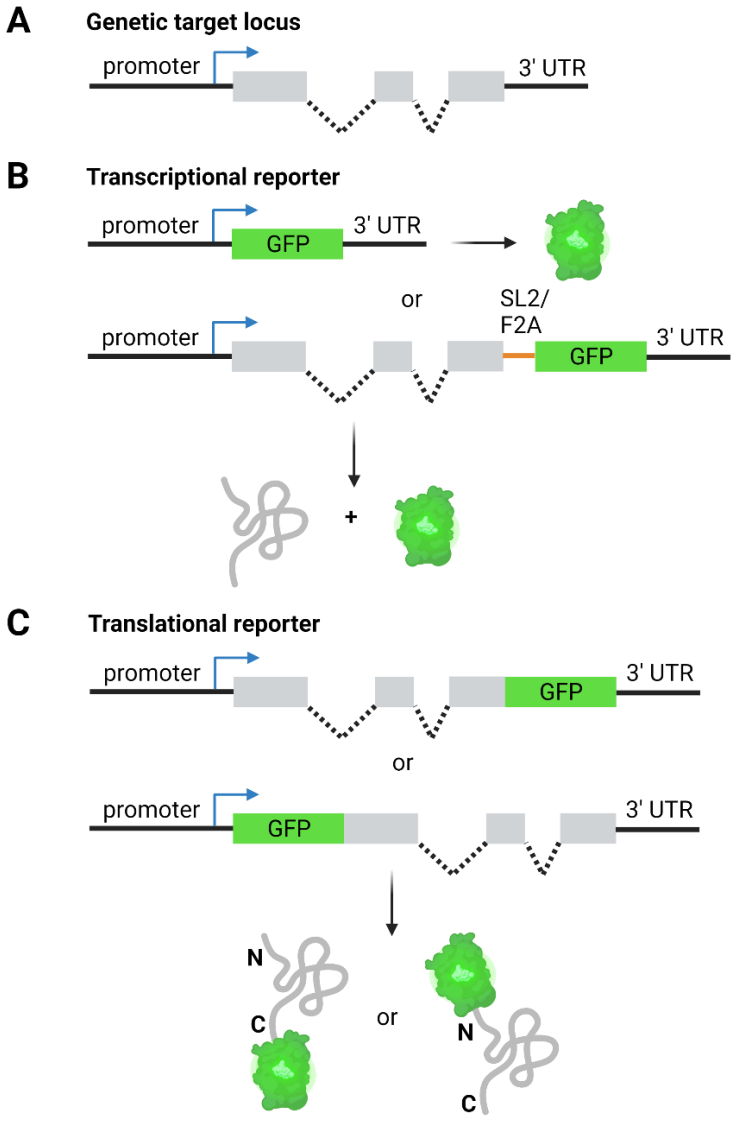

Figure 18. Transcriptional and translational fluorescent reporters. (A) The native gene structure is shown and consists of the promoter, exons (gray blocks), introns (broken lines), and the 3' UTR. The blue arrow indicates the direction of transcription. (B) In transcriptional reporters, the target gene coding sequence is replaced with the GFP coding sequence, resulting in GFP expression only. Alternatively, GFP may be expressed in the same transcript as the protein but without protein fusion by placing an SL2 trans-splicing sequence or a ribosomal skip sequence such as F2A. This leads to separate translation of the protein and (*continued on page 53*)

7.1. Transcriptional reporters

Transcriptional reporters consist of a promoter fragment from a gene of interest driving the expression of a fluorescent protein (FP) (**Figure 18**). In most cases, the first several kilobases upstream of the start of transcription contain sufficient regulatory information to provide a tentative expression pattern of the target endogenous gene (Boulin et al., 2006). However, regulatory information is also frequently found within introns, especially when the first intron is disproportionately large (Wenick & Hobert, 2004). In addition, the 3' untranslated region (UTR) can also exert transcriptional regulatory control (Conradt & Horvitz, 1999).

Alternatively, the FP can be expressed in the same transcript as the target gene but the two proteins can be translated separately by the addition of an SL2 trans-splicing sequence or a 2A peptide sequence between the two coding sequences. The SL2 trans-splicing sequence is a naturally occurring sequence commonly found in *C. elegans* operons. It facilitates the conversion of polycistronic mRNA into monocistronic mRNAs via cleavage and polyadenylation at the 3' ends of the upstream genes, accompanied by SL2-specific trans-splicing at the 5' ends of the downstream genes (Blumenthal, 2012). On the other hand, viral 2A peptide sequences can be used, triggering ribosomal skipping and ensuring efficient and concomitant expression of both the target protein and the FP reporter (Ahier & Jarriault, 2014).

(*continued from Figure 18, page 52*)
GFP. (C) In translational reporters, the GFP coding sequence may be placed immediately before the stop codon or immediately after the start codon, resulting in C-terminal or N-terminal protein::GFP fusions, respectively. Created with BioRender.com.

7.2. Translational reporters

Given the strategies above to maintain faithful representation of a gene's expression pattern, the FP can be simply fused in-frame with the genetic sequence of a protein-coding gene to create a tagged version of the target protein. In addition to retaining additional regulatory information from introns and 3' UTRs, translational reporters can provide information regarding subcellular localization and the temporal aspects of gene regulation. However, the use of translational reporters also has its drawbacks. First, if the FP is fused to an inherently unstable protein, the signal may appear dimmer or it may obscure post-transcriptional or post-translational levels of gene expression control (Hobert & Loria, 2005). Second, the insertion of the FP within the gene may interfere with protein function, and the chimeric product may even result in toxicity. Therefore, the FP must be preferably inserted in a location that does not interfere with protein function or topology. Finally, translational reporters than demonstrate subcellular location can hinder cell type identification since the shape of the cell may not be obvious (Boulin et al., 2006).

AIMS

1. To develop an efficient protocol for the generation of fluorescent endogenous reporters in *Caenorhabditis elegans*.

2. To expand genome editing possibilities in *Caenorhabditis elegans* using natural Cas12 nucleases and by optimizing the structurally engineered near-PAMless Cas9 variants SpG and SpRY.

RESULTS

PART I: Nested CRISPR

1. Nested CRISPR

This work describes an alternative cloning-free method for inserting large fragments of DNA in *Caenorhabditis elegans* with the primary goal of generating fluorescent endogenous reporters (**Figure 19**). This method was developed in light of the very low editing efficiencies we obtained from following another cloning-free approach that used PCR products with short 35-bp homology arms as repair templates (Paix et al., 2016). We have developed two modalities for achieving this goal. The first one is a two-step approach that uses ssODNs as repair template to first insert a short, locus-specific DNA fragment that serves as a "landing pad" for the subsequent insertion of a longer piece of DNA using a double-stranded PCR product as a repair template. Therefore, this approach must be carried out by performing two separate microinjections, producing an intermediate strain, and taking approximately three weeks to obtain the fluorescent reporter in homozygosis (**Figure 20A, Results Part I – Section 2**). However, the second approach, called one-shot Nested CRISPR, involves combining both steps in a single microinjection, dramatically reducing the time required to generate the same mutant to approximately a week (**Results Part I – Section 6**). Nested CRISPR can also be used to generate transcriptional reporters by using two gene-specific crRNAs in the first step. This produces an intermediate strain that knocks out the entire gene's CDS and subsequently inserts the partial fluorescent protein (FP) sequence. Step 2 is then similar to the approach used for the generation of translational reporters (**Figure 20B**).

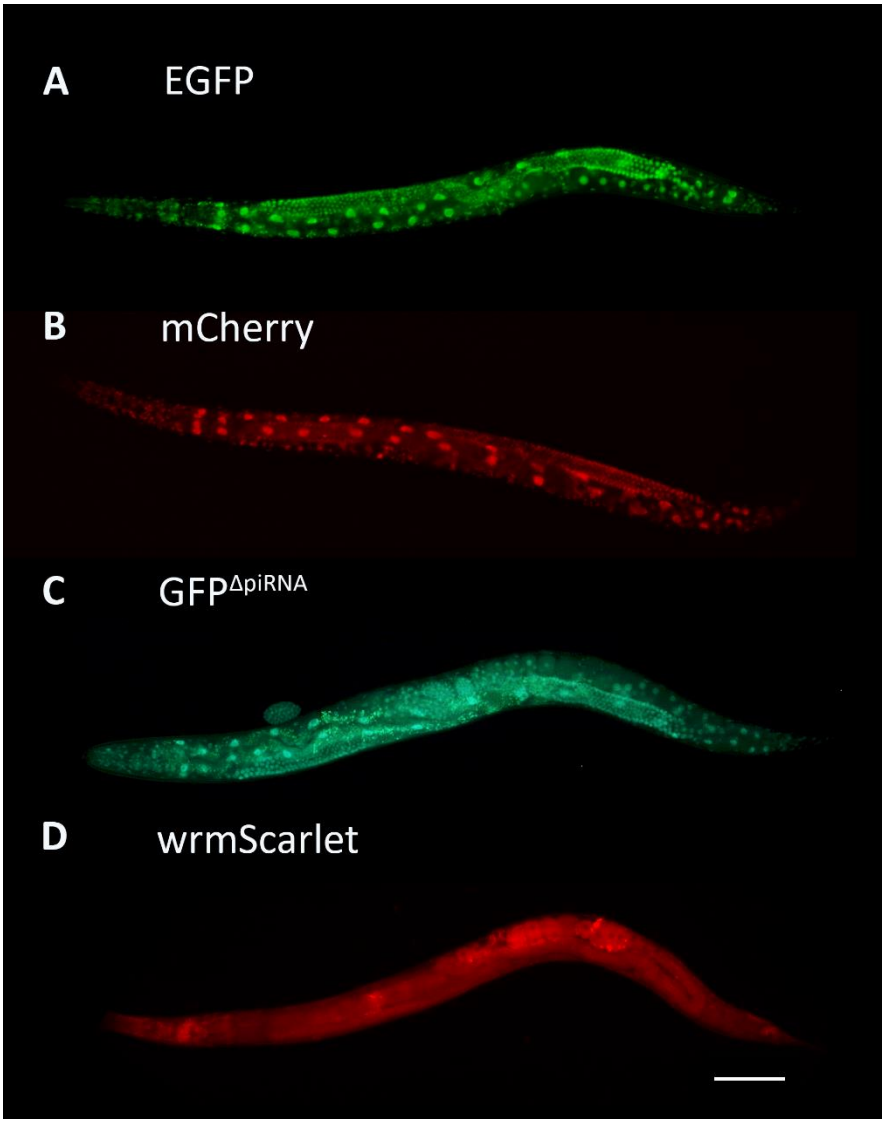

Figure 19: Representative images of fluorescent reporters generated via Nested CRISPR. (A) PRPF-4::EGFP, (B) PRPF-4::mCherry, (C) RPB-2::GFP$^{\Delta piRNA}$::degron::3xFLAG, (D) GTBP-1::wrmScarlet. Scale bar: 100 µM. PRPF-4::EGFP and PRPF-4::mCherry images were contributed by Xènia Serrat.

2. Two-step Nested CRISPR

2.1. Step 1 is highly efficient but not error-free

The first step of Nested CRISPR involves the generation of an intermediate strain that serves as a "landing pad" for the longer step 2 insertions. As expected with HDR-mediated repair with ssODN donors, step 1 insertions are almost always successful, albeit with variable efficiencies ranging from 5 to 90%, depending on the locus (**Table 5**). Moreover, the efficiency can widely vary even in the same locus (e.g., *prpf-4*, 13.0% to 90.6%) and could be attributed to inter-day and inter-injector variabilities such as differences in worm rearing conditions prior to injection or the exact developmental stage of the injected hermaphrodites. In step 1, F_1 individuals were screened for the edit of interest via PCR and were considered *positive* based on the resultant amplicon size. Most of these initial experiments were performed with a Cas9 concentration of 250 ng/µl. In the three cases (*prpf-4*::EGFP, *gtbp-1*::EGFP, and *pgl-1*::EGFP step 1) where the experiment was also performed with a higher Cas9 concentration up to a maximum of 1,640 ng/µL (10.0 µM), the efficiencies were always better at 250 ng/µl Cas9 (1.5 µM) (**Table 6**).

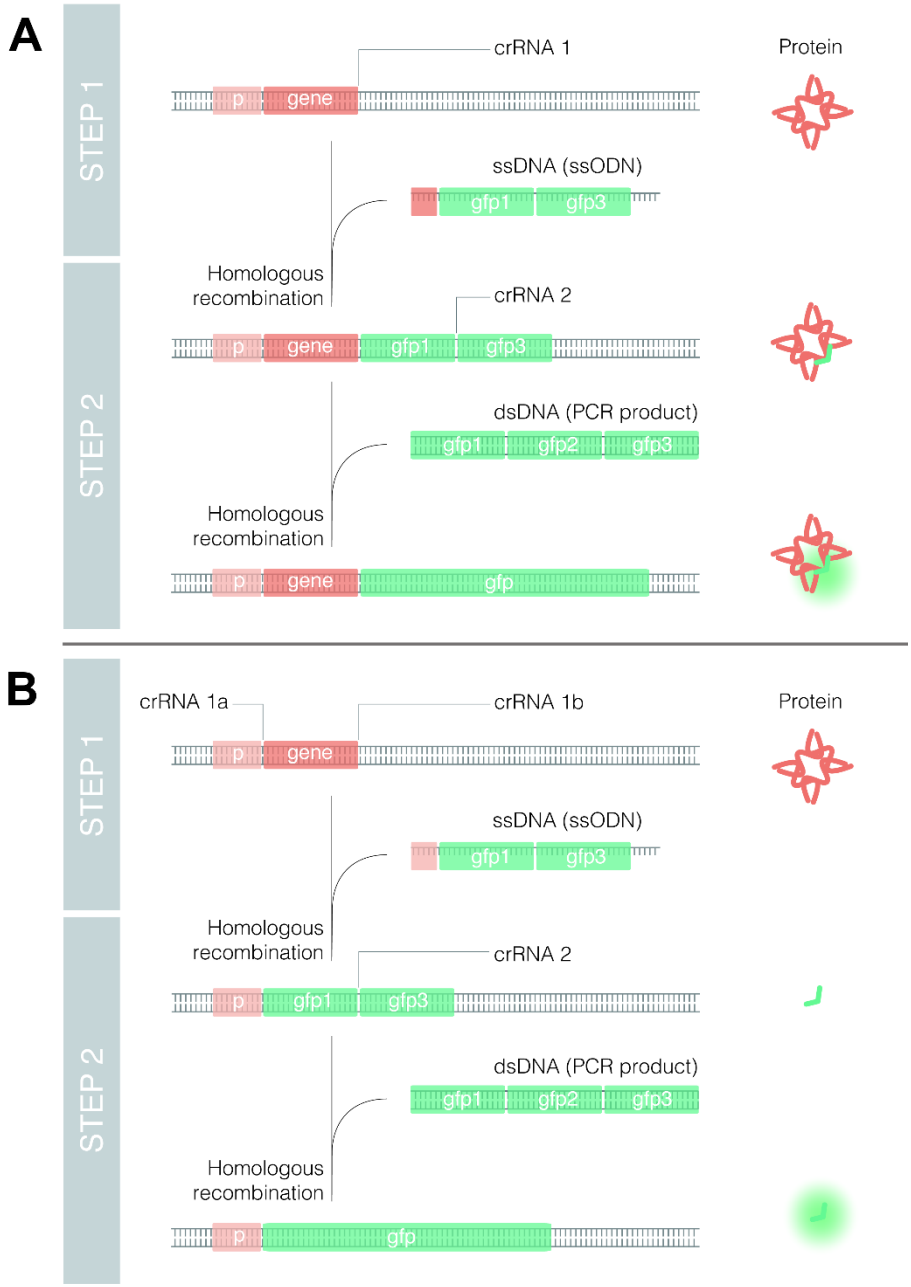

Figure 20. Scheme of molecular events to generate fluorescent reporters by Nested CRISPR. (A) Translational reporters. A gene-specific crRNA (crRNA 1) is required to assemble Cas9 RNP complexes that cut at the 5' or 3' end of the gene. Along with these RNPs, the injection mix contains an ssODN with two homology
(*continued on page 65*)

It is also important to note that the step 1 efficiencies for translational and transcriptional reporters should be considered separately, since translational reporters require only one target crRNA whereas transcriptional reporters require two. In the case of transcriptional reporters, the efficiency was sometimes lower since both crRNAs must cut effectively to carry out the deletion, then subsequent insertion of the 1-3 fragment. The efficiency of step 1 in translational reporters ranged from 13 to 91% whereas that of transcriptional reporters ranged from 5 to 71%. Considering both types of reporters, we observed that 32 of 51 (63%) insertions were correct (complete and in-frame) after sequencing. The most common errors include the lack of one or several nucleotides or the incorporation of a few additional nucleotides (**Figure 21**).

(*continued from Figure 20, page 64*)
arms of 35–45 bp (depending on the distance from the cut site) that is inserted via homologous recombination. In the second step, RNPs contain a universal crRNA (crRNA 2) that cuts the 1–3-specific (*gfp* in the example) target sequence. Then, a universal dsDNA molecule, resulting from PCR amplification of GFP, is used as a repair template to generate a translational reporter. (B) Transcriptional reporters. Two gene-specific crRNAs (crRNA 1a and crRNA 1b) and an ssODN donor are required to produce a deletion of the gene and an in-frame insertion of fragment 1–3. In the second step, RNPs contain a universal crRNA (crRNA 2) that cuts the *gfp* 1–3-specific target sequence. Then, a universal dsDNA molecule, resulting from PCR amplification of GFP, is used as a repair template to generate a transcriptional reporter.

Table 5. Summary of two-step Nested CRISPR efficiencies.

Experiment	Step 1 efficiency[1] (%)	N	Step 1 in-frame insertions	Step 2 efficiency (%)	N
Translational					
prpf-4::egfp	**56**	50	3 of 3	**Table 6**[2]	**Table 6**[2]
prpf-4::mCherry	**13**	12	2 of 3	**37.2**	28
prpf-4::2xTY1:: egfp::3xflag[3]	**90.6**	32	3 of 3	**0.6**	164
gtbp-1::egfp	**71.2**	52	2 of 3	**21.7**	46
gtbp-1::mCherry	**68.8**	32	1 of 3	**11.2**	62
pgl-1::egfp	**62.5**	40	2 of 5	**7.7**	13
pgl-1::mCherry	**53.3**	45	2 of 5	**35.9**	39
ubh-4::egfp[3]	**Table 6**[2]	**Table 6**[2]	**Table 6**[2]	**10.3**	39
mCherry::stfb-1[3]	**86.2**	29	3 of 3	**33.3**	3
egfp::nfki-1	**NP**	NP	NP	**7.7**	26
rbp-2::gfp::degron::3xflag	**63.3**	30	2 of 2	**24.1**	112
gei-3::SL2::mCherry	**NP**	NP	NP	**4.5**	67
hcf-1::gfp::degron::3xflag	**NP**	NP	NP	**41.8**	67
gtbp-1::wrmScarlet	**64.3**	28	2 of 3	**NP**	NP
nhr-1::2xTY1::egfp::3xflag	**NP**	NP	NP	**33**	100

Table 5. Summary of two-step Nested CRISPR efficiencies (*continued*).

Experiment	Step 1 efficiency[1] (%)	N	Step 1 in-frame insertions	Step 2 efficiency (%)	N
Transcriptional					
K12C11.3*p::mCherry*	**37.5**	56	3 of 3	**8.6**	35
K12C11.6*p::mCherry*	**4.6**	65	2 of 3	**73.5**	68
F58G6.9*p::wrmScarlet*	**12.5**	24	1 of 2	**2.5**	40
comt-4p::mCherry[3]	**22.2**	19	2 of 2	**7.4**	54
comt-4p::gfp::H2B[3]	**47.7**	47	1 of 2	**5.0**	20
comt-5p::gfp::H2B[3]	**78.1**	34	1 of 3	**19.1**	47
Y53C10A.5p::wrmScarlet	**60**	100	0 of 3	**NP**	NP
ads-1p::wrmScarlet	**40**	30	NS	**NP**	NP

[1] Efficiency is expressed as the percentage of F_1 individuals containing the edit of interest as a proportion of the number of F_1 screened (N). All experiments were performed with a Cas9 concentration of 250 ng/µl.

[2] All other experiments using a different Cas9 concentration are summarized in Table 6. NP means that the corresponding experiment was not performed. NS signifies that the insertion was not sequenced.

[3] Data contributed by Carmen Martínez, Xènia Serrat, and Dmytro Kukhtar

Table 6. Summary of Nested CRISPR experiments using Cas9 concentrations other than 250 ng/µl

Experiment	Efficiency (%)	N	Step 1 in-frame insertions	Cas9 concentration (ng/ul)	Efficiency (%) at 250 ng/µl
prpf-4::egfp Step 1	**26.1**	23	2 of 2	1500	56.0
prpf-4::egfp Step 2	**40.6**	32	N/A	1640	N/A
gtbp-1::egfp Step 1[1]	**5.0**	60	1 of 3	1000	71.2
pgl-1::egfp Step 1[1]	**14.0**	50	1 of 1	1000	62.5
ubh-4::egfp Step 1[1]	**26.7**	30	1 of 1	500	N/A

[1] Data contributed by Carmen Martínez and Xènia Serrat

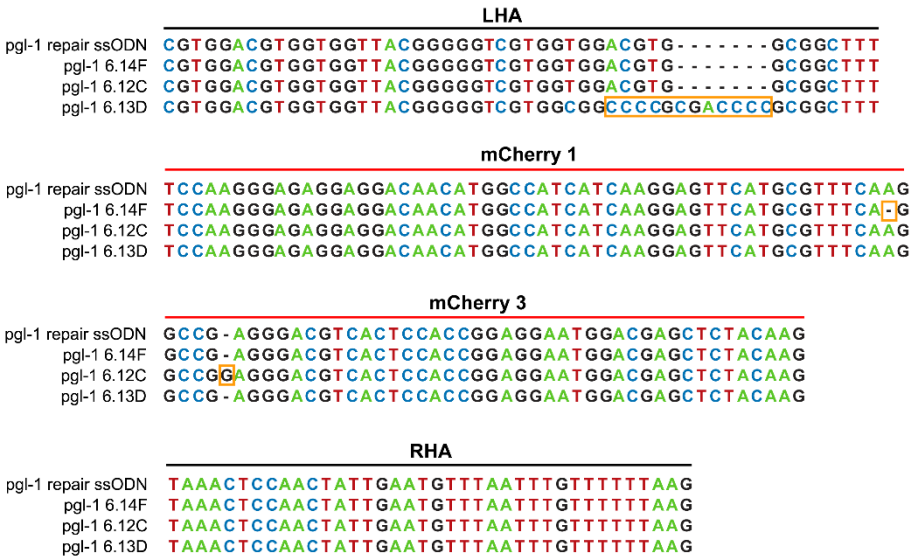

Figure 21. Sequence alignment of three *pgl-1*::mCherry step 1 insertions with errors using an ssODN repair template. The reference ssODN sequence containing the left homology arm (LHA), mCherry 1, mCherry 3, and right homology arm (RHA) sections is shown at the top. The sequences from three independent editing events then follow, with orange boxes highlighting the errors.

2.2. Step 2 can efficiently insert long (~1 kbp) sequences using dsDNA donors

In step 2, F1 individuals were screened either via PCR, fluorescence microscopy, or both. Efficiencies ranged from 0.6% (*prpf-4::2xTY1::egfp::3xflag*, 927 bp) to 73.5% (K12C11.6*p*::mCherry, 756 bp insertion). In most cases, all individuals found positive via PCR were also positive via fluorescence microscopy. Some exceptions include the ELT-2::wrmScarlet, COMT-4p::mCherry, and GEI-3::EGFP reporters where the FP tag was confirmed to be successfully inserted in-frame by sequencing but was not fluorescent upon visual examination. This might be due to improper folding or maturation of FPs upon linkage to the target protein or low endogenous expression levels, resulting in failure to detect fluorescence. Despite this, most attempts to generate various types of reporters result in fluorescence. The different varieties of reporters and their uses are summarized in **Table 7**. In addition, linkers may also be used to create distance between the protein of interest and the fluorophore, facilitating proper protein folding.

Table 7. Types of reporters integrated using Nested CRISPR

Reporter	Fragment length in bp (step 2)[1]	Uses
Classic fluorophores (EGFP, mCherry, wrmScarlet)	752, 756, and 582, respectively	*In vivo* cellular and subcellular localization, quantification of expression, and observation of protein dynamics via fluorescence microscopy.
2xTY1::EGFP::3xFLAG	927	All of the above functions are accomplished by the EGFP component whereas the 2xTY1 and 3xFLAG epitopes allow alternative examination via immunostaining.
SL2::mCherry	1003	The SL2 sequence facilitates the trans-splicing of the mCherry mRNA to the SL2 spliced leader, producing a transcriptional reporter since the fluorophore is not linked to the protein of interest.
$GFP^{\Delta piRNA}$::degron::3xFLAG	1008	The removal of piRNA sites from GFP prevents its silencing in the germline, the degron sequence allows controlled depletion of a protein of interest via the auxin-inducible degron (AID) system, and the 3xFLAG peptide can be used for immunostaining.
GFP::H2B	1215	The inclusion of the histone H2B sequence results in nuclear import of the tagged protein.

[1] The fragment length represents the length of the insertion in Step 2 of Nested CRISPR. The complete transgenes are approximately 90 to 120 bp longer, with these bases inserted during step 1 to serve as homology arms for step 2.

3. crRNA + tracrRNA vs. sgRNA

Since the structure of the guide RNA can influence the activity of Cas9 (Lim et al., 2016), we also compared the use of the dual crRNA and tracrRNA system to single guide RNA (sgRNA), which, as the name implies, is a single RNA molecule that contains both the custom-designed crRNA fused to the scaffold tracrRNA sequence. We observed that while sgRNAs are functional, they do not present an improvement over pre-annealed crRNA and tracrRNA (**Table 8**).

Other studies that compared the performance of the two gRNA modalities observed that neither the sgRNA nor the dual RNA system universally outperformed the other, with sgRNA performing better in some target sites, and the two-part gRNA working better in others; and that these differences may be attributed to the cell type or the gene target itself (Basila et al., 2017; Su et al., 2018; Turk & Spencer, 2019). However, it must be noted that these studies were performed in human cells, and that we only performed limited testing of both gRNA systems with a single target in three different loci. Therefore, a more systematic investigation of sgRNA vs. crRNA:tracrRNA efficiencies in *C. elegans* is warranted.

Table 8. Comparison of efficiencies between sgRNA and pre-annealed crRNA and tracrRNA

Experiment	Efficiency (%): sgRNA	N	Efficiency (%): crRNA + tracrRNA	N
prpf-4::*egfp* Step 2	**8.3**	24	**40.6**[1]	32
prpf-4::*mCherry* Step 2	**24.1**	108	**37.2**	28
gtbp-1::*egfp* Step 2	**8.9**	34	**21.7**	46

[1] All experiments were performed with a Cas9 concentration of 250 ng/µl except for *prpf-4::egfp* Step 2 with pre-annealed crRNA and tracrRNA which was done at 1640 ng/µl.

4. Long single-stranded DNA (megamers) as repair templates.

We performed experiments to determine whether the double-stranded PCR product can be substituted with long single-stranded DNA (megamers) as an effective repair template. The use of megamers for creating precise insertions has been demonstrated in mouse zygotes (Quadros et al., 2017), and in *Xenopus* (Nakayama et al., 2020) and zebrafish (Ranawakage et al., 2021) embryos. Therefore, we sought to test the use of megamers in *C. elegans* and hypothesized that the repair mechanisms that facilitate high repair efficiencies with the use of ssODNs in step 1 would also operate in step 2 if an ssDNA repair template were to be used. The drawback of this approach is that the synthesis of megamers is currently expensive and often presents difficulties in the synthesis of complex or repetitive regions. Therefore, we designed universal megamers that contain only the coding sequence for GFP or mCherry (872 and 702 nt, respectively) that do not possess homology with the target gene. Two different approaches were used to integrate the megamer: First, the single-step, direct integration of the megamer using two short ssODNs (70 nt each) that bridged the target locus to the megamer (**Figure 22A**). This process of using multiple overlapping fragments with concordant polarity to facilitate the homology-directed insertion of a complete sequence is called recombineering and has been proven to be effective in *C. elegans* (Paix et al., 2016). Second, integration of the megamer into a step 1 strain that contains either GFP 1-3 or mCherry 1-3 fragments, as in the normal two-step Nested CRISPR approach but substituting the dsDNA repair template (**Figure 22B**). Unfortunately, both methods only resulted in partial insertions ranging from 100 bp to 200 bp (**Table 9**) and could be due to the short length of the 5' homology arm. It is suggested that endogenous exonuclease activity may degrade the 5' end of

long ssDNA fragments, resulting in incomplete HDR (Ranawakage et al., 2021; Yoshimi et al., 2016).

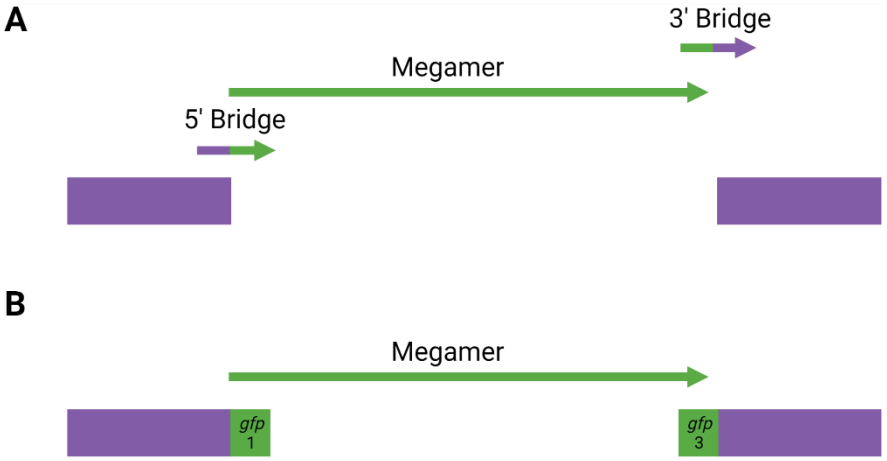

Figure 22. Scheme for the insertion of fluorescent protein sequences with megamers. (A) Direct insertion: three ssDNA donors of concordant polarity are used to integrate the FP in the target locus. This involves two bridges with homology arms to either the 5' or 3' end of the target gene, and a megamer with homology to one side of both bridges. (B) Step 2 insertion: the strategy follows the same process as Nested CRISPR step 2 insertions, with the dsDNA donor being substituted with a megamer than contains homology to the previously inserted *gfp*1 and *gfp*3 sequences. The arrowheads indicate the 3' end of the ssODN. Created with BioRender.com.

Table 9. Summary of experiments with megamers[1]

Locus, ssODN orientation (megamer concentration)	ssODN bridges or Step 2	Plates with *dpy-10* edits/injected worms	Positives[2]/worms screened (%)	Partial insertions	Cas9 (ng/µl)
gfp::sftb-1, sense2 (20 ng/ul)[1]	Bridges	10/28	0/175 (65 pools, 2-3 worms/pool)	3	1500
gfp::sftb-1, sense[3] (20 ng/ul)	Bridges	22/25	0/150 (42 pools, 2-3 worms/pool)	3	1500
gfp::sftb-1, antisense[3] (20 ng/ul)	Bridges	3/15	0/31 (14 pools, 2-3 worms/pool)	2	1500
gfp::ubh-4, antisense[3] (20 ng/ul)	Bridges	7/15	0/250 (40 pools, 2-3 worms/pool)	0	1500
gtbp-1::gfp, sense[3] (41 ng/ul)	Step 2	23/37	0/200 (40 pools, 2-3 worms/pool)	0	1500
pgl-1::gfp, sense[3] (41 ng/ul)	Step 2	14/20	0/460 (100 pools, 4-6 worms/pool)	0	1500
prpf-4::gfp, sense (41 ng/ul)	Step 2	3/20	0/219 (100 pools, 2-3 worms/pool)	1	1500
prpf-4::mCherry, antisense (210 ng/ul)	Step 2	8/34	0/41	1	250

[1] Data for the *sftb-1*, *ubh-4*, *gtbp-1*, and *pgl-1* loci were contributed by Carmen Martínez and Xènia Serrat

[2] Based on PCR genotyping (amplicons of the correct size are considered positives) and visual screening of jackpot plates (plates with ≥ 15 *dpy-10* co-edits). For experiments using bridges, the distance of the insertion from the DSB is 5 bases upstream (in both *sftb-1* and *ubh-4*) whereas for experiments using megamers as repair templates in step 2 of Nested CRISPR, the insertions are designed to be integrated exactly at the DSB. We utilized both sense and antisense ssODNs. However, ssODN polarity has marginal effects on editing efficiency in proximal edits (<10 bp), and a specific polarity is only favored in distal edits (Paix et al., 2017).

5. Co-CRISPR enriches successful edits

The microinjection of an individual P_0 hermaphrodite may give rise to either a few or many *dpy-10* co-edits. Jackpot plates are those which have a high incidence of dumpy and roller progeny (Paix et al., 2016). By plotting the number of successful editing events in the target locus against the number of separated *dpy-10* co-edits, it can be seen that there is a strong positive correlation between the number of separated *dpy-10* co-edited progeny and the number of successful edits at the target locus in step 1 experiments, whereas a moderate positive correlation is observed in step 2 experiments (**Figure 23**). While this does not preclude successful editing in plates with less co-edits, priority should be given to screening jackpot plates, especially when it is to be done by genotyping.

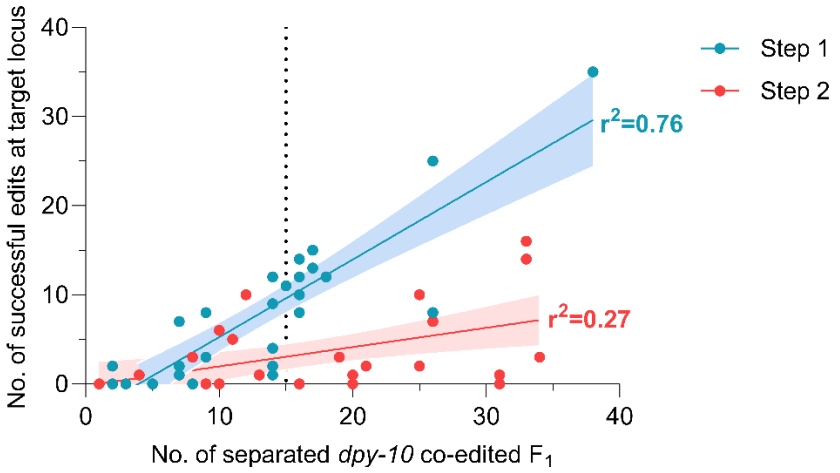

Figure 23. No. of successful edits at the target locus as a function of the number of separated *dpy-10* F_1 progeny. Each point represents an injected P_0 worm giving rise to *dpy-10* co-edited F_1 progeny. The broken vertical line divides jackpot plates from non-jackpot plates. r^2 is the coefficient of determination. The solid, colored lines represent the best-fit line based on a simple linear regression analysis and are surrounded by error bands that represent the 95% confidence interval. The data included in this analysis are derived from EGFP or mCherry experiments only to (*continued on page 76*)

6. One-shot Nested CRISPR

In an attempt to reduce the two-step approach into a single one, we combined both step 1 and step 2 crRNAs in the injection mix to generate translational reporters. Therefore, transgenic strains can be isolated in homozygosis in as little as eight days, instead of the usual three weeks for the two-step approach. The one-shot approach often works well for the insertion of shorter fragments such as EGFP, mCherry, or wrmScarlet (**Table 10**). However, it failed to produce full insertions (equivalent to step 2) when the fragments were longer such as in the case of SL2::mCherry, 2xTY1::EGFP::3xFLAG, and GFP::degron::3xFLAG. However, in all cases, step 1 insertions were obtained, and these were homozygosed to serve as intermediate strains for step 2 injections. Therefore, compared to the two-step approach, the one-shot method has the merit of possibly leading to complete insertions, with the assurance of at least producing step 1 insertions. The higher frequency of step 1 insertions compared to step 2 insertions is demonstrated in **Figure 24**.

(*continued from Figure 23, page 75*)
control for insertion size. The step 1 data come from 27 P_0s from 9 independent experiments while the step 2 data come from 29 P_0s from 10 independent experiments.

Table 10. Summary of one-shot Nested CRISPR experiments

Experiment	Step 1 efficiency[1] (%)	N	Step 1 in-frame insertions	Step 2 efficiency (%)	N[2]
prpf-4::mCherry	**65.8**	38	NS	**20.8**	77
gtbp-1::EGFP	**7.5**	40	NS	**0**	40
pgl-1::EGFP	**16**	25	NS	**4**	25
F27C1.2::wrmScarlet	**17.5**	40	NS	**4.9**	144
EGFP::*nfki-1*	**40**	70	1 of 2	**0**	70
wrmScarlet::F27C1.2	**43.8**	16	NS	**31.3**	16
gei-3::SL2::mCherry	**16.7**	30	1 of 2	**0**	30
nhr-1::2xTY1::EGFP::3xFLAG[3]	**20**	30	1 of 1	**0**	30
hcf-1::GFP::degron::3xFLAG	**81.25**	32	1 of 3	**0**	32
*comt-3*p::GFP::H2B[4]	**10.0**	40	1 of 2	**0**	40

[1] Efficiency is expressed as the percentage of F_1 individuals containing the edit of interest as a proportion of the number of F_1 screened (N).

[2] The N for screening Step 2 insertions may be larger than the N for Step 1 insertions if worms are screened via fluorescence microscopy in addition to PCR.

[3] Due to the unavailability of a suitable NGG PAM, the one-shot approach was carried out with a combination of AsCas12a (Step 1) and Cas9 (Step 2).

[4] Data contributed by Dmytro Kukhtar

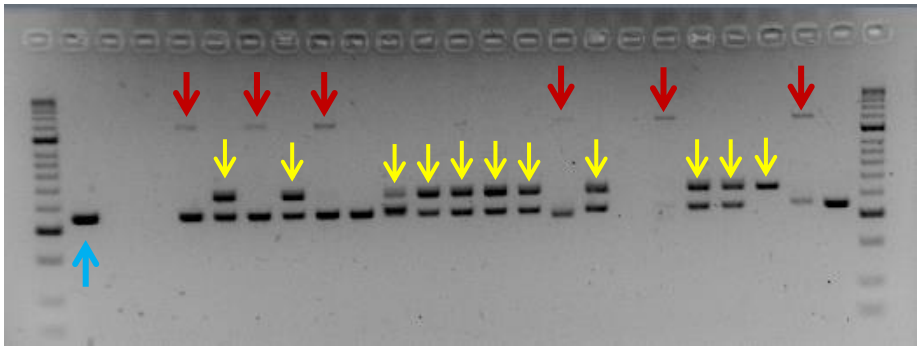

Figure 24. Representative gel image of insertions obtained via one-shot Nested CRISPR (*prpf-4::mCherry*). The wild-type band is marked with the blue arrow and is 348 bp long, step 1 bands are marked with yellow arrows and are 447 bp long, and step 2 bands are marked with red arrows and are 1203 bp long.

7. Transgenerational efficiency

To determine whether the efficiency of step 2 is affected by the number of generations that have passed after obtaining the step 1 entry strain, two frozen stocks of the *gtbp-1*::EGFP 1-3 entry strain (CER371) were thawed and cultivated at 25°C such that F_5 and F_{15} progeny were obtained at the same time points (the F_{15} progeny line was obtained from a frozen stock that was thawed 10 generations earlier than the F_5 progeny line). The F_5 and F_{15} step 1 strains were simultaneously injected for step 2 in addition to a freshly thawed stock that was left to grow to young adults prior to injection. The *gtbp-1* locus was chosen for this experiment since its high expression levels and ubiquitous expression pattern facilitates its screening via fluorescence under the stereomicroscope.

EGFP positives were obtained in all three groups after injection, regardless of the generation number (**Table 11**). This means that step 1 strains can be frozen indefinitely for storage until the step 2 injection is carried out. This experiment was only performed once in a single locus, but nevertheless indicates that neither freezing nor passage number is not an issue for two-step Nested CRISPR. This could imply that there are no changes in chromatin state within the immediate vicinity of the locus after cutting with Cas9. Worms are starved prior to freezing, and starvation can potentially trigger global changes in the chromatin landscape (Larance et al., 2015), erasing any chromatin marks accumulated across previous generations. However, these results demonstrate that the previously edited region remains equally accessible by the time the worms are thawed, as well as in succeeding generations.

Table 11. Summary of the step 2 transgenerational efficiency experiment for the insertion of EGFP at the *gtbp-1* locus

Generation	No.of P_0 Injected	Plates w/ *dpy-10* co-edits	Jackpot plates[1] w/ EGFP	Non-jackpot plates[1] w/ EGFP	Notes
CER371 (recently thawed)	16	4	2	0	Plates 3 and 13 with positives in WT-like worms
F_5	15	6	4	0	Plate 9 with positives in WT-like worms; Plate 12 with positives in both WT-like worms and rollers; Plates 13 and 14 with positives in rollers
F_{15}	19	2	0	3	Plates 6, 11, and 13 with positives in WT-like worms

[1] In this experiment, few F_1 rollers were seen in plates and a *jackpot plate* in this case is defined as a plate with at least one *dpy-10* co-edited F_1. Nevertheless, most EGFP+ worms were wild-type-like in appearance (not co-edited at the *dpy-10* locus). Specifically, in the F_{15} entry strain, positives were found in plates without F_1 rollers, suggesting that the problem may be due to a poor *dpy-10* crRNA aliquot.

8. Editing efficiency is inversely related to insertion length

To systematically address the trend that we observed regarding editing efficiencies and the length of the insert, we simultaneously performed insertions of three wrmScarlet sequences which were varied in length by inserting PATC-rich introns (**Figure 25, Supplementary Table 10**). First, Nested CRISPR step 1 was carried out at the *gtbp-1* locus to create an intermediate wrmScarlet 1-3 insertion. Step 2 was then carried out over this strain with varying insertion lengths of 582 bp, 1068 bp, and 1,608 bp.

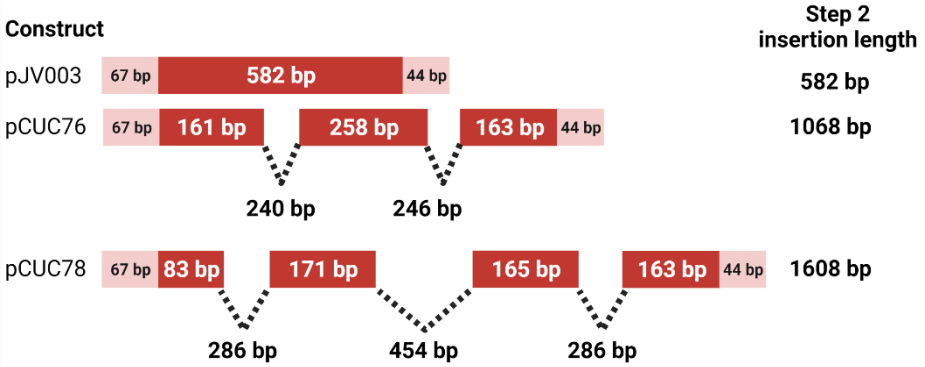

Figure 25. Diagram of three different wrmScarlet constructs with varying lengths. The original wrmScarlet sequence from the pJV003 plasmid does not contain introns. To vary the length, two different constructs were produced: pCUC76 and pCUC78, that contained two and three introns, respectively. Red blocks are exons and pink blocks represent the homology arms (which are also part of the exons and correspond to the wrmScarlet 1 and wrmScarlet 3 sequences in step 1 insertions). The broken lines represent introns. Created with BioRender.com.

The editing efficiencies across the three different fragment lengths at the *gtbp-1* locus is shown in **Figure 26**. To control for injection quality, only P_0s that gave rise to at least 10 *dpy-10* co-edited progeny are included in the analysis. A significant drop in editing efficiency is observed when the

length of the insertion increases from 582 bp to 1068 bp. However, no significant difference is observed between insertions of 1068 bp and 1608 bp. Therefore, insertions of standard FP constructs of ~600 to 750 long are moderately efficient and should be relatively easy to achieve. Nevertheless, longer insertions of up to ~1600 bp can still be obtained, albeit more worms need to be screened due to the lower editing efficiencies. Likewise, it must be emphasized that these results come from one experiment at a single locus, and it remains to be seen whether this trend can be extrapolated to other loci or not.

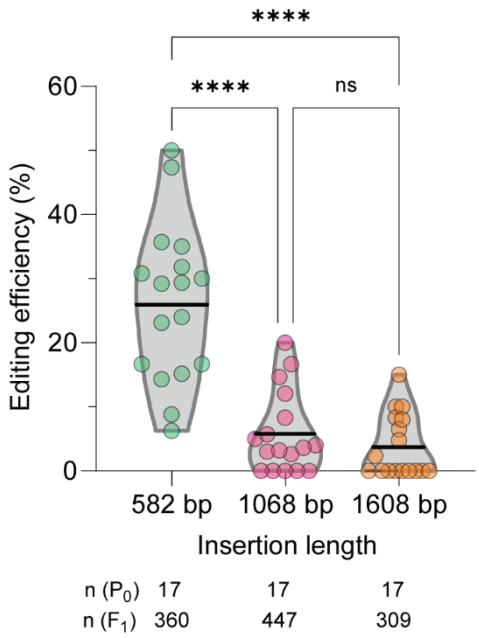

Figure 26. Editing efficiencies with varying wrmScarlet construct lengths at the *gtbp-1* locus. Editing efficiency is defined as the number of F_1 worms exhibiting fluorescence divided by the total number of separated *dpy-10* co-edited F_1s. Each point represents the editing efficiency in each individual P_0 that yielded at least 10 *dpy-10* co-edited F_1s. The numbers below the graph indicate the number of P_0s and F_1s included in the analysis and come from a single experiment. The horizontal bar indicates the mean. ns: no significant difference, $p<0.0001$ **** (One-way ANOVA followed by Tukey's test for multiple comparisons)

RESULTS

PART IIA: Expanded targeting range with natural Cas12 orthologs

1. Cas12a can be used for HDR-mediated genome editing in *C. elegans*

SpCas9 requires a 5'-NGG-3' PAM sequence, and while this does not severely limit its targeting range, there are cases where a T-rich PAM, such as that of some Cas12 nucleases, is more convenient for the desired application. For instance, for the construction of the NHR-1::2xTY1:: EGFP::3xFLAG reporter, the AsCas12a nuclease with a TTTV PAM was used instead of Cas9 for step 1 of the Nested CRISPR pipeline since a suitable NGG PAM close to the stop codon was unavailable. Therefore, we decided to further explore the capacity of Cas12 orthologs for genome editing in *C. elegans*.

In the context of Nested CRISPR, the use of Cas12a was explored in two different ways: first, as a substitute for Cas9 in the second step of the two-step approach, and second, as a substitute for Cas9 in the second step of the one-shot approach. In the latter case, Cas9 was combined with Cas12a in the same injection mix, with each nuclease carrying out steps 1 and 2, respectively. To perform this experiment, we first modified the step 1 wrmScarlet repair template to introduce an NGG PAM for Cas9 and a TTTV PAM for Cas12a that can induce DSBs at similar locations (**Figure 27**). This proof of concept was first performed at the F27C1.2 locus since it facilitated the screening of positive HDR events in the F_1 using a stereomicroscope (**Figure 28**).

GTCAGCAAGGGAGAGGCAGTTATCAAGGAGTTTATGCGTTTCAAGGTC
|GGAC/GGCACTCCACCGGAGGAATGGACGAGCTCTACAAG

Figure 27. Modified wrmScarlet 1-3 sequence for comparing Cas9 and Cas12a efficiencies. The wrmScarlet 1 and wrmScarlet 3 sequences are in green and red, respectively. Silent mutations for introducing a TTTV PAM for Cas12a and an NGG PAM for Cas9 are in orange. The PAMs are underlined. The vertical bar represents the blunt DSB site induced by Cas9 (3 bp upstream of the PAM) and the forward slash represents the DSB site produced by Cas12a at the target strand (18 bp downstream of the PAM).

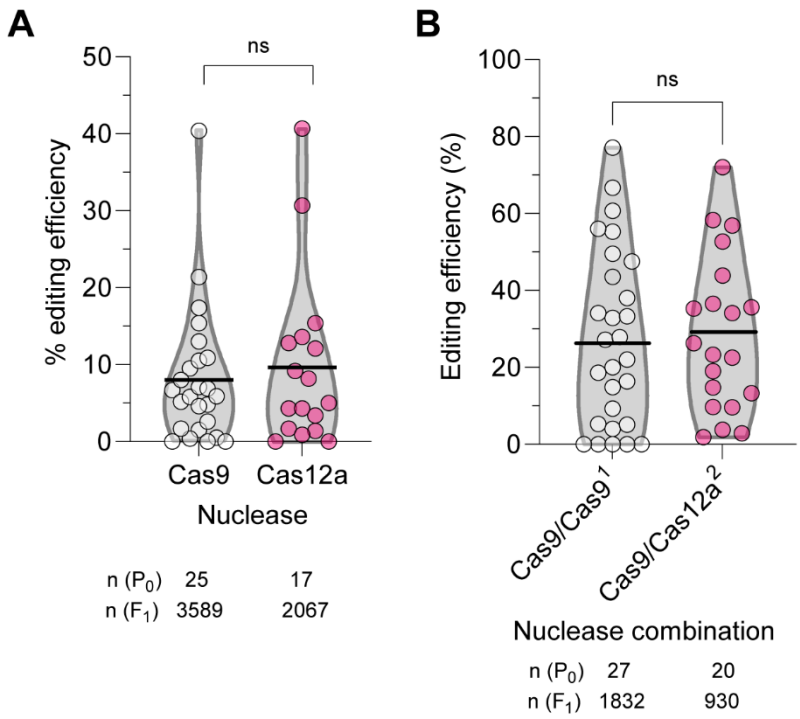

Figure 28. Comparative editing efficiencies of Cas9 and Cas12a at the F27C1.2 locus. (A) Cas9 vs. Cas12a editing efficiency in Nested CRISPR Step 2. Each point represents the editing efficiency in each individual P_0 and is defined as the number of F_1 worms exhibiting fluorescence divided by the total number of F_1s (co-CRISPR was not used since *dpy-10* co-editing was not possible in the Cas12a group using the wild-type N2 background). The data are derived from two independent replicates. (B) Cas9/Cas9 vs. Cas9/Cas12a editing efficiency in one-shot Nested CRISPR. The first and second nucleases in each combination signify which (*continued on page 86*)

Both Cas9 and Cas12a can both carry out step 2 insertions efficiently, with a marginal improvement observed with the use of Cas12a (Cas9 efficiency: 8.0% vs Cas12a efficiency: 9.6%) (**Figure 28A**). Meanwhile, the one-shot approach demonstrates the same trend, with the Cas9/Cas12a (28.6%) combination demonstrating a marginal improvement over the Cas9/Cas9 (26.6%) setup (**Figure 28B**). The efficiencies in the one-shot experiment are higher than in the step 2 experiment since *dpy-10* co-CRISPR was not applied to the latter group, and therefore, it was not possible to enrich for successful F_1 editing events (and moreover, since injections were performed only at a single gonad arm, RNPs were delivered to only half of the population in the step 2 group). Nevertheless, these results prove that Cas12a has sufficient *in vivo* activity for stimulating HDR in *C. elegans* and that the combination of two different nucleases in the injection mix does not negatively impact editing efficiencies.

In the F27C1.2 experiment, the total nuclease concentration was higher in the Cas9/Cas12a group than the Cas9 group alone. Therefore, to determine whether the higher efficiency was due to the higher total nuclease concentration, the experiment was repeated at the *gtbp-1* locus using similar nuclease concentrations (**Figure 29**).

(*continued from Figure 28, page 85*)
nuclease was paired with the step 1 and step 2 guide RNAs, respectively. Each point represents the editing efficiency in each individual P_0 that yielded at least 15 *dpy-10* co-edited F_1s. The data are derived from a single experiment. The numbers below the graph indicate the number of P_0s and F_1s included in the analysis. The horizontal bar indicates the mean, ns: no significant difference (Student's *t*-test).

[1] 1.5 µM Cas9

[2] 1.5 µM Cas9 + 1.5 µM Cas12a (3.0 µM total)

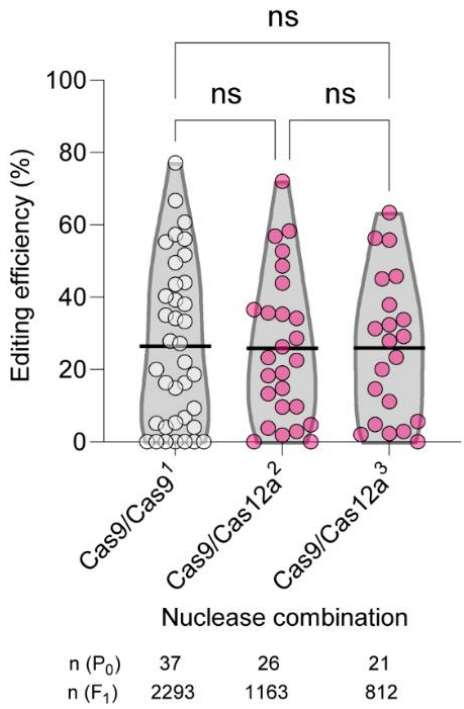

Figure 29. Comparative editing efficiencies of Cas9 and Cas12a combinations at the *gtbp-1* locus. The first and second nucleases in each combination signify which nuclease was paired with the step 1 and step 2 guide RNAs, respectively. Each point represents the editing efficiency in each individual P_0 that yielded at least 15 *dpy-10* co-edited F_1s. The data are derived from two independent experiments. The numbers below the graph indicate the number of P_0s and F_1s included in the analysis. The horizontal bar indicates the mean, ns: no significant difference (One-way ANOVA followed by Tukey's test for multiple comparisons)

[1] 1.5 µM Cas9

[2] 1.5 µM Cas9 + 1.5 µM Cas12a (3.0 µM total)

[3] 1.0 µM Cas9 + 0.75 µM Cas12a (1.75 µM total)

The experiment at the *gtbp-1* locus provides evidence that the lower nuclease concentrations in the Cas9 only group is not limiting and that increasing the total nuclease concentration does not add any advantage in terms of editing efficiency. All in all, our results demonstrate that AsCas12a for genome editing with TTTV PAMs has similar editing efficiencies as SpCas9 with NGG PAMs in *C. elegans*.

2. Characterization of Cas12f1 activity in *C. elegans*

Three different Cas12f1 effectors were tested in this study. Two of them, AsCas12f1 and SpCas12f1 belong to the type V-U3 family; and the other, Un1Cas12f1, belongs to the type V-F family (Karvelis et al., 2020). One peculiarity of these CRISPR–Cas12f systems is that they utilize long sgRNA molecules of about 200 nt long. The nucleases were tested in two loci: *dpy-10* and EGFP.

We chose *dpy-10* as the target gene for the *in vivo* characterization of AsCas12f1 and Un1Cas12f1 since we expected it to provide facile readout of dominant phenotypes in the F_1. To facilitate this, we modified the *dpy-10* sequence in the wild-type N2 background by CRISPR–Cas9 to introduce a TTTA PAM that was compatible with both Un1Cas12f1 (TTTR) and AsCas12f1 (YTTN), resulting in the CER603 strain (**Figure 30**). On the other hand, several gRNAs were designed to target EGFP (**Figure 31**), facilitating the screening of knockouts in the F_2.

ATG-AGA-TTT-ACT-GGA-AAC-CGT-ACC-GCT-CGT-GGT-G/CC-TAT

Figure 30. Modified *dpy-10* sequence to accommodate Un1Cas12f1 and AsCas1f1 target recognition. The sequence in the immediate vicinity of the *cn64* allele is shown. The *cn64* allele is described as the change of the C nucleotide (in red) to a T, resulting in a missense mutation that recodes arginine (CGT) to cysteine (TGT), [M85F]. The two mutations for introducing a TTTR PAM are in orange. These two mutations result in the recoding of methionine (ATG) to phenylalanine (TTT). The PAM is underlined and the forward slash represents the DSB site produced by Un1Cas12f1 and AsCas12f1 at the target strand (24 bp downstream of the PAM).

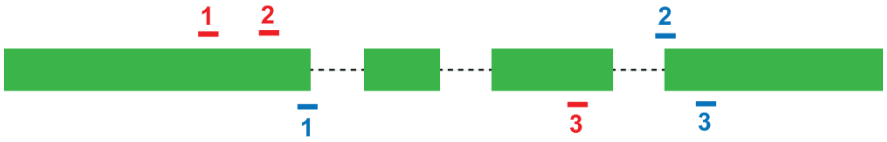

Figure 31. EGFP targets for the three Cas12f1 variants. Figure is drawn to scale. The green boxes represent the EGFP exons and the broken lines represent introns. The protospacer sequences are represented as colored lines and their positions correspond to their orientation (above: sense, below: antisense). The blue guides are for use with Un1Cas12f1 and AsCas12f1 while the red guides are for use with SpCas12f1.

2.1. Cas12f1 variants exhibit *in vitro* activity at high temperatures only (50°C)

The *in vitro* assays demonstrate that Un1Cas12f1 and AsCas12f1 were capable of cleaving dsDNA targets in a PAM-dependent manner, but at an optimal temperature of 50°C (**Figure 32**), beyond the tolerable temperatures for *C. elegans*. In addition, the activity is enhanced by the addition of Mg^{2+} ions. However, SpCas12f1 did not show significant *in vitro* activity for any of the targets tested even at 50°C, and therefore, this nuclease was not further characterized *in vivo*.

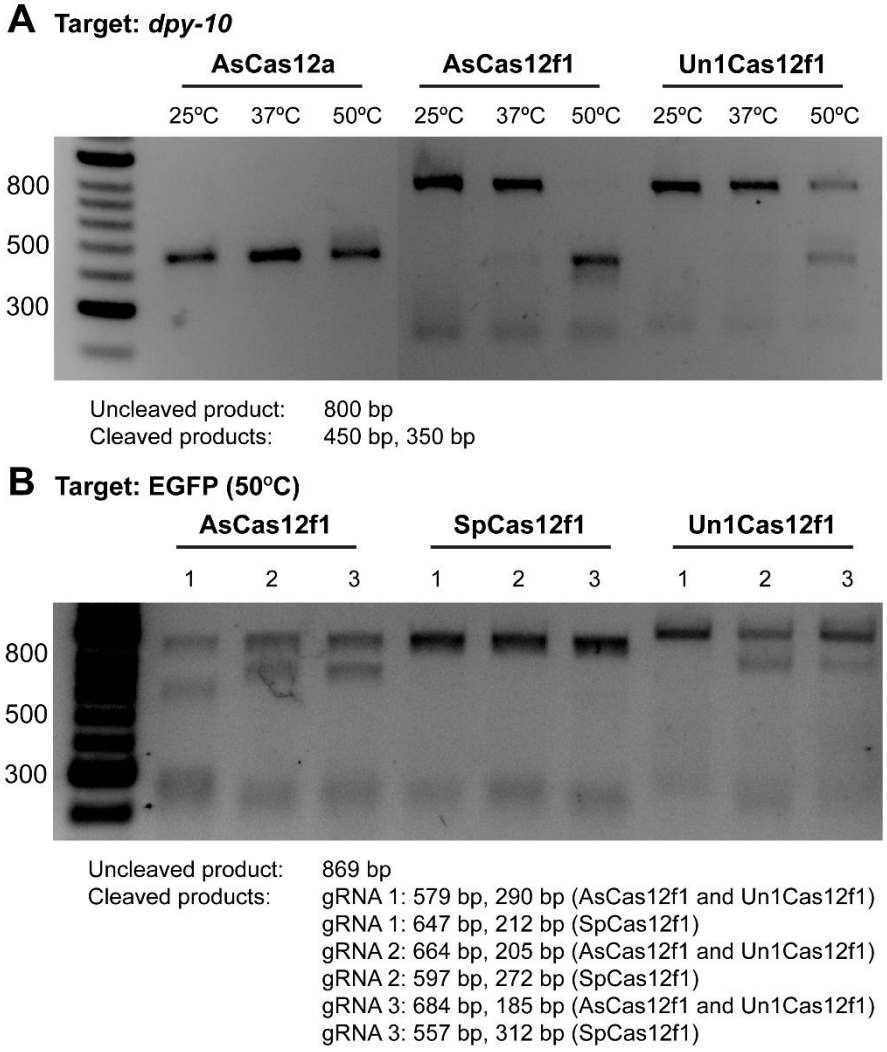

Figure 32. *In vitro* activity of the Cas12f1 variants in *dpy-10* and EGFP targets. (A) The ability of the AsCas12f1 and Un1Cas12f1 variants to cleave the *dpy-10* PCR product were tested together with AsCas12a as control. AsCas12a was capable of cleaving all dsDNA substrate at all three temperatures whereas AsCas12f1 showed strong cleavage only at 50°C (with weak cleavage at 37°C), and Un1Cas12f1 only showed weak cleavage at 50°C. [Results from SpCas12f1 are not included in the image but it did not exhibit any cleavage at any of the temperatures tested.] (B) The ability of the three Cas12f1 variants to cleave the EGFP PCR product were tested using three distinct guide RNAs at three different temperatures [only the image from the 50°C experiment is included since no cleavage was detected at 25°C and 37°C]. Nonspecific 200–300 bp fragments in all samples come from gRNA.

2.2. AsCas12f1 and Un1Cas12f1 are not capable of genome editing in the germline.

Four attempts were made to characterize AsCas12f1 and Un1Cas12f1 *in vivo* (**Table 12**). In the first experiment, AsCas12f1 or Un1Cas12f1 were injected with the *sqt-1* or *dpy-10* gRNAs, respectively, at the standard concentration of 1.5 µM (equivalent to 77 ng/µl for AsCas12f1 or 98 ng/µl for Un1Cas12f1). Both nucleases failed to yield F_1 rollers. Since UnCas12f1 is not capable of plasmid DNA interference (Karvelis et al., 2020), it therefore does not function as a *bona fide* CRISPR-Cas system, at least in *E. coli* cells. Thus, this nuclease was not further characterized and subsequent experiments focused on AsCas12f1.

In the second and third experiments, the *dpy-10* locus was targeted with AsCas12f1 at two different concentrations with Mg^{2+} supplementation based on the fact that the Un1Cas12f1 RNP complex is magnesium-dependent (Karvelis et al., 2020), and that the same may be true for AsCas12f1. Both attempts yielded phenotypes, including: slightly shorter worms compared to wild-type (semi-Dpy), locomotion variants characterized by lifting of the head in an upward twisting motion (Lif), and a solitary F_1 roller. However, none of these F_1 phenotypes exhibited Mendelian segregation, and all phenotypes were eventually lost in subsequent generations. In addition, DNA from candidate worms that exhibited phenotypes were sequenced, but all of them were genetically wild-type. Therefore, we speculate that these phenotypes could have arisen due to the capacity of the nucleases to degrade mRNA or to act in a manner akin to dCas9.

Table 12. Summary of Cas12f1 *in vivo* experiments

Expe-riment	Nuclease	Locus	Concen-tration	Mg^{2+}	Phenotypes observed
1	UnCas12f1 AsCas12f1	*sqt-1* *dpy-10*	1.5 µM	0 mM	None
2	AsCas12f1	*dpy-10*	1.5 µM	10 mM	Semi-Dpy, Lif, Rol
3	AsCas12f1	*dpy-10*	10.0 µM	10 mM	Semi-Dpy, Lif
4	AsCas12f1	EGFP	10.0 µM	10 mM	None

Finally, to test AsCas12f1 using an alternative phenotype, RNPs consisting of AsCas12f1 and three anti-EGFP guides were simultaneously injected into the gonads of young adult hermaphrodites (**Figure 33**). Most editing events at this locus would produce a frameshift, resulting in EGFP knockout and loss of fluorescence. To control for injection quality and to aid in the separation of F_1 heterozygotes, *dpy-10* co-CRISPR (using Cas9) was used as a marker. However, all of the isolated F_1 rollers failed to yield EGFP knockouts. Therefore, considering the results of all four *in vivo* experiments, it can be concluded that Cas12f1 variants are incapable of genome editing in *C. elegans*, and could be due to their high temperature requirements for optimal activity.

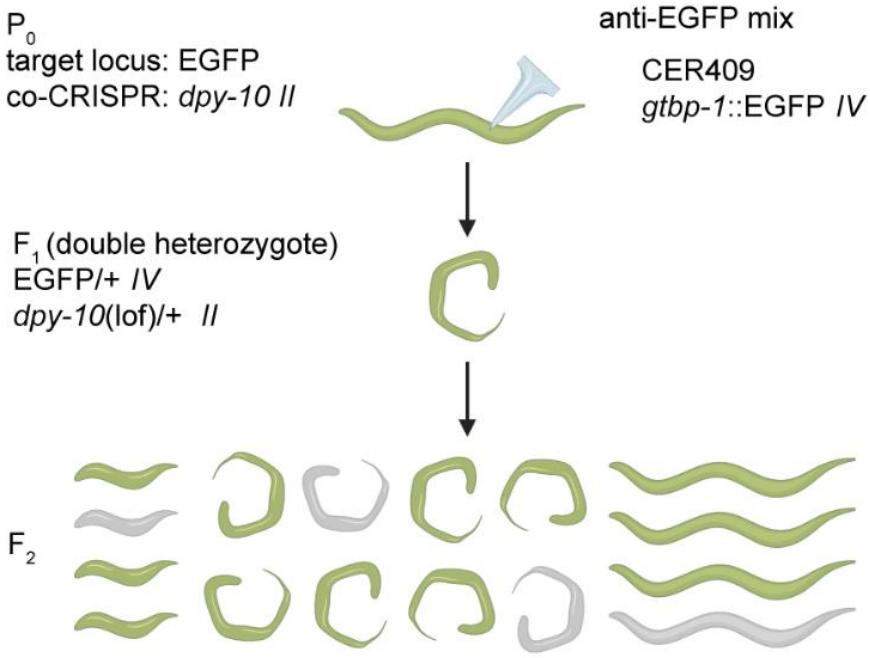

Figure 33. Schematic representation of the EGFP knockout assay. CER409 worms harboring an endogenous *gtbp-1*::EGFP reporter are injected with a mixture containing three anti-EGFP guides and a *dpy-10* guide for co-CRISPR. F_1 worms with the Rol or Dpy phenotypes are separated onto individual plates and allowed to lay F_2 progeny, which display Mendelian segregation from a doubly heterozygous F_1 hermaphrodite. Created with BioRender.com.

RESULTS

PART IIB: Expanded targeting range with engineered Cas9 variants

1. Characterization of SpG and SpRY in NGG PAMs

1.1. SpG and SpRY have *in vitro* activities similar to WT SpCas9

Since the activity of Cas9 orthologs found in diverse microbes varies with temperature (Gasiunas et al., 2020), the activity of the engineered SpG and SpRY variants was first examined to determine temperature sensitivity as it could hamper their use in organisms growing at temperatures below 37°C. Therefore, these proteins were initially tested *in vitro* at different temperatures including 15, 25, 37, and 50°C. The two engineered variants, along with two versions of wild-type Cas9 (purified in-house and commercial), generated targeted DNA double-strand breaks on a substrate harboring an NGG PAM with similar efficiencies (**Figure 34**)**.** Therefore, the SpG and SpRY variants are active at the standard rearing temperatures for *C. elegans*.

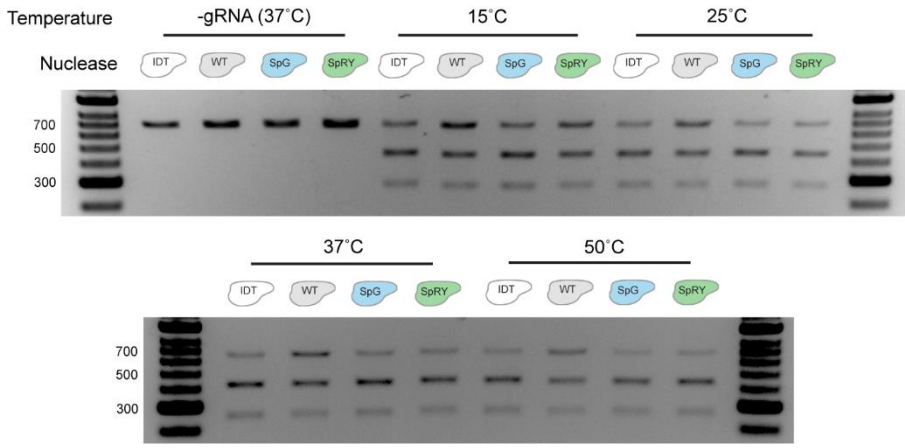

Figure 34. Comparative activities of IDT Cas9, WT SpCas9, SpG, and SpRY against the *dpy-10* NGG target *in vitro*. Four different RNP combinations comprised of each guide and IDT Cas9, WT SpCas9, SpG, or SpRY were tested *in vitro* at 15, 25, 37, and 50 °C by incubating the RNPs with a PCR product amplified from the *dpy-10* locus for one hour. Negative controls without the guide RNA (-gRNA) were tested at 37 °C. The top row of bands shows uncleaved PCR product at 698 bp, the middle row of bands shows cleaved products at 432 bp, and the bottom row of bands shows cleaved products at 266 bp.

1.2. SpG and SpRY, like WT SpCas9, exhibit low tolerance to mismatches in the protospacer

To analyze the specificity of these proteins, we investigated their sensitivity to mismatches located in the protospacer sequence. Remarkably, SpG and SpRY were similarly sensitive to mismatches proximal to the PAM (positions +1 and +5) at both 25 and 37°C (**Figure 35A)**. Then, we validated the tolerance to mismatches *in vivo* by scoring a dominant phenotype caused by *dpy-10* targeting, using SpG with the matched guide and a guide with a mismatch at position +5 (**Figure 35B).** We observed that a single mismatch almost completely abolished the *in vivo* activity of SpG, and therefore, the amino acid substitutions in this variant do not lead to

relaxed recognition of the protospacer sequence relative to SpCas9, which is important for maintaining specificity.

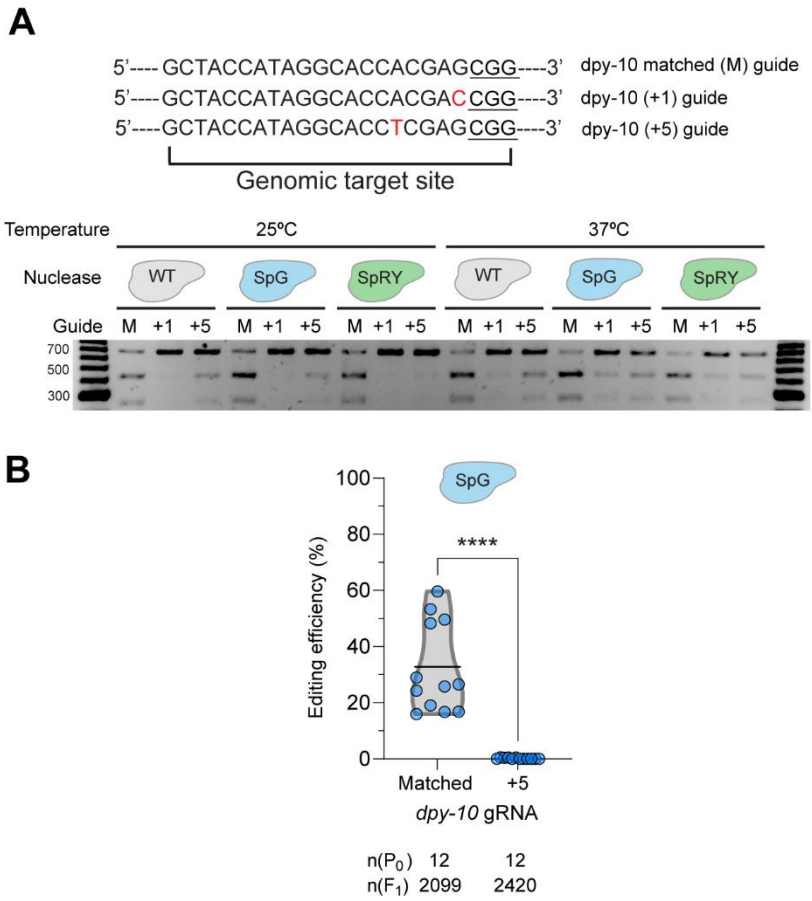

Figure 35. *In vitro* and *in vivo* testing of the mismatch tolerance of SpG and SpRY. (A) Sequences of three guides targeting *dpy-10*: a spacer with perfect complementarity (*dpy-10* matched guide), a spacer with a mismatch 1 nt upstream of the PAM (*dpy-10* +1 guide), and a spacer with a mismatch 5 nt upstream of the PAM (*dpy-10* +5 guide). Nine different RNP combinations comprised of each guide and WT SpCas9, SpG, or SpRY were tested *in vitro* at 25 °C and 37 °C by incubating the RNPs with a *dpy-10* PCR product for one hour. The top row of bands shows uncleaved PCR product at 698 bp, the middle row of bands shows cleaved products at 432 bp, and the bottom row of bands shows cleaved products at 266 bp. (B) The *dpy-10* matched and +5 guides were tested for *in vivo* activity in *C. elegans* by injecting a single gonad arm. The editing efficiency is defined as the number of
(*continued on page 99*)

1.3. SpG and SpRY have lower editing efficiencies in NGG PAMs compared to WT SpCas9

We first used the standard gRNA and ssDNA repair template (to generate the *cn64* allele) for *dpy-10* as used in co-CRISPR assays and found that WT SpCas9 was more efficient than SpG and SpRY in producing *dpy-10* mutations with an NGG PAM. Since the half-life of these nucleases is limited, we scored their efficiency at two different periods and observed that it was lower after 24 hours (**Figure 36**).

(*continued from Figure 35, page 98*)

F_1 progeny with Rol or Dpy phenotypes divided by the total number of F_1 progeny laid by each P_0. Each dot represents the editing efficiency in each individual P_0 that produced at least 100 F_1s. The numbers below the graph indicate the number of P_0s and F_1s included in the analysis. The results are obtained from two independent experiments, with both conditions carried out in parallel injections. The horizontal bars represent the mean. $p<0.0001$ **** (Student's *t*-test)

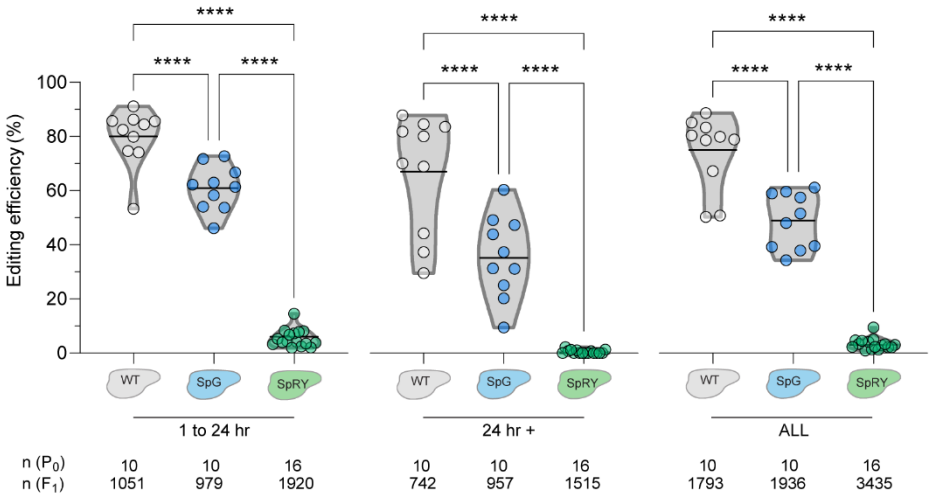

Figure 36. Comparison of WT Cas9 (WT), SpG, and SpRY editing efficiencies at the *dpy-10* locus. RNP concentration at 1.6 µM (250 ng/µl). The left panel includes F_1 progeny laid between 1 and 24 hr post-injection, the middle panel includes F_1 progeny laid after 24 hr post-injection, and the right panel includes all F_1 progeny, all from the same set of injected P_0s. The editing efficiency is defined as the number of F_1 progeny with Rol or Dpy phenotypes divided by the total number of F_1 progeny laid by each P_0. Each dot represents the editing efficiency in each individual P_0 that produced at least 100 F_1s. The numbers below the graph indicate the number of P_0s and F_1s included in the analysis. The data are derived from two independent experiments, with all three conditions carried out in parallel injections. The horizontal bars represent the mean. $p<0.0001$ **** (One-way ANOVA followed by Tukey's test for multiple comparisons).

We targeted an additional locus to confirm the gradient of efficiency SpCas9 > SpG > SpRY on NGG PAMs by scoring for the absence of fluorescence in F_2 animals using an endogenous *gtbp-1*::wrmScarlet reporter. The experimental workflow is similar to the EGFP knockout experiments performed with AsCas12f1 (**Figure 33)**. The results of this experiment corroborated the gradient of activity among the distinct Cas nucleases targeting an NGG PAM, with SpCas9 again having the highest efficiency, and SpRY the least (**Figure 37**).

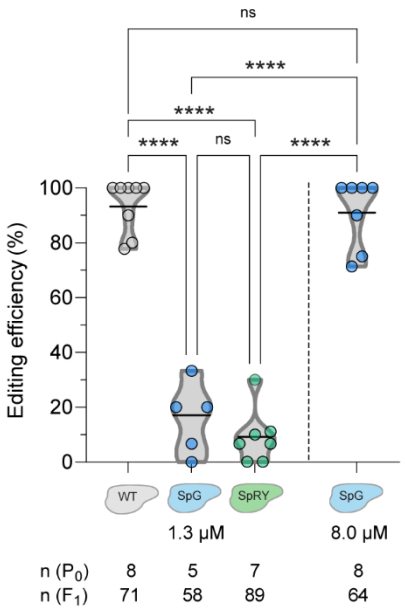

Figure 37. Comparison of WT Cas9 (WT), SpG, and SpRY editing efficiencies at the wrmScarlet locus. An anti-wrmScarlet guide with NGG PAM was complexed with SpCas9, SpG, or SpRY to compare their *in vivo* efficiencies in *C. elegans*. Each of the three RNP combinations were injected in parallel at a final concentration of 1.3 µM (1x, 200 ng/µl); and in a separate experiment, the SpG-anti-wrmScarlet (NGG) RNP was injected at a final concentration of 8.0 µM (6x, 1,200 ng/µl). The editing efficiency is defined as the number of F_1 worms exhibiting loss of fluorescence in the F_2 divided by the total number of separated *dpy-10* co-edited F_1s. Each dot represents the editing efficiency in each individual P_0 that produced at least five Dpy or Rol F_1s. The data are derived from a single experiment. The numbers below the graph indicate the number of P_0s and F_1s included in the analysis. The horizontal bars represent the mean. ns: no significant difference, $p<0.0001$ **** (One-way ANOVA followed by Tukey's test for multiple comparisons).

The results of the initial Nested CRISPR experiments demonstrated that Cas9 concentrations can be raised six-fold without any apparent toxicity. Thus, when a six-fold higher concentration (8µM in the injection mix) of SpG was used, the efficiency of wrmScarlet targeting by SpG increased to a level similar to that of WT SpCas9 (**Figure 37**).

2. Characterization of SpG and SpRY in NGC and NAC PAMs.

We characterized the activity of SpG and SpRY using the wrmScarlet knockout approach. In human cells, SpG and SpRY work on NGN and NYN targets, respectively (Walton et al., 2020). Since it has been demonstrated that WT SpCas9 already has minor activity in non-canonical NGA and NAG targets (Walton et al., 2020; Yilan Zhang et al., 2014), focus was given on the characterization of SpG and SpRY activities in NGC and NAC targets, respectively (**Figure 38**).

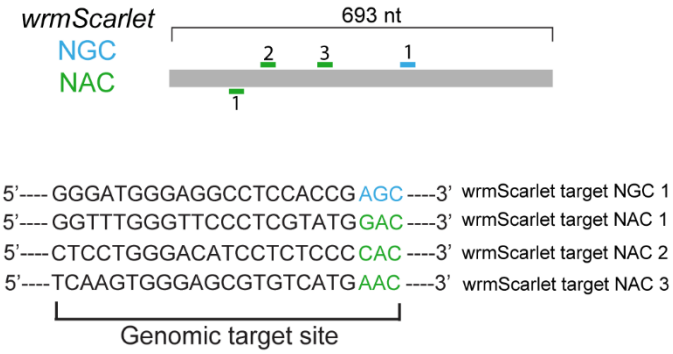

Figure 38. Location of NGC and NAC targets at the wrmScarlet locus. Diagram illustrating one crRNA with an NGC PAM (blue) and three crRNAs with NAN PAMs (green) targeting wrmScarlet.

2.1. SpG activity in an NGC target is concentration-dependent

To implement the use of SpG for genome editing in *C. elegans*, it was necessary to check whether RNP concentration is also critical for SpG efficiency on NGC PAMs. Similar to observations in the NGG PAM target using the wrmScarlet knockout approach (**Figure 37**), the efficiency of SpG is enhanced when the concentration is increased from 1.3 to 3.7 to 8.0 µM (**Figure 39**).

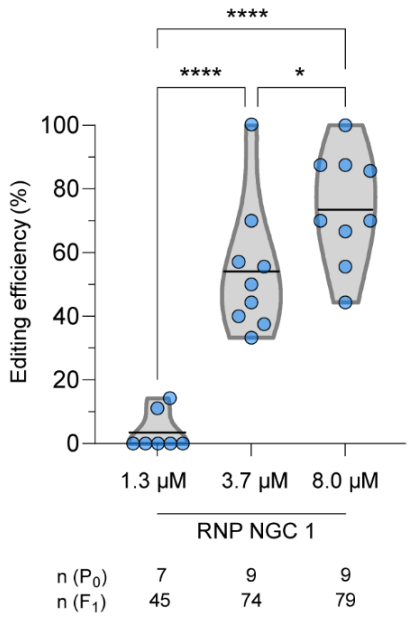

Figure 39. Titration of SpG RNP concentration in *C. elegans*. Three distinct concentrations of SpG RNP, with the anti-wrmScarlet NGC guide 1, were tested in a strain expressing the *gtbp-1*::wrmScarlet reporter (CER541). Editing efficiency is defined as the number of F_1 worms exhibiting loss of fluorescence in the F_2 divided by the total number of separated *dpy-10* co-edited F_1s. Each dot represents the editing efficiency in each individual P_0 that produced at least ten Dpy or Rol F_1s. The numbers below the graph indicate the number of P_0s and F_1s included in the analysis. The data are derived from a single experiment and all three conditions were carried out in parallel injections. The horizontal bars represent the mean. $p<0.05$ *, $p<0.0001$ **** (One-way ANOVA followed by Tukey's test for multiple comparisons)

2.2. SpG activity is not affected by high salt concentrations

Since the purified nucleases are stored in a high salt buffer (500 mM KCl), it was necessary to test whether the higher salt concentrations accompanying the increasing nuclease concentrations would have an effect on editing efficiency. Therefore, two injection mixes containing the standard (50 mM) and six-fold higher (300 mM) KCl concentrations were tested in a CRISPR-SpG experiment targeting an NGC or NGG PAM while keeping the nuclease concentration constant (1.3 µM). Similar editing efficiencies were observed at the wrmScarlet (NGC) and *dpy-10* (NGG) loci in both conditions. Thus, the higher salt concentrations due to a six-fold increase in nuclease volume in the injection mix does not affect editing efficiency (**Figure 40**).

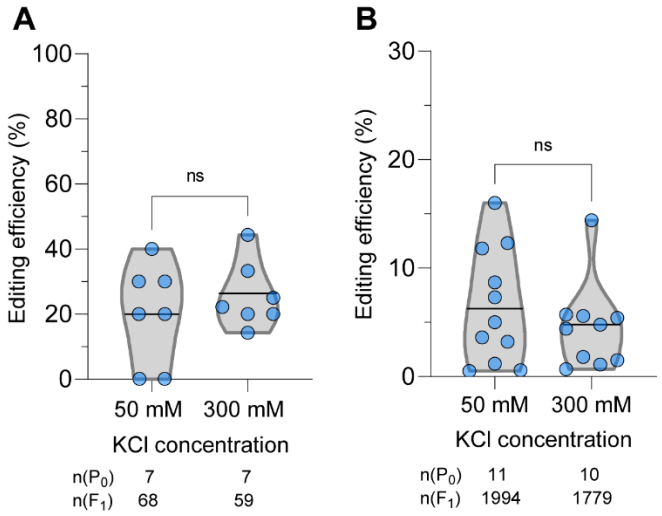

Figure 40. High salt concentrations do not affect the editing efficiency of SpG RNPs *in vivo*. The standard 1.3 µM RNP concentration was used in this experiment. (A) wrmScarlet knockout assay (NGC PAM). The editing efficiency is defined as the number of F_1 worms exhibiting loss of fluorescence in the F_2 divided by the total number of separated *dpy-10* co-edited F_1s. Each dot represents the editing efficiency in each individual P_0 that produced at least eight Dpy or Rol F_1s. (B) *dpy-10* assay (NGG PAM). The editing efficiency is defined as the number of F_1 progeny with Rol or Dpy phenotypes divided by the total number of F_1 progeny laid by each P_0. Each dot represents the editing efficiency in each individual P_0 that produced at least 100 F_1. The horizontal bars represent the mean. The data are derived from a single experiment, with both conditions carried out in parallel injections. ns: no significant difference (Student's *t*-test).

2.3. SpG is more efficient than WT SpCas9 for targeting an NGC PAM.

To compare the efficiency of SpCas9 and SpG for targeting sites with NGC PAMs, experiments were performed using these nucleases at the highest concentration (8 µM) to produce mutations in *gtbp-1*:wrmScarlet. We observed that SpG was more efficient than SpCas9 when targeting a site with an NGC PAM (**Figure 41**).

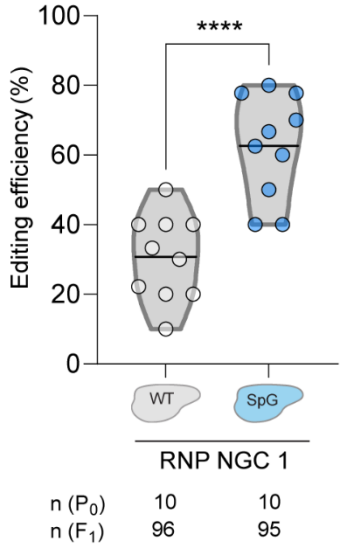

Figure 41. Comparison of editing efficiencies between WT SpCas9 and SpG in a wrmScarlet NGC target. The RNP concentration used in all conditions is 8.0 µM. Editing efficiency is defined as the number of F_1 worms exhibiting loss of fluorescence in the F_2 divided by the total number of separated *dpy-10* co-edited F_1s. Each dot represents the editing efficiency in each individual P_0 that produced at least ten Dpy or Rol F_1s. The numbers below the graph indicate the number of P_0s and F_1s included in the analysis. The data are derived from two experiments with one replicate each, and conditions belonging to parallel injections are separated by a dashed line. The horizontal bars represent the mean. ns: no significant difference, $p<0.0001$ **** (Student's *t*-test)

2.4. SpRY activity in NAC targets is concentration-dependent

Since SpRY has a wider targeting range than SpG, further analysis was focused on the evaluation of SpRY activity in three different NAC targets in the *gtbp-1*:wrmScarlet locus. First, the *in vitro* capacity of WT SpCas9, SpG, and SpRY to cleave dsDNA targets with NAC PAMs was assessed. *In vitro*, SpRY had the highest cutting efficiency at all three target sites harboring an NAC PAM (**Figure 42**). As expected, SpG was also capable of efficiently cutting two of the targets *in vitro*. This may be due to the minor but still detectable SpG activity as previously observed at NAC sites in mammalian cells (Walton et al., 2020).

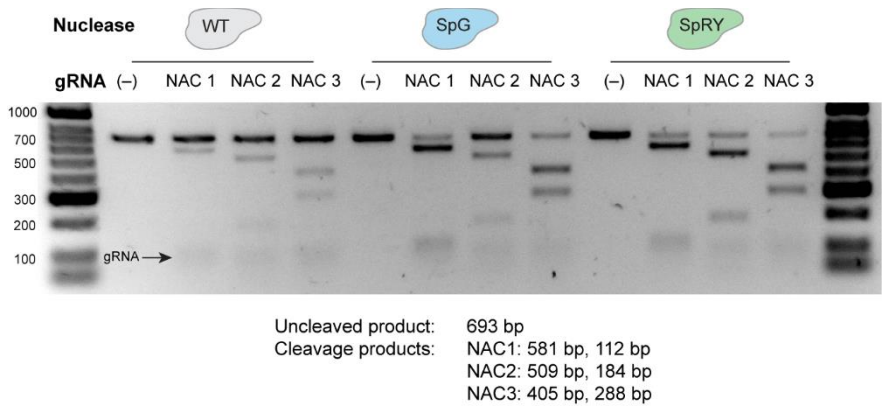

Figure 42. *In vitro* analysis of the cleavage activities of three anti-wrmScarlet NAC RNPs. Different RNP combinations comprised of each guide and WT SpCas9, SpG, or SpRY were tested *in vitro* at 37°C by incubating the RNPs with wrmScarlet PCR product for one hour. The top row of bands shows uncleaved PCR product at 693 bp and the specific cleavage products for each guide are specified in the figure. The gRNA appears as a faint band at approximately 100 bp.

When tested *in vivo*, higher concentrations of SpRY RNP significantly enhanced its activity in one of the analyzed targets, similar to observations of concentration-dependent activity in SpG (**Figure 43**). Finally, the

efficiencies of SpRY and WT SpCas9 in one of the targets with a high level of mutagenesis (NAC 2) were compared, and results demonstrate that SpRY is much more effective than SpCas9 for editing NAC PAMs *in vivo* (**Figure 40**).

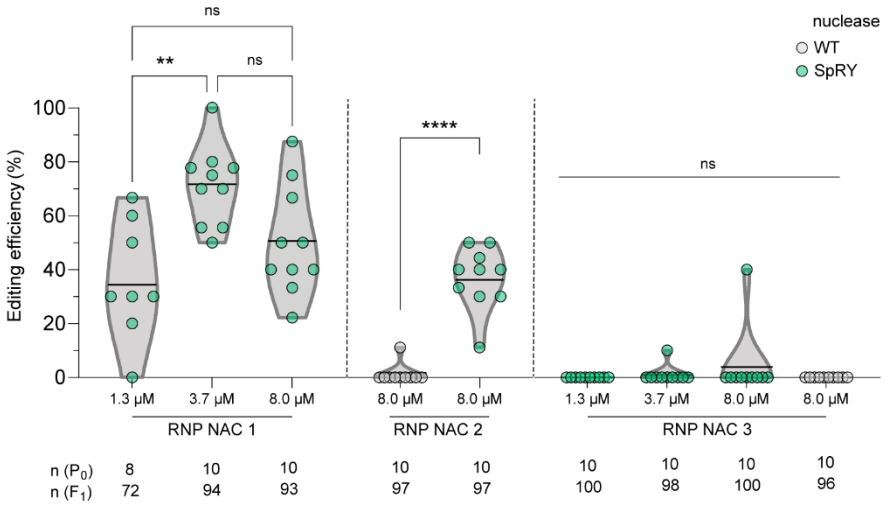

Figure 43. *In vivo* analysis of the three anti-wrmScarlet NAC gRNAs. A titration of three distinct SpRY RNP concentrations was performed for guides 1 and 3 while guide 2 was tested at 8.0 µM only. Additionally, the editing efficiency of WT SpCas9 in NAC sites was evaluated using guides 2 and 3. Editing efficiency is defined as the number of F_1 worms exhibiting loss of fluorescence in the F_2 divided by the total number of separated *dpy-10* co-edited F_1s. Each dot represents the editing efficiency in each individual P_0 that produced at least ten Dpy or Rol F_1s. The numbers below the graph indicate the number of P_0s and F_1s included in the analysis. The data are derived from three experiments with one replicate each, and conditions belonging to parallel injections are separated by a dashed line. The horizontal bars represent the mean. ns: no significant difference, $p<0.01$ **, $p<0.0001$ **** (One-way ANOVA followed by Tukey's test for multiple comparisons [NAC 1 and 3], Student's *t*-test [NAC 2]).

By sequencing some of the worms that had wrmScarlet knockouts, it can be seen that the DSBs produced by both SpG and SpRY lead to the formation of indels near the cut site, analogously to SpCas9, regardless of the PAM (**Figure 44**).

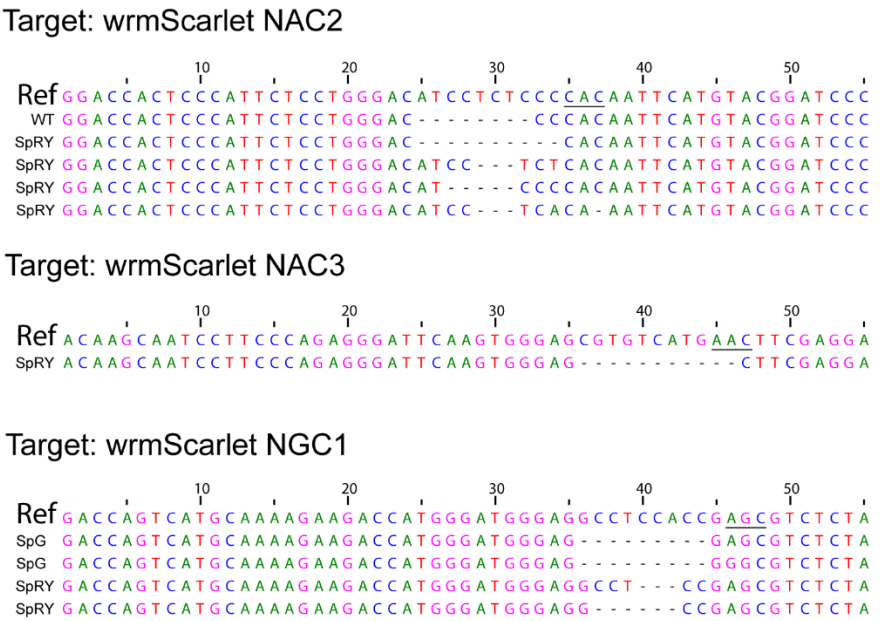

Figure 44. Examples of mutations obtained with WT SpCas9, SpG, and SpRY RNPs in wrmScarlet targets. Each sequence is derived from individual worms consisting of F_2 wrmScarlet knockouts. WT, SpG, and SpRY indicate the nuclease used to edit the genome. The reference sequence (Ref) is provided as the first sequence in each group of alignments. The PAM sequence is underlined; -: deletion.

3. The predictive gRNA efficiency algorithm CRISPRscan mirrors *in vivo* editing efficiencies

It is interesting to note that a correlation was found between *in vivo* efficiency and CRISPRscan[1] scores in the wrmScarlet locus, in which five targets were tested (**Figure 45**). For example, while the NAC 3 target with a CRISPRscan score of 39 showed very low activity even in optimized conditions (4%), targets predicted to be highly efficient (NAC 1, NAC 2, NGC1 and NGG), with scores of more than 70, showed a drastic increase in activity. However, it must be noted that CRISPRscan is based on the

analysis of the efficiencies of *in vitro* transcribed gRNAs in zebrafish (Moreno-Mateos et al., 2015). A different approach was used in *C. elegans* wherein RNPs were injected, which can influence the final SpG or SpRY activity since RNPs can protect from *in vivo* gRNA degradation and increase the half-life of unstable gRNAs (Burger et al., 2016; P. Liu et al., 2019; Moreno-Mateos et al., 2017). Nevertheless, the *in vivo* results obtained in *C. elegans* suggest that CRISPRscan could help in the selection of the most efficient targets for SpG and SpRY.

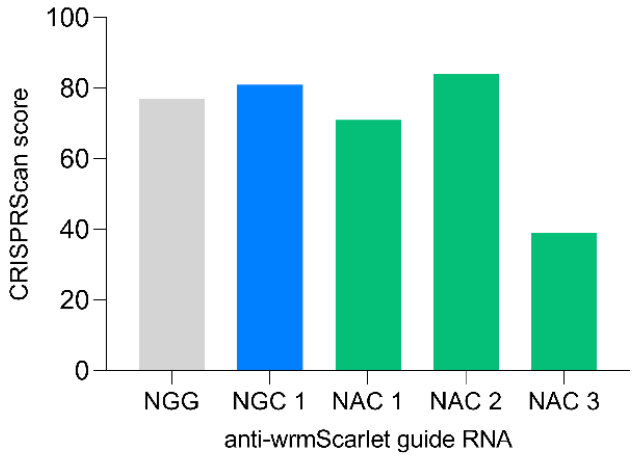

Figure 45. CRISPRscan scores for the anti-wrmScarlet guide RNAs. Each set of PAMs were evaluated with the corresponding algorithm (NGG evaluation for the NGG guide, NGN evaluation for the NGC 1 guide, and NYN evaluation for the three NAC guides).

4. SpG and SpRY can facilitate HDR-mediated genome editing

To further support the use of SpG and SpRY in *C. elegans*, the efficiency of SpG and SpRY for precise HDR-mediated genome editing was evaluated by generating missense mutations and fluorescent reporters. First, by choosing an NGN PAM target closer to the edit of interest compared to a site with an NGG PAM, the R350C substitution (which mimics a human cancer mutation) was introduced into the *C. elegans* protein SWSN-4/SMARCA4 with an efficiency of 10% among *dpy-10* co-edited animals (**Figure 46A**). Then, using SpG, translational reporters were generated by fusing wrmScarlet at the C-terminal end of two genes (*usp-48* and *trx-1*) which lack an NGG PAM proximal to the stop codon (**Figure 46B**). Specifically, SpG was used to facilitate step 1 of the Nested CRISPR protocol. Among *dpy-10* co-edited worms, 19.7% and 13.1% of inserts were obtained at the USP-48 and TRX-1 C-terminal ends, respectively. In addition, a GFP:H2B transcriptional reporter was generated by replacing the entire W05H9.1 coding sequence for the GFP:H2B tag. In this case, SpCas9 was used to cut at the C-terminal end, and SpG to cut at the N-terminal end (**Figure 46B**). The step 1 Nested CRISPR efficiency for this reporter was 6.6% among *dpy-10* co-edited worms. Finally, a translational reporter for *cep-1* was created using SpRY with the stop codon TAA serving as an NAA PAM, with a step 1 efficiency of 4.8% among *dpy-10* co-edited worms (**Figure 46B**).

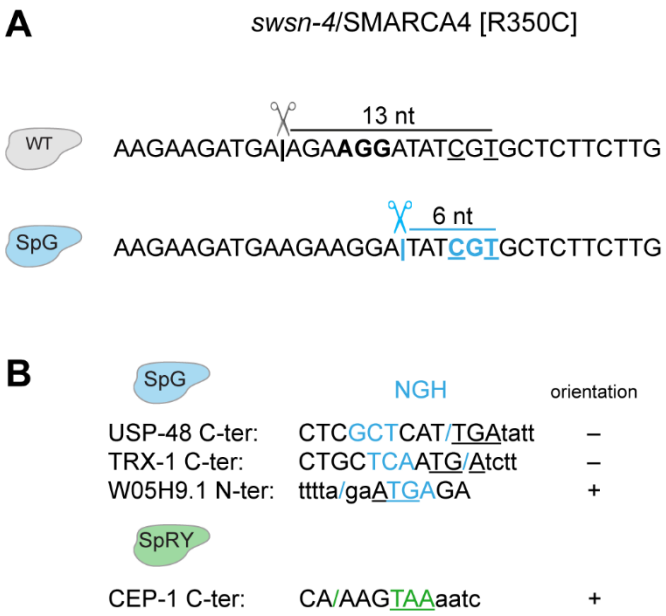

Figure 46. Utility of SpG and SpRY RNPs for precise genome editing. (A) Use of SpG for the generation of the *swsn-4*/SMARCA4 [R350C] substitution. Nucleotide substitutions corresponding to the amino acid change are underlined and PAMs for each nuclease are indicated in bold. (B) Use of SpG and SpRY for the insertion of DNA sequences via HDR. By Nested CRISPR, the USP-48, TRX-1, and CEP-1 proteins were tagged endogenously with wrmScarlet at their C-terminus while a GFP::H2B transcriptional reporter was generated for W05H9.1. In the case of *usp-48* and *trx-1* which required a single cut near the stop codon (underlined), SpG-targetable NGH PAMs (blue) were selected. In the case of W05H9.1, an SpG-targetable NGH PAM (blue) was chosen near the start codon (underlined). In the case of *cep-1*, an SpRY-targetable NAN PAM (green) was at the stop codon (underlined). /: cut site, +: sense orientation, -: antisense orientation. The SWSN-4, TRX-1, W05H9.1, and CEP-1 experiments were performed by David Brena and Mariona Cots.

The widespread use of Cas9 variants in *C. elegans* can be promoted by the creation of transgenic strains that endogenously express these nucleases in the germline. Starting from a strain expressing SpCas9 in the germline (SpCas9e) under the control of the *mex-5* promoter (B. Yang et al., 2020), we introduced mutations by CRISPR to obtain a modified strain that produces SpG instead of SpCas9. By injecting only crRNA and tracrRNA, the mutagenic capacity of these two strains were tested on an NGT *dpy-10* PAM target. We observed that animals expressing SpG endogenously in the germline (SpGe) were more efficient than those expressing SpCas9 when targeting this NGT PAM (**Figure 47**). Both dominant and recessive phenotypes for *dpy-10* were observed. However, there were no obvious discriminatory features between the pattern of indels generated in both phenotypes (**Figure 48**).

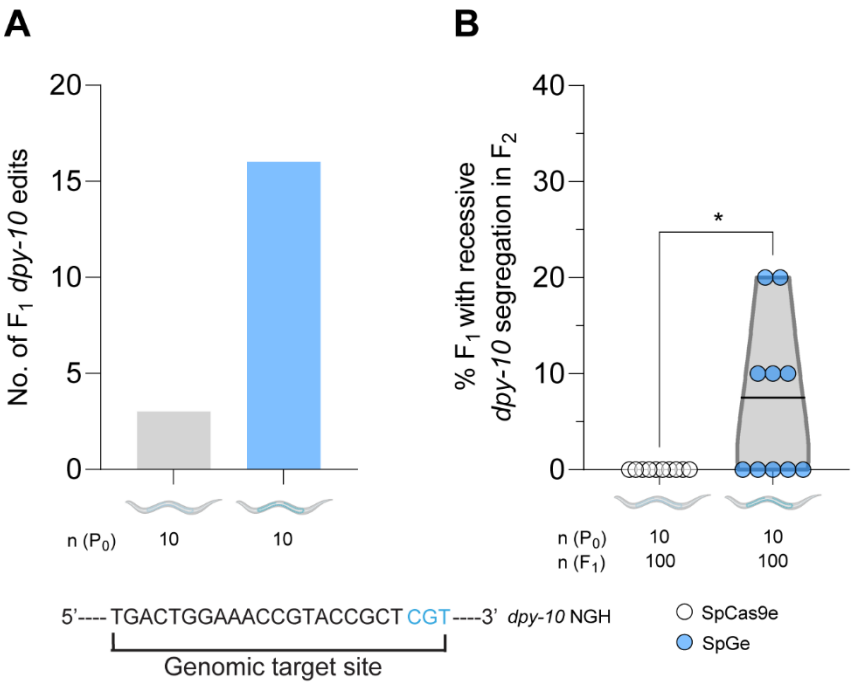

Figure 47. SpGe is more efficient than SpCas9e in an NGT PAM. EG9615 and CER660 worms which express SpCas9 and SpG endogenously in the germline (SpCas9e and SpGe), respectively, were injected with tracrRNA and a crRNA targeting *dpy-10* with an NGT PAM. (A) The total number of F_1 progeny exhibiting dominant Rol or Dpy phenotypes was counted from 10 injected P_0 hermaphrodites. (B) The fluorescent markers *myo-2p*::mCherry and *myo-3p*::mCherry were used as co-injection markers. F_1 worms expressing mCherry in the pharynx or body wall muscle were singled out and the appearance of a recessive Dpy phenotype was screened in the F_2. Editing efficiency is defined as the number of F_1 worms that segregated Dpy progeny in the F_2 divided by the total number of separated F_1s. Each dot represents the editing efficiency in each individual P_0 that produced at least ten mCherry-expressing F_1s. The data are derived from a single experiment and all conditions were carried out in parallel injections. $p<0.05$ * (One-way ANOVA followed by Tukey's test for multiple comparisons). The CER660 strain was generated by Dmytro Kukhtar.

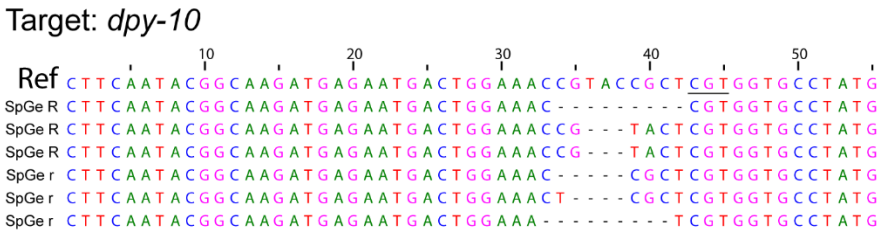

Figure 48. Examples of mutations obtained with SpGe in a *dpy-10* NGT target. Each sequence is derived from individual worms that exhibited either a dominant (R) or recessive (r) Dpy phenotype. SpGe indicates that the animals were edited using the endogenously expressed SpG from the germline. Ref is the reference sequence and the PAM sequence is underlined; -: deletion.

In summary, these experiments demonstrate that the near-PAMless Cas9 variants SpG and SpRY can efficiently mediate genome editing through both error-prone and precise repair mechanisms. Furthermore, it has been demonstrated that a strain that endogenously expresses SpG in the germline can facilitate genome editing in targets with an NGH PAM. However, this has currently only been tested in one target and further validation in more targets is required.

DISCUSSION

1. Pushing the limits of insertion: the origins of Nested CRISPR

Our lab initially attempted performing CRISPR–Cas9-mediated insertions of fluorescent tags in *C. elegans* using PCR products with 35-bp homology arms as donors (Paix et al., 2015). However, we found that this method was not as efficient as originally reported and this discrepancy has been corroborated by other colleagues within the field (Dokshin et al., 2018). One possible reason to explain this outcome is that the characterization of the cloning-free approach by Paix and colleagues was mostly centered on a single locus, *gtbp-1*. When the authors themselves tested their method on different loci, they recognized that the editing efficiency was influenced by the high efficiency of the sgRNA targeting *gtbp-1* (Paix et al., 2015). Another factor that may have influenced the reproducibility of results is the difference in the type of reagents used. Paix et al. purified their own proteins while we used commercial Cas9 whereas other reagents (tracrRNA and crRNA) were purchased from different suppliers.

Although Nested CRISPR was initially conceived to produce reporters with standard FPs, it can also be adapted for gene replacements in the future. The size limit of insertions is relevant in gene replacement studies, where orthologs in model organisms are replaced with their human counterparts with the aim of observing phenotypic rescue to confirm its functional conservation. If the human protein is functional, then the impact of human pathogenic variants or chemical inhibitors can be evaluated. The first report of gene replacement in *C. elegans* involves the replacement of the worm *daf-18* ortholog with the human PTEN (phosphatase and tensin) coding sequence which is 1,209 bp long (McDiarmid et al., 2018). Considering that the average human protein-coding gene has ten 160-bp coding exons (Piovesan et al., 2019), and that introns may need to be included to

modulate gene expression, the size limit of insertions should be constantly pushed to facilitate replacement with larger genes in the future.

In the second step of Nested CRISPR, we have efficiently inserted DNA fragments ranging from 582 bp (wrmScarlet) to 1215 bp (GFP::H2B). By generating constructs of wrmScarlet with varying lengths, I was able to systematically study the relationship between insertion length and editing efficiency. Thus far, insertions of up to 1,608 bp have been successful. Although the efficiency obtained was quite low (4%), it is sufficient for obtaining at least two independent lines by screening a reasonable number of F_1 progeny (e.g., in this case, 50 F_1s given an editing efficiency of 4%). However, this trend has only been assessed in one target and further validation of this observation is required.

Other studies in *C. elegans* demonstrate variable success. Following the Paix protocol, Silva-García et al. (2019) used a very efficient *dpy-10* gRNA to insert a **2.3 kbp** fragment into their single-copy knock-in loci for defined gene expression (SKI LODGE) strains with an efficiency of 2%. Meanwhile, using a recombineering approach, Paix and colleagues (2016) demonstrated that a fragment of identical size can be inserted with an efficiency of 5% using three overlapping PCR products. Using a similar recombineering approach involving four overlapping PCR products, Philip et al. (2019) inserted a **3.5 kbp** fragment in a method called *Mos1* element-mediated CRISPR integration (mmCRISPi) with an efficiency of 9%. This method involved using three crRNAs that targeted the *Mos1* transposon at three defined loci at chromosomes I, II, and IV, facilitating the creation of multiple *Mos1* insertions using the same reagents.

On the other hand, Dickinson and colleagues (2015) compared the use of plasmids with long homology arms (500–700 bp) and PCR products with short homology arms (35–40 bp) for inserting a **6.5 kbp** fragment. The former was successful in 7 of 8 loci tested whereas the latter was successful in only 2 of 8 loci, meaning that the use of plasmids with long homology arms is more desirable when attempting longer insertions. However, if the insertion is large (several kbp) but the distance from the cut site to the insertion is small (short-range HDR), plasmids with either long or short homology arms can be used as repair templates as both result in similar editing efficiencies (Schwartz & Jorgensen, 2016). Finally, by first generating two DSBs that result in a 340 bp deletion, Farboud et al. (2019) were able to insert a long dsDNA template of **9.3 kbp** provided as a plasmid. This strategy led to a 5% co-conversion rate whereas attempts to insert a DNA fragment of this length were unsuccessful when only one DSB was generated. This may indicate that spatial or topological constraints may act during templated repair.

One avenue that is currently unexplored in *C. elegans* is the insertion of large DNA fragments via CRISPR–dCas9-mediated transposition. In particular, *piggyBac* (PB) transposable elements have been widely used for the integration of transgenes in mammalian cells and other species (Eckermann et al., 2018; S. C. Y. Wu et al., 2006; Yusa et al., 2011). The fusion of transposases to dCas9 proteins is an attractive approach due to its minimal cellular toxicity (Eckermann et al., 2018) and large cargo capacities of up to **100 kbp** (M. A. Li et al., 2011).

1.1 Advantages of Nested CRISPR

The Nested CRISPR approach has several advantages and has shortened the time needed to create endogenous reporters in our lab. While we previously spent months performing CRISPR experiments attempting to generate reporters of six distinct genes and being successful only once, by following the Nested CRISPR method we have succeeded in most of our attempts to make endogenous fluorescent reporters (**Table 6**). Since all the required elements are commercially available and the reagents and conditions for the second step are universal, other researchers should be able to reproduce our success rate. Thus, this method is feasible for researchers with limited knowledge of molecular cloning and will facilitate the production of endogenous reporters that more closely reflect the real expression patterns of a given gene, as compared to extrachromosomal arrays or when randomly integrated into genome as multicopies.

The **first step** of Nested CRISPR takes advantage of the fact that the insertion of shorter fragments of DNA of up to ~130 bp using ssODNs is a highly efficient process (Paix et al., 2016; Ward, 2015). This is of great value considering that the first step is locus-specific and must therefore use a different gRNA for each target gene. Therefore, step 1 insertions can be obtained with relative ease despite potential differences in gRNA efficiency. In addition, step 1 injections for the transcriptional reporter pipeline result in a useful intermediate strain that is comprised of a deletion mutant.

On the other hand, the **second step** involves the more challenging process of inserting long dsDNA fragments. However, the use of highly efficient, universal gRNAs means that editing efficiencies are not undermined by using gRNAs with poor stability or activity. In addition, due to the universal nature of the second step, the same injection mix can be used for the same type of FP tag, demonstrating the scalability of Nested CRISPR.

The modular and flexible nature of the second step of Nested CRISPR provides the opportunity to customize the FP construct after successful step 1 injections. For instance, once the 1-3 fragment is inserted, the sequence of the dsDNA repair template for the second step can be modified to avoid piRNA-mediated transgene silencing in the germline (Frøkjær-Jensen et al., 2016; W.-S. Wu et al., 2018) or to alter protein expression levels by modifying codons according to the codon adaptation index (Redemann et al., 2011). The number, length, and sequences of introns can also be modified in the second step. This is relevant because the number and length of introns can influence the transcriptional rate, and the sequence of these introns can influence germline silencing (Frokjaer-Jensen, 2013; Heyn et al., 2015). In fact, one of the synthetic PATC introns we added to the original wrmScarlet construct to increase its length from 693 bp to 1,179 bp resulted in a reduction in the expression of the GTBP-1::wrmScarlet reporter.

1.2 Limitations of Nested CRISPR

Compared to other methods, the Nested CRISPR approach requires two rounds of injections, and the intermediate strains from the translational reporter pipeline do not serve another purpose aside from serving as a landing pad for the larger dsDNA insertion step. In addition, separate step 1 injections must be performed for each different FP tag that the researcher wishes to introduce in the same locus (e.g., a *gtbp-1*::EGFP1-3 step 1 strain will not serve for the creation of *gtbp-1*::mCherry or *gtbp-1*::wrmScarlet reporters).

To circumvent this issue, we developed the one-shot Nested CRISPR approach that facilitates the generation of endogenous fluorescent reporters in as short as six to eight days (in homozygosis). Despite the variable success of the one-shot approach (**Table 10**), in-frame step 1 insertions are always obtained and can be used for a succeeding round of step 2 injections in cases where the complete FP sequence fail to be inserted in a single injection.

On other hand, the need for homozygous animals with the 1-3 fragment in our deletion plus transcriptional reporter pipeline is a handicap for essential genes (approximately 20% of genes) whose deletions need to be maintained as heterozygous strains. In these cases, the one-shot approach can be considered as an option, followed by crossing of the heterozygous transcriptional reporter to a genetic balancer.

Finally, the injection mixes for Nested CRISPR typically require very high concentrations of PCR product (~1 uM or ~500 ng/ul for EGFP, **Table 19**). Although the step 2 injection mix is universal and can be used for several rounds of microinjection, the amounts of purified PCR product from eight 50-µL reactions are usually sufficient for preparing up to only two 10-µL injection mixes. In addition, high-fidelity polymerases must be used to ensure that the repair template is as accurate as possible. Therefore, the use of plasmids as repair templates in Nested CRISPR should also be investigated as it has been previously demonstrated that plasmid donors with short homology arms of just 50-60 bp can efficiently direct insertion into the *C. elegans* genome (Schwartz & Jorgensen, 2016). Alternatively, Ghanta & Mello (2020) have proposed that melted dsDNA templates could efficiently channel HDR with donor concentrations as low as 6.25 ng/µl (12.5 pM).

1.3. Practical considerations for endogenous fluorescent reporters

1.3.1. Endogenous expression levels

In some cases, the endogenous expression levels may be so low that GFP fluorescence cannot be observed. There are several approaches to address this problem. The most obvious approach is to use brighter fluorophores, such as mScarlet (Bindels et al., 2017; El Mouridi et al., 2017) or mNeonGreen (Hostettler et al., 2017; Shaner et al., 2013).

In one particular case, the *comt-4p*::mCherry reporter did not exhibit detectable fluorescence probably due to its low endogenous expression level. However, by changing the mCherry tag to GFP::H2B, the FP becomes concentrated in the nucleus, facilitating its visualization. However, as a consequence, any information regarding subcellular localization is lost.

Another approach is to use a split-GFP system wherein the first 10 β-strands (GFP_{1-10}) spontaneously interact with its shorter complement which contains the 11^{th} β-strand (GFP_{11}), reconstituting the barrel-like GFP structure (Cabantous et al., 2005). The target protein is then tagged with multiple copies of GFP_{11}, resulting in signal amplification (He et al., 2019; Kamiyama et al., 2016). The use of brighter split-FP systems such as split super-folder GFP (sfGFP) and split-wrmScarlet has been tested and validated in *C. elegans* (Goudeau et al., 2021; Hefel & Smolikove, 2019).

1.3.2. Autofluorescence

Another common concern with reporter gene fusions is autofluorescence emitted by intestinal lysosome-related gut particles that contain anthranilic acid (Coburn et al., 2013). In addition, bright green autofluorescence appears diffusely throughout the whole body of *C. elegans* upon organismal death, and thus, extreme caution must be exercised when interpreting GFP measures in very old transgenic animals (Pincus et al., 2016). To circumvent this issue, red FPs can be used instead of green FPs, or alternatively, microscopes can be equipped with special filter sets that can separate GFP signal from autofluorescence (Teuscher & Ewald, 2018).

1.3.3. FP properties

Finally, consideration must be given to the fluorophore itself as each FP has key characteristics that might affect their practical use. First, the sensitivity and signal-to-noise ratio of any fluorescence detection technique greatly relies on the brightness of the fluorophore employed. Brighter FPs are advantageous since they require a lower dose of excitation light, translating to lower phototoxic effects (Chudakov et al., 2010). Next, given the rapid development of *C. elegans*, a fluorophore with a fast maturation rate is a very important feature when choosing which FP to use. FP fluorescence occurs after protein folding and chromophore maturation, which involves several successive covalent modifications, and are particularly extensive in orange or red FPs (Chudakov et al., 2010). For instance, long fluorophore maturation times preclude co-translational imaging of FP-tagged nascent peptide chains as well as imaging of short-lived transcription factors critical for development and embryogenesis. By the time the FP folds, matures, and fluoresces, translation may already be over or transcription factors may have already degraded (N. Zhao et al., 2019).

In our hands, there have been a few instances when the integration of FP tags did not result in fluorescence despite positive confirmation of successful insertions via sequencing. In the case of GEI-3::EGFP, this may be due to the intrinsic instability of the target protein fused to the FP, leading to improper folding of either or both proteins. This issue was resolved after using the SL2 trans-splicing sequence to create a transcriptional reporter instead of a protein fusion. In addition, the position of the fusion (C-ter or N-ter) can have different effects depending on the importance of the domains present at each end of the target protein. For instance, the wrmScarlet::F27C1.2 N-terminal fusion resulted in complete sterility in homozygosis whereas the F27C1.2::wrmScarlet C-terminal fusion only led to reduced brood size.

A myriad of other factors can affect the choice of FP when creating reporter gene fusions. These include photostability and undesirable photoconversions, the oligomeric nature of the FP and its tendency to aggregate, as well as pH stability. These factors are extensively reviewed in Chudakov et al. (2010) and other practical considerations for the applications of FPs in *C. elegans* is reviewed in Hutter (2012). Furthermore, recommendations for choosing the appropriate FP for *in vivo* imaging applications in *C. elegans* embryos can be found in Heppert et al., (2016). Finally, FPbase[5] is a free and open-source database for FPs and their properties and is useful for choosing appropriate FPs for specific applications.

2. *C. elegans* is a plausible model for optimizing CRISPR–Cas technologies

The Cas9 nuclease from *Streptococcus pyogenes* (SpCas9) is the most popular enzyme for CRISPR technologies. However, a massive number of Cas effectors are being, and will be, identified and characterized in the search of optimal Cas variants for each of the many applications of CRISPR (Gasiunas et al., 2020; Makarova et al., 2020). In this context, *Caenorhabditis elegans* is a versatile and efficient multicellular system for evaluating different aspects of Cas effectors such as toxicity, specificity, and efficiency (**Figure 49**). Several features make *C. elegans* convenient for genome editing experiments, even though it also has its drawbacks (**Table 13**).

[5] https://www.fpbase.org/

As an example, advances in gRNA design first elucidated in *C. elegans* such as the use of guides with a 3' GG motif immediately before the PAM to increase the frequency of genome editing has been adapted to and/or confirmed in other organisms such as fungi including various *Candida* species (Demuyser et al., 2020; Grahl et al., 2017; Silao et al., 2019); plants such as *Arabidopsis* (De Pater et al., 2018; Pyott et al., 2016; H. Shen et al., 2017) and *Solanum* (Butler et al., 2015); *Drosophila* (Itakura et al., 2018; Tianfang Ge et al., 2016) and other non-model flies (Paulo et al., 2019); and mice (Miyata et al., 2016; Perrin et al., 2017). In addition, the ease of gRNA optimization in *C. elegans* has even led to the insertion of the nematode's DNA sequences into human cells in order to replicate the high degree of gRNA reliability and activity for applications such as labeling and imaging endogenous protein-coding genes.(B. Chen et al., 2018) These examples demonstrate that advancements in *C. elegans* CRISPR design can also be applied to other model and non-model organisms.

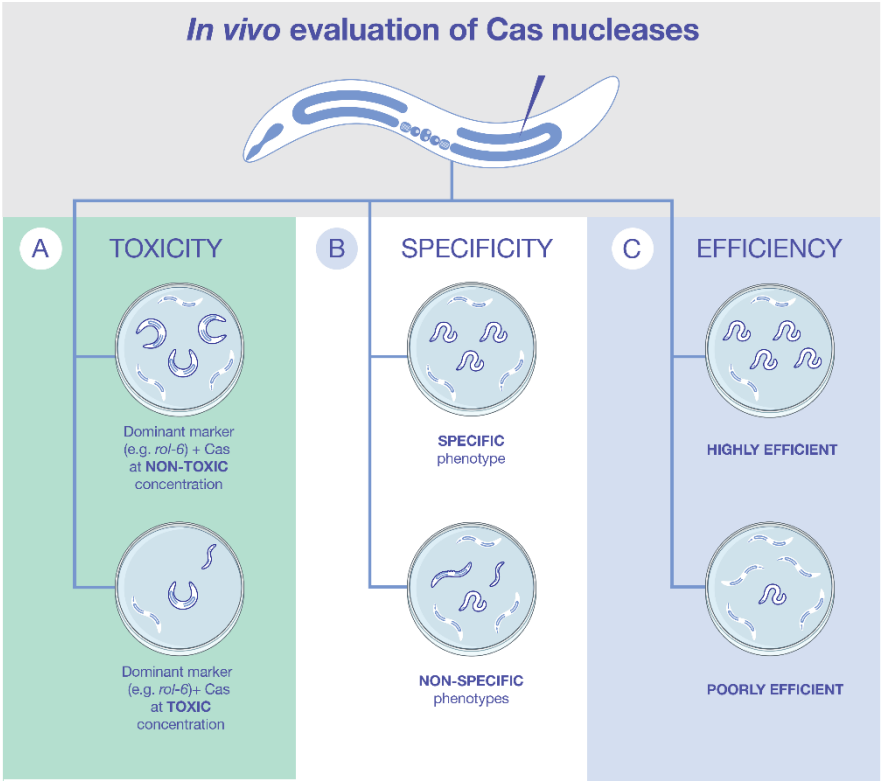

Figure 49. Evaluation of toxicity, specificity, and efficiency for Cas nucleases in *C. elegans*. (A) Toxic effects of Cas nucleases can be inferred from reduced progeny and the presence of unexpected phenotypes in the F_1. The titration of RNP concentrations while keeping a constant dominant marker concentration has been used to reach a compromise between high efficiency and low toxicity (Dokshin et al., 2018). (B) Cas specificity can be evaluated by the number of nonspecific phenotypes observed, indicating tolerance to crRNAs mismatches. (C) The efficiency of Cas nucleases and gRNAs can be easily determined by scoring the proportion of animals which display the expected phenotype. Curved animals represent the dominant roller phenotype caused by a *rol-6* gain-of-function mutation; small animals represent larval arrest, worm with multiple vulvas is representative of unexpected phenotypes, and empty worms represent sterile animals. Reproduced from Vicencio & Cerón, 2021.

Table 13. Strengths and weaknesses of *C. elegans* for genome editing studies

Strengths	Weaknesses
Its rapid life cycle (3 days at 22°C) accelerates CRISPR studies in a multicellular animal and facilitates the investigation of transgenerational impacts of genome editing.	Microinjection can be time-consuming and is a bottleneck for high-throughput approaches.
Multiple offspring can be edited in a single microinjection due to its syncytial germline, facilitating the quantitative evaluation of editing efficiencies.	
Editing events can be easily isolated in homozygosis without the need for crossing with males due to its hermaphroditic state.	Some mechanisms of genome editing and the factors that influence it act differently between *C. elegans* and human cells.
Several mutations can be easily combined through genetic crosses and defined mutants can be used to study genetic pathways influencing CRISPR.	
Its transparency facilitates gene expression and protein localization studies *in vivo*.	CRISPR experiments in *C. elegans* are restricted to its growth temperatures from 15°C to 25°C.
As an invertebrate, *C. elegans* is an animal free from ethical issues for use in CRISPR experiments.	

2.1. Toxicity

In *C. elegans*, dose-dependent Cas9 toxicity has been observed when using concentrations from 25 ng/µl to 500 ng/µl in the injection mix (Dokshin et al., 2018). In addition, there is evidence that donor concentrations higher than 200 ng/µl for ~1 kb donors can be toxic, leading to a reduction in the number of roller transgenics (Ghanta & Mello, 2020; Mello et al., 1991). However, we did not observe any apparent toxicity in our Nested CRISPR experiments wherein some injection mixes contained as much as 1,640 ng/µl of Cas9 (*prpf-4*::egfp Step 2) and up to 1,080 ng/µl of PCR product (*gtbp-1::wrmScarlet*, 1,608 bp construct). This may be due to differences in the purity of the reagents used or the absolute volume of injection mix delivered into the gonad.

Furthermore, the toxicity of CRISPR effectors cannot be quantified by simply counting the progeny since not all microinjections are equal and excessive liquid can flow into the proximal bend of the gonad arm during microinjection, halting oocyte production (Berkowitz et al., 2008). However, by titrating RNP concentrations, Dokshin and colleagues determined that lower concentrations of Cas9 were less toxic but were as equally efficient compared to higher concentrations (Dokshin et al., 2018). By contrast, in our titrations of RNP concentrations for SpG and SpRY, we found that higher concentrations of RNP were necessary for efficient genome editing, but we did not observe any toxic effects when increasing the concentration from 250 ng/µl all the way to 1,200 ng/µl.

The recent discovery of the nuclease *Cje*Cas9 (from the pathogenic bacteria *Campylobacter jejuni*) capable of cleaving DNA even in the absence of gRNA has raised concerns about the toxicity of new Cas nucleases.(Saha et al., 2020) The capacity of these nucleases to generate nonspecific DSBs could be evaluated in *C. elegans* by analyzing apoptosis or using reporters for DSBs (Koury et al., 2018; Lant & Derry, 2013).

Finally, different types of repair templates also appear to have varying degrees of toxicity. For instance, the use of long ssDNA in zebrafish was found to be less toxic than PCR product or plasmid DNA donors when injected at the same mass (Ranawakage et al., 2021). This suggests that the use of ssDNAs may be advantageous since the template copy numbers can be increased without also increasing toxicity. Therefore, even though we were not successful in our attempts to use megamers for HDR-mediated repair, further optimization of their properties may eventually lead to their successful use in *C. elegans*.

2.2. Specificity

An important consideration for any Cas effector is off-targeting, which is the consequence of relaxed specificity in protospacer and PAM recognition. *C. elegans* can help detect off-target effects in different ways. First, guide RNAs (gRNAs) with mismatches can be designed, and their efficiency in cutting and producing mutations could be evaluated via whole-genome sequencing (WGS) of mutant worms (Au et al., 2019; Chiu et al., 2013; Paix et al., 2014). Alternatively, sequencing can be limited to candidate loci that closely resemble the guide sequence instead of performing WGS (Dickinson et al., 2013; Friedland et al., 2013). While these studies demonstrated the rarity of off-target effects induced by Cas9, the case may be different for other nucleases. Thus, it would be prudent to test the

specificity of new Cas effectors as off-target effects may affect important genes for cellular homeostasis or viability.

Specificity is heavily influenced by the gRNA and, therefore, several guidelines for gRNA design relating to the number and position of mismatches have been formulated to reduce off-targeting (Cong et al., 2013; Hsu et al., 2013; W. Jiang et al., 2013; Jinek et al., 2012). Moreover, mismatch tolerance is concentration dependent since lower concentrations of Cas9 and gRNA reduce off-target cleavage (but also reduce on-target cleavage) (Hsu et al., 2013).

In *C. elegans*, it has been repeatedly demonstrated that mismatches at the 5' end of the gRNA can be tolerated (Farboud & Meyer, 2015; Katic & Großhans, 2013; Paix et al., 2014; Ward, 2015). However, mismatches at the 3' end are not tolerated, and is reflected by our results using the Cas9 variant, SpG (**Figure 35**).

2.3. Efficiency

While the generation of missense mutations and knockouts via error-prone repair mechanisms is quite straightforward, the insertion of long DNA fragments via HDR remains more challenging. Therefore, *C. elegans* researchers have tested different strategies to enhance the efficiency of HDR-mediated repair.

2.3.1. Repair template modifications

A few studies have proposed modifications in dsDNA templates to improve the efficiency of genome editing. These studies suggest the use of 5' modifications in the dsDNA donors (Ghanta et al., 2018) and the use of hybrid PCR products with 120 bp of ssDNA overhangs (Dokshin et al., 2018). The generation of hybrid PCR products requires long primers (140 nt) that may need to be optimized, whereas in comparison, the PCR conditions for the second step in Nested CRISPR are already optimized, and the product can be reused for several experiments. More recently, Ghanta & Mello (2020) have suggested that melting, then reannealing, of dsDNA donors increases knock-in efficiencies via an unknown mechanism. However, it is currently unknown if this phenomenon is sequence-independent, as it has only been reported with GFP. We have attempted to replicate this protocol in our lab for wrmScarlet and GFP::H2B insertions with very limited success.

2.3.2. Modulating the balance between DSB repair mechanisms

A key dynamic in the repair of DSBs is the modulation between the different repair pathways. Even though HDR is already the preferred pathway for the repair of DSBs in the *C. elegans* germline (Clejan et al., 2006b), different strategies for tipping the balance even further towards HDR have been tested, especially in the context of CRISPR–Cas genome editing, albeit with mixed results.

First, Ward (2015) demonstrated that temporary inhibition of the NHEJ pathway by performing RNAi of the Ku80 *C. elegans* homolog *cku-80* boosted the efficiency of HDR as an increase in the number of knock-ins were detected when using ssDNA as a repair template. However, since a canonical role for NHEJ has been ruled out for CRISPR–Cas9-mediated germ cell transformation (van Schendel et al., 2015), this suggests that HDR may occur outside the germline. Indeed, experiments by Farboud et al., (2019) demonstrate that genome editing can occur in embryos after pronuclear fusion.

By contrast, inhibition of the TMEJ pathway by using *polq-1*-deficient animals did not improve the efficiency of HDR (van Schendel et al., 2015). However, as the main pathway implicated in error-prone repair in the *C. elegans* germline, the inhibition of TMEJ resulted in the reduction of successful CRISPR-Cas9 targeting by six-fold while also leading to ~1,000-fold larger deletions (van Schendel et al., 2015).

2.4. Limitations of screening approaches

During our investigations of the *in vivo* activity of several Cas effectors, one of the challenges that we encountered was to find a high-throughput screening approach that permitted the quantitative evaluation of editing efficiencies. While the EGFP and wrmScarlet knockout assays were straightforward and did not rely on HDR, it entailed the separation of hundreds of F_2 progeny, translating to both increased hands-on time and resources. Therefore, screening should be ideally performed in F_1 animals.

We attempted to use *dpy-10* for this purpose since we expected that most mutations in the highly conserved RXXR motif (Kramer & Johnson, 1993) would lead to a dominant phenotype, as in the case of the R91C substitution in the *cn64* allele. Our initial experiments with Cas12a in the CER603 strain supported this hypothesis, since sequencing of F_1 rollers revealed that the dominant phenotype was not caused by a specific mutation, but rather, by small indels within the RXXR motif that led to the gain or loss of a few amino acids, or by indels that led to frameshifts. However, to our surprise, we discovered that this approach did not work as well for the near-PAMless Cas9 variants, with some mutations producing recessive phenotypes instead (**Figure 48**).

Therefore, a plausible screening strategy would be one that combines the discrete on/off properties of a FP knockout approach and screening in the F_1 generation. One example is by using the traffic light reporter (TLR) approach (Certo et al., 2011) which is based on the targeting of a “broken” GFP sequence followed by a frameshifted mCherry reporter. The advantage of this method is that it can distinguish between precise and imprecise editing events, based on whether green or red fluorescence is observed. HDR-mediated repair produces a green signal whereas imprecise repair restores the reading frame in a subset of indels, producing red fluorescence.

In addition, technologies such as the COPAS worm sorter (Union Biometrica) can be used to separate worms as a function of fluorescence (Pulak, 2006), permitting high-throughput screening that facilitates the study of editing efficiencies .

3. Expanding the targeting range: going beyond wild-type SpCas9

There are hundreds of thousands of CRISPR effectors in nature, and this diversity would grow exponentially if we consider our capacity to modify their protein sequences (F. Zhang, 2019). An expanded catalog of Cas proteins would help advance genome editing and would allow researchers to better adapt to distinct requirements. For instance, SpCas9, which has about 1500 amino acid residues (AARs), could be considered bulky for packaging inside nanoparticles. Instead, variants of CasX (Cas12e) (≈ 1000 AARs) or Cas12f (≈ 500 AARs) are considerably smaller and can better fit inside nanoparticles (Karvelis et al., 2020; J. J. Liu et al., 2019; Savage, 2019). Another reason to explore alternative Cas systems is to find nucleases with optimal activities at different temperatures or other environmental conditions. Although Cas enzymes are usually active in a wide range of temperatures, a Cas protein with an optimal activity at 37°C would be ideal for human cells, but inefficient for genome editing in ectothermic organisms or other biotechnological processes. For instance, although LbCpf1 and AsCpf1 have similar cleavage activities at 37°C *in vitro*, LbCpf1 is more efficient in zebrafish and *Xenopus* than AsCpf1 due to the lower activity of the former enzyme at 25 and 28°C (Moreno-Mateos et al., 2017).

3.1. Type V CRISPR effectors

3.1.1. Type V-A: AsCas12a

The type V effectors that were characterized in this thesis, while having more restrictive PAMs, were made interesting by the fact that they produce 5' staggered overhangs in contrast to the blunt DSBs produced by SpCas9. This is interesting from the perspective of HDR since the cleavage pattern may be a determinant of repair pathway choice (Yeh et al., 2019). Blunt, unprocessed DSBs undergo NHEJ, whereas resection reveals homologies that can channel MMEJ or HDR (Chang et al., 2017). Therefore, if an alternative HDR repair mechanism is used by Cas12 effectors, then competition for repair machinery can be avoided by dedicating different nucleases to steps 1 and 2 of the Nested CRISPR process, potentially increasing its efficiency. However, our results demonstrate that AsCas12a does not provide a significant increase in efficiency over Cas9, and therefore, blunt ends or overhangs do not appear to influence HDR efficiencies in the *C. elegans* germline (**Figures 28 and 29**). Nevertheless, its comparable efficiency to Cas9 means that T-rich regions in the *C. elegans* genome are also available for targeting.

3.1.2. Type V-F and Type V-U3

On the other hand, the results we obtained using the Type V-F effector Un1Cas12f1 and Type V-U3 effectors AsCas12f1 and SpCas12f1 were not surprising. The high optimal temperatures of these nucleases were not suitable for an ectothermic organism such as *C. elegans*. In addition, of the Cas12f proteins tested, only Un1Cas12f1 was shown to act as a *bona-fide* CRISPR system in bacterial cells (Karvelis et al., 2020). Another drawback for using Cas12f1 nucleases is that the synthesis of long sgRNA molecules is not cost-efficient for routine use.

Upon testing Un1Cas12f1 and AsCas12f1 in the *dpy-10* locus, we observed low frequency phenotypes that did not segregate as expected. Although we do not know the exact mechanism by which it could occur, it is possible that these Cas12f1 nucleases could interfere with gene expression. Type V nucleases have many practical applications such as transcriptional regulation (Ramesh et al., 2020; Y. Wu et al., 2020; X. Zhang et al., 2017) and base editing (X. Li et al., 2018), and its capacity for both specific and non-specific ssDNA cleavage can be leveraged for the detection of nucleic acids (S. Y. Li et al., 2018) and small molecules (M. Liang et al., 2019). Therefore, a deeper investigation of these nucleases could potentially uncover a new host of applications that are currently not supported by existing Cas derivatives.

3.2. Near-PAM-less Cas9 variants

While the NGG PAM requirement of SpCas9 is not severely limiting, it is still a major barrier for genome editing applications that require high-resolution target site positioning such as the targeting of small genetic elements (Canver et al., 2015), base editing (Huang et al., 2021; Komor et al., 2016), multiplex HDR (Findlay et al., 2014), or for diagnosing specific mutations (Y. Li et al., 2019). In order to circumvent this limitation, efforts are being centered on the search for natural Cas9 orthologs and on engineering Cas9 variants with minimal PAM requirements (Collias & Beisel, 2021). Among engineered Cas9 variants, the near-PAMless SpG and SpRY variants present the most relaxed PAM requirements to date, and consequently, can target a greater fraction of the genome (**Figure 50**). The activity of these nucleases has been well described in human cell lines (Walton et al., 2020) and more recently in plants (J. Li et al., 2021; Ren et al., 2021; Xu et al., 2021; C. Zhang et al., 2021). However, SpG and SpRY

have never been applied in animals. In this thesis, I demonstrate for the first time that SpG and SpRY are functional in *C. elegans*.

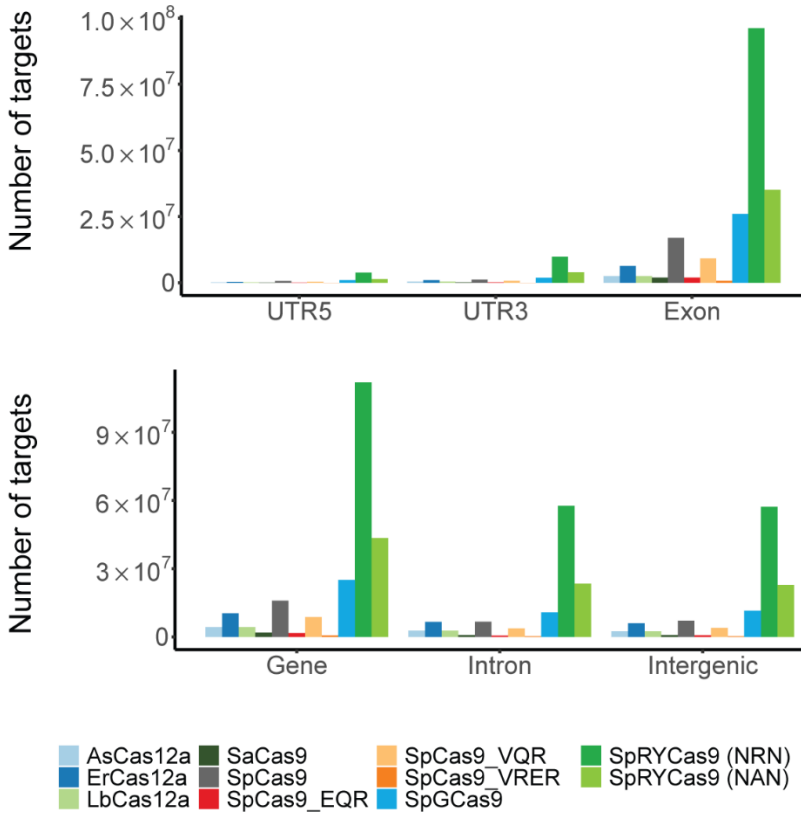

Figure 50. Targeting range of various Cas9 and Cas12a nucleases. Bar graphs show the number of targets of the indicated nucleases in the *C. elegans* genome, separated into 5' UTRs, 3' UTRs, exons, genes, introns, and intergenic regions. AsCas12a: *Acidaminococcus* spp. Cas12a; ErCas12a: *Eubacterium rectale* Cas12a; LbCas12a: *Lachnospiraceae bacterium* Cas12a; SaCas9: *Staphylococcus aureus* Cas9; SpCas9: *Streptococcus pyogenes* Cas9; SpCas9 EQR: *S. pyogenes* Cas9 EQR variant; SpCas9VQR: *S. pyogenes* Cas9 VQR variant; SpCas9VRER: *S. pyogenes* Cas9 VRER variant; SpGCas9: *S. pyogenes* Cas9 SpG variant; and SpRYCas9: *S. pyogenes* Cas9 SpRY variant. Adapted from Vicencio et al., 2021.

3.2.1. Expanded targeting range comes at a price

Our results show that there is a tradeoff between the relaxed PAM requirements of SpG and SpRY and *in vivo* editing efficiency. When using similar standard concentrations of CRISPR reagents (Cas9 and gRNA), SpG and SpRY did not perform as successfully as SpCas9. However, we showed that SpG and SpRY activity benefits from an increased concentration of CRISPR–Cas reagents. This is in contrast with our results using the commercial Cas9 from IDT, where lower nuclease concentrations promoted greater editing efficiencies. However, the need for higher SpG and SpRY concentrations could be due to the more extensive target scanning that occurs when more PAMs fit within the requirements of the nuclease (Moreb et al., 2020). We speculate that this reduced SpG and SpRY activity was not detected in human cell cultures or plant experiments because the gRNA and nuclease were expressed from strong, constitutive promoters that likely drove their cellular concentrations to saturating levels. Therefore, our results in *C. elegans* indicate that SpG and SpRY exhibit a trade-off between versatility and efficiency that could be balanced by increasing the concentration of the RNP.

Another possible drawback when using SpG and SpRY is the potential increase in off-targeting (Walton et al., 2020). However, we have observed that WT SpCas9, SpG, and SpRY have similar mismatch tolerance profiles, and therefore, such off-targeting could be predicted by current algorithms (Doench et al., 2016). Moreover, the use of transient approaches such as RNP delivery will help reduce potential off-targets compared to when gRNA and Cas9 are expressed from plasmids or stable integrations in the genome that provide a longer window of opportunity for off-target mutagenesis. Finally, high-fidelity versions can decrease off-target activity as shown in mammalian cells (Walton et al., 2020).

3.2.2. Taking genome editing one step further in *C. elegans*

Aside from demonstrating the capacity of SpG and SpRY to generate indels, we also demonstrated that these variants can be harnessed for HDR-mediated precision genome editing by mimicking a missense mutation and creating endogenous reporters in targets that are inaccessible for SpCas9. In addition, as proof of principle, we have also produced an SpG transgenic nematode that will further accelerate the use of the technology in this animal. This strategy, combined with the use of tissue-specific promoters and inducible gene expression systems, opens the possibility of taking advantage of these nucleases for somatic editing in distinct developmental stages (W. Li et al., 2015; Muñoz-Jimenez et al., 2017; Z. Shen et al., 2014; Tian et al., 2015). Altogether, we believe that our SpG and SpRY optimizations will contribute to the expansion of the CRISPR–Cas toolbox for *in vivo* applications not only in *C. elegans*, but also in other organisms.

4. Future prospects of CRISPR genome editing

Over the last few years, the CRISPR genome editing technology has gained popularity, and with the recent awarding of the 2020 Nobel Prize in Chemistry to Jennifer Doudna and Emmanuelle Charpentier, it has even started to become a household name. Due to the far-reaching social and biotechnological implications of CRISPR, never has there been such an accelerated development of any other technology in a similar scale.

Ultimately, as with any scientific advancement, the goal of CRISPR is to improve society not only through the betterment of healthcare, but also of agriculture and the environment. To name some examples, CRISPR can address food security by developing a line of climate-resilient and disease-resistant crops (Massel et al., 2021; Zaidi et al., 2020), mitigate climate change by abating greenhouse gas emissions (Nagaraju et al., 2016) or by enhancing the yield of biofuels (Ajjawi et al., 2017) and bio-based chemicals (Ting & Ng, 2020), and introduce gene drives to eliminate invasive species (Scudellari, 2019).

In terms of human health, CRISPR is opening new avenues for gene therapy as demonstrated by recent developments in the treatment of sickle cell disease and β-thalassemia (Frangoul et al., 2021). However, the treatment of other genetic diseases warrant *in vivo* genome editing, such as in the case of a form of childhood blindness known as Leber's congenital amaurosis (Ledford, 2020). To reduce the risks related with off-target effects, researchers are evaluating the use of more precise approaches such as through the use of Cas9 nickases for the treatment of Huntington's disease (Dabrowska et al., 2018) or through the use of base editors for the treatment of cystic fibrosis (Geurts et al., 2020) or progeria (Koblan et al., 2021). A great leap towards the goal of safely performing *in vivo* gene editing in patients was taken by the research team behind the recent demonstration of

base editing in monkeys to lower cholesterol levels by targeting the *PCSK9* gene (Musunuru et al., 2021).

In light of the COVID-19 pandemic, CRISPR technology has been rapidly put to use in the development of Cas12-based (Broughton et al., 2020) or Cas13a-based (Fozouni et al., 2021) assays for viral detection. In addition to its diagnostic utility, CRISPR–Cas13 may also provide therapeutic options for COVID-19 patients based on the simultaneous targeting of multiple RNA regions for degradation, paving the way for a pivotal pan-coronavirus targeting strategy (Abbott et al., 2020; Blanchard et al., 2021).

The contributions of *C. elegans* to the breakthrough of CRISPR technologies is beyond doubt, and this thesis demonstrates that it is a well-suited model organism for testing different CRISPR–Cas systems. As one of the simplest *in vivo* model systems, *C. elegans* can synergistically advance disease modeling with the use of near-PAMless nucleases which permits the targeting of virtually any genomic site. Due to the availability of powerful genetic tools and high-throughput approaches in *C. elegans*, it will continue to be a relevant and paramount model organism for many years to come.

CONCLUSIONS

1. Nested CRISPR is an efficient and flexible method for creating endogenous fluorescent reporters and can be accomplished in one or two rounds of microinjection.

2. The use of synthetic sgRNAs do not demonstrate clear benefits for genome editing in *C. elegans*, and the use of megamers is not straightforward and may require further optimization.

3. The efficiency of long dsDNA insertions in step 2 of Nested CRISPR is not affected by freezing/thawing nor by the generation number.

4. Editing efficiency is inversely related to insertion length.

5. Cas12a opens up targeting in TTTV PAMs and has similar efficiency as Cas9 for genome editing in *C. elegans*.

6. The Cas12f1 nucleases Un1Cas12f1, AsCas12f1, and SpCas12f1 do not induce DSBs *in vivo* in *C. elegans* and may be due to their high optimal temperatures.

7. The activity of the near-PAMless variants SpG and SpRY is concentration-dependent, and requires higher concentrations compared to Cas9 to efficiently produce genome editing events.

8. SpG and SpRY dramatically expands the number of targetable sites in the *C. elegans* genome, and facilitates precise genome editing in previously inaccessible sites via homology-directed repair.

9. Endogenously expressed SpG in the germline, under the control of *mex-5* promoter, can successfully perform genome editing in *C. elegans*, albeit at lower efficiencies compared to the use of RNPs.

MATERIALS AND METHODS

1. *Caenorhabditis elegans* strains

The Bristol N2 strain was used as the wild-type background and worms were maintained on Nematode Growth Medium (NGM) plates seeded with *Escherichia coli* OP50 bacteria (Stiernagle, 2006). CER371 was used for the transgenerational efficiency experiment by propagating the thawed strain for up to 15 generations. CER531 was used for studying the influence of insertion length on editing efficiencies. N2 and CER544 were used for comparing Cas9 and Cas12a efficiencies in *gtbp-1* (one-shot) and F27C1.2 (one-shot and Step 2), respectively. The CER409 strain harboring an endogenous *gtbp-1*::EGFP reporter was used for EGFP knockout assays and the CER541 strain with an endogenous *gtbp-1*::wrmScarlet reporter was used for wrmScarlet knockout assays. The CER603 strain with a modified *dpy-10* locus containing a TTTN PAM was used for the characterization of the Cas12f1 variants. The EG9615 strain expressing Cas9 in the germline was a gift from Dr. Matthew Schwartz and Dr. Erik Jorgensen. Six amino acid substitutions were introduced in this strain to generate CER660 which expresses SpG in the germline. All strains used in this study are listed in **Table 14** and all strains generated in this study are listed in **Supplementary Table 1**.

Table 14. List of strains used in this thesis

Strain	Genotype	Reference
N2	Wild-type background	CGC
CER371	*gtbp-1(cer53[gtbp-1::EGFP1-3]) IV*	This study
CER531	*gtbp-1(cer146[gtbp-1::wrmScarlet1-3]) IV*	This study
CER544	F27C1.2*(cer152[*F27C1.2*::wrmScarlet1-3]) I*	This study
CER409	*gtbp-1(cer89[gtbp-1::EGFP]) IV*	This study
CER541	*gtbp-1(cer149[gtbp-1::wrmScarlet]) IV*	This study
CER603	*dpy-10(cer192*[M85F]*) II*	This study
EG9615	*oxSi1091[mex-5p::Cas9(smu-2 introns) unc-119(+)] II; unc-119(ed3) III*	B. Yang et al., 2020
CER660	*cer227[mex-5p::SpG(smu-2 introns) unc-119(+)] II; unc-119(ed3) III*	This study

2. PCR genotyping

Lysis buffer was prepared by adding 1 µl of Proteinase K (10 mg/mL) for every 150 µL of 1x MyTaq Reaction Buffer (Bioline, #37111). Single or pooled worms were picked into 0.2 mL PCR tubes containing 10 µL of lysis buffer. In order to lyse the animals, the tubes were frozen at -80°C for at least 10 minutes then incubated at 60°C for 1 hour followed by incubation at 95°C for 15 minutes to inactivate the proteinase K. 40 µL of sterile water (Braun) were added to dilute the worm lysates and 3 µL were subsequently used as templates for polymerase chain reaction (PCR) amplification using the MyTaq™ DNA polymerase (Bioline, #21107) according to the touchdown PCR conditions specified in **Table 15**. The primers used for genotyping are listed in **Supplementary Table 2**.

Table 15. Touchdown PCR conditions for genotyping

Phase	Temperature	Duration	Cycles
Initial denaturation	95°C	2 min	
Denaturation	95°C	15 sec	11 cycles
Annealing	64°C (decrease by 0.5°C/cycle)	15 sec	
Extension	72°C	30 sec per1000 kb	
Denaturation	95°C	15 sec	24 cycles
Annealing	59°C	15 sec	
Extension	72°C	30 sec per 1000 kb	
Final extension	72°C	10 min	

3. crRNA and ssODN design

3.1. Nested CRISPR

The 20-nucleotide protospacer sequences were selected with the help of CCTop (Stemmer et al., 2015), which contains CRISPR–Cas9 target predictors. The following criteria were considered for crRNA selection: predicted efficiency, number of potential off-target sites, and distance of the DSB to the desired edit site. The crRNAs were ordered as 2 nmol products from IDT (www.idtdna.com) and were resuspended in 20 µL of nuclease-free duplex buffer (30 mM HEPES, pH 7.5; 100 mM potassium acetate. IDT, #11-01-03-01) to yield a stock concentration of 100 µM.

Once the cut site had been determined, ssODN donors for C-terminal fusions were designed in such a way that the FP 1-3 sequences were inserted in-frame immediately before the stop codon of the gene of interest or within a few amino acids before the stop codon (*gtbp-1* and *ubh-4*), depending on the availability of a PAM sequence. In contrast, N-terminal fusions rely on ssODN donors that facilitate in-frame insertions immediately after the start codon. The standard design involves flanking the FP 1-3 sequence with 35–45 nt-long homology arms. The exact lengths of the homology arms depend

on the distance of the insertion from the cut site and include adjustments to ensure that the FP 1-3 fragment is inserted in-frame. In addition, silent mutations are introduced to break the PAM or protospacer when needed, and silent mutations are also placed within homologous sequences that lie at a distance from the DSB.

3.2. Expanded targeting with Cas variants

3.2.1. Cas12a

To compare Cas9 and Cas12a efficiencies in the same locus, the original wrmScarlet sequence from the pJV003 plasmid was modified to introduce an NGG PAM for Cas9 and a TTTV PAM for Cas12a that can induce DSBs at similar locations (**Figure 27**). The corresponding homology arms for F27C1.2 and *gtbp-1* were then added. The crRNAs and ssODNs were purchased from IDT and are listed in **Supplementary Table 5**.

3.2.2. Cas12f1 variants

The *dpy-10* sequence in the N2 background was modified by CRISPR–Cas9 to introduce a TTTA PAM that was compatible with both Un1Cas12f1 (TTTR) and AsCas12f1 (YTTN) (**Figure 30**).

Three gRNAs targeting EGFP were also designed based on the PAM requirements of Un1Cas12f1, AsCas12f1, and SpCas12f1 for use in the EGFP knockout assay (**Figure 33**). The guide RNAs were synthesized as sgRNAs via *in vitro* transcription and were gifts from Tautvydas Karvelis and Virginijus Šikšnys. The gRNA sequences are listed in **Supplementary Table 6**

3.2.3. Near-PAMless Cas9 variants

For experiments in the *dpy-10* locus, the *dpy-10* gRNA with NGG PAM used in co-CRISPR was used as the reference sequence (Arribere et al., 2014). Mismatches were then introduced into the protospacer at one (+1) or five (+5) nucleotides upstream of the PAM (**Figure 35A**). Meanwhile, a protospacer with an NGC PAM was chosen based on proximity to the reference NGG sequence to maintain the cut site within the RXXR domain of *dpy-10* which is responsible for the production of the dominant dumpy and roller phenotypes, such as that of the *cn64* allele (Kramer & Johnson, 1993). Five targets with distinct PAM requirements were selected for wrmScarlet: one NGG, one NGC, and three NAC (**Figure 38**). For HDR experiments in *swsn-4*, *usp-48*, *trx-1*, W05H9.1, and *cep-1*, gRNAs were selected based on the proximity of the DSB from the desired edit site (**Figure 46**). A list of all crRNAs and ssODNs used with the near-PAMless Cas9 variants is given in **Supplementary Tables 7** and **8**, respectively.

4. Preparation of dsDNA donors

dsDNA donors were amplified via PCR from existing plasmids or from plasmids generated via the integration of gBlocks™ gene fragments (IDT) into the pDONR221 backbone via Gateway® cloning (ThermoFisher) (**Table 16**). Primers were designed to amplify the complete sequences of the FPs and additional motifs using the Phusion High-Fidelity DNA Polymerase (Thermo Fisher Scientific, Cat. No. F530S) (**Table 17**). PCR mixes sufficient for eight 50-µL reactions were prepared and subject to PCR following the conditions specified in **Table 18**. Finally, 5 µL of PCR product were run on a 2% agarose gel to verify correct amplification of the fragments and the products were purified with the MinElute PCR purification kit (QIAGEN, Cat. No. 28004) with a yield of between 800 to 1200 ng/µL.

Table 16. List of plasmids for the preparation of dsDNA donors

Plasmid	FP	Source	Addgene #
pJJR82	EGFP	Mike Boxem	75027
pJJR83	mCherry	Mike Boxem	75028
pJV003	wrmScarlet	Denis Dupuy	N/A
WRM0625C_F10 (fosmid)	2xTY1::EGFP::3xFLAG	TransgeneOme Resource	N/A
pNES001	$GFP^{\Delta piRNA}$::degron::3xFLAG	Nicholas Stroustrup	N/A
IR88	SL2::mCherry	Inja Radman	N/A
pCM1.35	GFP::H2B	Geraldine Seydoux	17248
pCUC76	wrmScarlet (2 introns)	This study	N/A
pCUC77	wrmScarlet (with Cas9 and Cas12a PAM)	This study	N/A
pCUC78	wrmScarlet (3 introns)	This study	N/A

Table 17. List of primers used for amplifying dsDNA donors

FP	Primer #	Sequence (5' to 3')	Orientation
2xTY1::EGFP::3xFLAG	1545	ATACCAATCAGGACCCGCTG	Fwd
2xTY1::EGFP::3xFLAG	1546	TGTCGTCGTCATCCTTGTAGT	Rev
EGFP	1478	CCAAGGGAGAGGAGCTCTTCA	Fwd
EGFP	1479	CTTGTAGAGCTCGTCCATTC	Rev
GFP::H2B	1668	AGTAAAGGAGAAGAACTTTTCACTGG	Fwd
GFP::H2B	1667	CTTGCTGGAAGTGTACTTGGTG	Rev
GFP$^{\Delta piRNA}$::degron::3xFLAG	1563	AGGAGAAGAACTTTTCACTGGAG	Fwd
GFP$^{\Delta piRNA}$::degron::3xFLAG	1564	TGTCATCGTCATCCTTGTAATCG	Rev
mCherry	1485	TCCAAGGGAGAGGAGGACAA	Fwd
mCherry	1486	CTTGTAGAGCTCGTCCATTC	Rev
SL2::mCherry	1581	GCTGTCTCATCCTACTTTCACC	Fwd
SL2::mCherry	1582	CAATTCATCCATGCCACCTGT	Rev
wrmScarlet (all forms)	1519	GTCAGCAAGGGAGAGGCAGTTAT	Fwd
wrmScarlet (all forms)	1520	CTTGTAGAGCTCGTCCATTCCT	Rev

Table 18. Reagents and conditions for the preparation of dsDNA donors

PCR mix

Component	Volume	
H_2O	260.0 µL	
5x Phusion HF buffer	80.0 µL	
Fwd primer 10 µM	20.0 µL	(final concentration 0.5 µM)
Rev primer 10 µM	20.0 µL	(final concentration 0.5 µM)
Plasmid (10 ng/µl)	8.0 µL	(final concentration 0.2 ng/µl)
Phusion DNA polymerase	4.0 µL	
dNTPs 10 mM	8.0 µL	
TOTAL	**400.0 µL**	split into 8 x 50-µl reactions

Table 18. Reagents and conditions for the preparation of dsDNA donors (*continued*)

I. PCR conditions – all FPs except wrmScarlet

Temperature	Duration	Cycles
98º	2 min	
98º	30 sec	x35 cycles
See below	30 sec	
72º	45 sec	
72º	10 min	
4º	∞	

Annealing temperatures

FP	Plasmid	Annealing temperature
2xTY1::EGFP::3xFLAG	WRM0625C_F10	60º
EGFP	pJJR82	60º
GFP::H2B	pCM1.35	60º
GFP$^{\Delta piRNA}$::degron::3xFLAG	pNES001	61º
mCherry	pJJR83	67º
SL2::mCherry	IR88	58º

II. PCR conditions – wrmScarlet

Temperature	Duration	Cycles
98º	30 sec	
98º	10 sec	x35 cycles
See below	15 sec	
72º	See below	
72º	10 min	
4º	∞	

Annealing temperatures and extension durations

Plasmid	Annealing temperature	Extension duration
pJV003	51º	15 sec
pCUC76	55º	30 sec
pCUC77	51º	15 sec
pCUC78	70º	30 sec

5. Cas proteins

Alt-R® S.p. Cas9 Nuclease V3 (#1081058) and Alt-R® A.s. Cas12a (Cpf1) Ultra (#10001272) were purchased from IDT. The Cas12f1 proteins Un1Cas12f1, AsCas12f1, and SpCas12f1 were gifts from Tautvydas Karvelis and Virginijus Šikšnys. The Cas9 proteins WT SpCas9, SpG, and SpRY were synthesized at the Biomolecular Screening & Protein Technologies Facility at the Centre for Genomic Regulation (Barcelona) by Natalia Rodrigo Melero and Carlo Carolis.

6. RNP *in vitro* cleavage assay

For Cas9 assays, the gRNA was prepared by pre-annealing 3.2 µL of 32 µM ALT-R tracrRNA (IDT, #1072532) and 1 µL of 100 µM crRNA with 5.8 µL of nuclease-free duplex buffer (IDT) at 95°C for 5 minutes. On the other hand, no pre-annealing is required for Cas12a and Cas12f1 gRNAs. Dilutions of the components, namely gRNA, nuclease, and PCR product were prepared at 300 nM, 900 nM, and 90 nM, respectively. Then, the RNP complex was assembled by incubating 9 µL of gRNA with 3 µL of nuclease in 12 µL of nuclease-free H2O with 3 µL of 10x Cas9 reaction buffer (New England Biolabs, #B0386) at 37 °C for 15 minutes. 3 µL of the DNA substrate (PCR product) containing the target site was then added to achieve a final molar ratio of nuclease, guide RNA, and target site of 10:10:1 (90 nM:90 nM:9 nM). The 30-µl reactions were incubated at different temperatures (15, 25, 37, and 50 °C) for 60 minutes. To release the DNA substrate from the RNP complex, 2 µl Proteinase K (10 mg/mL) was added to the reaction and incubated at 56°C for 10 minutes. The cleaved products were analyzed through agarose gel electrophoresis using a 2% gel stained with SYBR® safe DNA gel stain (ThermoFisher Scientific, #S33102).

7. RNP delivery in *C. elegans*

7.1. Preparation of injection mixes

Injection mixes were prepared by combining Cas9 nuclease, tracrRNA, and crRNA, which were incubated at 37 °C for 15 minutes. When necessary, ssODN and/or dsDNA repair templates were added after incubation and the mixture centrifuged at 13,200 rpm for two minutes to settle particulate matter. The injection mixes were kept on ice prior to loading of the needles and any excess was stored at -20°C. The standard step 1, step 2, and one-shot Nested CRISPR injection mixes are shown in **Table 19**. Experiment-specific injection mixes that do not follow the standard composition are shown in **Supplementary Table 9**.

Table 19. Standard Nested CRISPR injection mixes

Step 1 Translational Reporter

Component	**Volume**	**Initial concentration**		**Final concentration**	
	µL	µM	ng/µL[1]	µM	ng/µL[1]
Cas9 (IDT)	0.25	61	10000	1.53	250.00
tracrRNA	0.50	32	709.8	1.60	35.5
dpy-10 crRNA	0.40	10	115.1	0.40	4.6
target gene crRNA	1.20	10	~120	1.20	~14.4
dpy-10(cn64) ssODN	0.28	32.7	1000	0.92	28.00
Step 1 repair ssODN	0.22	100	~5300	2.20	~116.6
Nuclease-free H_2O	7.15				
Total volume	**10.00**				

[1] Concentrations in ng/µl will vary depending on the sequence of the crRNA and the length of the ssODN.

Table 19. Standard Nested CRISPR injection mixes (*continued*)

Step 1 Transcriptional Reporter

Component	**Volume**	**Initial concentration**		**Final concentration**	
	µL	µM	ng/µL[1]	µM	ng/µL[1]
Cas9 (IDT)	0.25	61.0	10000	1.53	250.0
tracrRNA	0.50	32.0	710	1.60	35.5
dpy-10 crRNA	0.40	10.0	115.1	0.40	4.6
target gene 5' crRNA	0.60	10.0	~120	0.60	~7.2
target gene 3' crRNA	0.60	10.0	~120	0.60	~7.2
dpy-10(cn64) ssODN	0.28	32.7	1000	0.92	28.0
Step 1 repair ssODN	0.22	100.0	~5300	2.20	~116.6
Nuclease-free H_2O	7.15				
Total volume	**10.00**				

Step 2

Component	**Volume**	**Initial concentration**		**Final concentration**	
	µL	µM	ng/µL[1]	µM	ng/µL[1]
Cas9 (IDT)	0.25	61.0	10000	1.53	250.0
tracrRNA	0.50	32.0	710	1.60	35.5
dpy-10 crRNA	0.40	10.0	115	0.40	4.6
target gene crRNA	1.20	10.0	~120	1.20	~14.4
dpy-10(cn64) ssODN	0.28	32.7	1000	0.92	28.0
Step 2 PCR product[2]	5.25	~1.9	~1000	~1.00	~525.0
Nuclease-free H_2O	2.12				
Total volume	**10.00**				

[1] Concentrations in ng/µl vary depending on crRNA sequence and ssODN length.

[2] The volume was adjusted according to the molecular weight of the PCR product to reach a final concentration of 1.0 µM.

Table 19. Standard Nested CRISPR injection mixes (*continued*)

One-shot Nested CRISPR

Component	Volume	Initial concentration		Final concentration	
	µL	µM	ng/µL[1]	µM	ng/µL[1]
Cas9 (IDT)	0.25	61.0	10000	1.53	250.0
tracrRNA	0.50	32.0	710	1.60	35.5
dpy-10 crRNA	0.40	10.0	115	2.00	23.02
target gene crRNA	0.60	10.0	~120	0.60	~7.2
Step 2 crRNA	0.60	10.0	~120	0.60	~7.2
Step 1 repair ssODN	0.22	100.0	~5300	2.20	~116.6
dpy-10(cn64) ssODN	0.28	32.7	1000	0.92	28.0
Step 2 PCR product[2]	5.25	~1.9	~1000	~1.00	~525.0
Nuclease-free H_2O	1.90				
Total volume	**10.00**				

[1] Concentrations in ng/µl vary depending on crRNA sequence and ssODN length.

[2] The volume was adjusted according to the molecular weight of the PCR product to reach a final concentration of 1.0 µM.

7.2. *C. elegans* microinjection

Microinjections were carried out using standard *C. elegans* microinjection technique (Mello & Fire, 1995). Eppendorf Femtotips® capillary tips (Eppendorf, #930000035) for microinjection were loaded with 2 µl of the injection mix and were fixed onto the XenoWorks Microinjection System (Sutter Instrument) coupled to a Nikon Eclipse Ti-S inverted microscope with Nomarski optics. Approximately 15–20 young adult hermaphrodites were injected for each experimental condition. The worms were fixed on 2% agarose pads with halocarbon oil in groups of five and were injected in one or both gonad arms. Injected worms were recovered in M9 buffer and were individually separated onto nematode growth medium (NGM) agar plates. The worms were incubated at 25 °C for three days.

8. Screening

8.1. Nested CRISPR

dpy-10 co-edited animals (F_1 Rol or Dpy) were transferred onto NGM plates, individually or in pools, and were left to lay F_2 progeny. Single-worm or pooled (two to three worms) PCR was then performed on the F_1 worms. Primers were designed for each target gene and amplicon size shifts on 2% agarose gel were indicative of insertion events. If the PCR product was of the correct size, eight wild-type like F_2 progeny were individually transferred onto NGM plates to outsegregate the *dpy-10* comarker and to homozygose the step 1 insertion. PCR products from homozygous animals were then purified using the QIAquick PCR purification kit (QIAGEN, #28104) and were sent for Sanger sequencing (Stabvida) to verify the accuracy of the insertions. After step 2 injections, screening is initially performed visually through fluorescence microscopy using a Nikon SMZ800 stereomicroscope with GFP and mCherry filters linked to a Nikon Intensilight C-HGFI epi-fluorescence illuminator. Green or red fluorescence were indicative of complete, in-frame insertion events. When a fluorescent signal cannot be detected due to low endogenous expression levels, genotyping is then carried out via single-worm PCR.

8.2. *dpy-10* assay

Bristol N2 worms were injected with *dpy-10* RNPs and screened for the presence of Dpy and/or Rol phenotypes. The editing efficiency from each injected P_0 was calculated by counting the proportion of Dpy or Rol F_1 progeny over the total number of F_1 progeny laid by each P_0 worm. Since mutations in *dpy-10* can produce both dominant and recessive phenotypes (**Figure 51**), injections targeting the *dpy-10* locus occasionally included pCFJ90 (myo-2p:: mCherry) and pCFJ104 (myo-3p::mCherry) as co-markers to facilitate the screening of recessive Dpy phenotypes in the F_2.

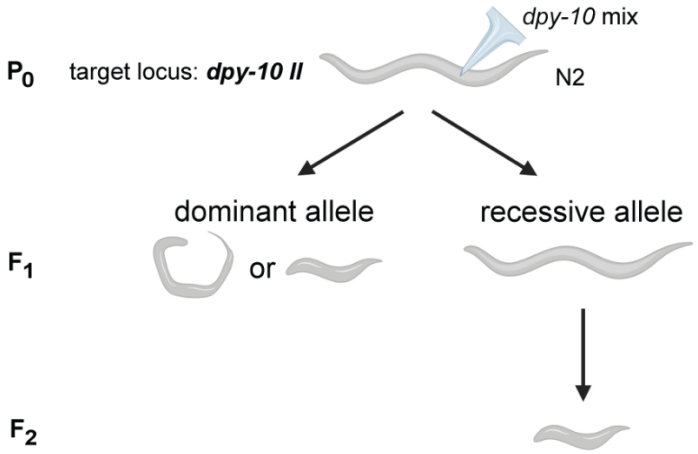

Figure 51. Schematic representation of *in vivo* experiments in *C. elegans* targeting *dpy-10*. N2 worms are injected with a mixture containing a guide against the *dpy-10* locus. Mutations leading to dominant Rol or Dpy phenotypes are detected in the F_1. In some experiments, wild type-like F_1 progeny are singled out to screen for recessive Rol or Dpy phenotypes in the F_2.

8.3. EGFP and wrmScarlet knockout assay

CER409 worms harboring a homozygous *gtbp-1*::EGFP reporter or CER541 worms harboring a homozygous *gtbp-1*::wrmScarlet reporter were injected with anti-EGFP or anti-wrmScarlet RNPs, respectively, combined with *dpy-10* RNP as co-CRISPR marker (**Figure 33**). From each injected P_0, between five to ten Dpy or Rol F_1s were separated and allowed to lay F_2 progeny. The F_2 progeny were then visually screened for EGFP or wrmScarlet knockouts via fluorescence microscopy. The editing efficiency from each injected P_0 was calculated by counting the proportion of separated F_1 progeny that gave rise to non-fluorescent F_2 worms. Non-fluorescent worms were indicative of indels arising from error-prone repair of DSBs.

9. Generation of endogenous germline SpG-expressing strains

EG9615 *(oxSi1091[mex-5p::Cas9(smu-2 introns) unc-119(+)] II; unc-119(ed3) III)*, a strain carrying a transgene that expresses SpCas9 in the germline, was a gift from Dr. Matthew Schwartz and Dr. Erik Jorgensen (unpublished). EG9615 hermaphrodites were injected with three crRNAs and three ssODN repair templates to introduce the six amino acid substitutions to convert SpCas9 to SpG. Each crRNA and ssODN repair template introduced the D1135L and S1136W, G1218K and E1219Q, and R1335Q and T1337R substitutions by pairs. The first round of injections contained all three crRNAs at a final concentration of 1 µM each, tracrRNA at 3.2 µM, the three ssODN repair templates at 2.2 µM each, pCFJ90 at 2.5 ng/µL, and pCFJ104 at 5.0 ng/µL. F_1 progeny with visible mCherry expression in the pharynx or body wall were singled out and were

genotyped via single worm lysis and PCR after laying F_2 progeny. From the first set of injections, a strain with the D1135L and S1136W substitutions was successfully isolated. Then, a second round of injections was made over this strain to introduce the remaining substitutions. However, in an attempt to increase the editing efficiency, the remaining two crRNAs were combined with tracrRNA and Cas9 (IDT) at a final concentration of 2.1 µM to form RNPs. Worms were injected with this injection mixture and genotyped as previously described. The four remaining substitutions were successfully isolated and three independent lines were kept and frozen (CER658, CER659, and CER660).

10. Statistical analysis

No statistical methods were used to predetermine sample size. The experiments were not randomized and there was no blinding during experiments and outcome assessment. Data come from one or two independent experiments, with all data derived from parallel injections unless otherwise specified in the figure legend. Student's *t*-test, one-way ANOVA (all values shown are two-sided) with Tukey's test for multiple comparisons, and creation of graphs were performed using Prism (GraphPad Software v9, La Jolla, CA, USA).

SUPPLEMENTARY TABLES

Supplementary Table 1. List of strains generated by Nested CRISPR

Strain	Genotype	Description
CER352	*prpf-4(cer40[prpf-4::EGFP1-3]) I*	*prpf-4* EGFP Step 1
CER353	*prpf-4(cer72[prpf-4::EGFP1-3]) I*	*prpf-4* EGFP Step 1
CER371	*gtbp-1(cer53[gtbp-1::EGFP1-3]) IV*	*gtbp-1* EGFP Step 1
CER372	*prpf-4(cer54[prpf-4::EGFP]) I*	*prpf-4* EGFP Step 2
CER373	*prpf-4(cer78[prpf-4::EGFP]) I*	*prpf-4* EGFP Step 2
CER376	*pgl-1(cer57[pgl-1::EGFP1-3]) IV*	*pgl-1* EGFP Step 1
CER378	*ubh-4(cer67[ubh-4::EGFP1-3) II*	*ubh-4* EGFP Step 1
CER379	*gtbp-1(cer66[gtbp-1:: EGFP]) IV*	*gtbp-1* EGFP Step 2
CER380	*gtbp-1(cer59[gtbp-1::mCherry1-3]) IV*	*gtbp-1* mCherry Step 1
CER381	*pgl-1(cer60[pgl-1::mCherry1-3]) IV*	*pgl-1* mCherry Step 1
CER382	*pgl-1(cer61[pgl-1::mCherry1-3]) IV*	*pgl-1* mCherry Step 1
CER383	*prpf-4(cer62[prpf-4::mCherry1-3]) I*	*prpf-4* mCherry Step 1
CER384	*prpf-4(cer63[prpf-4::mCherry1-3]) I*	*prpf-4* mCherry Step 1
CER385	*gei-3(cer64[gei-3::EGFP1-3]) X*	*gei-3* EGFP Step 1
CER386	*gei-3(cer65[gei-3::EGFP1-3]) X*	*gei-3* EGFP Step 1
CER395	*ubh-4(cer68[ubh-4::EGFP])II*	*ubh-4* EGFP Step 2
CER396	K12C11.3*(cer69[*K12C11.3*p::mCherry1-3]) I*	K12C11.3p Step 1
CER397	K12C11.3*(cer79[*K12C11.3*p::mCherry1-3]) I*	K12C11.3p Step 1
CER398	*prpf-4(cer80[prpf-4::mCherry]) I*	*prpf-4* mCherry Step 2

Supplementary Table 1. List of strains generated by Nested CRISPR (*continued*)

Strain	Genotype	Description
CER399	*prpf-4(cer81[prpf-4::mCherry]) I*	*prpf-4* mCherry Step 2
CER402	*prpf-4(cer82[prpf-4::EGFP]) I*	*prpf-4* EGFP Step 2 (sgRNA)
CER403	*prpf-4(cer83[prpf-4::EGFP]) I*	*prpf-4* EGFP Step 2 (sgRNA)
CER404	*prpf-4(cer84[prpf-4::mCherry]) I*	*prpf-4* mCherry Step 2 (sgRNA)
CER405	*prpf-4(cer85[prpf-4::mCherry]) I*	*prpf-4* mCherry Step 2 (sgRNA)
CER406	K12C11.3*(cer86[*K12C11.3*p::mCherry]) I*	K12C11.3p::mCherry Step 2
CER407	K12C11.3*(cer87[*K12C11.3*p::mCherry]) I*	K12C11.3p::mCherry Step 2
CER408	*gtbp-1(cer88[gtbp-1::EGFP]) IV*	*gtbp-1* EGFP Step 2
CER409	*gtbp-1(cer89[gtbp-1::EGFP]) IV*	*gtbp-1* EGFP Step 2
CER410	*gtbp-1(cer90[gtbp-1::EGFP]) IV*	*gtbp-1* EGFP Step 2 (sgRNA)
CER411	*gtbp-1(cer91[gtbp-1::EGFP]) IV*	*gtbp-1* EGFP Step 2 (sgRNA)
CER412	*gtbp-1(cer92[gtbp-1::mCherry]) IV*	*gtbp-1* mCherry Step 2
CER413	*gtbp-1(cer93[gtbp-1::mCherry]) IV*	*gtbp-1* mCherry Step 2
CER414	*pgl-1(cer70[pgl-1::mCherry]) IV*	*pgl-1* mCherry Step 2
CER415	*pgl-1(cer71[pgl-1::mCherry]) IV*	*pgl-1* mCherry Step 2
CER416	*gei-3(cer94[gei-3::EGFP) X*	*gei-3* EGFP Step 2
CER417	*gei-3(cer95[gei-3::EGFP) X*	*gei-3* EGFP Step 2
CER418	*pgl-1(cer96[pgl-1::EGFP]) IV*	*pgl-1* EGFP Step 2
CER419	*prpf-4(cer97[prpf-4::mCherry]) I*	*prpf-4* mCherry Step 2

Supplementary Table 1. List of strains generated by Nested CRISPR (*continued*)

Strain	Genotype	Description
CER421	*comt-4(cer99[comt-4p::mCherry 1-3]) V*	*comt-4p* mCherry Step 1
CER422	*comt-4(cer100[comt-4p::mCherry]) V*	*comt-4p* mCherry Step 2
CER423	*comt-4(cer101[comt-4p::mCherry]) V*	*comt-4p* mCherry Step 2
CER426	*sftb-1(cer103[mCherry1-3::sftb-1]) III*	*sftb-1* mCherry Step 1
CER427	*sftb-1(cer104[mCherry1-3::sftb-1]) III*	*sftb-1* mCherry Step 1
CER428	*sftb-1(cer105[mCherry1-3::sftb-1]) III*	*sftb-1* mCherry Step 1
CER431	*prpf-4(cer108[prpf-4::mCherry]) I*	*prpf-4* mCherry Step 2 (one-shot)
CER432	*pgl-1(cer96[pgl-1::EGFP]) IV*	*pgl-1* EGFP Step 2 (one-shot)
CER438	F27C1.2*(cer111[*F27C1.2*::wrmscarlet]) I*	F27C1.2 wrmScarlet Step 2 (one-shot)
CER439	F27C1.2*(cer112[*F27C1.2*::wrmscarlet]) I*	F27C1.2 wrmScarlet Step 2 (one-shot)
CER444	*sftb-1(cer114[mCherry::sftb-1]) III*	*sftb-1* mCherry Step 2
CER461	*nfki-1(cer116[EGFP::nfki-1]) X*	*nfki-1* EGFP Step 2
CER467	*nfki-1(cer120[EGFP::nfki-1]) X*	*nfki-1* EGFP Step 2
CER469	*nfki-1(cer121[EGFP1-3::nfki-1]) X*	*nfki-1* EGFP Step 1
CER470	*prpf-4(cer122[prpf-4::2xTY1::3xFLAG]) I*	*prpf-4* 2xTY1::EGFP::3xFLAG Step 1
CER471	*prpf-4(cer123[prpf-4::2xTY1::3xFLAG]) I*	*prpf-4* 2xTY1::EGFP::3xFLAG Step 1
CER472	*prpf-4(cer124[prpf-4::2xTY1::EGFP::3xFLAG]) I*	*prpf-4* 2xTY1::EGFP::3xFLAG Step 2
CER494	*comt-5(cer126 [comt-5p::GFP::H2B1-3]) V*	*comt-5p* GFP::H2B Step 1
CER495	*comt-5(cer126 [comt-5p::GFP::H2B1-3]) V*	*comt-5p* GFP::H2B Step 1

Supplementary Table 1. List of strains generated by Nested CRISPR (*continued*)

Strain	Genotype	Description
CER496	*comt-4(cer128[comt-4p::GFP::H2B1-3]) V*	*comt-4p* GFP::H2B Step 1
CER500	*comt-4(cer131[comt-4p::GFP::H2B]) V*	*comt-4p* GFP::H2B Step 2
CER501	*comt-5(cer132[comt-5p::GFP::H2B]) V*	*comt-5p* GFP::H2B Step 2
CER506	*rpb-2(cer133[rpb-2::GFPΔpiRNA::degron::3xFLAG1-3]) III*	*rpb-2* GFP::degron::3xFLAG Step 1
CER507	*rpb-2(cer134[rpb-2::GFPΔpiRNA::degron::3xFLAG1-3) III*	*rpb-2* GFP::degron::3xFLAG Step 1
CER510	*rpb-2(cer135[rpb-2::GFPΔpiRNA::degron::3xFLAG]) III*	*rpb-2* GFP::degron::3xFLAG Step 2
CER511	*rpb-2(cer136[rpb-2::GFPΔpiRNA::degron::3xFLAG]) III*	*rpb-2* GFP::degron::3xFLAG Step 2
CER512	*rpb-2(cer137[rpb-2::GFPΔpiRNA::degron::3xFLAG]) III*	*rpb-2* GFP::degron::3xFLAG Step 2
CER519	*gei-3(cer139[gei-3::SL2-1::mCherry1-3]) X*	*gei-3* SL2::mCherry Step 1
CER526	*gei-3(cer141[gei-3::SL2::mCherry]) X*	*gei-3* SL2::mCherry Step 2
CER527	*gei-3(cer142[gei-3::SL2::mCherry]) X*	*gei-3* SL2::mCherry Step 2
CER528	*gei-3(cer143[gei-3::SL2::mCherry]) X*	*gei-3* SL2::mCherry Step 2
CER531	*gtbp-1(cer146[gtbp-1::wrmScarlet1-3]) IV*	*gtbp-1* wrmScarlet Step 1
CER532	*gtbp-1(cer147[gtbp-1::wrmScarlet1-3]) IV*	*gtbp-1* wrmScarlet Step 1
CER533	F58G6.9*(cer148[*F58G6.9*p::wrmScarlet1-3]) IV*	F58G6.9p wrmScarlet Step 1
CER541	*gtbp-1(cer149[gtbp-1::wrmScarlet]) IV*	*gtbp-1* wrmScarlet without introns (pJV003)
CER543	*gtbp-1(cer151[gtbp-1::wrmScarlet]) IV*	*gtbp-1* wrmScarlet with two introns (pCUC76)
CER544	F27C1.2*(cer152[*F27C1.2*::wrmScarlet1-3]) I*	F27C1.2 wrmScarlet Step 1 (one-shot Cas9/Cas12a)
CER545	F27C1.2*(cer153[*F27C1.2*::wrmScarlet]) I*	F27C1.2 wrmScarlet Step 2 (one-shot Cas9/Cas12a)

Supplementary Table 1. List of strains generated by Nested CRISPR (*continued*)

Strain	Genotype	Description
CER547	K12C11.6*(cer154[*K12C11.6*p::mCherry1-3]) I*	K12C11.6p mCherry Step 1
CER548	K12C11.6*(cer155[*K12C11.6*p::mCherry1-3]) I*	K12C11.6p mCherry Step 1
CER549	*hcf-1(cer156[hcf-1::GFPΔpiRNA::degron::3xFLAG1-3]) IV*	*hcf-1* GFP::degron::3xFLAG Step 1
CER554	*comt-4(cer157[comt-4p::GFP::H2B]) V*	*comt-4p* GFP::H2B Step 2
CER555	F58G6.9*(cer158[*F58G6.9*p::wrmScarlet]) IV*	F58G6.9p wrmScarlet Step 2
CER556	*hcf-1(cer159[hcf-1::GFPΔpiRNA::degron::3xFLAG]) IV*	*hcf-1* GFP::degron::3xFLAG Step 2
CER557	*hcf-1(cer160[hcf-1::GFPΔpiRNA::degron::3xFLAG]) IV*	*hcf-1* GFP::degron::3xFLAG Step 2
CER558	K12C11.6*(cer161[*K12C11.6*p::mCherry]) I*	K12C11.6p mCherry Step 2
CER559	K12C11.6*(cer162[*K12C11.6p*::mCherry]) I*	K12C11.6p mCherry Step 2
CER582	*nhr-1(cer177[nhr-1::2xTY1::3xFLAG]) X*	*nhr-1* 2xTY1::EGFP::3xFLAG Step 1
CER583	*nhr-1(cer178[nhr-1::2xTY1::3xFLAG]) X*	*nhr-1* 2xTY1::EGFP::3xFLAG Step 1
CER584	*gtbp-1(cer179[gtbp-1::wrmScarlet] IV*	*gtbp-1* wrmScarlet with three introns (pCUC78)
CER585	*gtbp-1(cer180[gtbp-1::wrmScarlet] IV*	*gtbp-1* wrmScarlet with three introns (pCUC78)
CER589	*nhr-1(cer182[nhr-1::2xTY1::EGFP::3xFLAG]) X*	*nhr-1* 2xTY1::EGFP::3xFLAG Step 2
CER590	*nhr-1(cer183[nhr-1::2xTY1::EGFP::3xFLAG]) X*	*nhr-1* 2xTY1::EGFP::3xFLAG Step 2
CER591	Y53C10A.5*(cer184) I*	Y53C10A.5p wrmScarlet Step 1 (imprecise)
CER592	Y53C10A.5*(cer185) I*	Y53C10A.5p wrmScarlet Step 1 (imprecise)
CER593	Y53C10A.5*(cer186) I*	Y53C10A.5p wrmScarlet Step 1 (imprecise)
CER598	Y53C10A.5*(cer187[*Y53C10A.5*::wrmScarlet1-3]) I*	Y53C10A.5 wrmScarlet Step 1

Supplementary Table 1. List of strains generated by Nested CRISPR (*continued*)

Strain	Genotype	Description
CER602	*dpy-10(cer191[M85F]) II*	*dpy-10* TTTA PAM modification
CER603	*dpy-10(cer192[M85F]) II*	*dpy-10* TTTA PAM modification
CER608	Y53C10A.5*(cer196[*Y53C10A.5*::wrmScarlet]) I*	Y53C10A.5 wrmScarlet Step 2 (Cas9)
CER609	Y53C10A.5*(cer197[*Y53C10A.5*::wrmScarlet]) I*	Y53C10A.5 wrmScarlet Step 2 (Cas12a)
CER630	*usp-48(cer211[usp-48::wrmScarlet1-3]) I*	*usp-48* wrmScarlet Step 1 (SpG)
CER631	*usp-48(cer212[usp-48::wrmScarlet1-3]) I*	*usp-48* wrmScarlet Step 1 (SpG)
CER636	*trx-1(cer216[trx-1::wrmScarlet1-3]) II*	*trx-1* wrmScarlet Step 1 (SpG)
CER652	*usp-48(cer220[usp-48::wrmScarlet]) I*	*usp-48* wrmScarlet Step 2
CER653	*usp-48(cer221[usp-48::wrmScarlet]) I*	*usp-48* wrmScarlet Step 2
CER657	*trx-1(cer224[trx-1::wrmScarlet]) II*	*trx-1* wrmScarlet Step 2
CER658	*cer225[mex-5p::Cas9 SpG(smu-2 introns) unc-119(+)] II; unc-119(ed3) III*	Germline SpG
CER659	*cer226[mex-5p::Cas9 SpG(smu-2 introns) unc-119(+)] II; unc-119(ed3) III*	Germline SpG
CER660	*cer227[mex-5p::Cas9 SpG(smu-2 introns) unc-119(+)] II; unc-119(ed3) III*	Germline SpG
CER664	*trx-1(cer230[trx-1::wrmScarlet]) II*	*trx-1* wrmScarlet Step 2
CER669	*swsn-4(cer232(swsn-4[R350C]) IV*	*swsn-4* R350C substitution (SpG)
CER673	W05H9.1*(cer236(*W05H9.1*p::GFP::H2B1-3)) X*	W05H9.1 GFP::H2B Step 1 (SpG)
CER674	W05H9.1*(cer237(*W05H9.1*p::GFP::H2B)) X*	W05H9.1 GFP::H2B Step 2
CER675	*cep-1(cer238(cep-1::wrmScarlet1-3)) I*	*cep-1* wrmScarlet Step 1 (SpRY)

Supplementary Table 2. List of primers for genotyping

Locus	Primer #	Sequence (5' to 3')	Description
ads-1	281A	CCGGTACACTTAATCACAACCA	5'UTR Fwd
ads-1	282A	TCGGCAGGCGAAATACTAGT	3'UTR Rev
ads-1	283A	TGATGAAACGCGAGGCAAAA	Internal Fwd
cep-1	1746	CGATGAAGAGAAGTCGCTGT	C-ter Fwd
cep-1	1819	CGTCGACAGACTCGTTTTGT	3'UTR Rev
comt-3	1551	TCTTTTGCCTCCCCAATCCA	5'UTR Fwd
comt-3	1552	TGTCTACTTTGCCCCCAATG	3'UTR Rev
comt-4	1495	TGTTGCCAAGAGTTACTCCAAG	5'UTR Fwd
comt-4	1496	GCAGAACAATTTTGTCTTGAGC	3'UTR Rev
comt-5	1553	CCCTCCAAACAGCTATTGAAACG	5'UTR Fwd
comt-5	1554	ACATGAGTTCCATCGCCAAGA	C-ter Rev
dpy-10	279A	GAGTTGGTCCCTTATCTCCAG	Sequencing/*in vitro* Fwd
dpy-10	280A	GCGTCAGATGATCTACCGGT	Sequencing/*in vitro* Rev
dpy-10	396A	AATACGGCAAGATGAGAATG	WT-specific Fwd
dpy-10	397A	AATACGGCAAGATGCGATTT	Mutant-specific Fwd
dpy-10	398A	CACGAACTTGGTTGAGTGGG	Common Rev
F27C1.2	1521	GCAGTTCTCCAACTCCGAAA	C-ter Fwd
F27C1.2	1522	CCGCAGGAGAGAAACTAAGG	3'UTR Rev
F27C1.2	175A	CACCGGCTGTCAGTTCAGTA	5'UTR Fwd

Supplementary Table 2. List of primers for genotyping (*continued*)

Locus	Primer #	Sequence (5' to 3')	Description
F27C1.2	176A	TGTCTGCAGCTTGTGCGTAA	N-ter Rev
F58G6.9	1480	ACACCAAATCGAAAGCAAACC	5'UTR Fwd
F58G6.9	1481	ACTTCCAGCTGCTTCACTCT	3'UTR Rev
F58G6.9	1473	AAATCGACTTTCACTGATAACGG	Internal Rev
gei-3	1589	TCCGAGAAGTACGCCAAAGA	C-ter Fwd
gei-3	1590	GAGACAGGGGTGTGCTTTTG	3'UTR Rev
gtbp-1	1457	AGCTCAGGCTGAATCGGAAA	C-ter Fwd
gtbp-1	1458	ACAAGAAGGAAAAAGGAGAACGGA	3'UTR Rev
hcf-1	233A	ATATGGCCCGGCTACTCAAG	C-ter Fwd
hcf-1	234A	GCGGCAAAGTTGGAAAAGGT	3'UTR Rev
K12C11.3	1487	CTTTGAGCGGAGTGTCGTTG	5'UTR Fwd
K12C11.3	1488	AAGTTCATTGGAGCGCGTTT	3'UTR Rev
K12C11.3	1489	GGAGCCATCGTAGACGTGTT	Internal Rev
K12C11.6	1578	ACGCGCTCCAATGAACTTTT	5'UTR Fwd
K12C11.6	1579	ACGAGGAGTACATCAAGAGGT	3'UTR Rev
K12C11.6	1580	CGGTCACATTCCACGTCTTG	Internal Rev
mCherry	1490	TCCCACAACGAGGACTACAC	Internal Fwd
mCherry	1491	TTGGGTTCCCTCGTATGGAC	Internal Rev
mex-5p::Cas9	441A	AGTACGGAGGATTCGACTC	WT-specific Fwd: D1335, S1336

Supplementary Table 2. List of primers for genotyping (*continued*)

Locus	Primer #	Sequence (5' to 3')	Description
mex-5p::Cas9	442A	TACGGAGGATTCCTGTGG	Mutant-specific Fwd: D1135L, S1136W
mex-5p::Cas9	443A	AAGCGTCCACTCATCGAGAC	Sequencing Fwd: D1135L, S1136W
mex-5p::Cas9	444A	GTAAGCACCTTCTTGACCTCC	Common Rev: D1135L, S1136W
mex-5p::Cas9	445A	TATGCTCGCCTCCGCCGGAGAG	WT-specific Fwd: G1218, E1219
mex-5p::Cas9	446A	TATGCTCGCCTCCGCCAAACAG	Mutant-specific Fwd: G1218K, E1219Q
mex-5p::Cas9	447A	TTTCCAGGACCTCATCATCAAGC	Sequencing Fwd: G1218K, E1219Q
mex-5p::Cas9	448A	GGATGATGTTCTCGGCCTGCT	Common Rev: G1218K, E1219Q
mex-5p::Cas9	449A	TCCTTGGTGGAGGTGTAACG	WT-specific Rev: R1335Q, T1337R
mex-5p::Cas9	450A	TCCTTGGTGGAACGGTACTG	Mutant-specific Rev: R1335Q, T1337R
mex-5p::Cas9	451A	TGGCAAGCTTCTTCGCGTTT	Sequencing Rev: R1335Q, T1337R
mex-5p::Cas9	452A	GAGCTCGAGAACGGACGTAA	Common Fwd: R1335Q, T1337R
nfki-1	1446	TATAGTTCAACCGGCAGAG	5'UTR Fwd
nfki-1	1147	TGAATGTCGTGCTGAGAAAT	N-ter Rev
nhr-1	182A	TCCCGACTGGAGTTCAGAAATA	C-ter Fwd
nhr-1	183A	CAGCCGAAGTCAAAAGTCAA	3'UTR Rev
pgl-1	1454	AGGAAACCACAGTTGCTGACA	C-ter Fwd
pgl-1	1455	AATGTGCGTAAAACGTGTAAGT	3'UTR Rev
prpf-4	1206	GGCAGAGGACATGAAGATCCA	C-ter Fwd
prpf-4	1248	GGTTCGTCCTGGGAACATGA	3'UTR Rev

Supplementary Table 2. List of primers for genotyping (*continued*)

Locus	Primer #	Sequence (5' to 3')	Description
rpb-2	1574	GTAAGCTGCTCTTCCAGGAGT	C-ter Fwd
rpb-2	1575	TTAACCGGAAAAGTCCGTGAT	3'UTR Rev
sftb-1	1356	AGCTATCGAAGTTTAGGATGTTGTT	5'UTR Fwd
sftb-1	1357	CGGTTCCAATCGAGTCTAGGTA	N-ter Rev
swsn-4	1806	GCTCAAGATCGTGCACATCGT	WT-specific Fwd
swsn-4	1807	GCTCAAGATCGTGCTCACTGC	Mutant-specific Fwd
swsn-4	1808	ACTAAACCAGACGAGCGTGG	Sequencing Fwd
swsn-4	1809	TCAGATGGTTGCTCGCTCAG	Common Rev
trx-1	1748	CAAGATGATGCCGACTTTCA	C-ter Fwd
trx-1	1750	TGTTGACTCCCAACACCCTT	3'UTR Rev
ubh-4	1471	CGTCACAATTATACTCCG	C-ter Fwd
ubh-4	1315	CAAAAACAATCAAGAACCC	3'UTR Rev
usp-48	808A	CGGCGGTGAACAGTTTGATG	C-ter Fwd
usp-48	809A	GATCCAGCGAACAAAAGGGG	3'UTR Rev

Supplementary Table 2. List of primers for genotyping (*continued*)

Locus	Primer #	Sequence (5' to 3')	Description
W05H9.1	1796	CATACTGGGCGGACGTTAAT	5' UTR Fwd
W05H9.1	1797	TGTCTACGAACGGCTCGAC	Internal Fwd
W05H9.1	1798	AAAGACAAGCAGCAGTGCAA	Internal Rev
W05H9.1	1799	TTTGAAGTTGACGTGGCATT	3' UTR Rev
Y53C10A.5	276A	TGATGTGCCAAAGAAGGGGT	5'UTR Fwd
Y53C10A.5	277A	CACATTTATAAGGGAAACGAGGG	3'UTR Rev
Y53C10A.5	278A	ACATGGCATGATAGTACAAACGTC	Internal Rev
Y53C10A.5	284A	AACCCTAAAGTACGCCCTCT	C-ter Fwd

Supplementary Table 3. List of crRNAs for Nested CRISPR experiments

Locus	Sequence (5' to 3')	Orientation	Purpose	DSB to edit distance
ads-1	ACTCGACTTGCAATAAATGT	-	Step 1 N-ter crRNA	2 bp
ads-1	ATTATCTACAACTTGCAATG	+	Step 1 C-ter crRNA	9 bp
comt-3	CGCAAAAAGCTACAAGAGCT	+	Step 1 N-ter crRNA	19 bp
comt-3	TCGCTTTTAAGAAGTGAATT	+	Step 1 C-ter crRNA	0 bp
comt-4	TATTGTTGCCAAGAGTTACG	+	Step 1 N-ter crRNA	2 bp
comt-4	TTCACTTCTTAAAAGCCATG	+	Step 1 C-ter crRNA	1 bp
comt-5	TAAGGATGCCGATCCAGTGG	+	Step 1 N-ter crRNA	1 bp
comt-5	AATTTCCAGAGCCTTCGCGG	+	Step 1 C-ter crRNA	0 bp
F27C1.2	TCAGATCATGGGTACACAAT	+	Step 1 N-ter crRNA	7 bp
F27C1.2	CAATTATTAATGACACGCAT	-	Step 1 C-ter crRNA	8 bp
F58G6.9	ATGAGCATGACAACAATGTC	-	Step 1 N-ter crRNA	2 bp
F58G6.9	TTTGTTTTTGCTTCAAGAAC	+	Step 1 C-ter crRNA	1 bp
gei-3	GATGATATCAATGAGTTCGG	-	Step 1 C-ter crRNA (EGFP)	1 bp
gei-3	TCATCGTCTGATTCTACTCT	+	Step 1 C-ter crRNA (wrmScarlet)	9 bp
gtbp-1	CCACGAGGTGGTATGCGCAG	+	Step 1 C-ter crRNA	1 bp
hcf-1	TTTCGATCATCAGTAAACCA	+	Step 1 C-ter crRNA	4 bp
K12C11.3	GAGCCATCGTAGACGTGTTA	-	Step 1 N-ter crRNA	8 bp
K12C11.3	GCTATTTTTTCTTCGGATCT	+	Step 1 C-ter crRNA	9 bp

Supplementary Table 3. List of crRNAs for Nested CRISPR experiments (*continued*)

Locus	Sequence (5' to 3')	Orientation	Purpose	DSB to edit distance
K12C11.6	CATATGCATGAAAGGCGGTC	-	Step 1 N-ter crRNA	13 bp
K12C11.6	AATGGAACAATCTTGAGCGG	+	Step 1 C-ter crRNA	4 bp
nfki-1	CTTGGGGGCAACGGTTGCCA	-	Step 1 N-ter crRNA	1 bp
nhr-1	TATGAAGAGAGCATAAACGC	+	Step 1 C-ter crRNA (Cas12a)	5 bp
pgl-1	GGGGGTCGTGGTGGACGCGG	+	Step 1 C-ter crRNA	10 bp
prpf-4	TGGGAAATGTATTATTTGAT	-	Step 1 C-ter crRNA	3 bp
rpb-2	AACAATGAGCGCGATGGCTT	-	Step 1 C-ter crRNA	4 bp
sftb-1	TGTAGATCGATGTCTCGTTC	+	Step 1 N-ter crRNA	5 bp
ubh-4	TTTTCTCTTCAATTCAAGCT	-	Step 1 C-ter crRNA	0 bp
Y53C10A.5	CTTCAGAATGACATCCAGTT	+	Step 1 N-ter crRNA	7 bp
Y53C10A.5	GGCGGGGGGTTACTGTAACT	-	Step 1 C-ter crRNA	5 bp
EGFP	CGTCGAGCTCGACGGAGTCA	+	Step 2 universal crRNA	0 bp
mCherry	GTTCATGCGTTTCAAGGCCG	+	Step 2 universal crRNA	0 bp
wrmScarlet	CATGGAGGGATCCATGACCG	+	Step 2 universal crRNA	0 bp
SL2::mCherry	TGCTTCTCTTTAGTATCTGA	+	Step 2 universal crRNA	0 bp
GFP::H2B	AGAAGAACTTTTCACTGGAG	+	Step 2 universal crRNA	2 bp
2xTY1::EGFP::3xFLAG	CACAAACCAAGATCCACTCG	+	Step 2 universal crRNA	3 bp
2xTY1::EGFP::3xFLAG	TCTCCATCGTGGTCTTTGAG	-	Step 2 universal crRNA	0 bp
GFP::degron::FLAG	CACTGGAGTTGTCCCAATCC	+	Step 2 universal crRNA	0 bp

Supplementary Table 4. List of ssODNs for Nested CRISPR experiments

Locus	Reporter[1]	FP	Orien-tation	Sequence (5' to 3')
ads-1	TC	wrmScarlet	+	GATTCAGATCTTCGCCACTCGACTTGCAATAAATGGTCTCCAAGGGAGAGG CCGTCATCAAGGAGTTTATGCGTTTCAAGGTCGGACGGCACTCCACCGGAG GAATGGACGAGCTCTACAAGTAGATAATCATTGTTTCGTTTTTTATTATTAT TGG
comt-4	TC	mCherry	+	CAAAACTCCAAAAATGTCTATTGTTGCCAAGAGTTACTCCAAGGGAGAGG AGGACAACATGGCCATCATCAAGGAGTTCATGCGTTTCAAGGCCGAGGGA CGTCACTCCACCGGAGGAATGGACGAGCTCTACAAGTGAATGGATATTTA AATGAGAATTTTATTTTATTGT
comt-4	TC	GFP::H2B	+	TCCAAAACTCCAAAAATGTCTATTGTTGCCAAGAGTCCAAGTTTGTACAAA AAAGCAGGCTCCATGAGTAAAGGAGAAGAACTTTTCACTGGAGAGGGAAC CAAGGCCGTCACCAAGTACACTTCCAGCAAGTAAGAATGGATATTTAAAT GAGAATTTTATTTTATTGTC
comt-3	TC	GFP::H2B	+	TTTCAGTTTTTTTTTCCGAAAAAAAAAATGTCCAACCCAAGTTTGTACAAA AAAGCAGGCTCCATGAGTAAAGGAGAAGAACTTTTCACTGGAGAGGGAAC CAAGGCCGTCACCAAGTACACTTCCAGCAAGTAAATTAGGGGCTTTTTTTT TAATTTTGAATTATATTTA
comt-5	TC	GFP::H2B	+	GTTGTCGCTAAGAGTTATCATAAGGATGCCGATCCACCAAGTTTGTACAAA AAAGCAGGCTCCATGAGTAAAGGAGAAGAACTTTTCACTGGAGAGGGAAC CAAGGCCGTCACCAAGTACACTTCCAGCAAGTAACGGTGGCTCCGTAGCTG ACGAGAAAAGACGAGAAGA
F27C1.2	C-ter	wrmScarlet	+	TGATGGAGAAGTGACGGATTCGTTCCAAACCGATGCTTGCCACGTCAGCAA GGGAGAGGCAGTTATCAAGGAGTTCATGCGTTTCAAGGTCCACATGGAGG GATCCATGACCGAGGGACGTCACTCCACCGGAGGAATGGACGAGCTCTAC AAGTAATAATTGCGATCTCCAATCTCAATCCTCAAACA

[1] C-ter: C-terminal translational reporter, N-ter: N-terminal translational reporter, TC: transcriptional reporter

Supplementary Table 4. List of ssODNs for Nested CRISPR experiments (*continued*)

Locus	Reporter[1]	FP	Orien-tation	Sequence (5' to 3')
F27C1.2	N-ter	wrmScarlet	+	GATTTTCATGTTACGTCATATATTTTCAGATCATGGTCAGCAAGGGAGAGG CAGTTATCAAGGAGTTCATGCGTTTCAAGGTCCACATGGAGGGATCCATGA CCGAGGGACGTCACTCCACCGGAGGAATGGACGAGCTCTACAAGGGA-ACC-CAG-CTT-GCCATCCTAGGATGGTTGGCTGTGGCTTTG
F58G6.9	TC	wrmScarlet	+	TGAGAATGAACATGATGAACATGAGCATGACAACAGTCAGCAAGGGAGAG GCAGTTATCAAGGAGTTCATGCGTTTCAAGGTCCACATGGAGGGATCCATG ACCGAGGGACGTCACTCCACCGGAGGAATGGACGAGCTCTACAAGACTGG ATCATCGCTATAGAATTGCTCAAATGAAAG
gei-3	C-ter	EGFP	+	ACAAGCTACCGACCTCCAGCTTCTCGTCATCCACCTCCAAGGGAGAGGAGC TCTTCACCGGAGTCGTCCCAATCCTCGTCGAGCTCGACGGAGTCAAGGAGT TCGTCACCGCTGCCGGAATCACCCACGGAATGGACGAGCTCTACAAGGAA CTCATTGATATCATCGTCTGATTCTACTCTGG
gei-3	C-ter	SL2:: mCherry	+	TCTCGTCATCCACCGAACTCATTGATATCATCGTCGCTGTCTCATCCTACTT TCACCTAGTTAACTGCTTGTCTTAAAATCTATGCTTCTCTTTAGTATCTGAA GGGCGGCACTCGACAGGTGGCATGGATGAATTGTATAAGTGATTCTACTCT GGGCCATTACTTTTTTCCAATCACCTTTTTTA
gtbp-1	C-ter	EGFP	+	CGGTTCGGGTGGTGCTCCACGAGGTGGTATGCGCTCCAAGGGAGAGGAGC TCTTCACCGGAGTCGTCCCAATCCTCGTCGAGCTCGACGGAGTCAAGGAGT TCGTCACCGCTGCCGGAATCACCCACGGAATGGACGAGCTCTACAAGAGC GGTTTCCAAAATGCGGGACAAAATTAGAAG
gtbp-1	C-ter	mCherry	+	CGGTTCGGGTGGTGCTCCACGAGGTGGTATGCGCTCCAAGGGAGAGGAGG ACAACATGGCCATCATCAAGGAGTTCATGCGTTTCAAGGCCGAGGGACGT CACTCCACCGGAGGAATGGACGAGCTCTACAAGAGCGGTTTCCAAAATGC GGGACAAAATTAGAAG

[1] C-ter: C-terminal translational reporter, N-ter: N-terminal translational reporter, TC: transcriptional reporter

Supplementary Table 4. List of ssODNs for Nested CRISPR experiments (*continued*)

Locus	Reporter[1]	FP	Orien-tation	Sequence (5' to 3')
gtbp-1	C-ter	wrmScarlet	+	GGCGGTTCGGGTGGTGCTCCACGAGGTGGTATGCGCGTCAGCAAGGGAGA GGCAGTTATCAAGGAGTTCATGCGTTTCAAGGTCCACATGGAGGGATCCAT GACCGAGGGACGTCACTCCACCGGAGGAATGGACGAGCTCTACAAGAGCG GTTTCCAAAATGCGGGACAAAATTAGAAGCT
hcf-1	C-ter	GFP:: degron:: 3xFLAG	+	GTGGTCAGCAAAAGAGAGCTCGTTTCGATCATCAGAGTAAAGGAGAAGAA CTTTTCACTGGAGTTGTCCCAATCCTGGACTACAAAGACCATGACGGTGAT TATAAAGATCATGATATCGATTACAAGGATGACGATGACAAGTAAACCAT GGGATGGACTGATCGTTTTCTTATTTATGAT
K12C11.3	TC	mCherry	+	GCCTGACTATACTTATTTTTTATGAGCAGAAAATGTCCAAGGGAGAGGAGG ACAACATGGCCATCATCAAGGAGTTCATGCGTTTCAAGGCCGAGGGACGT CACTCCACCGGAGGAATGGACGAGCTCTACAAGTGAATCGATCGATAATG TTTATATAATTTTTGTTT
K12C11.6	TC	mCherry	+	GCCACGATAAATTTTAAAATTTCCAGAAAAAAATGTCCAAGGGAGAGGAG GACAACATGGCCATCATCAAGGAGTTCATGCGTTTCAAGGCCGAGGGACG TCACTCCACCGGAGGAATGGACGAGCTCTACAAGTGAGCGGCGGCAAGCG CGCTCTATTGCTAAGTTTG
nfki-1	N-ter	EGFP	+	GTTTTCCAAAATTACGTCGTTTGTTTTCAGCCATGTCCAAGGGAGAGGAGC TCTTCACCGGAGTCGTCCCAATCCTCGTCGAGCTCGACGGAGTCAAGGAGT TCGTCACCGCTGCCGGAATCACCCACGGAATGGACGAGCTCTACAAGGCA ACCGTTGCCCCCAAGGGAAACTGCCTTGTCGCT
nhr-1	C-ter	2xTY1:: EGFP:: 3xFLAG	+	ATCCATTTGTCAAGGAACTTTGTATGAAGAGAGCAGAAGTGCATACCAATC AGGACCCGCTGGATGAAGTCCACACAAACCAAGATCCACTC/AAAGACCAC GATGGAGACTATAAAGATCATGACATTGACTACAAGGATGACGACGACAA GTAAACGCGAAATTTGTTTATTATAAATATATTGAAGTTTT

[1] C-ter: C-terminal translational reporter, N-ter: N-terminal translational reporter, TC: transcriptional reporter

Supplementary Table 4. List of ssODNs for Nested CRISPR experiments (*continued*)

Locus	Reporter[1]	FP	Orien-tation	Sequence (5' to 3')
pgl-1	C-ter	EGFP	+	CGTGGACGTGGTGGTTACGGGGGTCGTGGTGGACGTGGCGGCTTTTCCAAG GGAGAGGAGCTCTTCACCGGAGTCGTCCCAATCCTCGTCGAGCTCGACGGA GTCAAGGAGTTCGTCACCGCTGCCGGAATCACCCACGGAATGGACGAGCT CTACAAGTAAACTCCAACTATTGAATGTTTAATTTGTTTTTTAAG
pgl-1	C-ter	mCherry	+	CGTGGACGTGGTGGTTACGGGGGTCGTGGTGGACGTGGCGGCTTTTCCAAG GGAGAGGAGGACAACATGGCCATCATCAAGGAGTTCATGCGTTTCAAGGC CGAGGGACGTCACTCCACCGGAGGAATGGACGAGCTCTACAAGTAAACTC CAACTATTGAATGTTTAATTTGTTTTTTAAG
prpf-4	C-ter	EGFP	-	TTAGAGATCACCGAAAAAATTTGGGAAATGTATTACTTGTAGAGCTCGTCC ATTCCGTGGGTGATTCCGGCAGCGGTGACGAACTCCTTGACTCCGTCGAGC TCGACGAGGATTGGGACGACTCCGGTGAAGAGCTCCTCTCCCTTGGACTTG ATAGGTATGGTGAAGAATGGGTGTTTGAGAGCCT
prpf-4	C-ter	mCherry	-	TTAGAGATCACCGAAAAAATTTGGGAAATGTATTACTTGTAGAGCTCGTCC ATTCCTCCGGTGGAGTGACGTCCCTCGGCCTTGAAACGCATGAACTCCTTG ATGATGGCCATGTTGTCCTCCTCTCCCTTGGACTTGATAGGTATGGTGAAG AATGGGTGTTTGAGAGCCT
prpf-4	C-ter	2xTY1:: EGFP:: 3xFLAG	-	TTAGAGATCACCGAAAAAATTTGGGAAATGTATTACTTGTCGTCGTCATCC TTGTAGTCAATGTCATGATCTTTATAGTCTCCTCGAGTGGATCTTGGTTTGT GTGGACTTCATCCAGCGGGTCCTGATTGGTATGCACTTCCTTGATAGGTAT GGTGAAGAATGGGTGTTTGAGAGCCT
rpb-2	C-ter	GFP:: degron:: 3xFLAG	+	GACAATCAAAACGTTCAAAACATCAATCGGAAGCCAGTAAAGGAGAAGAA CTTTTCACTGGAGTTGTCCCAATCCTGGACTACAAAGACCATGACGGTGAT TATAAAGATCATGATATCGATTACAAGGATGACGATGACAAGTAAGCCAT CGCGCTCATTGTTCGATGAATTTATTCTAAT

[1] C-ter: C-terminal translational reporter, N-ter: N-terminal translational reporter, TC: transcriptional reporter

Supplementary Table 4. List of ssODNs for Nested CRISPR experiments (*continued*)

Locus	Reporter[1]	FP	Orien-tation	Sequence (5' to 3')
sftb-1	N-ter	mCherry	+	CTTCCATATAATCAATATTGATTGTAGATCGATGTCCAAGGGAGAGGAGGA CAACATGGCCATCATCAAGGAGTTCATGCGTTTCAAGGCCGAGGGACGTC ACTCCACCGGAGGAATGGACGAGCTCTACAAGTCAAGATCTGGCGAGGCT TATGCGCAGGAGTTGAACCGCAAAAG
ubh-4	C-ter	EGFP	+	AAGAAAAATCCAAGCTGAATACAGACATAACCAAGTCCAAGGGAGAGGA GCTCTTCACCGGAGTCGTCCCAATCCTCGTCGAGCTCGACGGAGTCAAGGA GTTCGTCACCGCTGCCGGAATCACCCACGGAATGGACGAGCTCTACAAGCT TGAATTGAAGAGAAAACAATAGATATTGCATTCT
Y53C10A.5	TC	wrmScarlet	+	CAAAAACCTTTGCAAAAATCAATAACTTCAGAATGGTCAGCAAGGGAGAG GCAGTTATCAAGGAGTTCATGCGTTTCAAGGTCCACATGGAGGGATCCATG ACCGAGGGACGTCACTCCACCGGAGGAATGGACGAGCTCTACAAGTAACC CCCCGCCTGCCTTCTCGCCTACAGTACCCC
Y53C10A.5	C-ter	wrmScarlet	-	GGGGTACTGTAGGCGAGAAGGCAGGCGGGGGGTTACTTGTAGAGCTCGTC CATTCCTCCGGTGGAGTGCCGTCCGACCTTGAAACGCATAAACTCCTTGAT GACGGCCTCTCCCTTGGAGACCTGTAACTTGGTGGCCCACTTCAAATCGTC CTCTCGTGGT
dpy-10 (co-CRISPR)	N/A	N/A	+	CACTTGAACTTCAATACGGCAAGATGAGAATGACTGGAAACCGTACCGCA TGCGGTGCCTATGGTAGCGGAGCTTCACATGGCTTCAGACCAACAGCCTAT

[1] C-ter: C-terminal translational reporter, N-ter: N-terminal translational reporter, TC: transcriptional reporter

Supplementary Table 4. List of ssODNs for Nested CRISPR experiments (*continued*)

FP	Orien-tation	Sequence (5' to 3')[2]
GFP (megamer)	+	TCCAAGGGAGAGGAGCTCTTCACCGGAGTCGTCCCAATCCTCGTCGAGCTCGACGGAGACGTCAACGGACACA AGTTCTCCGTCTCAGGAGAGGGAGAGGGAGACGCCACCTACGGAAAGCTCACCCTCAAGTTCATCTGCACCAC CGGAAAGCTCCCAGTCCCATGGCCAACCCTCGTCACCACCTTCACTTACGGAGTCCAATGCTTCTCCCGTTACCC AGACCACATGAAGCGTCACGACTTCTTCAAGTCCGCCATGCCAGAGGGATACGTCCAAGAGCGTACCATCTTCT TCAAGgtaagtttaaacattaattaatactaactaaccctgattatttaaattttcagGACGACGGAAACTACAAGACCCGTGCCGAGGTCAAGTTC GAGGGAGACACCCTCGTCAACCGTATCGAGCTCAAGgtaagtttaaacagttcggtactaactaaccatacatatttaaattttcagGGAATCGA CTTCAAGGAGGACGGAAACATCCTCGGACACAAGCTCGAATACAACTACAACTCCCACAACGTCTACATCATG GCCGACAAGCAAAAGAACGGAATCAAGGTCAACTTCAAGATCCGTCACAACATCGAGGACGGATCTGTCCAAC TCGCCGACCACTACCAACAAAACACCCCAATCGGAGACGGACCAGTCCTCCTCCCAGACAACCACTACCTCTCC ACCCAATCCGCCCTCTCCAAGGACCCAAACGAGAAGCGTGACCACATGGTCCTCAAGGAGTTCGTCACCGCTGC CGGAATCACCCACGGAATGGACGAGCTCTACAAG
GFP (megamer)	-	CTTGTAGAGCTCGTCCATTCCGTGGGTGATTCCGGCAGCGGTGACGAACTCCTTGAGGACCATGTGGTCACGCT TCTCGTTTGGGTCCTTGGAGAGGGCGGATTGGGTGGAGAGGTAGTGGTTGTCTGGGAGGAGGACTGGTCCGTCT CCGATTGGGGTGTTTTGTTGGTAGTGGTCGGCGAGTTGGACAGATCCGTCCTCGATGTTGTGACGGATCTTGAA GTTGACCTTGATTCCGTTCTTTTGCTTGTCGGCCATGATGTAGACGTTGTGGGAGTTGTAGTTGTATTCGAGCTT GTGTCCGAGGATGTTTCCGTCCTCCTTGAAGTCGATTCCctgaaaatttaaatatgtatggttagttagtaccgaactgtttaaacttacCTTGAG CTCGATACGGTTGACGAGGGTGTCTCCCTCGAACTTGACCTCGGCACGGGTCTTGTAGTTTCCGTCGTCctgaaaatttt aaataatcagggttagttagtattaattaatgtttaaacttacCTTGAAGAAGATGGTACGCTCTTGGACGTATCCCTCTGGCATGGCGGACT TGAAGAAGTCGTGACGCTTCATGTGGTCTGGGTAACGGGAGAAGCATTGGACTCCGTAAGTGAAGGTGGTGAC GAGGGTTGGCCATGGGACTGGGAGCTTTCCGGTGGTGCAGATGAACTTGAGGGTGAGCTTTCCGTAGGTGGCGT CTCCCTCTCCCTCTCCTGAGACGGAGAACTTGTGTCCGTTGACGTCTCCGTCGAGCTCGACGAGGATTGGGACG ACTCCGGTGAAGAGCTCCTCTCCCTTGGA

Supplementary Table 4. List of ssODNs for Nested CRISPR experiments (*continued*)

FP	Orien-tation	Sequence (5' to 3')[2]
mCherry (megamer)	-	CTTGTAGAGCTCGTCCATTCCTCCGGTGGAGTGACGTCCCTCGGCACGCTCGTATTGCTCGACGATGGTGTAGTC CTCGTTGTGGGAGGTGATGTCGAGCTTGATGTTGACGTTGTAGGCTCCTGGGAGTTGGACTGGCTTCTTGGCCTT GTAGGTGGTCTTGACCTCGGCGTCGTAGTGTCCTCCGTCCTTGAGCTTGAGACGTTGCTTGATCTCTCCCTTGAG GGCTCCGTCCTCTGGGTACATACGCTCGGAGGAGGCCTCCCATCCCATGGTCTTCTTTTGCATGACTGGTCCGTC GGATGGGAAGTTGGTTCCACGGAGCTTGACCTTGTAGATGAACTCTCCGTCTTGGAGGGAGGAGTCTTGGGTGA CGGTGACGACTCCTCCGTCCTCGAAGTTCATGACACGCTCCCACTTGAATCCCTCTGGGAAGGAGAGCTTGAGG TAGTCTGGGATGTCGGCTGGGTGCTTGACGTAGGCCTTTGATCCGTACATGAATTGTGGGGAGAGGATGTCCCA GGCGAATGGGAGTGGTCCTCCCTTGGTGACCTTGAGCTTGGCGGTTTGGGTTCCCTCGTATGGACGTCCCTCTCC CTCTCCCTCGATCTCGAACTCGTGTCCGTTGACTGATCCCTCCATGTGGACCTTGAAACGCATGAACTCCTTGAT GATGGCCATGTTGTCCTCCTCTCCCTTGGA

[1] C-ter: C-terminal translational reporter, N-ter: N-terminal translational reporter, TC: transcriptional reporter

[2] Exons in uppercase, introns in lowercase

Supplementary Table 5. List of crRNAs and ssODNs for Cas12a experiments

crRNAs

Locus	Nuclease	Sequence (5’ to 3’)	Purpose
dpy-10	Cas9	TACGGCAAGATGAGAATGAC	Introduction of TTTV PAM
dpy-10	Cas12a	CTGGAAACCGTACCGCTCGT	Generation of *cn64* point mutation

ssODNs

Locus	Nuclease	Sequence (5’ to 3’)	Purpose
dpy-10	Cas9	ACGAGGCTGCACTTGAACTTCAATACGGCAAGATG CGATTTACTGGAAACCGTACCGCTCGTGGTGCCTAT GGTAG	Introduction of TTTV PAM
dpy-10	Cas12a	ACGGCAAGATGCGATTTACTGGAAACCGTACCGCT TGTGGTGCCTATGGTAGCGGAGCTTCACATGGCTTC AGACCA	Generation of *cn64* point mutation

Supplementary Table 6. List of sgRNAs for Cas12f1 experiments

sgRNA	Nuclease	Sequence (5' to 3')	Purpose
dpy-10	Un1Cas12f1 AsCas12f1	CTGGAAACCGTACCGCTCGT	Generation of *cn64* point mutation
EGFP1	Un1Cas12f1 AsCas12f1	AACTTACCTTGAAGAAGATG	EGFP knockout assay
EGFP2	Un1Cas12f1 AsCas12f1	AATTTTCAGATCCGTCACAA	EGFP knockout assay
EGFP3	Un1Cas12f1 AsCas12f1	TTGGTAGTGGTCGGCGAGTT	EGFP knockout assay
EGFP1	SpCas12f1	ACTTACGGAGTCCAATGCTT	EGFP knockout assay
EGFP2	SpCas12f1	AAGTCCGCCATGCCAGAGGG	EGFP knockout assay
EGFP3	SpCas12f1	TTTTGCTTGTCGGCCATGAT	EGFP knockout assay

Supplementary Table 7. List of crRNAs for Near-PAMless Cas9 variants experiments

Locus	Protospacer (5' to 3')	PAM	Orientation	Purpose	DSB to edit distance[1]
cep-1	AAGCGATGAAACTGCCAAAG	TAA(A)	+	*cep-1* wrmScarlet Step 1	3 bp
dpy-10	GCTACCATAGGCACCACGAG	CGG(T)	-	Screening for Rol or Dpy phenotypes	0 bp
dpy-10	TGACTGGAAACCGTACCGCT	CGT(G)	+	Screening for Rol or Dpy phenotypes	3 bp
swsn-4	AAGAAGATGAAGAAGGATAT	CGT(G)	+	R350C substitution	6 bp
trx-1	AGCAGATGGTCGAAGATCAT	TGA(G)	-	*trx-1* wrmScarlet Step 1 (C-ter)	2 bp
usp-48	TCTGTGAAAAAATATCAATG	AGC(G)	-	*usp-48* wrmScarlet Step 1 (C-ter)	0 bp
W05H9.1	TTATCATTAACATTTTAGAA	TGA(G)	+	W05H9.1 GFP H2B Step 1 (N-ter)	14 bp
W05H9.1	AATTTTATAATACAATCACA	TGG(T)	-	W05H9.1 GFP H2B Step 1 (C-ter)	5 bp
wrmScarlet	GGGAGAGGGACGTCCATACG	AGG(G)	+	wrmScarlet knockout assay	N/A
wrmScarlet	GGGATGGGAGGCCTCCACCG	AGC(G)	+	wrmScarlet knockout assay	N/A
wrmScarlet	GGTTTGGGTTCCCTCGTATG	GAC(G)	-	wrmScarlet knockout assay	N/A
wrmScarlet	CTCCTGGGACATCCTCTCCC	CAC(A)	+	wrmScarlet knockout assay	N/A
wrmScarlet	TCAAGTGGGAGCGTGTCATG	AAC(T)	+	wrmScarlet knockout assay	N/A

[1] N/A: wrmScarlet knockouts do not require HDR and thus, the DSB to edit distance is not specified.

Supplementary Table 8. List of ssODNs for Near-PAMless Cas9 variants experiments

Locus	Orientation	Purpose	Sequence (5' to 3')
cep-1	+	C-ter wrmScarlet reporter	GCTTTTACCGCATCCAGGAAGCGATGAAACTGCCAAAGGTCAGCAAGGGAGA GGCAGTTATCAAGGAGTTCATGCGTTTCAAGGTCCACATGGAGGGATCCATGA CCGAGGGACGTCACTCCACCGGAGGAATGGACGAGCTCTACAAGTAAAAATC ATATCACCACCTGGTTTAATCGCCTAATTT
swsn-4	+	R350C substitution	CGTATGCAAAAACTGATGCAAGAAGATGAAGAAGGCTACTGCGCTCTTCTTGA TGAGAAGAAAGATCAACGTCTTGT
trx-1	+	C-ter wrmScarlet reporter	AACTGCGTCAAAAAGTGTTGGAGCACGTATCTGCTCAAGTCAGCAAGGGAGA GGCAGTTATCAAGGAGTTCATGCGTTTCAAGGTCCACATGGAGGGATCCATGA CCGAGGGACGTCACTCCACCGGAGGAATGGACGAGCTCTACAAGTGATCTTCG ACCATCTGCTTTTAAACCAATCATCT
usp-48	+	C-ter wrmScarlet reporter	CCCCGGAGCGTGGTTTCGTGGATACAGCGCTCGCTCATGTCAGCAAGGGAGAG GCAGTTATCAAGGAGTTCATGCGTTTCAAGGTCCACATGGAGGGATCCATGAC CGAGGGACGTCACTCCACCGGAGGAATGGACGAGCTCTACAAGTGATATTTTT TCACAGACAATGTTTAATTCTTATA
W05H9.1	+	GFP::H2B transcriptional reporter	TCTGTATTGATTTTTATCATTAACATTTTAGAATGCCAAGTTTGTACAAAAAAG CAGGCTCCATGAGTAAAGGAGAAGAACTTTTCACTGGAGAGGGAACCAAGGC CGTCACCAAGTACACTTCCAGCAAGTAAACTTTGTTCGATAACCATGTGATTGT ATTATA

Supplementary Table 9. Miscellaneous CRISPR injection mixes

I. dpy-10 experiments

1. WTSpCas9 RNP

Component	**Volume**	**Initial concentration**		**Final concentration**	
	µL	µM	ng/µL	µM	ng/µL
WT SpCas9	2.50	6.3	1000.0	1.58	250.0
tracrRNA	0.50	32.0	7098.3	1.60	354.9
dpy-10 crRNA	1.60	10.0	1151.0	1.60	184.2
dpy-10 (cn64) ssODN	0.25	32.7	1000.0	0.82	25.0
Nuclease-free H_2O	5.15				
Total volume	**10.00**				

2. SpG RNP

Component	**Volume**	**Initial concentration**		**Final concentration**	
	µL	µM	ng/µL	µM	ng/µL
Cas9 SpG	1.25	12.6	2000.0	1.57	250.0
tracrRNA	0.50	32.0	7098.3	1.60	354.9
dpy-10 crRNA	1.60	10.0	1151.0	1.60	184.2
dpy-10 (cn64) ssODN	0.28	32.7	1000.0	0.91	28.0
Nuclease-free H_2O	6.37				
Total volume	**10.00**				

3. SpRY RNP

Component	**Volume**	**Initial concentration**		**Final concentration**	
	µL	µM	ng/µL	µM	ng/µL
Cas9 SpRY	1.25	12.61	2000.0	1.58	250.0
tracrRNA	0.50	32.0	709.8	1.60	35.5
dpy-10 crRNA	1.60	10.0	115.1	1.60	18.4
dpy-10 (cn64) ssODN	0.28	32.7	1000.0	0.91	28.0
Nuclease-free H_2O	6.37				
Total volume	**10.00**				

Supplementary Table 9. Miscellaneous CRISPR injection mixes (*continued*)

4. SpG endogenous

Component	**Volume**	**Initial concentration**		**Final concentration**	
	µL	µM	ng/µL	µM	ng/µL
dpy-10 crRNA	1.00	100	1151.0	10.00	115.1
tracrRNA	0.32	320	7098.3	10.24	227.2
pCFJ90	0.21		117.5		2.5
pCFJ104	0.25		204.5		5.1
Duplex buffer	8.22				
Total volume	**10.00**				

II. wrmScarlet experiments

1. WT SpCas9/SpG/SpRY 1.3 µM, 50 mM KCl

Component	**Volume**	**Initial concentration**		**Final concentration**	
	µL	µM	ng/µL	µM	ng/µL
Cas9	1.40	11.0	1750.0	1.54	245.0
tracrRNA	0.50	32.0	709.8	1.60	35.5
anti-wrmScarlet crRNA	1.60	10.0	118.0	1.60	18.9
Nuclease-free H_2O	6.50				
Total volume	**10.00**				

2. SpG/SpRY 3.7 µM

Component	**Volume**	**Initial concentration**		**Final concentration**	
	µL	µM	ng/µL	µM	ng/µL
Cas9	4.00	11.0	1750.0	4.41	700.0
tracrRNA	1.40	32.0	709.8	4.60	99.4
anti-wrmScarlet crRNA	4.60	10.0	118.0	4.48	54.3
Nuclease-free H_2O	0.00				
Total volume	**10.00**				

Supplementary Table 9. Miscellaneous CRISPR injection mixes (*continued*)

3. WT SpCas9/SpG/SpRY 8.0 µM

Component	Volume	Initial concentration		Final concentration	
	µL	µM	ng/µL	µM	ng/µL
Cas9	8.65	11.0	1750.0	9.54	1513.8
tracrRNA	1.40	320.0	7098.0	10.30	227.2
anti-wrmScarlet crRNA	4.60	100.0	1180.0	10.24	12.2
Nuclease-free H_2O	0.00				
Total volume	**10.00**				

4. SpG 1.3 µM, 300 mM KCl

Component	Volume	Initial concentration		Final concentration	
	µL	µM	ng/µL	µM	ng/µL
Cas9	1.40	11.0	1750.0	1.54	245.0
tracrRNA	0.50	32.0	709.8	1.60	35.5
anti-wrmScarlet crRNA	1.60	10.0	118.0	1.60	18.9
KCl	2.50	1 M		250 mM	
Nuclease-free H_2O	4.00				
Total volume	**10.00**				

5. *dpy-10* RNP 6x

Component	Volume	Initial concentration		Final concentration	
	µL	µM	ng/µL	µM	ng/µL
WT SpCas9 or SpG	6.97	11.0	1750.0	7.69	1219.8
tracrRNA	0.32	320.0	7098.0	10.30	227.2
dpy-10 crRNA	1.03	100.0	1151.0	10.24	118.6
dpy-10 (cn64) ssODN	1.68	32.7	1000.0	0.91	28.0
Total volume	**10.00**				

To assemble: Take 5 parts of anti-wrmScarlet mix and add 1 part of *dpy-10* 6x mix (8.33 uL anti-wrmScarlet mix + 1.67 uL *dpy-10* x6 mix)

Supplementary Table 9. Miscellaneous CRISPR injection mixes (*continued*)

III. *usp-48*::wrmScarlet

Component	**Volume**	**Initial concentration**		**Final concentration**	
	µL	µM	ng/µL	µM	ng/µL
SpG	8.00	12.6	2000.0	10.07	1600.0
tracrRNA	0.32	320.0	7098.3	10.24	227.1
dpy-10 crRNA	0.20	100.0	1151.0	2.00	23.0
usp-48 C-ter crRNA	0.80	100.0	1187.7	8.00	95.0
dpy-10 (cn64) ssODN	0.28	32.7	1000.0	0.91	28.0
usp-48 Step 1 ssODN	0.22	100.0	5004.4	2.20	110.1
Nuclease-free H_2O	0.18				
Total volume	**10.00**				

IV. *trx-1*::wrmScarlet

Component	**Volume**	**Initial concentration**		**Final concentration**	
	µL	µM	ng/µL	µM	ng/µL
SpG	8.00	11.0	1750.0	8.82	1400.0
tracrRNA	0.32	320.0	709.8	10.24	22.7
dpy-10 crRNA	0.10	100.0	1151.0	1.00	11.5
trx-1 C-ter crRNA	0.90	100.0	1185.2	9.00	106.7
dpy-10 (cn64) ssODN	0.28	32.7	1000.0	0.91	28.0
trx-1 Step 1 ssODN	0.22	100.0	5693.4	2.20	125.3
Nuclease-free H_2O	0.18				
Total volume	**10.00**				

Supplementary Table 9. Miscellaneous CRISPR injection mixes (*continued*)

V. W05H9.1::GFP::H2B

Component	Volume	Initial concentration		Final concentration	
	µL	µM	ng/µL	µM	ng/µL
SpG	7.70	11.0	1750.0	8.49	1347.5
tracrRNA	0.50	320.0	709.8	16.00	35.5
dpy-10 crRNA	0.10	100.0	1151.0	1.00	11.5
W05H9.1 N-ter crRNA	0.60	100.0	1168.1	6.00	70.1
W05H9.1 C-ter crRNA	0.60	100.0	1168.7	6.00	70.1
dpy-10 (cn64) ssODN	0.28	32.7	1000.0	0.91	28.0
W05H9.1 Step 1 ssODN	0.22	100.0	5996.5	2.20	131.9
Total volume	**10.00**				

VI. *cep-1*::wrmScarlet

Component	Volume	Initial concentration		Final concentration	
	µL	µM	ng/µL	µM	ng/µL
SpRY	8.29	11.0	1750.0	9.14	1450.8
tracrRNA	0.29	320.0	709.8	9.28	20.6
dpy-10 crRNA	0.24	100.0	1151.0	2.40	27.6
cep-1 C-ter crRNA	0.68	100.0	1185.8	6.80	80.6
dpy-10 ssODN	0.28	32.7	1000.0	0.91	28.0
cep-1 Step 1 ssODN	0.22	100.0	5786.8	2.20	127.3
Total volume	**10.00**				

VII. *swsn-4*[R350C]

Component	Volume	Initial concentration		Final concentration	
	µL	µM	ng/µL	µM	ng/µL
SpG	8.00	11.0	1750.0	8.82	1400.0
tracrRNA	0.32	320.0	709.8	10.24	22.7
dpy-10 crRNA	0.10	100.0	1151.0	1.00	11.5
swsn-4 crRNA	0.90	100.0	1194.7	9.00	107.5
dpy-10 (cn64) ssODN	0.28	32.7	1000.0	0.91	28.0
swsn-4 [R350C] ssODN	0.22	100.0	2388.5	2.20	52.5
Nuclease-free H_2O	0.18				
Total volume	**10.00**				

Supplementary Table 9. Miscellaneous CRISPR injection mixes (*continued*)

VIII. Generation of CER658, CER659, and CER660 (germline endogenous SpG) from the base strain EG9615

1. D1135L and S1136W (crRNA 158, ssODN 118), G1218K and E1219Q (crRNA 159, ssODN 119), and R1335Q and T1337R (crRNA 160, ssODN 120)

Component	**Volume**	**Initial concentration**		**Final concentration**	
	µL	µM	ng/µL	µM	ng/µL
tracrRNA	1.00	32.0	709.8	3.20	71.0
crRNA 158	1.00	10.0	119.4	1.00	11.9
crRNA 159	1.00	10.0	116.7	1.00	11.7
crRNA 160	1.00	10.0	118.6	1.00	11.9
ssODN 118	0.22	100.0	2465.2	2.20	54.2
ssODN 119	0.22	100.0	2329.1	2.20	51.2
ssODN 120	0.22	100.0	2432.4	2.20	53.5
pCFJ90	0.29		86.0		2.5
pCFJ104	0.50		100.0		5.0
Nuclease-free H_2O	4.55				
Total volume	**10.00**				

2. G1218K and E1219Q (crRNA 159, ssODN 119), and R1335Q and T1337R (crRNA 160, ssODN 120) via RNP delivery

Component	**Volume**	**Initial concentration**		**Final concentration**	
	µL	µM	ng/µL	µM	ng/µL
Cas9 (IDT)	0.35	61.0	10000.0	2.14	350.0
tracrRNA	0.65	32.0	709.8	2.08	46.1
crRNA 159	1.00	10.0	116.7	1.00	11.7
crRNA 160	1.00	10.0	118.6	1.00	11.9
ssODN 119	0.22	100.0	2329.1	2.20	51.2
ssODN 120	0.22	100.0	2432.4	2.20	53.5
pCFJ90	0.29		86.0		2.5
pCFJ104	0.50		100.0		5.0
Nuclease-free H_2O	5.77				
Total volume	**10.00**				

Supplementary Table 10. List of PATC introns used in the pCUC76 and pCUC78 constructs[1]

Construct (Intron No., length)	Sequence (5' to 3')[2]
pCUC76 (Intron 1, 240 bp) *Reduced Synthetic Intron 1*	GTAAGTTTTCTcgTTTTctAAAAAAAAgaatgaTTTTTgcatg TTTTcggTTTAAAAAAtctgAAAAgtaacgcAAAAAgcaatAAA AAgcaagTTTTTcatcTTTTaatctagtAAAAAtgatAAAAtagtccT TTTTatcgtAAAAcagtgcTTTTTTAAAtagTTTTcccAAAAAAt gccgttAAAAAAgcTTTTTcgAAAAtAAAAcgcgtgtAAAActtc gTTTTAGATTTTCAG
pCUC76 (Intron 2, 246 bp) *Reduced Synthetic Intron 3*	GTAAGTTCTTTTaTTTTagtaccTTTTggagcAAAAAgacggTT TTgtagcagTTTTTctatagAAAAAAgtcAAAAgacctggTTTTccT TTAAAATTTaacAAAAgctatatgTTTTggtaacAAAAgagagAA AAgaatccTTTTattgctaTTTTctaatggAAAAAtcaccTTTTgctatA AAATTTTcAAAAAggagtgAAAAccagagcaTTTTacagcaTTT TAAAAGTAATTTTCAG
pCUC78 (Intron 1, 286 bp) *Y54F10AL.1*	GTAAGTTCTTTacggagAAAAtgcggAAAAttgtgAAAATAA AAcacTTTTTTgaatgAAAAAtcgAAATTTTTcgtaTTTTTTact gAAAAAAtcggaaTTTTTcgtattaTTTagtgAAAAAAtcgAAAA AtgttataaTTTTTgacgAAATTTatagcAAAAAAtcacaaTTTTTg ccaTTTctagtcgTTTTcattgtAAAAAccagAAAAttgtatgaTTTTg acagAAAAAttcaagaaTTTgagcgTTTTTTaaccAAAAAAAAAc tgGTAATTTTCAG
pCUC78 (Intron 2, 454 bp) *F20G4.3*	GTAAGTTTTCTtgtcgatagctaacaattcttcattgaatatAAAtattctcgtc aagctggttgtcgtcTTTTggcgTTTacataagcctaagatgcggTTTcTTTc gtagcaattcTTTgtggcgaTTTaacccccctaactcagaggaaccagctcAAAtt atagaataagTTTcAAAgtagAAATTTTgtAAAtggaccggcttctgccat tcccggagaTTTTcctatattgaaccttgctgtgaccTTTatctctaagaaggaatac agttaTTTctgtagTTTgataatcTTTTTatcaggtgagatatAAAAtatgca gaacgtctcaaccggtcgttggTTTTTaataatcaagagatcctgatgaccTTTgc aacaTTTcAAAtaTTTaTTTaaggcAAAAActtatacaTTTatatAA Atatcaatcgaattat AGATTTTCAG
pCUC78 (Intron 3, 286 bp) *Y54F10AL.1*	GTAAGTTCTTTacggagAAAAtgcggAAAAttgtgAAAAAAA AAcacTTTTTTgaatgAAAAAtcgAAATTTTTcgtaTTTTTTact gAAAAAAtcggaaTTTTTcgtattaTTTagtgAAAAAAtcgAAAA AtgttataaTTTTTgacgAAATTTatagcAAAAAAtcacaaTTTTTg ccaTTTctagtcgTTTTcattgtAAAAAccagAAAAttgtatgaTTTTg acagAAAAAttcaagaaTTTgagcgTTTTTTaaccAAAAAAAAAc tgGTAATTTTCAG

[1] Reference: Frøkjær-Jensen et al., 2016

[2] Underlined sequences represent splice junctions

BIBLIOGRAPHY

Bibliography

Abbott, T. R., Dhamdhere, G., Liu, Y., Lin, X., Goudy, L., Zeng, L., Chemparathy, A., Chmura, S., Heaton, N. S., Debs, R., Pande, T., Endy, D., La Russa, M. F., Lewis, D. B., & Qi, L. S. (2020). Development of CRISPR as an Antiviral Strategy to Combat SARS-CoV-2 and Influenza. *Cell*, *181*(4), 865-876.e12. https://doi.org/10.1016/j.cell.2020.04.020

Adamo, A., Collis, S. J., Adelman, C. A., Silva, N., Horejsi, Z., Ward, J. D., Martinez-Perez, E., Boulton, S. J., & La Volpe, A. (2010). Preventing Nonhomologous End Joining Suppresses DNA Repair Defects of Fanconi Anemia. *Molecular Cell*, *39*(1), 25–35. https://doi.org/10.1016/j.molcel.2010.06.026

Ahier, A., & Jarriault, S. (2014). Simultaneous expression of multiple proteins under a single promoter in *Caenorhabditis elegans* via a versatile 2A-based toolkit. *Genetics*, *196*(3), 605–613. https://doi.org/10.1534/genetics.113.160846

Ahmad, A., Robinson, A. R., Duensing, A., van Drunen, E., Beverloo, H. B., Weisberg, D. B., Hasty, P., Hoeijmakers, J. H. J., & Niedernhofer, L. J. (2008). ERCC1-XPF Endonuclease Facilitates DNA Double-Strand Break Repair. *Molecular and Cellular Biology*, *28*(16), 5082–5092. https://doi.org/10.1128/mcb.00293-08

Ajjawi, I., Verruto, J., Aqui, M., Soriaga, L. B., Coppersmith, J., Kwok, K., Peach, L., Orchard, E., Kalb, R., Xu, W., Carlson, T. J., Francis, K., Konigsfeld, K., Bartalis, J., Schultz, A., Lambert, W., Schwartz, A. S., Brown, R., & Moellering, E. R. (2017). Lipid production in Nannochloropsis gaditana is doubled by decreasing expression of a single transcriptional regulator. *Nature Biotechnology*, *35*(7), 647–652. https://doi.org/10.1038/nbt.3865

Al-Minawi, A. Z., Saleh-Gohari, N., & Helleday, T. (2008). The ERCC1/XPF endonuclease is required for efficient single-strand annealing and gene conversion in mammalian cells. *Nucleic Acids Research*, *36*(1), 1–9. https://doi.org/10.1093/nar/gkm888

Albert Hubbard, E. J., & Greenstein, D. (2000). The *Caenorhabditis elegans* gonad: A test tube for cell and developmental biology. *Developmental Dynamics*, *218*(1), 2–22. https://doi.org/10.1002/(SICI)1097-0177(200005)218:1<2::AID-DVDY2>3.0.CO;2-W

Aljohani, M. D., El Mouridi, S., Priyadarshini, M., Vargas-Velazquez, A. M., & Frøkjær-Jensen, C. (2020). Engineering rules that minimize germline silencing of transgenes in simple extrachromosomal arrays in *C. elegans*. *Nature Communications*, *11*(1), 1–14. https://doi.org/10.1038/s41467-020-19898-0

Altun, Z. F., & Hall, D. H. (2009). Introduction to *C. elegans* Anatomy. In *WormAtlas*. https://doi.org/doi:10.3908/wormatlas.1.1

Anders, C., Niewoehner, O., Duerst, A., & Jinek, M. (2014). Structural basis of PAM-dependent target DNA recognition by the Cas9 endonuclease. *Nature*, *513*(7519), 569–573. https://doi.org/10.1038/nature13579

Anzalone, A. V, Randolph, P. B., Davis, J. R., Sousa, A. A., Koblan, L. W., Levy, J. M., Chen, P. J., Wilson, C., Newby, G. A., Raguram, A., & Liu, D. R. (2019). Search-and-replace genome editing without double-strand breaks or donor DNA. *Nature*, *576*(August), 149–157. https://doi.org/10.1038/s41586-019-1711-4

Arribere, J. A., Bell, R. T., Fu, B. X. H., Artiles, K. L., Hartman, P. S., & Fire, A. Z. (2014). Efficient marker-free recovery of custom genetic modifications with CRISPR/Cas9 in *Caenorhabditis elegans*. *Genetics*, *198*(3), 837–846. https://doi.org/10.1534/genetics.114.169730

Au, V., Li-leger, E., Raymant, G., Flibotte, S., Chen, G., Martin, K., Fernando, L., Doell, C., Rosell, F. I., Wang, S., Edgley, M. L., Rougvie, A. E., Hutter, H., & Moerman, D. G. (2019). CRISPR/Cas9 Methodology for the Generation of Knockout Deletions in *Caenorhabditis elegans*. *G3: Genes, Genomes, Genetics*, *9*(January), 135–144. https://doi.org/10.1534/g3.118.200778

Barnes, T. M., Kohara, Y., Coulson, A., & Hekimi, S. (1995). Meiotic recombination, noncoding DNA and genomic organization in *Caenorhabditis elegans*. *Genetics*, *141*(1), 159–179. https://doi.org/https://dx.doi.org/10.1093/genetics/141.1.159

Barrangou, R., Fremaux, C., Deveau, H., Richards, M., Boyaval, P., Moineau, S., Romero, D. A., & Horvath, P. (2007). CRISPR provides acquired resistance against viruses in prokaryotes. *Science*, *315*(5819), 1709–1712. https://doi.org/10.1126/science.1138140

Basila, M., Kelley, M. L., & Smith, A. V. B. (2017). Minimal 2'-O-methyl phosphorothioate linkage modification pattern of synthetic guide RNAs for increased stability and efficient CRISPR-Cas9 gene editing avoiding cellular toxicity. *PLoS ONE*, *12*(11), 1–19. https://doi.org/10.1371/journal.pone.0188593

Berkowitz, L. A., Knight, A. L., Caldwell, G. A., & Caldwell, K. A. (2008). Generation of stable transgenic *C. elegans* using microinjection. *Journal of Visualized Experiments*, *18*, 2–5. https://doi.org/10.3791/833

Bessereau, J. L., Wright, A., Williams, D. C., Schuske, K., Davis, M. W., & Jorgensen, E. M. (2001). Mobilization of a *Drosophila* transposon in the, *Caenorhabditis elegans* germ line. *Nature*, *413*(6851), 70–74. https://doi.org/10.1038/35092567

Bhargava, R., Onyango, D. O., & Stark, J. M. (2016). Regulation of Single-Strand Annealing and its Role in Genome Maintenance. *Trends in Genetics*, *32*(9), 566–575. https://doi.org/10.1016/j.tig.2016.06.007

Bindels, D. S., Haarbosch, L., van Weeren, L., Postma, M., Wiese, K. E., Mastop, M., Aumonier, S., Gotthard, G., Royant, A., Hink, M. A., & Gadella, T. W. J. J. (2017). mScarlet: a bright monomeric red fluorescent protein for cellular imaging. *Nature Methods*, *14*(1), 53–56. https://doi.org/10.1038/nmeth.4074

Blanchard, E. L., Vanover, D., Bawage, S. S., Tiwari, P. M., Rotolo, L., Beyersdorf, J., Peck, H. E., Bruno, N. C., Hincapie, R., Michel, F., Murray, J., Sadhwani, H., Vanderheyden, B., Finn, M. G., Brinton, M. A., Lafontaine, E. R., Hogan, R. J., Zurla, C., & Santangelo, P. J. (2021). Treatment of influenza and SARS-CoV-2 infections via mRNA-encoded Cas13a in rodents. *Nature Biotechnology*. https://doi.org/10.1038/s41587-021-00822-w

Blumenthal, T. (2012). Trans-splicing and operons in *C. elegans*. *WormBook : The Online Review of C. elegans Biology*, 1–11. https://doi.org/10.1895/wormbook.1.5.2

Blumenthal, T., Evans, D., Link, C. D., Guffanti, A., Lawson, D., Thierry-Mieg, J., Thierry-Mieg, D., Chiu, W. L., Duke, K., Kiraly, M., & Kim, S. K. (2002). A global analysis of *Caenorhabditis elegans* operons. *Nature*, *417*(6891), 851–854. https://doi.org/10.1038/nature00831

Blumenthal, T., & Steward, K. (1997). RNA Processing and Gene Structure. In D. L. Riddle, T. Blumenthal, B. J. Meyer, & J. R. Priess (Eds.), *C. elegans II* (2nd editio).

Bolotin, A., Quinquis, B., Sorokin, A., & Dusko Ehrlich, S. (2005). Clustered regularly interspaced short palindrome repeats (CRISPRs) have spacers of extrachromosomal origin. *Microbiology*, *151*(8), 2551–2561. https://doi.org/10.1099/mic.0.28048-0

Boulin, T., Etchberger, J. F., & Hobert, O. (2006). Reporter gene fusions. *WormBook : The Online Review of C. elegans Biology*, 1–23. https://doi.org/10.1895/wormbook.1.106.1

Brenner, S. (1974). The Genetics of *Caenorhabditis elegans*. *Genetics*, *77*(1), 71–94. https://doi.org/10.1002/cbic.200300625

Broughton, J. P., Deng, X., Yu, G., Fasching, C. L., Servellita, V., Singh, J., Miao, X., Streithorst, J. A., Granados, A., Sotomayor-Gonzalez, A., Zorn, K., Gopez, A., Hsu, E., Gu, W., Miller, S., Pan, C. Y., Guevara, H., Wadford, D. A., Chen, J. S., & Chiu, C. Y. (2020). CRISPR–Cas12-based detection of SARS-CoV-2. *Nature Biotechnology*, *38*(7), 870–874. https://doi.org/10.1038/s41587-020-0513-4

Burger, A., Lindsay, H., Felker, A., Hess, C., Anders, C., Chiavacci, E., Zaugg, J., Weber, L. M., Catena, R., Jinek, M., Robinson, M. D., & Mosimann, C. (2016). Maximizing mutagenesis with solubilized CRISPR-Cas9 ribonucleoprotein complexes. *Development (Cambridge)*, *143*(11), 2025–2037. https://doi.org/10.1242/dev.134809

Butler, N. M., Atkins, P. A., Voytas, D. F., & Douches, D. S. (2015). Generation and inheritance of targeted mutations in potato (*Solanum tuberosum* L.) Using the CRISPR/Cas System. *PLoS ONE*, *10*(12), e0144591. https://doi.org/10.1371/journal.pone.0144591

Cabantous, S., Terwilliger, T. C., & Waldo, G. S. (2005). Protein tagging and detection with engineered self-assembling fragments of green fluorescent protein. *Nature Biotechnology*, *23*(1), 102–107. https://doi.org/10.1038/nbt1044

Canver, M. C., Smith, E. C., Sher, F., Pinello, L., Sanjana, N. E., Shalem, O., Chen, D. D., Schupp, P. G., Vinjamur, D. S., Garcia, S. P., Luc, S., Kurita, R., Nakamura, Y., Fujiwara, Y., Maeda, T., Yuan, G. C., Zhang, F., Orkin, S. H., & Bauer, D. E. (2015). BCL11A enhancer dissection by Cas9-mediated in situ saturating mutagenesis. *Nature*, *527*(7577), 192–197. https://doi.org/10.1038/nature15521

Caplen, N. J., Parrish, S., Imani, F., Fire, A., & Morgan, R. A. (2001). Specific inhibition of gene expression by small double-stranded RNAs in invertebrate and vertebrate systems. *Proceedings of the National Academy of Sciences of the United States of America*, *98*(17), 9742–9747. https://doi.org/10.1073/pnas.171251798

Castillo-Davis, C. I., Mekhedov, S. L., Hartl, D. L., Koonin, E. V., & Kondrashov, F. A. (2002). Selection for short introns in highly expressed genes. *Nature Genetics*, *31*(4), 415–418. https://doi.org/10.1038/ng940

Ceccaldi, R., Rondinelli, B., & D'Andrea, A. D. (2016). Repair Pathway Choices and Consequences at the Double-Strand Break. *Trends in Cell Biology*, *26*(1), 52–64. https://doi.org/10.1016/j.tcb.2015.07.009

Certo, M. T., Ryu, B. Y., Annis, J. E., Garibov, M., Jarjour, J., Rawlings, D. J., & Scharenberg, A. M. (2011). Tracking genome engineering outcome at individual DNA breakpoints. *Nature Methods*, *8*(8), 671–676. https://doi.org/10.1038/nmeth.1648

Chalfie, M., Tu, Y., Euskirchen, G., Ward, W. W., & Prasher, D. C. (1994). Green fluorescent protein as a marker gene expression. *Science*, *263*(5148), 802–805. https://doi.org/10.1126/science.8303295

Chan, S. H., Yu, A. M., & McVey, M. (2010). Dual roles for DNA polymerase theta in alternative end-joining repair of double-strand breaks in *Drosophila*. *PLoS Genetics*, *6*(7), 1–16. https://doi.org/10.1371/journal.pgen.1001005

Chang, H. H. Y., Pannunzio, N. R., Adachi, N., & Lieber, M. R. (2017). Non-homologous DNA end joining and alternative pathways to double-strand break repair. *Nature Reviews Molecular Cell Biology*, *18*(8), 495–506. https://doi.org/10.1038/nrm.2017.48

Chatterjee, P., Jakimo, N., Lee, J., Amrani, N., Rodríguez, T., Koseki, S. R. T., Tysinger, E., Qing, R., Hao, S., Sontheimer, E. J., & Jacobson, J. (2020). An engineered ScCas9 with broad PAM range and high specificity and activity. *Nature Biotechnology*, *38*(10), 1154–1158. https://doi.org/10.1038/s41587-020-0517-0

Chatterjee, P., Lee, J., Nip, L., Koseki, S. R. T., Tysinger, E., Sontheimer, E. J., Jacobson, J. M., & Jakimo, N. (2020). A Cas9 with PAM recognition for adenine dinucleotides. *Nature Communications*, *11*(1), 1–6. https://doi.org/10.1038/s41467-020-16117-8

Chen, B., Zou, W., Xu, H., Liang, Y., & Huang, B. (2018). Efficient labeling and imaging of protein-coding genes in living cells using CRISPR-Tag. *Nature Communications*, *9*(1). https://doi.org/10.1038/s41467-018-07498-y

Chen, F., Pruett-Miller, S. M., & Davis, G. D. (2014). Gene Editing Using ssODNs with Engineered Nucleases. In S. M. Pruett-Miller (Ed.), *Chromosomal Mutagenesis. Methods in Molecular Biology (Methods and Protocols), vol 1239* (2nd editio, Issue December 2014, pp. 251–265). Humana Press. https://doi.org/10.1007/978-1-4939-1862-1

Cheng, A. W., Wang, H., Yang, H., Shi, L., Katz, Y., Theunissen, T. W., Rangarajan, S., Shivalila, C. S., Dadon, D. B., & Jaenisch, R. (2013). Multiplexed activation of endogenous genes by CRISPR-on, an RNA-guided transcriptional activator system. *Cell Research*, *23*(10), 1163–1171. https://doi.org/10.1038/cr.2013.122

Chin, G. M., & Villeneuve, A. M. (2001). *C. elegans* mre-11 is required for meiotic recombination and DNA repair but is dispensable for the meiotic G2 DNA damage checkpoint. *Genes and Development*, *15*(5), 522–534. https://doi.org/10.1101/gad.864101

Chiu, H., Schwartz, H. T., Antoshechkin, I., & Sternberg, P. W. (2013). Transgene-Free Genome Editing in *Caenorhabditis elegans* Using CRISPR-Cas. *Genetics*, *195*(November), 1167–1171. https://doi.org/10.1534/genetics.113.155879

Cho, S. W., Lee, J., Carroll, D., Kim, J.-S., & Lee, J. (2013). Heritable gene knockout in *Caenorhabditis elegans* by direct injection of Cas9-sgRNA ribonucleoproteins. *Genetics*, *195*(3), 1177–1180. https://doi.org/10.1534/genetics.113.155853

Chudakov, D. M., Matz, M. V., Lukyanov, S., & Lukyanov, K. A. (2010). Fluorescent proteins and their applications in imaging living cells and tissues. *Physiological Reviews*, *90*(3), 1103–1163. https://doi.org/10.1152/physrev.00038.2009

Clejan, I., Boerckel, J., & Ahmed, S. (2006a). Developmental modulation of nonhomologous end joining in *Caenorhabditis elegans*. *Genetics*, *173*(3), 1301–1317. https://doi.org/10.1534/genetics.106.058628

Clejan, I., Boerckel, J., & Ahmed, S. (2006b). Developmental modulation of nonhomologous end joining in *Caenorhabditis elegans*. *Genetics*, *173*(3), 1301–1317. https://doi.org/10.1534/genetics.106.058628

Coburn, C., Allman, E., Mahanti, P., Benedetto, A., Cabreiro, F., Pincus, Z., Matthijssens, F., Araiz, C., Mandel, A., Vlachos, M., Edwards, S. A., Fischer, G., Davidson, A., Pryor, R. E., Stevens, A., Slack, F. J., Tavernarakis, N., Braeckman, B. P., Schroeder, F. C., … Gems, D. (2013). Anthranilate Fluorescence Marks a Calcium-Propagated Necrotic Wave That Promotes Organismal Death in *C. elegans*. *PLoS Biology*, *11*(7). https://doi.org/10.1371/journal.pbio.1001613

Collias, D., & Beisel, C. L. (2021). CRISPR technologies and the search for the PAM-free nuclease. *Nature Communications*, *12*(1), 1–12. https://doi.org/10.1038/s41467-020-20633-y

Cong, L., Ran, F. A., Cox, D., Lin, S., Barretto, R., Habib, N., Hsu, P. D., Wu, X., Jiang, W., Marraffini, L. a, & Zhang, F. (2013). Multiplex genome engineering using CRISPR/Cas systems. *Science*, *339*(6121), 819–823. https://doi.org/10.1126/science.1231143

Conradt, B., & Horvitz, H. R. (1999). The TRA-1A sex determination protein of *C. elegans* regulates sexually dimorphic cell deaths by repressing the egl-1 cell death activator gene. *Cell*, *98*(3), 317–327. https://doi.org/10.1016/S0092-8674(00)81961-3

Cook, S. J., Jarrell, T. A., Brittin, C. A., Wang, Y., Bloniarz, A. E., Yakovlev, M. A., Nguyen, K. C. Q., Tang, L. T. H., Bayer, E. A., Duerr, J. S., Bülow, H. E., Hobert, O., Hall, D. H., & Emmons, S. W. (2019). Whole-animal connectomes of both *Caenorhabditis elegans* sexes. *Nature*, *571*(7763), 63–71. https://doi.org/10.1038/s41586-019-1352-7

Corsi, A. K., Wightman, B., & Chalfie, M. (2015). A Transparent window into biology: A primer on *Caenorhabditis elegans*. *WormBook : The Online Review of C. elegans Biology*, 1–31. https://doi.org/10.1895/wormbook.1.177.1

Cutter, A. D., Dey, A., & Murray, R. L. (2009). Evolution of the *Caenorhabditis elegans* genome. *Molecular Biology and Evolution*, *26*(6), 1199–1234. https://doi.org/10.1093/molbev/msp048

Dabrowska, M., Juzwa, W., Krzyzosiak, W. J., & Olejniczak, M. (2018). Precise Excision of the CAG Tract from the Huntingtin Gene by Cas9 Nickases. *Frontiers in Neuroscience*, *12*(February), 1–8. https://doi.org/10.3389/fnins.2018.00075

De Pater, S., Klemann, B. J. P. M., & Hooykaas, P. J. J. (2018). True gene-targeting events by CRISPR/Cas-induced DSB repair of the PPO locus with an ectopically integrated repair template. *Scientific Reports*, *8*(1), 2–11. https://doi.org/10.1038/s41598-018-21697-z

Deltcheva, E., Chylinski, K., Sharma, C. M., Gonzales, K., Chao, Y., Pirzada, Z. A., Eckert, M. R., Vogel, J., & Charpentier, E. (2011). CRISPR RNA maturation by trans-encoded small RNA and host factor RNase III. *Nature*, *471*(7340), 602–607. https://doi.org/10.1038/nature09886

Demuyser, L., Palmans, I., Vandecruys, P., & Dijck, P. Van. (2020). Molecular Elucidation of Riboflavin Production and Regulation in *Candida albicans*, toward a Novel Antifungal Drug Target. *MSphere*, *5*(4), e00714-20. https://doi.org/https://doi.org/10.1128/mSphere.00714-20.

Dickinson, D. J., & Goldstein, B. (2016). CRISPR-based methods for *Caenorhabditis elegans* genome engineering. *Genetics*, *202*(3), 885–901. https://doi.org/10.1534/genetics.115.182162

Dickinson, D. J., Pani, A. M., Heppert, J. K., Higgins, C. D., & Goldstein, B. (2015). Streamlined Genome Engineering with a Self-Excising Drug Selection Cassette. *Genetics*, *200*(4), 1035–1049. https://doi.org/10.1534/genetics.115.178335

Dickinson, D. J., Ward, J. D., Reiner, D. J., & Goldstein, B. (2013). Engineering the *Caenorhabditis elegans* genome using Cas9-triggered homologous recombination. *Nature Methods*, *10*(10), 1028–1034. https://doi.org/10.1038/nmeth.2641

Doench, J. G., Fusi, N., Sullender, M., Hegde, M., Vaimberg, E. W., Donovan, K. F., Smith, I., Tothova, Z., Wilen, C., Orchard, R., Virgin, H. W., Listgarten, J., & Root, D. E. (2016). Optimized sgRNA design to maximize activity and minimize off-target effects of CRISPR-Cas9. *Nature Biotechnology*, *34*(2), 184–191. https://doi.org/10.1038/nbt.3437

Doitsidou, M., Poole, R. J., Sarin, S., Bigelow, H., & Hobert, O. (2010). *C. elegans* mutant identification with a one-step whole-genome-sequencing and SNP mapping strategy. *PLoS ONE*, *5*(11), 1–7. https://doi.org/10.1371/journal.pone.0015435

Dokshin, G. A., Ghanta, K. S., Piscopo, K. M., & Mello, C. C. (2018). Robust Genome Editing With Short Single-Stranded and Long, Partially Single-Stranded DNA Donors in *Caenorhabditis elegans*. *Genetics*. https://doi.org/10.1534/genetics.118.301532

Doudna, J. A., & Charpentier, E. (2014). The new frontier of genome engineering with CRISPR-Cas9. *Science*, *346*(6213). https://doi.org/10.1126/science.1258096

Dupuy, D., Li, Q. R., Deplancke, B., Boxem, M., Hao, T., Lamesch, P., Sequerra, R., Bosak, S., Doucette-Stamm, L., Hope, I. A., Hill, D. E., Walhout, A. J. M., & Vidal, M. (2004). A first version of the *Caenorhabditis elegans* promoterome. *Genome Research*, *14*(10 B), 2169–2175. https://doi.org/10.1101/gr.2497604

East-Seletsky, A., Connell, M. R. O., Knight, S. C., Burstein, D., Cate, J. H. D., Tjian, R., & Doudna, J. A. (2016). Two distinct RNase activities of CRISPR-C2c2 enable guide-RNA processing and RNA detection. *Nature*, *538*(7624), 270–273. https://doi.org/10.1038/nature19802

Eckermann, K. N., Ahmed, H. M. M., KaramiNejadRanjbar, M., Dippel, S., Ogaugwu, C. E., Kitzmann, P., Isah, M. D., & Wimmer, E. A. (2018). Hyperactive piggyBac transposase improves transformation efficiency in diverse insect species. *Insect Biochemistry and Molecular Biology*, *98*(April), 16–24. https://doi.org/10.1016/j.ibmb.2018.04.001

El Mouridi, S., Lecroisey, C., Tardy, P., Mercier, M., Leclercq-Blondel, A., Zariohi, N., & Boulin, T. (2017). Reliable CRISPR/Cas9 genome engineering in *Caenorhabditis elegans* using a single efficient sgRNA and an easily recognizable phenotype. *G3: Genes, Genomes, Genetics*, *7*(5), 1429–1437. https://doi.org/10.1534/g3.117.040824

Elbashir, S. M., Harborth, J., Lendeckel, W., Yalcin, A., Weber, K., & Tuschl, T. (2001). Duplexes of 21-nucleotide RNAs mediate RNA interference in cultured mammalian cells. *Nature*, *411*(6836), 494–498. https://doi.org/10.1038/35078107

Evans, T. (2006). Transformation and microinjection. *WormBook*, 1–15. https://doi.org/10.1895/wormbook.1.108.1

Farboud, B., & Meyer, B. J. (2015). Dramatic enhancement of genome editing by CRISPR/cas9 through improved guide RNA design. *Genetics*, *199*(4), 959–971. https://doi.org/10.1534/genetics.115.175166

Farboud, B., Severson, A. F., & Meyer, B. J. (2019). Strategies for efficient genome editing using CRISPR-Cas9. *Genetics*, *211*(2), 431–457. https://doi.org/10.1534/genetics.118.301775

Findlay, G. M., Boyle, E. A., Hause, R. J., Klein, J. C., & Shendure, J. (2014). Saturation editing of genomic regions by multiplex homology-directed repair. *Nature*, *513*(7516), 120–123. https://doi.org/10.1038/nature13695

Fire, A., Harrison, S. W., & Dixon, D. (1990). A modular set of lacZ fusion vectors for studying gene expression in *Caenorhabditis elegans*. *Gene*, *93*(2), 189–198. https://doi.org/10.1016/0378-1119(90)90224-F

Fire, A., Xu, S., Montgomery, M. K., Kostas, S. A., Driver, S. E., & Mello, C. C. (1998). Potent and specific genetic interference by double-stranded RNA in *Caenorhabditis elegans*. *Nature*, *391*(February), 806–811. https://doi.org/10.1038/35888

Fonfara, I., Richter, H., BratoviÄ, M., Le Rhun, A., & Charpentier, E. (2016). The CRISPR-associated DNA-cleaving enzyme Cpf1 also processes precursor CRISPR RNA. *Nature*, *532*(7600), 517–521. https://doi.org/10.1038/nature17945

Fozouni, P., Son, S., Díaz de León Derby, M., Knott, G. J., Gray, C. N., D'Ambrosio, M. V., Zhao, C., Switz, N. A., Kumar, G. R., Stephens, S. I., Boehm, D., Tsou, C. L., Shu, J., Bhuiya, A., Armstrong, M., Harris, A. R., Chen, P. Y., Osterloh, J. M., Meyer-Franke, A., … Ott, M. (2021). Amplification-free detection of SARS-CoV-2 with CRISPR-Cas13a and mobile phone microscopy. *Cell*, *184*(2), 323-333.e9. https://doi.org/10.1016/j.cell.2020.12.001

Frangoul, H., Altshuler, D., Cappellini, M. D., Chen, Y.-S., Domm, J., Eustace, B. K., Foell, J., de la Fuente, J., Grupp, S., Handgretinger, R., Ho, T. W., Kattamis, A., Kernytsky, A., Lekstrom-Himes, J., Li, A. M., Locatelli, F., Mapara, M. Y., de Montalembert, M., Rondelli, D., … Corbacioglu, S. (2021). CRISPR-Cas9 Gene Editing for Sickle Cell Disease and β-Thalassemia. *New England Journal of Medicine*, *384*(3), 252–260. https://doi.org/10.1056/nejmoa2031054

Friedland, A. E., Tzur, Y. B., Esvelt, K. M., Colaiacovo, M. P., Church, G. M., & Calarco, J. A. (2013). Heritable genome editing in *C. elegans* via a CRISPR-Cas9 system. *Nature Methods*, *10*(8), 741–743. https://doi.org/10.1038/nmeth.2532

Frokjaer-Jensen, C. (2013). Exciting prospects for precise engineering of *Caenorhabditis elegans* genomes with CRISPR/Cas9. *Genetics*, *195*(3), 635–642. https://doi.org/10.1534/genetics.113.156521

Frøkjær-Jensen, C., Jain, N., Hansen, L., Davis, M. W., Li, Y., Zhao, D., Rebora, K., Millet, J. R. M., Liu, X., Kim, S. K., Dupuy, D., Jorgensen, E. M., & Fire, A. Z. (2016). An Abundant Class of Non-coding DNA Can Prevent Stochastic Gene Silencing in the *C. elegans* Germline. *Cell*, *166*(2), 343–357. https://doi.org/10.1016/j.cell.2016.05.072

Frøkjær-Jensen, C., Wayne Davis, M., Hopkins, C. E., Newman, B. J., Thummel, J. M., Olesen, S. P., Grunnet, M., & Jorgensen, E. M. (2008). Single-copy insertion of transgenes in *Caenorhabditis elegans*. *Nature Genetics*, *40*(11), 1375–1383. https://doi.org/10.1038/ng.248

Garneau, J. E., Dupuis, M. È., Villion, M., Romero, D. A., Barrangou, R., Boyaval, P., Fremaux, C., Horvath, P., Magadán, A. H., & Moineau, S. (2010). The CRISPR/cas bacterial immune system cleaves bacteriophage and plasmid DNA. *Nature*, *468*(7320), 67–71. https://doi.org/10.1038/nature09523

Gasiunas, G., Barrangou, R., Horvath, P., & Siksnys, V. (2012). Cas9-crRNA ribonucleoprotein complex mediates specific DNA cleavage for adaptive immunity in bacteria. *Proceedings of the National Academy of Sciences of the United States of America*, *109*(39), E2579-86. https://doi.org/10.1073/pnas.1208507109

Gasiunas, G., Young, J. K., Karvelis, T., Kazlauskas, D., Urbaitis, T., Jasnauskaite, M., Grusyte, M. M., Paulraj, S., Wang, P. H., Hou, Z., Dooley, S. K., Cigan, M., Alarcon, C., Chilcoat, N. D., Bigelyte, G., Curcuru, J. L., Mabuchi, M., Sun, Z., Fuchs, R. T., … Siksnys, V. (2020). A catalogue of biochemically diverse CRISPR-Cas9 orthologs. *Nature Communications*, *11*(1). https://doi.org/10.1038/s41467-020-19344-1

Gaudelli, N. M., Komor, A. C., Rees, H. A., Packer, M. S., Badran, A. H., Bryson, D. I., & Liu, D. R. (2017). Programmable base editing of T to G C in genomic DNA without DNA cleavage. *Nature*, *551*(7681), 464–471. https://doi.org/10.1038/nature24644

Geurts, M. H., de Poel, E., Amatngalim, G. D., Oka, R., Meijers, F. M., Kruisselbrink, E., van Mourik, P., Berkers, G., de Winter-de Groot, K. M., Michel, S., Muilwijk, D., Aalbers, B. L., Mullenders, J., Boj, S. F., Suen, S. W. F., Brunsveld, J. E., Janssens, H. M., Mall, M. A., Graeber, S. Y., … Clevers, H. (2020). CRISPR-Based Adenine Editors Correct Nonsense Mutations in a Cystic Fibrosis Organoid Biobank. *Cell Stem Cell*, *26*(4), 503-510.e7. https://doi.org/10.1016/j.stem.2020.01.019

Ghanta, K. S., Dokshin, G. A., Mir, A., Krishnamurthy, P. M., Gneid, H., Edraki, A., Watts, J. K., Sontheimer, E. J., & Mello, C. C. (2018). 5′ Modifications Improve Potency and Efficacy of DNA Donors for Precision Genome Editing. *BioRxiv*. http://biorxiv.org/content/early/2018/06/22/354480.abstract

Ghanta, K. S., & Mello, C. C. (2020). Melting dsDNA donor molecules greatly improves precision genome editing in *Caenorhabditis elegans*. *Genetics*, *216*(3), 643–650. https://doi.org/10.1534/genetics.120.303564

Gilbert, L. A., Larson, M. H., Morsut, L., Liu, Z., Brar, G. A., Torres, S. E., Stern-ginossar, N., Brandman, O., Whitehead, E. H., Doudna, J. A., Lim, W. A., Weissman, J. S., & Qi, L. S. (2013). Resource CRISPR-Mediated Modular RNA-Guided Regulation of Transcription in Eukaryotes. *Cell*, *154*(2), 442–451. https://doi.org/10.1016/j.cell.2013.06.044

Goshayeshi, L., Yousefi Taemeh, S., Dehdilani, N., Nasiri, M., Ghahramani Seno, M. M., & Dehghani, H. (2021). CRISPR/dCas9-mediated transposition with specificity and efficiency of site-directed genomic insertions. *FASEB Journal : Official Publication of the Federation of American Societies for Experimental Biology*, *35*(2), e21359. https://doi.org/10.1096/fj.202001830RR

Gottlieb, T. M., & Jackson, P. (1993). The DNA-dependent protein kinase: Requirement for DNA ends and association with Ku antigen. *Cell*, *72*, 131–142. https://doi.org/https://doi.org/10.1016/0092-8674(93)90057-W

Goudeau, J., Sharp, C. S., Paw, J., Savy, L., Leonetti, M. D., York, A. G., Updike, D. L., Kenyon, C., & Ingaramo, M. (2021). Split-wrmScarlet and split-sfGFP: tools for faster, easier fluorescent labeling of endogenous proteins in *Caenorhabditis elegans*. *Genetics*, *217*(4). https://doi.org/10.1093/genetics/iyab014

Grabowski, M. M., Svrzikapa, N., & Tissenbaum, H. A. (2005). Bloom syndrome ortholog HIM-6 maintains genomic stability in *C. elegans*. *Mechanisms of Ageing and Development*, *126*(12), 1314–1321. https://doi.org/10.1016/j.mad.2005.08.005

Grahl, N., Demers, E. G., Crocker, A. W., & Hogan, D. A. (2017). Use of RNA-Protein Complexes for Genome Editing in Non-*albicans Candida* Species. *MSphere*, *2*(3), e00218-17. https://doi.org/https://doi.org/10.1128/mSphere.00217-17.

Hall, D. H., Herndon, L. A., & Altun, Z. F. (2017). Introduction to *C. elegans* Embryo Anatomy. In *WormAtlas*. https://doi.org/doi:10.3908/wormatlas.4.1

Hannon, G. J. (2002). RNA interference. *Nature*, *418*(July), 244–251. https://doi.org/https://doi-org.sare.upf.edu/10.1038/418244a

Harmsen, T., Klaasen, S., Van De Vrugt, H., & Te Riele, H. (2018). DNA mismatch repair and oligonucleotide end-protection promote base-pair substitution distal from a CRISPR/Cas9-induced DNA break. *Nucleic Acids Research*, *46*(6), 2945–2955. https://doi.org/10.1093/nar/gky076

Harrington, L. B., Burstein, D., Chen, J. S., Paez-Espino, D., Ma, E., Witte, I. P., Cofsky, J. C., Kyrpides, N. C., Banfield, J. F., & Doudna, J. A. (2018). Programmed DNA destruction by miniature CRISPR-Cas14 enzymes. *Science*, *362*(6416), 839–842. https://doi.org/10.1126/science.aav4294

Harris, T. W., Arnaboldi, V., Cain, S., Chan, J., Chen, W. J., Cho, J., Davis, P., Gao, S., Grove, C. A., Kishore, R., Lee, R. Y. N., Muller, H. M., Nakamura, C., Nuin, P., Paulini, M., Raciti, D., Rodgers, F. H., Russell, M., Schindelman, G., … Sternberg, P. W. (2020). WormBase: A modern Model Organism Information Resource. *Nucleic Acids Research*, *48*(D1), D762–D767. https://doi.org/10.1093/nar/gkz920

Hayashi, M., Chin, G. M., & Villeneuve, A. M. (2007). *C. elegans* germ cells switch between distinct modes of double-strand break repair during meiotic prophase progression. *PLoS Genetics*, *3*(11), 2068–2084. https://doi.org/10.1371/journal.pgen.0030191

He, S., Cuentas-Condori, A., & Miller, D. M. (2019). *NATF (Native and Tissue-Specific Fluorescence): A Strategy for Bright, Tissue-Specific GFP Labeling of Native Proteins in Caenorhabditis elegans*. *212*(June), 387–395. https://doi.org/https://doi.org/10.1534/genetics.119.302063

Hefel, A., & Smolikove, S. (2019). Tissue-specific split sfGFP system for streamlined expression of GFP tagged proteins in the *Caenorhabditis elegans* germline. *G3: Genes, Genomes, Genetics*, *9*(6), 1933–1943. https://doi.org/10.1534/g3.119.400162

Heler, R., Samai, P., Modell, J. W., Weiner, C., Goldberg, G. W., Bikard, D., & Marraffini, L. A. (2015). Cas9 specifies functional viral targets during CRISPR-Cas adaptation. *Nature*, *519*(7542), 199–202. https://doi.org/10.1038/nature14245

Heppert, J. K., Dickinson, D. J., Pani, A. M., Higgins, C. D., Steward, A., Ahringer, J., Kuhn, J. R., & Goldstein, B. (2016). Comparative assessment of fluorescent proteins for in vivo imaging in an animal model system. *Molecular Biology of the Cell*, *27*(22), 3385–3394. https://doi.org/10.1091/mbc.E16-01-0063

Heyn, P., Kalinka, A. T., Tomancak, P., & Neugebauer, K. M. (2015). Introns and gene expression: cellular constraints, transcriptional regulation, and evolutionary consequences. *BioEssays : News and Reviews in Molecular, Cellular and Developmental Biology*, *37*(2), 148–154. https://doi.org/10.1002/bies.201400138

Hillier, L. D. W., Coulson, A., Murray, J. I., Bao, Z., Sulston, J. E., & Waterston, R. H. (2005). Genomics in *C. elegans*: So many genes, such a little worm. *Genome Research*, *15*(12), 1651–1660. https://doi.org/10.1101/gr.3729105

Hirano, H., Gootenberg, J. S., Horii, T., Abudayyeh, O. O., Kimura, M., Hsu, P. D., Nakane, T., Ishitani, R., Hatada, I., Zhang, F., Nishimasu, H., & Nureki, O. (2016). Structure and Engineering of Francisella novicida Cas9. *Cell*, *164*(5), 950–961. https://doi.org/10.1016/j.cell.2016.01.039

Hirsh, D., Oppenheim, D., & Klass, M. (1976). Development of the reproductive system of *Caenorhabditis elegans*. *Developmental Biology*, *49*(1), 200–219. https://doi.org/10.1016/0012-1606(76)90267-0

Hobert, O. (2002). PCR fusion-based approach to create reporter Gene constructs for expression analysis in transgenic *C. elegans*. *BioTechniques*, *32*(4), 728–730. https://doi.org/10.2144/02324bm01

Hobert, O., & Loria, P. (2005). Uses of GFP in *Caenorhabditis elegans*. *Methods of Biochemical Analysis*, *47*, 203–226. https://doi.org/10.1002/0471739499.ch10

Hodgkin, J. (2005). Karyotype, ploidy, and gene dosage. *WormBook : The Online Review of C. elegans Biology*, 1–9. https://doi.org/10.1895/wormbook.1.3.1

Hostettler, L., Grundy, L., Käser-Pébernard, S., Wicky, C., Schafer, W. R., & Glauser, D. A. (2017). The bright fluorescent protein mNeonGreen facilitates protein expression analysis in vivo. *G3: Genes, Genomes, Genetics*, *7*(2), 607–615. https://doi.org/10.1534/g3.116.038133

Howe, K., Davis, P., Paulini, M., Tuli, M. A., Williams, G., Yook, K., Durbin, R., Kersey, P., & Sternberg, P. (2012). WormBase: Annotating many nematode genomes. *Worm*, *1*(1), 15–21. https://doi.org/10.4161/worm.19574

Hsu, P. D., Scott, D. A., Weinstein, J. A., Ran, F. A., Konermann, S., Agarwala, V., Li, Y., Fine, E. J., Wu, X., Shalem, O., Cradick, T. J., Marraffini, L. A., Bao, G., & Zhang, F. (2013). DNA targeting specificity of RNA-guided Cas9 nucleases. *Nature Biotechnology*, *31*(9), 827–832. https://doi.org/10.1038/nbt.2647

Hu, J. H., Miller, S. M., Geurts, M. H., Tang, W., Chen, L., Sun, N., Zeina, C. M., Gao, X., Rees, H. A., Lin, Z., & Liu, D. R. (2018). Evolved Cas9 variants with broad PAM compatibility and high DNA specificity. *Nature*, *556*(7699), 57–63. https://doi.org/10.1038/nature26155

Huang, T. P., Newby, G. A., & Liu, D. R. (2021). Precision genome editing using cytosine and adenine base editors in mammalian cells. *Nature Protocols*, *16*(2), 1089–1128. https://doi.org/10.1038/s41596-020-00450-9

Hubbard, E. J. A., & Greenstein, D. (2005). Introduction to the germ line. *WormBook : The Online Review of C. elegans Biology*, 1–4. https://doi.org/10.1895/wormbook.1.18.1

Hutter, H. (2012). Fluorescent Protein Methods: Strategies and Applications. In *Methods in Cell Biology* (Second Edi, Vol. 107). Elsevier Inc. https://doi.org/10.1016/B978-0-12-394620-1.00003-5

IDT. (n.d.). *CRISPR genome editing*. Retrieved June 9, 2021, from https://eu.idtdna.com/pages/products/crispr-genome-editing

Ishino, Y., Shinagawa, H., Makino, K., Amemura, M., & Nakatura, A. (1987). Nucleotide sequence of the iap gene, responsible for alkaline phosphatase isoenzyme conversion in *Escherichia coli*, and identification of the gene product. *Journal of Bacteriology*, *169*(12), 5429–5433. https://doi.org/10.1128/jb.169.12.5429-5433.1987

Itakura, Y., Inagaki, S., Wada, H., & Hayashi, S. (2018). Trynity controls epidermal barrier function and respiratory tube maturation in *Drosophila* by modulating apical extracellular matrix nano-patterning. *PLoS ONE*, *13*(12), e0209058. https://doi.org/10.1371/journal.pone.0209058

Jansen, R., Van Embden, J. D. A., Gaastra, W., & Schouls, L. M. (2002). Identification of genes that are associated with DNA repeats in prokaryotes. *Molecular Microbiology*, *43*(6), 1565–1575. https://doi.org/10.1046/j.1365-2958.2002.02839.x

Jiang, F., Zhou, K., Ma, L., Gressel, S., & Doudna, J. A. (2015). A Cas9-guide RNA complex preorganized for target DNA recognition. *Science*, *348*(6242), 1477–1481. https://doi.org/10.1126/science.aab1452

Jiang, W., Bikard, D., Cox, D., Zhang, F., & Marraffini, L. A. (2013). RNA-guided editing of bacterial genomes using CRISPR-Cas systems. *Nature Biotechnology*, *31*(3), 233–239. https://doi.org/10.1038/nbt.2508

Jinek, M., Chylinski, K., Fonfara, I., Hauer, M., & Doudna, J. A. (2012). A Programmable Dual-RNA – Guided DNA Endonuclease in Adaptive Bacterial Immunity. *Science*, *337*(June), 816–821. https://doi.org/10.1126/science.1225829

Jinek, M., East, A., Cheng, A., Lin, S., Ma, E., & Doudna, J. (2013). RNA-programmed genome editing in human cells. *ELife*, *2*, e00471. https://doi.org/10.7554/eLife.00471

Johnsen, R. C., Jones, S. J. M., & Rose, A. M. (2000). Mutational accessibility of essential genes on chromosome I(left) in *Caenorhabditis elegans*. *Molecular and General Genetics MGG*, *263*(2), 239–252. https://doi.org/10.1007/s004380051165

Jorgensen, E. M., & Mango, S. E. (2002). The art and design of genetic screens: *Caenorhabditis elegans*. *Nature Reviews Genetics*, *3*(5), 356–369. https://doi.org/10.1038/nrg794

Jung, H., Lee, J. A., Choi, S., Lee, H., & Ahn, B. (2014). Characterization of the *Caenorhabditis elegans* HIM-6/BLM helicase: Unwinding recombination intermediates. *PLoS ONE*, *9*(7). https://doi.org/10.1371/journal.pone.0102402

Kadandale, P., Chatterjee, I., & Singson, A. (2009). Germline transformation of *C. elegans* by injection. *Methods in Molecular Biology*, *518*, 122–133. https://doi.org/10.1007/978-1-59745-202-1_10

Kamath, R. S., Martinez-Campos, M., Zipperlen, P., Fraser, A. G., & Ahringer, J. (2001). Effectiveness of specific RNA-mediated interference through ingested double-stranded RNA in *Caenorhabditis elegans*. *Genome Biology*, *2*(1), 1–10. https://doi.org/10.1186/gb-2000-2-1-research0002

Kamath, Ravi S., Fraser, A. G., Dong, Y., Poulin, G., Durbin, R., Gotta, M., Kanapin, A., Le Bot, N., Moreno, S., Sohrmann, M., Welchman, D. P., Zipperien, P., & Ahringer, J. (2003). Systematic functional analysis of the *Caenorhabditis elegans* genome using RNAi. *Nature*, *421*(6920), 231–237. https://doi.org/10.1038/nature01278

Kamath, Ravi S, & Ahringer, J. (2003). Genome-wide RNAi screening in *Caenorhabditis elegans*. *Methods*, *30*, 313–321. https://doi.org/10.1016/S1046-2023(03)00050-1

Kamiyama, D., Sekine, S., Barsi-Rhyne, B., Hu, J., Chen, B., Gilbert, L. A., Ishikawa, H., Leonetti, M. D., Marshall, W. F., Weissman, J. S., & Huang, B. (2016). Versatile protein tagging in cells with split fluorescent protein. *Nature Communications*, *7*, 1–9. https://doi.org/10.1038/ncomms11046

Kan, Y., Ruis, B., Lin, S., & Hendrickson, E. A. (2014). The Mechanism of Gene Targeting in Human Somatic Cells. *PLoS Genetics*, *10*(4). https://doi.org/10.1371/journal.pgen.1004251

Kan, Y., Ruis, B., Takasugi, T., & Hendrickson, E. A. (2017). Mechanisms of precise genome editing using oligonucleotide donors. *Genome Research*, *27*(7), 1099–1111. https://doi.org/10.1101/gr.214775.116

Karvelis, T., Bigelyte, G., Young, J. K., Hou, Z., Zedaveinyte, R., Budre, K., Paulraj, S., Djukanovic, V., Gasior, S., Silanskas, A., Venclovas, C., & Siksnys, V. (2020). PAM recognition by miniature CRISPR-Cas12f nucleases triggers programmable double-stranded DNA target cleavage. *Nucleic Acids Research*, *48*(9), 5016–5023. https://doi.org/10.1093/nar/gkaa208

Katic, I., & Großhans, H. (2013). Targeted heritable mutation and gene conversion by Cas9-CRISPR in *Caenorhabditis elegans*. *Genetics*, *195*(3), 1173–1176. https://doi.org/10.1534/genetics.113.155754

Katic, I., Xu, L., & Ciosk, R. (2015). CRISPR/Cas9 Genome Editing in *Caenorhabditis elegans*: Evaluation of Templates for Homology-Mediated Repair and Knock-Ins by Homology-Independent DNA Repair. *G3 (Bethesda, Md.)*, *5*(8), 1649–1656. https://doi.org/10.1534/g3.115.019273

Kelly, W. G., Xu, S. Q., Montgomery, M. K., & Fire, A. (1997). Distinct requirements for somatic and germline expression of a generally expressed *Caenorhabditis elegans* gene. *Genetics*, *146*(1), 227–238.

Kennerdell, J. R., & Carthew, R. W. (1998). Use of dsRNA-mediated genetic interference to demonstrate that frizzled and frizzled 2 act in the wingless pathway. *Cell*, *95*(7), 1017–1026. https://doi.org/10.1016/S0092-8674(00)81725-0

Khan, S. H. (2019). Genome-Editing Technologies: Concept, Pros, and Cons of Various Genome-Editing Techniques and Bioethical Concerns for Clinical Application. *Molecular Therapy - Nucleic Acids*, *16*(June), 326–334. https://doi.org/10.1016/j.omtn.2019.02.027

Kim, H., Ishidate, T., Ghanta, K. S., Seth, M., Conte, D. J., Shirayama, M., & Mello, C. C. (2014). A co-CRISPR strategy for efficient genome editing in *Caenorhabditis elegans*. *Genetics*, *197*(4), 1069–1080. https://doi.org/10.1534/genetics.114.166389

Kim, H. K., Song, M., Lee, J., Menon, A. V., Jung, S., Kang, Y. M., Choi, J. W., Woo, E., Koh, H. C., Nam, J. W., & Kim, H. (2017). In vivo high-throughput profiling of CRISPR-Cpf1 activity. *Nature Methods*, *14*(2), 153–159. https://doi.org/10.1038/nmeth.4104

Kim, W., Underwood, R. S., Greenwald, I., & Shaye, D. D. (2018). Ortholist 2: A new comparative genomic analysis of human and *Caenorhabditis elegans* genes. *Genetics*, *210*(2), 445–461. https://doi.org/10.1534/genetics.118.301307

Kimble, J. E., & White, J. G. (1981). On the control of germ cell development in *Caenorhabditis elegans*. *Developmental Biology*, *81*(2), 208–219. https://doi.org/10.1016/0012-1606(81)90284-0

Kiontke, K. C., Félix, M. A., Ailion, M., Rockman, M. V., Braendle, C., Pénigault, J. B., & Fitch, D. H. A. (2011). A phylogeny and molecular barcodes for *Caenorhabditis*, with numerous new species from rotting fruits. *BMC Evolutionary Biology*, *11*(1). https://doi.org/10.1186/1471-2148-11-339

Kleinstiver, B. P., Pattanayak, V., Prew, M. S., Tsai, S. Q., Nguyen, N. T., Zheng, Z., & Joung, J. K. (2016). High-fidelity CRISPR-Cas9 nucleases with no detectable genome-wide off-target effects. *Nature*, *529*(7587), 490–495. https://doi.org/10.1038/nature16526

Kleinstiver, B. P., Prew, M. S., Tsai, S. Q., Topkar, V. V., Nguyen, N. T., Zheng, Z., Gonzales, A. P. W., Li, Z., Peterson, R. T., Yeh, J. R. J., Aryee, M. J., & Joung, J. K. (2015). Engineered CRISPR-Cas9 nucleases with altered PAM specificities. *Nature*, *523*(7561), 481–485. https://doi.org/10.1038/nature14592

Koblan, L. W., Erdos, M. R., Wilson, C., Cabral, W. A., Levy, J. M., Xiong, Z. M., Tavarez, U. L., Davison, L. M., Gete, Y. G., Mao, X., Newby, G. A., Doherty, S. P., Narisu, N., Sheng, Q., Krilow, C., Lin, C. Y., Gordon, L. B., Cao, K., Collins, F. S., … Liu, D. R. (2021). In vivo base editing rescues Hutchinson–Gilford progeria syndrome in mice. *Nature*, *589*(7843), 608–614. https://doi.org/10.1038/s41586-020-03086-7

Komiyama, M. (2014). Chemical modifications of artificial restriction DNA cutter (ARCUT) to promote its in vivo and in vitro applications. *Artificial DNA, PNA & XNA*, *5*(3), e1112457. https://doi.org/10.1080/1949095X.2015.1112457

Komor, A. C., Kim, Y. B., Packer, M. S., Zuris, J. A., & Liu, D. R. (2016). Programmable editing of a target base in genomic DNA without double-stranded DNA cleavage. *Nature*, *533*(7603), 420–424. https://doi.org/10.1038/nature17946

Konermann, S., Brigham, M. D., Trevino, A. E., Joung, J., Abudayyeh, O. O., Barcena, C., Hsu, P. D., Habib, N., Gootenberg, J. S., Nishimasu, H., Nureki, O., & Zhang, F. (2015). Genome-scale transcriptional activation by an engineered CRISPR-Cas9 complex. *Nature*, *517*(7536), 583–588. https://doi.org/10.1038/nature14136

Koole, W., van Schendel, R., Karambelas, A. E., van Heteren, J. T., Okihara, K. L., & Tijsterman, M. (2014). A polymerase theta-dependent repair pathway suppresses extensive genomic instability at endogenous G4 DNA sites. *Nature Communications*, *5*, 3216. https://doi.org/10.1038/ncomms4216

Koonin, E. V., Makarova, K. S., & Zhang, F. (2017). Diversity, classification and evolution of CRISPR-Cas systems. *Current Opinion in Microbiology*, *37*, 67–78. https://doi.org/10.1016/j.mib.2017.05.008

Koury, E., Harrell, K., & Smolikove, S. (2018). Differential RPA-1 and RAD-51 recruitment in vivo throughout the *C. elegans* germline, as revealed by laser microirradiation. *Nucleic Acids Research*, *46*(2), 748–764. https://doi.org/10.1093/nar/gkx1243

Kowalczykowski, S. C. (2015). An overview of the molecular mechanismsof recombinational DNA repair. *Cold Spring Harbor Perspectives in Biology*, *7*(11). https://doi.org/10.1101/cshperspect.a016410

Kramer, J. M., French, R. P., Park, E. C., & Johnson, J. J. (1990). The *Caenorhabditis elegans* rol-6 gene, which interacts with the sqt-1 collagen gene to determine organismal morphology, encodes a collagen. *Molecular and Cellular Biology*, *10*(5), 2081–2089. https://doi.org/10.1128/mcb.10.5.2081

Kramer, J. M., & Johnson, J. J. (1993). Analysis of mutations in the sqt-1 and rol-6 collagen genes of *Caenorhabditis elegans*. *Genetics*, *135*(4), 1035–1045. https://doi.org/10.1093/genetics/135.4.1035

Krogh, B. O., & Symington, L. S. (2004). Recombination proteins in yeast. *Annual Review of Genetics*, *38*, 233–271. https://doi.org/10.1146/annurev.genet.38.072902.091500

Kuwabara, P. E., & O'Neil, N. (2001). The use of functional genomics in *C. elegans* for studying human development and disease. *Journal of Inherited Metabolic Disease*, *24*, 127–138. http://www.wormbase.org/db/misc/paper?name=WBPaper00004637

Labuhn, M., Adams, F. F., Ng, M., Knoess, S., Schambach, A., Charpentier, E. M., Schwarzer, A., Mateo, J. L., Klusmann, J. H., & Heckl, D. (2018). Refined sgRNA efficacy prediction improves largeand small-scale CRISPR-Cas9 applications. *Nucleic Acids Research*, *46*(3), 1375–1385. https://doi.org/10.1093/nar/gkx1268

Labun, K., Montague, T. G., Krause, M., Cleuren, Y. N. T., & Valen, E. (2019). CHOPCHOP v3 : expanding the CRISPR web toolbox beyond genome editing. *Nucleic Acids Research*, *47*(May), 171–174. https://doi.org/10.1093/nar/gkz365

Lai, C. H., Chou, C. Y., Ch'ang, L. Y., Liu, C. S., & Lin, W. C. (2000). Identification of novel human genes evolutionarily conserved in *Caenorhabditis elegans* by comparative proteomics. *Genome Research*, *10*(5), 703–713. https://doi.org/10.1101/gr.10.5.703

Lambie, E. J. (2002). Cell proliferation and growth in C . elegans. *BioEssays*, *24*(1), 38–53. https://doi.org/10.1002/bies.10019

Lant, B., & Derry, W. B. (2013). Methods for detection and analysis of apoptosis signaling in the *C. elegans* germline. *Methods*, *61*(2), 174–182. https://doi.org/10.1016/j.ymeth.2013.04.022

Larance, M., Pourkarimi, E., Wang, B., Murillo, A. B., Kent, R., Lamond, A. I., & Gartner, A. (2015). Global proteomics analysis of the response to starvation in *C. elegans*. *Molecular and Cellular Proteomics*, *14*(7), 1989–2001. https://doi.org/10.1074/mcp.M114.044289

Ledford, H. (2020). CRISPR treatment inserted directly into the body for first time. *Nature*, *579*(7798), 185. https://doi.org/10.1038/d41586-020-00655-8

Lee, J. H., & Paull, T. T. (2004). Direct Activation of the ATM Protein Kinase by the Mre11/Rad50/Nbs1 Complex. *Science*, *304*(5667), 93–96. https://doi.org/10.1126/science.1091496

Lemmens, B., Johnson, N. M., & Tijsterman, M. (2013). COM-1 Promotes Homologous Recombination during *Caenorhabditis elegans* Meiosis by Antagonizing Ku-Mediated Non-Homologous End Joining. *PLoS Genetics*, *9*(2). https://doi.org/10.1371/journal.pgen.1003276

Lemmens, B., Van Schendel, R., & Tijsterman, M. (2015). Mutagenic consequences of a single G-quadruplex demonstrate mitotic inheritance of DNA replication fork barriers. *Nature Communications*, *6*, 1–8. https://doi.org/10.1038/ncomms9909

Li, J., Xu, R., Qin, R., Liu, X., Kong, F., & Wei, P. (2021). Genome editing mediated by SpCas9 variants with broad non-canonical PAM compatibility in plants. *Molecular Plant*, *14*(2), 352–360. https://doi.org/10.1016/j.molp.2020.12.017

Li, M. A., Turner, D. J., Ning, Z., Yusa, K., Liang, Q., Eckert, S., Rad, L., Fitzgerald, T. W., Craig, N. L., & Bradley, A. (2011). Mobilization of giant piggyBac transposons in the mouse genome. *Nucleic Acids Research*, *39*(22). https://doi.org/10.1093/nar/gkr764

Li, S. Y., Cheng, Q. X., Li, X. Y., Zhang, Z. L., Gao, S., Cao, R. B., Zhao, G. P., Wang, J., & Wang, J. M. (2018). CRISPR-Cas12a-assisted nucleic acid detection. *Cell Discovery*, *4*(1), 18–21. https://doi.org/10.1038/s41421-018-0028-z

Li, W., Yi, P., & Ou, G. (2015). Somatic CRISPR-Cas9-induced mutations reveal roles of embryonically essential dynein chains in *Caenorhabditis elegans* cilia. *Journal of Cell Biology*, *208*(6), 683–692. https://doi.org/10.1083/jcb.201411041

Li, X., Wang, Y., Liu, Y., Yang, B., Wang, X., Wei, J., Lu, Z., Zhang, Y., Wu, J., Huang, X., Yang, L., & Chen, J. (2018). Base editing with a Cpf1-cytidine deaminase fusion. *Nature Biotechnology*, *36*(4), 324–327. https://doi.org/10.1038/nbt.4102

Li, Y., Li, S., Wang, J., & Liu, G. (2019). CRISPR/Cas Systems towards Next-Generation Biosensing. *Trends in Biotechnology*, *37*(7), 730–743. https://doi.org/10.1016/j.tibtech.2018.12.005

Liang, L., Deng, L., Nguyen, S. C., Zhao, X., Maulion, C. D., Shao, C., & Tischfield, J. A. (2008). Human DNA ligases I and III, but not ligase IV, are required for microhomology-mediated end joining of DNA double-strand breaks. *Nucleic Acids Research*, *36*(10), 3297–3310. https://doi.org/10.1093/nar/gkn184

Liang, M., Li, Z., Wang, W., Liu, J., Liu, L., Zhu, G., Karthik, L., Wang, M., Wang, K. F., Wang, Z., Yu, J., Shuai, Y., Yu, J., Zhang, L., Yang, Z., Li, C., Zhang, Q., Shi, T., Zhou, L., … Zhang, L. X. (2019). A CRISPR-Cas12a-derived biosensing platform for the highly sensitive detection of diverse small molecules. *Nature Communications*, *10*(1). https://doi.org/10.1038/s41467-019-11648-1

Liang, X., Potter, J., Kumar, S., Ravinder, N., & Chesnut, J. D. (2017). Enhanced CRISPR/Cas9-mediated precise genome editing by improved design and delivery of gRNA, Cas9 nuclease, and donor DNA. *Journal of Biotechnology*, *241*, 136–146. https://doi.org/10.1016/j.jbiotec.2016.11.011

Lieber, M. R. (2010). The mechanism of double-strand DNA break repair by the nonhomologous DNA end-joining pathway. *Annual Review of Biochemistry*, *79*(D), 181–211. https://doi.org/10.1146/annurev.biochem.052308.093131

Lim, Y., Bak, S. Y., Sung, K., Jeong, E., Lee, S. H., Kim, J.-S., Bae, S., & Kim, S. K. (2016). Structural roles of guide RNAs in the nuclease activity of Cas9 endonuclease. *Nature Communications*, *7*, 13350. https://doi.org/10.1038/ncomms13350

Lino, C. A., Harper, J. C., Carney, J. P., & Timlin, J. A. (2018). Delivering crispr: A review of the challenges and approaches. *Drug Delivery*, *25*(1), 1234–1257. https://doi.org/10.1080/10717544.2018.1474964

Lints, R., & Hall, D. H. (2009). Male introduction. In *WormAtlas*. https://doi.org/doi:10.3908/wormatlas.2.1

Liu, J. J., Orlova, N., Oakes, B. L., Ma, E., Spinner, H. B., Baney, K. L. M., Chuck, J., Tan, D., Knott, G. J., Harrington, L. B., Al-Shayeb, B., Wagner, A., Brötzmann, J., Staahl, B. T., Taylor, K. L., Desmarais, J., Nogales, E., & Doudna, J. A. (2019). CasX enzymes comprise a distinct family of RNA-guided genome editors. *Nature*, *566*(7743), 218–223. https://doi.org/10.1038/s41586-019-0908-x

Liu, L., Li, X., Wang, J., Wang, M., Chen, P., Yin, M., Li, J., Sheng, G., & Wang, Y. (2017). Two Distant Catalytic Sites Are Responsible for C2c2 RNase Activities. *Cell*, *168*(1–2), 121-134.e12. https://doi.org/10.1016/j.cell.2016.12.031

Liu, P., Luk, K., Shin, M., Idrizi, F., Kwok, S., Roscoe, B., Mintzer, E., Suresh, S., Morrison, K., Frazão, J. B., Bolukbasi, M. F., Ponnienselvan, K., Luban, J., Zhu, L. J., Lawson, N. D., & Wolfe, S. A. (2019). Enhanced Cas12a editing in mammalian cells and zebrafish. *Nucleic Acids Research*, *47*(8), 4169–4180. https://doi.org/10.1093/nar/gkz184

Lo, T. W., Pickle, C. S., Lin, S., Ralston, E. J., Gurling, M., Schartner, C. M., Bian, Q., Doudna, J. A., & Meyer, B. J. (2013). Precise and heritable genome editing in evolutionarily diverse nematodes using TALENs and CRISPR/Cas9 to engineer insertions and deletions. *Genetics*, *195*(2), 331–348. https://doi.org/10.1534/genetics.113.155382

Makarova, K. S., Haft, D. H., Barrangou, R., Brouns, S. J. J., Charpentier, E., Horvath, P., Moineau, S., Mojica, F. J. M., Wolf, Y. I., Yakunin, A. F., van der Oost, J., & Koonin, E. V. (2011). Evolution and classification of the CRISPR-Cas systems. *Nature Reviews. Microbiology*, *9*(6), 467–477. https://doi.org/10.1038/nrmicro2577

Makarova, K. S., Wolf, Y. I., Alkhnbashi, O. S., Costa, F., Shah, S. A., Saunders, S. J., Barrangou, R., Brouns, S. J. J., Charpentier, E., Haft, D. H., Horvath, P., Moineau, S., Mojica, F. J. M., Terns, R. M., Terns, M. P., White, M. F., Yakunin, A. F., Garrett, R. A., Van Der Oost, J., … Koonin, E. V. (2015). An updated evolutionary classification of CRISPR-Cas systems. *Nature Reviews Microbiology*, *13*(11), 722–736. https://doi.org/10.1038/nrmicro3569

Makarova, K. S., Wolf, Y. I., Iranzo, J., Shmakov, S. A., Alkhnbashi, O. S., Brouns, S. J. J., Charpentier, E., Cheng, D., Haft, D. H., Horvath, P., Moineau, S., Mojica, F. J. M., Scott, D., Shah, S. A., Siksnys, V., Terns, M. P., Venclovas, Č., White, M. F., Yakunin, A. F., … Koonin, E. V. (2020). Evolutionary classification of CRISPR–Cas systems: a burst of class 2 and derived variants. *Nature Reviews Microbiology*, *18*(2), 67–83. https://doi.org/10.1038/s41579-019-0299-x

Marais, G., Mouchiroud, D., & Duret, L. (2001). Does recombination improve selection on codon usage? Lessons from nematode and fly complete genomes. *Proceedings of the National Academy of Sciences of the United States of America*, *98*(10), 5688–5692. https://doi.org/10.1073/pnas.091427698

Mariol, M. C., Walter, L., Bellemin, S., & Gieseler, K. (2013). A rapid protocol for integrating extrachromosomal arrays with high transmission rate into the *C. elegans* genome. *Journal of Visualized Experiments*, *82*, 1–7. https://doi.org/10.3791/50773

Marraffini, L. A., & Sontheimer, E. J. (2008). CRISPR interference limits horizontal gene transfer in staphylococci by targeting DNA. *Science*, *322*(5909), 1843–1845. https://doi.org/10.1126/science.1165771

Martin, J. S., Winkelmann, N., Petalcorin, M. I. R., Mcilwraith, M. J., & Boulton, S. J. (2005). RAD-51-Dependent and -Independent Roles of a. *Society*, *25*(8), 3127–3139. https://doi.org/10.1128/MCB.25.8.3127

Massel, K., Lam, Y., Wong, A. C. S., Hickey, L. T., Borrell, A. K., & Godwin, I. D. (2021). Hotter, drier, CRISPR: the latest edit on climate change. *Theoretical and Applied Genetics*, *0123456789*. https://doi.org/10.1007/s00122-020-03764-0

McDiarmid, T. A., Au, V., Loewen, A., Liang, J. J. H., Mizumoto, K., Moerman, D. G., & Rankin, C. H. (2018). CRISPR-Cas9 human gene replacement and phenomic characterization in *Caenorhabditis elegans* to understand the functional conservation of human genes and decipher variants of uncertain significance. *Disease Models & Mechanisms*, *11*, dmm036517. https://doi.org/10.1242/dmm.036517

McVey, M., Khodaverdian, V. Y., Meyer, D., Cerqueira, P. G., & Heyer, W. D. (2016). Eukaryotic DNA Polymerases in Homologous Recombination. *Annual Review of Genetics*, *50*, 393–421. https://doi.org/10.1146/annurev-genet-120215-035243

Mello, C. C., & Fire, A. Z. (1995). DNA Transformation. In H. F. Epstein & D. C. Shakes (Eds.), *Methods in Cell Biology* (pp. 451–482). https://doi.org/10.1016/S0091-679X(08)61399-0

Mello, C. C., Kramer, J. M., Stinchcomb, D., & Ambros, V. (1991). Efficient gene transfer in C.elegans: Extrachromosomal maintenance and integration of transforming sequences. *EMBO Journal*, *10*(12), 3959–3970. https://doi.org/10.1002/j.1460-2075.1991.tb04966.x

Miller, J. C., Tan, S., Qiao, G., Barlow, K. A., Wang, J., Xia, D. F., Meng, X., Paschon, D. E., Leung, E., Hinkley, S. J., Dulay, G. P., Hua, K. L., Ankoudinova, I., Cost, G. J., Urnov, F. D., Zhang, H. S., Holmes, M. C., Zhang, L., Gregory, P. D., & Rebar, E. J. (2011). A TALE nuclease architecture for efficient genome editing. *Nature Biotechnology*, *29*(2), 143–150. https://doi.org/10.1038/nbt.1755

Mimitou, E. P., & Symington, L. S. (2010). Ku prevents Exo1 and Sgs1-dependent resection of DNA ends in the absence of a functional MRX complex or Sae2. *EMBO Journal*, *29*(19), 3358–3369. https://doi.org/10.1038/emboj.2010.193

Minevich, G., Park, D. S., Blankenberg, D., Poole, R. J., & Hobert, O. (2012). CloudMap: A cloud-based pipeline for analysis of mutant genome sequences. *Genetics*, *192*(4), 1249–1269. https://doi.org/10.1534/genetics.112.144204

Miyata, H., Castaneda, J. M., Fujihara, Y., Yu, Z., Archambeault, D. R., Isotani, A., Kiyozumi, D., Kriseman, M. L., Mashiko, D., Matsumura, T., Matzuk, R. M., Mori, M., Noda, T., Oji, A., Okabe, M., Prunskaite-Hyyrylainen, R., Ramirez-Solis, R., Satouh, Y., Zhang, Q., … Matzuk, M. M. (2016). Genome engineering uncovers 54 evolutionarily conserved and testis-enriched genes that are not required for male fertility in mice. *Proceedings of the National Academy of Sciences of the United States of America*, *113*(28), 7704–7710. https://doi.org/10.1073/pnas.1608458113

Mojica, F. J.M., Díez-Villaseñor, C., García-Martínez, J., & Almendros, C. (2009). Short motif sequences determine the targets of the prokaryotic CRISPR defence system. *Microbiology*, *155*(3), 733–740. https://doi.org/10.1099/mic.0.023960-0

Mojica, F. J.M., Juez, G., & Rodriguez-Valera, F. (1993). Transcription at different salinities of Haloferax mediterranei sequences adjacent to partially modified PstI sites. *Molecular Microbiology*, *9*(3), 613–621. https://doi.org/10.1111/j.1365-2958.1993.tb01721.x

Mojica, Francisco J.M., & Rodriguez-Valera, F. (2016). The discovery of CRISPR in archaea and bacteria. *FEBS Journal*, *May*, 3162–3169. https://doi.org/10.1111/febs.13766

Mojica, Francisco J M, Diez-Villasenor, C., Garcia-Martinez, J., & Soria, E. (2005). Intervening sequences of regularly spaced prokaryotic repeats derive from foreign genetic elements. *Journal of Molecular Evolution*, *60*(2), 174–182. https://doi.org/10.1007/s00239-004-0046-3

Moreb, E. A., Hutmacher, M., & Lynch, M. D. (2020). CRISPR-Cas "non-Target" Sites Inhibit On-Target Cutting Rates. *CRISPR Journal*, *3*(6), 550–561. https://doi.org/10.1089/crispr.2020.0065

Moreno-Mateos, M. A., Fernandez, J. P., Rouet, R., Vejnar, C. E., Lane, M. A., Mis, E., Khokha, M. K., Doudna, J. A., & Giraldez, A. J. (2017). CRISPR-Cpf1 mediates efficient homology-directed repair and temperature-controlled genome editing. *Nature Communications*, *8*, 2024. https://doi.org/10.1038/s41467-017-01836-2

Moreno-Mateos, M. A., Vejnar, C. E., Beaudoin, J. D., Fernandez, J. P., Mis, E. K., Khokha, M. K., & Giraldez, A. J. (2015). CRISPRscan: Designing highly efficient sgRNAs for CRISPR-Cas9 targeting in vivo. *Nature Methods*, *12*(10), 982–988. https://doi.org/10.1038/nmeth.3543

Muñoz-Jimenez, C., Ayuso, C., Dobrzynska, A., Torres-Mendez, A., De la Cruz Ruiz, P., & Askjaer, P. (2017). An Efficient FLP-Based Toolkit for Spatiotemporal. *Genetics*, *206*(August), 1–16. https://doi.org/10.1534/genetics.117.201012/-/DC1.1

Musunuru, K., Chadwick, A. C., Mizoguchi, T., Garcia, S. P., DeNizio, J. E., Reiss, C. W., Wang, K., Iyer, S., Dutta, C., Clendaniel, V., Amaonye, M., Beach, A., Berth, K., Biswas, S., Braun, M. C., Chen, H.-M., Colace, T. V., Ganey, J. D., Gangopadhyay, S. A., … Kathiresan, S. (2021). In vivo CRISPR base editing of PCSK9 durably lowers cholesterol in primates. *Nature*, *593*(7859), 429–434. https://doi.org/10.1038/s41586-021-03534-y

Nagaraju, S., Davies, N. K., Walker, D. J. F., Köpke, M., & Simpson, S. D. (2016). Genome editing of Clostridium autoethanogenum using CRISPR/Cas9. *Biotechnology for Biofuels*, *9*(1), 1–8. https://doi.org/10.1186/s13068-016-0638-3

Nakade, S., Tsubota, T., Sakane, Y., Kume, S., Sakamoto, N., Obara, M., Daimon, T., Sezutsu, H., Yamamoto, T., Sakuma, T., & Suzuki, K. I. T. (2014). Microhomology-mediated end-joining-dependent integration of donor DNA in cells and animals using TALENs and CRISPR/Cas9. *Nature Communications*, *5*, 1–3. https://doi.org/10.1038/ncomms6560

Nakayama, T., Grainger, R. M., & Cha, S. W. (2020). Simple embryo injection of long single-stranded donor templates with the CRISPR/Cas9 system leads to homology-directed repair in Xenopus tropicalis and Xenopus laevis. *Genesis*, *58*(6). https://doi.org/10.1002/dvg.23366

Nance, J., & Frøkjær-Jensen, C. (2019). The *Caenorhabditis elegans* transgenic toolbox. *Genetics*, *212*(4), 959–990. https://doi.org/10.1534/genetics.119.301506

Nigon, V. M. (1949). Les modalites de la reproduction et le determinisme du sexe chez quelques nematodes libres. *Annales de Sciences Naturelles - Zool. Biol. Anim.*, *11*, 1–132.

Nimonkar, A. V., Genschel, J., Kinoshita, E., Polaczek, P., Campbell, J. L., Wyman, C., Modrich, P., & Kowalczykowski, S. C. (2011). BLM-DNA2-RPA-MRN and EXO1-BLM-RPA-MRN constitute two DNA end resection machineries for human DNA break repair. *Genes and Development*, *25*(4), 350–362. https://doi.org/10.1101/gad.2003811

Nishimasu, H., Shi, X., Ishiguro, S., Gao, L., Hirano, S., Okazaki, S., Noda, T., Abudayyeh, O. O., Gootenberg, J. S., Mori, H., Oura, S., Holmes, B., Tanaka, M., Seki, M., Hirano, H., Aburatani, H., Ishitani, R., Ikawa, M., Yachie, N., … Nureki, O. (2018). Engineered CRISPR-Cas9 nuclease with expanded targeting space. *Science*, *9*(September), 1259–1262. https://doi.org/10.1126/science.aas9129(2018)

Norris, A. D., Kim, H. M., Colaiácovo, M. P., & Calarco, J. A. (2015). Efficient genome editing in *Caenorhabditis elegans* with a toolkit of dual-marker selection cassettes. *Genetics*, *201*(2), 449–458. https://doi.org/10.1534/genetics.115.180679

Nuñez, J. K., Kranzusch, P. J., Noeske, J., & Wright, A. V. (2014). *Cas1 – Cas2 complex formation mediates spacer acquisition during CRISPR – Cas adaptive immunity*. *21*(6), 528–534.

O'Reilly, L. P., Luke, C. J., Perlmutter, D. H., Silverman, G. A., & Pak, S. C. (2014). *C. elegans* in high-throughput drug discovery. *Advanced Drug Delivery Reviews*, *69–70*, 247–253. https://doi.org/10.1016/j.addr.2013.12.001

Ochi, T., Wu, Q., & Blundell, T. L. (2014). The spatial organization of non-homologous end joining: From bridging to end joining. *DNA Repair*, *17*(June), 98–109. https://doi.org/10.1016/j.dnarep.2014.02.010

Orr-Weaver, T. L., Szostak, J. W., & Rothstein, R. J. (1981). Yeast transformation: A model system for the study of recombination. *Proceedings of the National Academy of Sciences of the United States of America*, *78*(10 I), 6354–6358. https://doi.org/10.1073/pnas.78.10.6354

Paix, A., Folkmann, A., Goldman, D. H., Kulaga, H., Grzelak, M. J., Rasoloson, D., Paidemarry, S., Green, R., Reed, R. R., & Seydoux, G. (2017). Precision genome editing using synthesis-dependent repair of Cas9-induced DNA breaks. *Proceedings of the National Academy of Sciences of the United States of America*, *114*(50), E10745–E10754. https://doi.org/10.1073/pnas.1711979114

Paix, A., Folkmann, A., Rasoloson, D., & Seydoux, G. (2015). High efficiency, homology-directed genome editing in *Caenorhabditis elegans* using CRISPR-Cas9ribonucleoprotein complexes. *Genetics*, *201*(1), 47–54. https://doi.org/10.1534/genetics.115.179382

Paix, A., Schmidt, H., & Seydoux, G. (2016). Cas9-assisted recombineering in *C. elegans*: genome editing using in vivo assembly of linear DNAs. *Nucleic Acids Research*, *44*(15), e128. https://doi.org/10.1093/nar/gkw502

Paix, A., Wang, Y., Smith, H. E., Lee, C.-Y. S., Calidas, D., Lu, T., Smith, J., Schmidt, H., Krause, M. W., & Seydoux, G. (2014). Scalable and versatile genome editing using linear DNAs with microhomology to Cas9 Sites in *Caenorhabditis elegans*. *Genetics*, *198*(4), 1347–1356. https://doi.org/10.1534/genetics.114.170423

Pâques, F., & Haber, J. E. (1999). Multiple Pathways of Recombination Induced by Double-Strand Breaks in Saccharomyces cerevisiae. *Microbiology and Molecular Biology Reviews*, *63*(2), 349–404. https://doi.org/10.1128/mmbr.63.2.349-404.1999

Paquet, D., Kwart, D., Chen, A., Sproul, A., Jacob, S., Teo, S., Olsen, K. M., Gregg, A., Noggle, S., & Tessier-Lavigne, M. (2016). Efficient introduction of specific homozygous and heterozygous mutations using CRISPR/Cas9. *Nature*, *533*(7601), 125–129. https://doi.org/10.1038/nature17664

Paulo, D. F., Williamson, M. E., Arp, A. P., Li, F., Sagel, A., Skoda, S. R., Sanchez-Gallego, J., Vasquez, M., Quintero, G., Pérez de León, A. A., Belikoff, E. J., Azeredo-Espin, A. M. L., McMillan, W. O., Concha, C., & Scott, M. J. (2019). Specific gene disruption in the major livestock pests *Cochliomyia hominivorax* and *Lucilia cuprina* using CRISPR/Cas9. *G3: Genes, Genomes, Genetics*, *9*(9), 3045–3055. https://doi.org/10.1534/g3.119.400544

Perrin, A., Rousseau, J., & Tremblay, J. P. (2017). Increased Expression of Laminin Subunit Alpha 1 Chain by dCas9-VP160. *Molecular Therapy - Nucleic Acids*, *6*(March), 68–79. https://doi.org/10.1016/j.omtn.2016.11.004

Philip, N. S., Escobedo, F., Bahr, L. L., Berry, B. J., & Wojtovich, A. P. (2019). Mos1 element-mediated CRISPR integration of transgenes in *Caenorhabditis elegans*. *G3: Genes, Genomes, Genetics*, *9*(8), 2629–2635. https://doi.org/10.1534/g3.119.400399

Pincus, Z., Mazer, T. C., & Slack, F. J. (2016). Autofluorescence as a measure of senescence in *C. elegans*: Look to red, not blue or green. *Aging*, *8*(5), 889–898. https://doi.org/10.18632/aging.100936

Piovesan, A., Antonaros, F., Vitale, L., Strippoli, P., Pelleri, M. C., & Caracausi, M. (2019). Human protein-coding genes and gene feature statistics in 2019. *BMC Research Notes*, *12*(1), 1–5. https://doi.org/10.1186/s13104-019-4343-8

Porta-de-la-Riva, M., Fontrodona, L., Villanueva, A., & Cerón, J. (2012). Basic *Caenorhabditis elegans* methods: Synchronization and observation. *Journal of Visualized Experiments*, *64*, 1–9. https://doi.org/10.3791/4019

Pourcel, C., Salvignol, G., & Vergnaud, G. (2005). CRISPR elements in Yersinia pestis acquire new repeats by preferential uptake of bacteriophage DNA, and provide additional tools for evolutionary studies. *Microbiology*, *151*(3), 653–663. https://doi.org/10.1099/mic.0.27437-0

Prachumwat, A., Devincentis, L., & Palopoli, M. F. (2004). Intron Size Correlates Positively With Recombination Rate in *Caenorhabditis elegans*. *Genetics*, *1590*(March), 1585–1590. https://doi.org/https://doi.org/10.1534/genetics.166.3.1585

Praitis, V., Casey, E., Collar, D., & Austin, J. (2001). Creation of low-copy integrated transgenic lines in *Caenorhabditis elegans*. *Genetics*, *157*(3), 1217–1226.

Prior, H., Jawad, A. K., MacConnachie, L., & Beg, A. A. (2017). Highly efficient, rapid and Co-CRISPR-independent genome editing in *Caenorhabditis elegans*. *G3: Genes, Genomes, Genetics*, *7*(11), 3693–3698. https://doi.org/10.1534/g3.117.300216

Pulak, R. (2006). Techniques for analysis, sorting, and dispensing of *C. elegans* on the COPAS flow-sorting system. *Methods in Molecular Biology (Clifton, N.J.)*, *351*, 275–286. https://doi.org/10.1385/1-59745-151-7:275

Pyott, D. E., Sheehan, E., & Molnar, A. (2016). Engineering of CRISPR/Cas9-mediated potyvirus resistance in transgene-free *Arabidopsis* plants. *Molecular Plant Pathology*, *17*(8), 1276–1288. https://doi.org/10.1111/mpp.12417

Qi, L. S., Larson, M. H., Gilbert, L. A., Doudna, J. A., Weissman, J. S., Arkin, A. P., & Lim, W. A. (2013). Repurposing CRISPR as an RNA-Guided Platform for Sequence-Specific Control of Gene Expression. *Cell*, *152*(5), 1173–1183. https://doi.org/10.1016/j.cell.2013.02.022

Quadros, R. M., Miura, H., Harms, D. W., Akatsuka, H., Sato, T., Aida, T., Redder, R., Richardson, G. P., Inagaki, Y., Sakai, D., Buckley, S. M., Seshacharyulu, P., Batra, S. K., Behlke, M. A., Zeiner, S. A., Jacobi, A. M., Izu, Y., Thoreson, W. B., Urness, L. D., … Gurumurthy, C. B. (2017). Easi-CRISPR: a robust method for one-step generation of mice carrying conditional and insertion alleles using long ssDNA donors and CRISPR ribonucleoproteins. *Genome Biology*, *18*(1), 92. https://doi.org/10.1186/s13059-017-1220-4

Ramesh, A., Ong, T., Garcia, J. A., Adams, J., & Wheeldon, I. (2020). Guide RNA Engineering Enables Dual Purpose CRISPR-Cpf1 for Simultaneous Gene Editing and Gene Regulation in Yarrowia lipolytica. *ACS Synthetic Biology*, *9*(4), 967–971. https://doi.org/10.1021/acssynbio.9b00498

Ramsden, D. A., & Geliert, M. (1998). Ku protein stimulates DNA end joining by mammalian DNA ligases: A direct role for Ku in repair of DNA double-strand breaks. *EMBO Journal*, *17*(2), 609–614. https://doi.org/10.1093/emboj/17.2.609

Ran, F. A., Cong, L., Yan, W. X., Scott, D. A., Gootenberg, J. S., Kriz, A. J., Zetsche, B., Shalem, O., Wu, X., Makarova, K. S., Koonin, E. V., Sharp, P. A., & Zhang, F. (2015). In vivo genome editing using Staphylococcus aureus Cas9. *Nature*, *520*(7546), 186–191. https://doi.org/10.1038/nature14299

Ran, F. A., Hsu, P. D., Lin, C. Y., Gootenberg, J. S., Konermann, S., Trevino, A. E., Scott, D. A., Inoue, A., Matoba, S., Zhang, Y., & Zhang, F. (2013). Double nicking by RNA-guided CRISPR cas9 for enhanced genome editing specificity. *Cell*, *154*(6), 1–10. https://doi.org/10.1016/j.cell.2013.08.021

Ranawakage, D. C., Okada, K., Sugio, K., Kawaguchi, Y., Kuninobu-Bonkohara, Y., Takada, T., & Kamachi, Y. (2021). Efficient CRISPR-Cas9-Mediated Knock-In of Composite Tags in Zebrafish Using Long ssDNA as a Donor. *Frontiers in Cell and Developmental Biology*, *8*(February), 1–20. https://doi.org/10.3389/fcell.2020.598634

Ranjha, L., Howard, S. M., & Cejka, P. (2018). Main steps in DNA double-strand break repair: an introduction to homologous recombination and related processes. *Chromosoma*, *127*(2), 187–214. https://doi.org/10.1007/s00412-017-0658-1

Redemann, S., Schloissnig, S., Ernst, S., Pozniakowsky, A., Ayloo, S., Hyman, A. A., & Bringmann, H. (2011). Codon adaptation-based control of protein expression in *C. elegans*. *Nature Methods*, *8*(3), 250–252. https://doi.org/10.1038/nmeth.1565

Ren, Q., Sretenovic, S., Liu, S., Tang, X., Huang, L., He, Y., Liu, L., Guo, Y., Zhong, Z., Liu, G., Cheng, Y., Zheng, X., Pan, C., Yin, D., Zhang, Y., Li, W., Qi, L., Li, C., Qi, Y., & Zhang, Y. (2021). PAM-less plant genome editing using a CRISPR–SpRY toolbox. *Nature Plants*, *7*(1), 25–33. https://doi.org/10.1038/s41477-020-00827-4

Renkawitz, J., Lademann, C. A., Kalocsay, M., & Jentsch, S. (2013). Monitoring Homology Search during DNA Double-Strand Break Repair In Vivo. *Molecular Cell*, *50*(2), 261–272. https://doi.org/10.1016/j.molcel.2013.02.020

Roerink, S. F., Schendel, R., & Tijsterman, M. (2014). Polymerase theta-mediated end joining of replication-associated DNA breaks in *C. elegans*. *Genome Research*, *24*(6), 954–962. https://doi.org/10.1101/gr.170431.113

Romano, N., & Macino, G. (1992). Quelling: transient inactivation of gene expression in Neurospora crassa by transformation with homologous sequences. In *Molecular Microbiology* (Vol. 6, Issue 22, pp. 3343–3353). https://doi.org/10.1111/j.1365-2958.1992.tb02202.x

Rual, J., Ceron, J., Koreth, J., Hao, T., Nicot, A., Hirozane-kishikawa, T., Vandenhaute, J., Orkin, S. H., Hill, D. E., Heuvel, S. Van Den, & Vidal, M. (2004). Toward Improving *Caenorhabditis elegans* Phenome Mapping With an ORFeome-Based RNAi Library. *Genome Research*, *14*, 2162–2168. https://doi.org/10.1101/gr.2505604.7

Rual, J. F., Klitgord, N., & Achaz, G. (2007). Novel insights into RNAi off-target effects using *C. elegans* paralogs. *BMC Genomics*, *8*, 1–8. https://doi.org/10.1186/1471-2164-8-106

Saha, C., Mohanraju, P., Stubbs, A., Dugar, G., Hoogstrate, Y., Kremers, G. J., Van Cappellen, W. A., Horst-Kreft, D., Laffeber, C., Lebbink, J. H. G., Bruens, S., Gaskin, D., Beerens, D., Klunder, M., Joosten, R., Demmers, J. A. A., Van Gent, D., Mouton, J. W., Van Der Spek, P. J., … Louwen, R. (2020). Guide-free Cas9 from pathogenic Campylobacter jejuni bacteria causes severe damage to DNA. *Science Advances*, *6*(25), eaaz4849. https://doi.org/10.1126/sciadv.aaz4849

San Filippo, J., Sung, P., & Klein, H. (2008). Mechanism of eukaryotic homologous recombination. *Annual Review of Biochemistry*, *77*, 229–257. https://doi.org/10.1146/annurev.biochem.77.061306.125255

Sartori, A. A., Lukas, C., Coates, J., Mistrik, M., Fu, S., Bartek, J., Baer, R., Lukas, J., & Jackson, S. P. (2007). Human CtIP promotes DNA end resection. *Nature*, *450*(7169), 509–514. https://doi.org/10.1038/nature06337

Savage, D. F. (2019). Cas14: Big Advances from Small CRISPR Proteins. *Biochemistry*, *58*(8), 1024–1025. https://doi.org/10.1021/acs.biochem.9b00035

Schwartz, M. L., & Jorgensen, E. M. (2016). SapTrap, a toolkit for high-throughput CRISPR/Cas9 gene modification in *Caenorhabditis elegans*. *Genetics*, *202*(4), 1277–1288. https://doi.org/10.1534/genetics.115.184275

Scudellari, M. (2019). Self-destructing mosquitoes and sterilized rodents: the promise of gene drives. *Nature*, *571*, 160–162. https://doi.org/https://doi.org/10.1038/d41586-019-02087-5

Scully, R., Panday, A., Elango, R., & Willis, N. A. (2019). DNA double-strand break repair-pathway choice in somatic mammalian cells. *Nature Reviews Molecular Cell Biology*, *20*(11), 698–714. https://doi.org/10.1038/s41580-019-0152-0

Semenova, E., Jore, M. M., Datsenko, K. A., Semenova, A., Westra, E. R., Wanner, B., Van Der Oost, J., Brouns, S. J. J., & Severinov, K. (2011). Interference by clustered regularly interspaced short palindromic repeat (CRISPR) RNA is governed by a seed sequence. *Proceedings of the National Academy of Sciences of the United States of America*, *108*(25), 10098–10103. https://doi.org/10.1073/pnas.1104144108

Seol, J. H., Shim, E. Y., & Lee, S. E. (2018). Microhomology-mediated end joining: Good, bad and ugly. *Mutation Research - Fundamental and Molecular Mechanisms of Mutagenesis*, *809*(February 2017), 81–87. https://doi.org/10.1016/j.mrfmmm.2017.07.002

Sfeir, A., & Symington, L. S. (2015). Microhomology-Mediated End Joining: A Back-up Survival Mechanism or Dedicated Pathway? *Trends in Biochemical Sciences*, *40*(11), 701–714. https://doi.org/10.1016/j.tibs.2015.08.006

Shaner, N. C., Lambert, G. G., Chammas, A., Ni, Y., Cranfill, P. J., Baird, M. A., Sell, B. R., Allen, J. R., Day, R. N., Israelsson, M., Davidson, M. W., & Wang, J. (2013). A bright monomeric green fluorescent protein derived from Branchiostoma lanceolatum. *Nature Methods*, *10*(5), 407–409. https://doi.org/10.1038/nmeth.2413

Shen, B., Zhang, W., Zhang, J., Zhou, J., Wang, J., Chen, L., Wang, L., Hodgkins, A., Iyer, V., Huang, X., & Skarnes, W. C. (2014). Efficient genome modification by CRISPR-Cas9 nickase with minimal off-target effects. *Nature Methods*, *11*(4), 399–402. https://doi.org/10.1038/nmeth.2857

Shen, H., Strunks, G. D., Klemann, B. J. P. M., Hooykaas, P. J. J., & de Pater, S. (2017). CRISPR/Cas9-induced double-strand break repair in *Arabidopsis* nonhomologous end-joining mutants. *G3: Genes, Genomes, Genetics*, *7*(1), 193–202. https://doi.org/10.1534/g3.116.035204

Shen, Z., Zhang, X., Chai, Y., Zhu, Z., Yi, P., Feng, G., Li, W., & Ou, G. (2014). Conditional knockouts generated by engineered CRISPR-Cas9 endonuclease reveal the roles of coronin in *C. elegans* neural development. *Developmental Cell*, *30*(5), 625–636. https://doi.org/10.1016/j.devcel.2014.07.017

Shim, E. Y., Chung, W. H., Nicolette, M. L., Zhang, Y., Davis, M., Zhu, Z., Paull, T. T., Ira, G., & Lee, S. E. (2010). Saccharomyces cerevisiae Mre11/Rad50/Xrs2 and Ku proteins regulate association of Exo1 and Dna2 with DNA breaks. *EMBO Journal*, *29*(19), 3370–3380. https://doi.org/10.1038/emboj.2010.219

Shmakov, S., Smargon, A., Scott, D., Cox, D., Pyzocha, N., Yan, W., Abudayyeh, O. O., Gootenberg, J. S., Makarova, K. S., Wolf, Y. I., Severinov, K., Zhang, F., & Koonin, E. V. (2017). Diversity and evolution of class 2 CRISPR-Cas systems. *Nature Reviews Microbiology*, *15*(3), 169–182. https://doi.org/10.1038/nrmicro.2016.184

Silao, F. G. S., Ward, M., Ryman, K., Wallström, A., Brindefalk, B., Udekwu, K., & Ljungdahl, P. O. (2019). Mitochondrial proline catabolism activates Ras1/cAMP/PKA-induced filamentation in *Candida albicans*. In *PLoS Genetics* (Vol. 15, Issue 2). https://doi.org/10.1371/journal.pgen.1007976

Silva-García, C. G., Lanjuin, A., Heintz, C., Dutta, S., Clark, N. M., & Mair, W. B. (2019). Single-copy knock-in loci for defined gene expression in *Caenorhabditis elegans*. *G3: Genes, Genomes, Genetics*, *9*(7), 2195–2198. https://doi.org/10.1534/g3.119.400314

Simmer, F., Tijsterman, M., Parrish, S., Koushika, S. P., Nonet, M. L., Fire, A., Ahringer, J., & Plasterk, R. H. A. (2002). Loss of the putative RNA-directed RNA polymerase RRF-3 makes *C. elegans* hypersensitive to RNAi. *Current Biology*, *12*(15), 1317–1319. https://doi.org/10.1016/S0960-9822(02)01041-2

Smolikov, S., Eizinger, A., Hurlburt, A., Rogers, E., Villeneuve, A. M., & Colaiácovo, M. P. (2007). Synapsis-defective mutants reveal a correlation between chromosome conformation and the mode of double-strand break repair during *Caenorhabditis elegans* meiosis. *Genetics*, *176*(4), 2027–2033. https://doi.org/10.1534/genetics.107.076968

Sonnhammer, E. L. L., & Durbin, R. (1997). Analysis of protein domain families in *Caenorhabditis elegans*. *Genomics*, *46*(2), 200–216. https://doi.org/10.1006/geno.1997.4989

Spieth, J., Lawson, D., Davis, P., Williams, G., & Howe, K. (2014). Overview of gene structure in *C. elegans*. *WormBook : The Online Review of C. elegans Biology*, 1–18. https://doi.org/10.1895/wormbook.1.65.2

Stemmer, M., Thumberger, T., Del Sol Keyer, M., Wittbrodt, J., & Mateo, J. L. (2015). CCTop: An Intuitive, Flexible and Reliable CRISPR/Cas9 Target Prediction Tool. *PloS One*, *10*(4), e0124633. https://doi.org/10.1371/journal.pone.0124633

Sternberg, S. H., Redding, S., Jinek, M., Greene, E. C., & Doudna, J. A. (2014). DNA interrogation by the CRISPR RNA-guided endonuclease Cas9. *Nature*, *507*(7490), 62–67. https://doi.org/10.1038/nature13011

Stiernagle, T. (2006). Maintenance of *C. elegans*. *WormBook : The Online Review of C. elegans Biology*, 1–11. https://doi.org/10.1895/wormbook.1.101.1

Stinchcomb, D. T., Shaw, J. E., Carr, S. H., & Hirsh, D. (1985). Extrachromosomal DNA transformation of *Caenorhabditis elegans*. *Molecular and Cellular Biology*, *5*(12), 3484–3496. https://doi.org/10.1128/mcb.5.12.3484

Sturzenegger, A., Burdova, K., Kanagaraj, R., Levikova, M., Pinto, C., Cejka, P., & Janscak, P. (2014). DNA2 cooperates with the WRN and BLM RecQ helicases to mediate long-range DNA end resection in human cells. *Journal of Biological Chemistry*, *289*(39), 27314–27326. https://doi.org/10.1074/jbc.M114.578823

Su, K. C., Tsang, M. J., Emans, N., & Cheeseman, I. M. (2018). CRISPR/Cas9-based gene targeting using synthetic guide RNAs enables robust cell biological analyses. *Molecular Biology of the Cell*, *29*(20), 2370–2377. https://doi.org/10.1091/mbc.E18-04-0214

Sugiyama, T., Zaitseva, E. M., & Kowalczykowski, S. C. (1997). A single-stranded DNA-binding protein is needed for efficient presynaptic complex formation by the Saccharomyces cerevisiae Rad51 protein. *Journal of Biological Chemistry*, *272*(12), 7940–7945. https://doi.org/10.1074/jbc.272.12.7940

Sulston, J. E., & Horvitz, H. R. (1977). Post-embryonic cell lineages of the nematode, *Caenorhabditis elegans*. *Developmental Biology*, *56*(1), 110–156. https://doi.org/10.1016/0012-1606(77)90158-0

Sulston, J. E., Schierenberg, E., White, J. G., & Thomson, J. N. (1983). The embryonic cell lineage of the nematode *Caenorhabditis elegans*. *Developmental Biology*, *100*(1), 64–119. https://doi.org/10.1016/0012-1606(83)90201-4

Sung, P., & Klein, H. (2006). Mechanism of homologous recombination: Mediators and helicases take on regulatory functions. *Nature Reviews Molecular Cell Biology*, *7*(10), 739–750. https://doi.org/10.1038/nrm2008

Tabara, H., Grishok, A., & Mello, C. C. (1998). RNAi in *C. elegans*: Soaking in the Genome sequence. *Science*, *282*(5388), 430–431. https://doi.org/10.1126/science.282.5388.430

Teuscher, A., & Ewald, C. (2018). Overcoming Autofluorescence to Assess GFP Expression During Normal Physiology and Aging in *Caenorhabditis elegans*. *Bio-Protocol*, *8*(14), 0–17. https://doi.org/10.21769/bioprotoc.2940

The *C. elegans* Deletion Mutant Consortium. (2012). Large-scale screening for targeted knockouts in the *Caenorhabditis elegans* genome. *G3: Genes, Genomes, Genetics*, *2*(11), 1415–1425. https://doi.org/10.1534/g3.112.003830

The *C. elegans* Sequencing Consortium. (1998). Genome sequence of the nematode *C. elegans*: A platform for investigating biology. *Science*, *282*(5396), 2012–2018. https://doi.org/10.1126/science.282.5396.2012

Thompson, O., Edgley, M., Strasbourger, P., Flibotte, S., Ewing, B., Adair, R., Au, V., Chaudhry, I., Fernando, L., Hutter, H., Kieffer, A., Lau, J., Lee, N., Miller, A., Raymant, G., Shen, B., Shendure, J., Taylor, J., Turner, E. H., … Waterston, R. H. (2013). The million mutation project: A new approach to genetics in *Caenorhabditis elegans*. *Genome Research*, *23*(10), 1749–1762. https://doi.org/10.1101/gr.157651.113

Tian, D., Diao, M., Jiang, Y., Sun, L., Zhang, Y., Chen, Z., Huang, S., & Ou, G. (2015). Anillin regulates neuronal migration and neurite growth by linking RhoG to the actin cytoskeleton. *Current Biology*, *25*(9), 1135–1145. https://doi.org/10.1016/j.cub.2015.02.072

Tianfang Ge, D., Tipping, C., Brodsky, M. H., & Zamore, P. D. (2016). Rapid screening for CRISPR-directed editing of th *Drosophila* genome using white coconversion. *G3: Genes, Genomes, Genetics*, *6*(10), 3197–3206. https://doi.org/10.1534/g3.116.032557

Timmons, L., & Fire, A. Z. (1998). Specific interference by ingested dsRNA. *Nature*, *395*(6705), 854. https://doi.org/10.1038/27579

Ting, W. W., & Ng, I. S. (2020). Metabolic manipulation through CRISPRi and gene deletion to enhance cadaverine production in *Escherichia coli*. *Journal of Bioscience and Bioengineering*, *130*(6), 553–562. https://doi.org/10.1016/j.jbiosc.2020.07.013

Truong, L. N., Li, Y., Shi, L. Z., Hwang, P. Y. H., He, J., Wang, H., Razavian, N., Berns, M. W., & Wu, X. (2013). Microhomology-mediated End Joining and Homologous Recombination share the initial end resection step to repair DNA double-strand breaks in mammalian cells. *Proceedings of the National Academy of Sciences of the United States of America*, *110*(19), 7720–7725. https://doi.org/10.1073/pnas.1213431110

Turk, R., & Spencer, N. Y. (2019). *A high degree of similarity in CRISPR-Cas9 editing efficiency is found between 2-part guide RNAs and single guide RNAs*. DECODED™ Online Newsletter. https://eu.idtdna.com/pages/education/decoded/article/a-high-degree-of-similarity-in-crispr-cas9-editing-efficiency-is-found-between-2-part-guide-rnas-and-single-guide-rnas

Urnov, F. D., Rebar, E. J., Holmes, M. C., Zhang, H. S., & Gregory, P. D. (2010). Genome editing with engineered zinc finger nucleases. *Nature Reviews Genetics*, *11*(9), 636–646. https://doi.org/10.1038/nrg2842

van Schendel, R., Roerink, S. F., Portegijs, V., van den Heuvel, S., & Tijsterman, M. (2015). Polymerase θ is a key driver of genome evolution and of CRISPR/Cas9-mediated mutagenesis. *Nature Communications*, *6*(May), 1–8. https://doi.org/10.1038/ncomms8394

van Schendel, R., van Heteren, J., Welten, R., & Tijsterman, M. (2016). Genomic Scars Generated by Polymerase Theta Reveal the Versatile Mechanism of Alternative End-Joining. *PLoS Genetics*, *12*(10), 1–21. https://doi.org/10.1371/journal.pgen.1006368

Verma, P., & Greenberg, R. A. (2016). Noncanonical views of homology-directed DNA repair. *Genes and Development*, *30*(10), 1138–1154. https://doi.org/10.1101/gad.280545.116

Vicencio, J., & Cerón, J. (2021). A Living Organism in your CRISPR Toolbox: *Caenorhabditis elegans* Is a Rapid and Efficient Model for Developing CRISPR-Cas Technologies. *CRISPR Journal*, *4*(1), 32–42. https://doi.org/10.1089/crispr.2020.0103

Vicencio, J., Martínez-fernández, C., Serrat, X., & Cerón, J. (2019). Efficient Generation of Endogenous Fluorescent Reporters by Nested CRISPR in *Caenorhabditis elegans*. *Genetics*, *211*(April), 1143–1154. https://doi.org/10.1534/genetics.119.301965

Vicencio, J., Sánchez-Bolaños, C., Moreno-Sánchez, I., Brena, D., Kukhtar, D., Ruiz-López, M., Cots-Ponjoan, M., Vejnar, C. E., Rubio, A., Rodrigo Melero, N., Carolis, C., Pérez-Pulido, A. J., Giráldez, A. J., Kleinstiver, B. P., Cerón, J., & Moreno-Mateos, M. A. (2021). Genome editing in animals with minimal PAM CRISPR-Cas9 enzymes Jeremy. *BioRxiv*. https://doi.org/https://doi.org/10.1101/2021.06.06.447255

Vujin, A., Jones, S. J., & Zetka, M. (2020). NHJ-1 is required for canonical nonhomologous end joining in *Caenorhabditis elegans*. *Genetics*, *215*(3), 635–651. https://doi.org/10.1534/genetics.120.303328

Waaijers, S., Portegijs, V., Kerver, J., Lemmens, B. B. L. G., Tijsterman, M., van den Heuvel, S., & Boxem, M. (2013). CRISPR/Cas9-targeted mutagenesis in *Caenorhabditis elegans*. *Genetics*, *195*(3), 1187–1191. https://doi.org/10.1534/genetics.113.156299

Walton, R. T., Christie, K. A., Whittaker, M. N., & Kleinstiver, B. P. (2020). Unconstrained genome targeting with near-PAMless engineered CRISPR-Cas9 variants. *Science*, *368*(6488), 290–296. https://doi.org/10.1126/science.aba8853

Ward, J. D. (2015). Rapid and precise engineering of the *Caenorhabditis elegans* genome with lethal mutation co-conversion and inactivation of NHEJ repair. *Genetics*, *199*(2), 363–377. https://doi.org/10.1534/genetics.114.172361

Waterhouse, P. M., Graham, M. W., & Wang, M. B. (1998). Virus resistance and gene silencing in plants can be induced by simultaneous expression of sense and antisense RNA. *Proceedings of the National Academy of Sciences of the United States of America*, *95*(23), 13959–13964. https://doi.org/10.1073/pnas.95.23.13959

Wei, Y., Terns, R. M., & Terns, M. P. (2015). Cas9 function and host genome sampling in type II-A CRISPR–cas adaptation. *Genes and Development*, *29*(4), 356–361. https://doi.org/10.1101/gad.257550.114

Wenick, A. S., & Hobert, O. (2004). Genomic cis-regulatory architecture and trans-acting regulators of a single interneuron-specific gene battery in *C. elegans*. *Developmental Cell*, *6*(6), 757–770. https://doi.org/10.1016/j.devcel.2004.05.004

Wiedenheft, B., Sternberg, S. H., & Doudna, J. a. (2012). RNA-guided genetic silencing systems in bacteria and archaea. *Nature*, *482*(7385), 331–338. https://doi.org/10.1038/nature10886

Winston, W. M., Molodowitch, C., & Hunter, C. P. (2002). Systemic RNAi in *C. elegans* requires the putative transmembrane protein SID-1. *Science*, *295*(March), 2456–2459. https://doi.org/doi:10.1126/science.1068836

Wood, A. J., Lo, T. W., Zeitler, B., Pickle, C. S., Ralston, E. J., Lee, A. H., Amora, R., Miller, J. C., Leung, E., Meng, X., Zhang, L., Rebar, E. J., Gregory, P. D., Urnov, F. D., & Meyer, B. J. (2011). Targeted genome editing across species using ZFNs and TALENs. *Science*, *333*(6040), 307. https://doi.org/10.1126/science.1207773

Wu, S. C. Y., Meir, Y. J. J., Coates, C. J., Handler, A. M., Pelczar, P., Moisyadi, S., & Kaminski, J. M. (2006). piggyBac is a flexible and highly active transposon as compared to Sleeping Beauty, Tol2, and Mos1 in mammalian cells. *Proceedings of the National Academy of Sciences of the United States of America*, *103*(41), 15008–15013. https://doi.org/10.1073/pnas.0606979103

Wu, W.-S., Huang, W.-C., Brown, J. S., Zhang, D., Song, X., Chen, H., Tu, S., Weng, Z., & Lee, H.-C. (2018). pirScan: a webserver to predict piRNA targeting sites and to avoid transgene silencing in *C. elegans*. *Nucleic Acids Research*, *46*(W1), W43–W48. https://doi.org/10.1093/nar/gky277

Wu, Y., Liu, Y., Lv, X., Li, J., Du, G., & Liu, L. (2020). CAMERS-B: CRISPR/Cpf1 assisted multiple-genes editing and regulation system for Bacillus subtilis. *Biotechnology and Bioengineering*, *117*(6), 1817–1825. https://doi.org/10.1002/bit.27322

Xu, Z., Kuang, Y., Ren, B., Yan, D., Yan, F., Spetz, C., Sun, W., Wang, G., Zhou, X., & Zhou, H. (2021). SpRY greatly expands the genome editing scope in rice with highly flexible PAM recognition. *Genome Biology*, *22*(1), 1–15. https://doi.org/10.1186/s13059-020-02231-9

Xue, C., & Greene, E. C. (2021). DNA Repair Pathway Choices in CRISPR-Cas9-Mediated Genome Editing. *Trends in Genetics : TIG*, *xx*(xx), 1–18. https://doi.org/10.1016/j.tig.2021.02.008

Yang, B., Schwartz, M., & McJunkin, K. (2020). In vivo CRISPR screening for phenotypic targets of the mir-35-42 family in *C. elegans*. *Genes & Development*, *34*, 1227–1238. https://doi.org/10.1101/gad.339333.120

Yang, H., Ren, S., Yu, S., Pan, H., Li, T., Ge, S., Zhang, J., & Xia, N. (2020). Methods favoring homology-directed repair choice in response to crispr/cas9 induced-double strand breaks. *International Journal of Molecular Sciences*, *21*(18), 1–20. https://doi.org/10.3390/ijms21186461

Yang, S. H., Zhou, R., Campbell, J., Chen, J., Ha, T., & Paull, T. T. (2013). The SOSS1 single-stranded DNA binding complex promotes DNA end resection in concert with Exo1. *EMBO Journal*, *32*(1), 126–139. https://doi.org/10.1038/emboj.2012.314

Yao, X., Wang, X., Liu, J., Hu, X., Shi, L., Shen, X., Ying, W., Sun, X., Wang, X., Huang, P., & Yang, H. (2017). CRISPR/Cas9 – Mediated Precise Targeted Integration In Vivo Using a Double Cut Donor with Short Homology Arms. *EBioMedicine*, *20*, 19–26. https://doi.org/10.1016/j.ebiom.2017.05.015

Yeh, C. D., Richardson, C. D., & Corn, J. E. (2019). Advances in genome editing through control of DNA repair pathways. *Nature Cell Biology*, *21*(12), 1468–1478. https://doi.org/10.1038/s41556-019-0425-z

Yoshimi, K., Kunihiro, Y., Kaneko, T., Nagahora, H., Voigt, B., & Mashimo, T. (2016). SsODN-mediated knock-in with CRISPR-Cas for large genomic regions in zygotes. *Nature Communications*, *7*, 1–10. https://doi.org/10.1038/ncomms10431

Yoshimura, J., Ichikawa, K., Shoura, M. J., Artiles, K. L., Gabdank, I., Wahba, L., Smith, C. L., Edgley, M. L., Rougvie, A. E., Fire, A. Z., Morishita, S., & Schwarz, E. M. (2019). Recompleting the *Caenorhabditis elegans* genome. *Genome Research*, *29*(6), 1009–1022. https://doi.org/10.1101/gr.244830.118

Yousefzadeh, M. J., Wyatt, D. W., Takata, K. ichi, Mu, Y., Hensley, S. C., Tomida, J., Bylund, G. O., Doublié, S., Johansson, E., Ramsden, D. A., McBride, K. M., & Wood, R. D. (2014). Mechanism of Suppression of Chromosomal Instability by DNA Polymerase POLQ. *PLoS Genetics*, *10*(10). https://doi.org/10.1371/journal.pgen.1004654

Yuen, K. W. Y., Nabeshima, K., Oegema, K., & Desai, A. (2011). Rapid de novo centromere formation occurs independently of heterochromatin protein 1 in *C. elegans* embryos. *Current Biology*, *21*(21), 1800–1807. https://doi.org/10.1016/j.cub.2011.09.016

Yusa, K., Zhou, L., Li, M. A., Bradley, A., & Craig, N. L. (2011). A hyperactive piggyBac transposase for mammalian applications. *Proceedings of the National Academy of Sciences of the United States of America*, *108*(4), 1531–1536. https://doi.org/10.1073/pnas.1008322108

Zaidi, S. S. e. A., Mahas, A., Vanderschuren, H., & Mahfouz, M. M. (2020). Engineering crops of the future: CRISPR approaches to develop climate-resilient and disease-resistant plants. *Genome Biology*, *21*(1), 1–19. https://doi.org/10.1186/s13059-020-02204-y

Zarkower, D. (2006). Somatic sex determination. *WormBook : The Online Review of C. elegans Biology*, 1–12. https://doi.org/10.1895/wormbook.1.84.1

Zetsche, B., Gootenberg, J. S., Abudayyeh, O. O., Slaymaker, I. M., Makarova, K. S., Essletzbichler, P., Volz, S. E., Joung, J., Van Der Oost, J., Regev, A., Koonin, E. V., & Zhang, F. (2015). Cpf1 Is a Single RNA-Guided Endonuclease of a Class 2 CRISPR-Cas System. *Cell*, *163*(3), 759–771. https://doi.org/10.1016/j.cell.2015.09.038

Zhang, C., Wang, Y., Wang, F., Zhao, S., Song, J., Feng, F., Zhao, J., & Yang, J. (2021). Expanding base editing scope to near-PAMless with engineered CRISPR/Cas9 variants in plants. *Molecular Plant*, *14*(2), 191–194. https://doi.org/10.1016/j.molp.2020.12.016

Zhang, D., & Glotzer, M. (2014). Efficient site-specific editing of the *C. elegans* genome. *BioRxiv*, 007344. https://doi.org/10.1101/007344

Zhang, F. (2019). Development of CRISPR-Cas systems for genome editing and beyond. *Quarterly Reviews of Biophysics*, *52*. https://doi.org/10.1017/s0033583519000052

Zhang, X., Wang, J., Wang, J., Cheng, Q., Zheng, X., & Zhao, G. (2017). Multiplex gene regulation by CRISPR-ddCpf1. *Cell Discovery*, *3*, 1–9. https://doi.org/10.1038/celldisc.2017.18

Zhang, Yan, Heidrich, N., Ampattu, B. J., Gunderson, C. W., Seifert, H. S., Schoen, C., Vogel, J., & Sontheimer, E. J. (2013). Processing-Independent CRISPR RNAs Limit Natural Transformation in Neisseria meningitidis. *Molecular Cell*, *50*(4), 488–503. https://doi.org/10.1016/j.molcel.2013.05.001

Zhang, Yilan, Ge, X., Yang, F., Zhang, L., Zheng, J., Tan, X., Jin, Z. B., Qu, J., & Gu, F. (2014). Comparison of non-canonical PAMs for CRISPR/Cas9-mediated DNA cleavage in human cells. *Scientific Reports*, *4*, 1–5. https://doi.org/10.1038/srep05405

Zhao, N., Kamijo, K., Fox, P. D., Oda, H., Morisaki, T., Sato, Y., Kimura, H., & Stasevich, T. J. (2019). A genetically encoded probe for imaging nascent and mature HA-tagged proteins in vivo. *Nature Communications*, *10*(1). https://doi.org/10.1038/s41467-019-10846-1

Zhao, P., Zhang, Z., Ke, H., Yue, Y., & Xue, D. (2014). Oligonucleotide-based targeted gene editing in *C. elegans* via the CRISPR/Cas9 system. *Cell Research*, *24*(2), 247–250. https://doi.org/10.1038/cr.2014.9

Zhu, J., Cheng, K. C. L., & Yuen, K. W. Y. (2018). Histone H3K9 and H4 Acetylations and Transcription Facilitate the Initial CENP-AHCP-3 Deposition and de Novo Centromere Establishment in *Caenorhabditis elegans* Artificial Chromosomes. *Epigenetics and Chromatin*, *11*(1), 1–20. https://doi.org/10.1186/s13072-018-0185-1

Zuryn, S., Le Gras, S., Jamet, K., & Jarriault, S. (2010). A strategy for direct mapping and identification of mutations by whole-genome sequencing. *Genetics*, *186*(1), 427–430. https://doi.org/10.1534/genetics.110.119230

LIST OF PUBLICATIONS

1. Vicencio, J., & Cerón, J. (2021). A Living Organism in your CRISPR Toolbox: *Caenorhabditis elegans* Is a Rapid and Efficient Model for Developing CRISPR-Cas Technologies. *CRISPR Journal*, *4*(1), 32–42. https://doi.org/10.1089/crispr.2020.0103

2. Vicencio, J., Martínez-Fernández, C., Serrat, X., & Cerón, J. (2019). Efficient Generation of Endogenous Fluorescent Reporters by Nested CRISPR in *Caenorhabditis elegans*. *Genetics*, *211*(April), 1143–1154. https://doi.org/10.1534/genetics.119.301965

3. Vicencio, J., Sánchez-Bolaños, C., Moreno-Sánchez, I., Brena, D., Kukhtar, D., Ruiz-López, M., Cots-Ponjoan, M., Vejnar, C. E., Rubio, A., Rodrigo Melero, N., Carolis, C., Pérez-Pulido, A. J., Giráldez, A. J., Kleinstiver, B. P., Cerón, J., & Moreno-Mateos, M. A. (2021). Genome editing in animals with minimal PAM CRISPR-Cas9 enzymes. *BioRxiv*. https://doi.org/https://doi.org/10.1101/2021.06.06.447255